ROLE OF SEDIMENT IN NON-POINT SOURCE SALT LOADING WITHIN THE UPPER COLORADO RIVER BASIN

by

H.W. Shen
J.B. Laronne
E.D. Enck
G. Sunday
K.K. Tanji
L.D. Whittig
J.W. Biggar

August 1981

COLORADO WATER RESOURCES RESEARCH INSTITUTE

Colorado State University
Fort Collins, Colorado

Completion Report No. 107

ROLE OF SEDIMENT IN NON-POINT SOURCE SALT LOADING WITHIN THE UPPER COLORADO RIVER BASIN

Combined Completion Report

OWRT Project Nos. B-137-COLO and B-170-COLO

by

H. W. Shen
Professor of Civil Engineering
Colorado State University

J. B. Laronne
Formerly Research Associate
Colorado State University
Now Lecturer, Department of Geography
Ben Gurion University of the Negev
Beer Sheva, Israel

E. D. Enck and G. Sunday
Graduate Research Assistants
Colorado State University

K. K. Tanji, L. D. Whittig and J. W. Biggar
Department of Land, Air and Water Resources
University of California
Davis, California

submitted to

Office of Water Research and Technology
U. S. Department of the Interior
Washington, D. C. 20240

August, 1981

The work upon which this report is based was supported (in part) by funds provided by the United States Department of the Interior, Office of Water Research and Technology, as authorized by the Water Resources Research Act of 1978, and pursuant to Grant Agreement Nos. 14-34-0001-6063 and 14-34-0001-8067.

COLORADO WATER RESOURCES RESEARCH INSTITUTE
Colorado State University
Fort Collins, Colorado
Norman A. Evans, Director

ACKNOWLEDGEMENTS

We wish to thank OWRT for their financial support for this Project No. B-137-COLO, B-170-COLO, and CSU Experiment Station-124-COLO. Robert Strand of the U.S. Water and Power Agencies, Norman Evans of Colorado State University, Keith Eggleston and Gordon Bently of the U.S. Bureau of Land Management, and J. Paul Riley and William Riney of Utah State University have given us stimulated discussions on this matter. Laboratory experiments and field investigations were undertaken and partly planned by D. Achterberg, B. Begin, A. Deyo, R. Fujii, and G. Zimpfer.

TABLE OF CONTENTS

Chapter | Page

LIST OF FIGURES

LIST OF TABLES

CHAPTER 1

INTRODUCTION

1.1. Statement of Problem and Scope of Study

The Colorado River Basin is the main water resource for the entire Southwest, providing water for irrigation, industry, power, municipal needs and recreation. A critical shortage of water and a deterioration of water quality plague this vital resource. The most serious water quality problem in the basin is salinity and the continued increase in salinity over the last century (U.S. Bureau of Reclamation, 1972). The Colorado River Basin is divided into the Upper and Lower Basins by the Colorado River Compact of 1922 (U.S. Congressional Record, 1928). The physical dividing point is Lees Ferry, Arizona (Fig. 1.1).

Salinity sources are categorized into two distinct groups: (1) Point sources are usually easy to identify because of the high solute concentrations involved. They include springs and large seeps as well as saline effluents of urban, industrial and agricultural origin; (2) diffuse sources frequently cover large tracts of land. Spatial variations in solute contribution within such large areas are not easily determined. This report deals only with the role of sediment in diffuse-source salt loading. The scope of this study includes:

1. A brief review of current knowledge;
2. Spatial variability of soluble mineral content (herein denoted SMC);
3. Identification of variables that determine the rate of solute pickup;
4. Role of sediment in salt loading of flows over hillslopes;

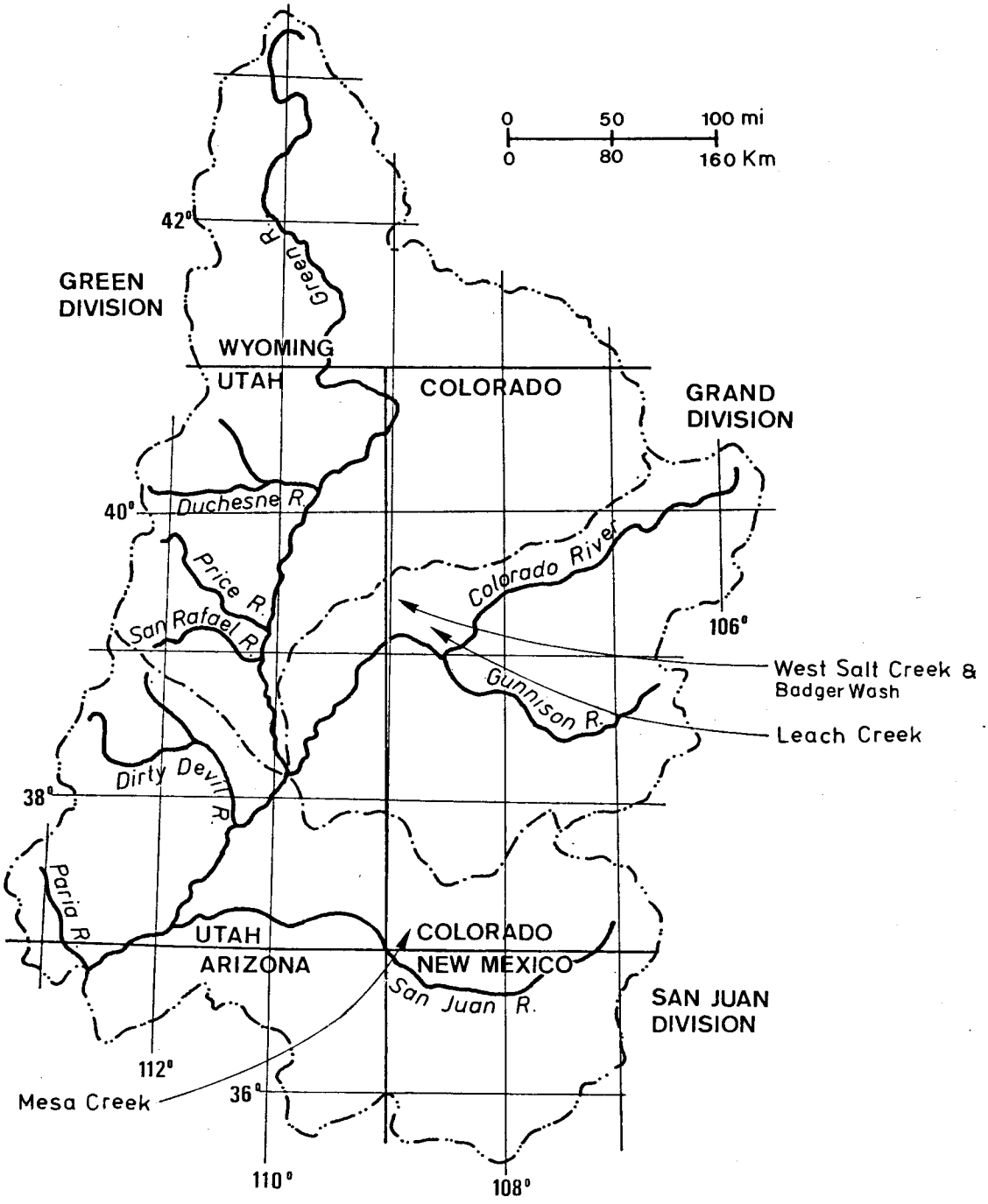

Figure 1.1. The Upper Colorado River Basin. Note the location of the principal study areas.

5. Movement of sediment and solutes in streams;
6. Preliminary estimation of diffuse, non-agricultural salt loading, and
7. Preliminary identification of areas where management and treatment practices will reduce salt loading.

1.2 Salinity Problem

The Colorado River Basin spans from Wyoming, Colorado and Utah down to Arizona and California with a drainage area of more than 200,000 square miles. At the headwaters the average salinity (concentration of solutes, or the misnomer total dissolved solids) in the Colorado River is less than 50 mg/1. This progressively increases downstream until, at Imperial Dam, the modified condition is 865 mg/1 (Maletic, 1973). Salinity values refer to the concentration of solutes and are reported in milligrams per liter (mg/1). This weight per volume unit of concentration is nearly equivalent to parts per million (ppm) up to concentrations of 7000 mg/1. "Present unmodified condition" refers to conditions during 1941-1968 modified to reflect all upstream existing projects in operation for the full period.

Projection of future salinity levels without a control program suggests that values of 1250 mg/1 or more will occur at Imperial Dam by the year 2000. One projection used in the Lower Colorado Region Comprehensive Framework Study (based on a U.S. Water Resource Council study) foresees such a level being reached by 1980. The salinity problem is especially severe due to the importance of this region of the nation for energy development, which almost unavoidable will result in increased salinity levels (Coos, 1973; Schmehl and McCaslin, 1973).

Should these increases in salinity levels occur, the agriculture in the Imperial, Coachella, Gila and Yuma Valleys would be further threatened. Also, a poorer water quality would be diverted to the Metropolitan Water District of Southern California and the Las Vegas Valley Water District, causing further economic losses to the very large block of domestic water users in California and Nevada. Upon completion of the Central Arizona Project, water users in the Phoenix and Tucson areas would be similarly affected.

The enactment of the Federal Water Pollution Control Act Amendments of 1972 (Public Law 92-600) and the conclusion of negotiations with Mexico regarding the control of salinity in waters delivered to Mexico have greatly increased the needs for salinity investigations in this river basin.

Various studies have been accomplished by different government agencies on the salinity problem in the Colorado River Basin. Because of non-uniformity in assumptions, data sets, and procedures, the findings of these studies differ. However, the conclusions derived are generally similar. The major conclusions (U.S. Bureau of Reclamation, 1974) are that the largest portion of the mineral burden was found to originate in the upper basin, that natural sources were thought to be the major contributors to the salt loading, that salinity was projected to continually increase in the lower reaches unless control programs are implemented, and that the impact of the increasing salinity levels was found to be primarily economic.

In order to evaluate the salinity problem, it is essential to identify the point and diffuse sources of salinity (Fig. 1.2) and to

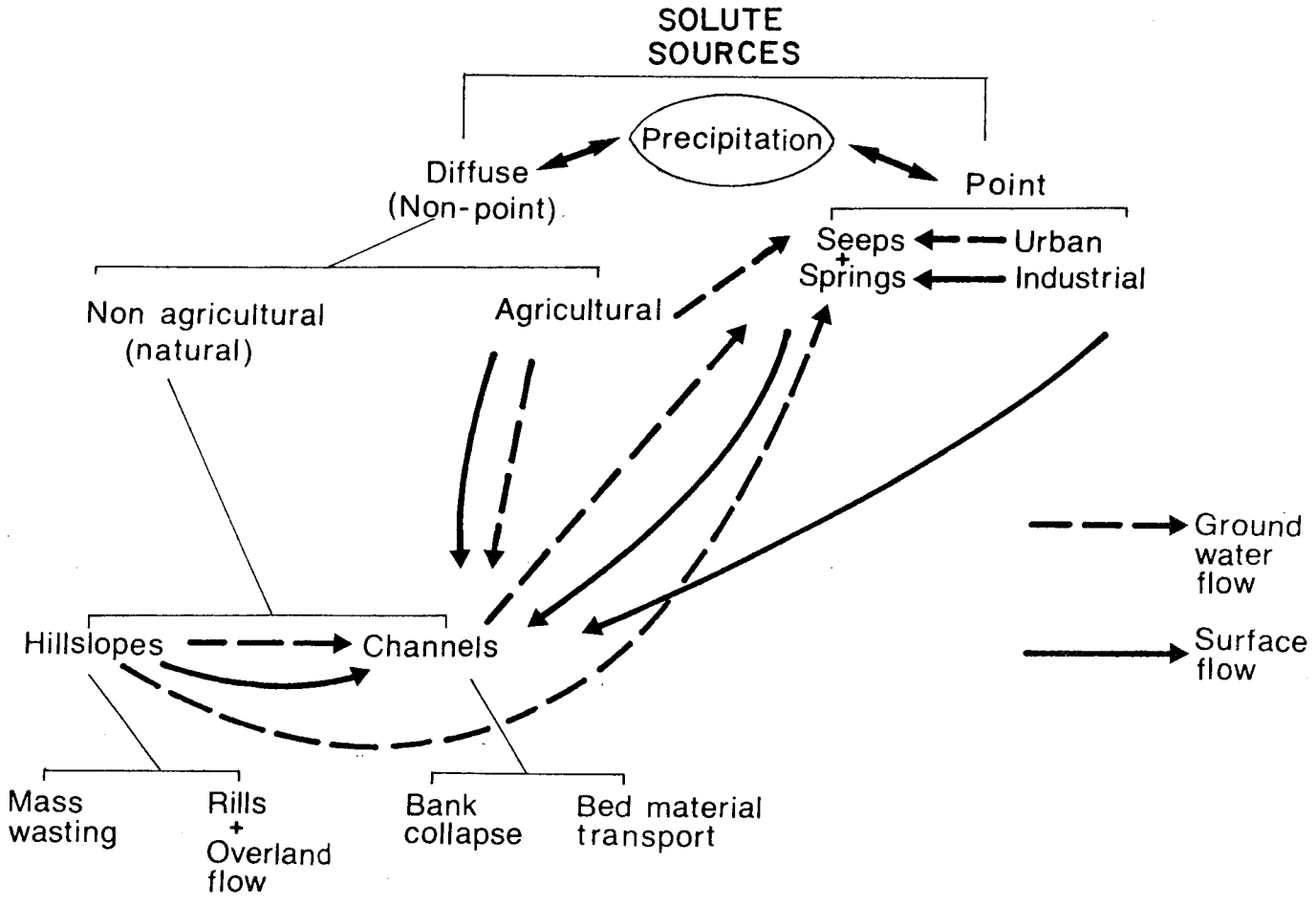

Figure 1.2. Transport of solutes and related sediment transport mechanisms.

understand the mechansims of salt transport. As shown on Figure 1.2, both ground water flow and surface flow carry the salt load from one source to another. The non-agricultural source of salt input is derived from hillslopes and channels. Dominant hillslope processes giving rise to salt input are either mass wasting or liquid flow in rills and as overland and rill flow. Channel sources arise from bank collapse and from bed material transport. In this study, the work is addressed to the role of sediment on salt loading from both hillslopes and channels.

Recent studies (U.S. Department of Agriculture, 1975; Whitmore, 1976; White, 1977; Ponce and Hawkins, 1978; Laronne, 1981; and Laronne and Schumm, 1981) as well as earlier reports recognize the large portion of solutes produced by diffuse sources (especially in the upper basin, Fig. 1.3) and the possibility that the transport of sediments is the cause for much of the solute pickup.

1.3 Description of Area

Most of the water in the upper Colorado River Basin originates from spring snow melt in the Rocky Mountains. These vegetated mountain ranges expose primarily crystalline rocks with derived soils that produce relatively insoluble weathering products. The mountains are also generally characterized by low sediment yields (Colorado Land Use Commission, 1974). The lower areas of the basin are principally underlain by sedimentary rocks, many of which (and specifically, the shales), are of marine origin. Figure 1.4 presents a photograph showing a general view of this area. Salts in the sediments eroded

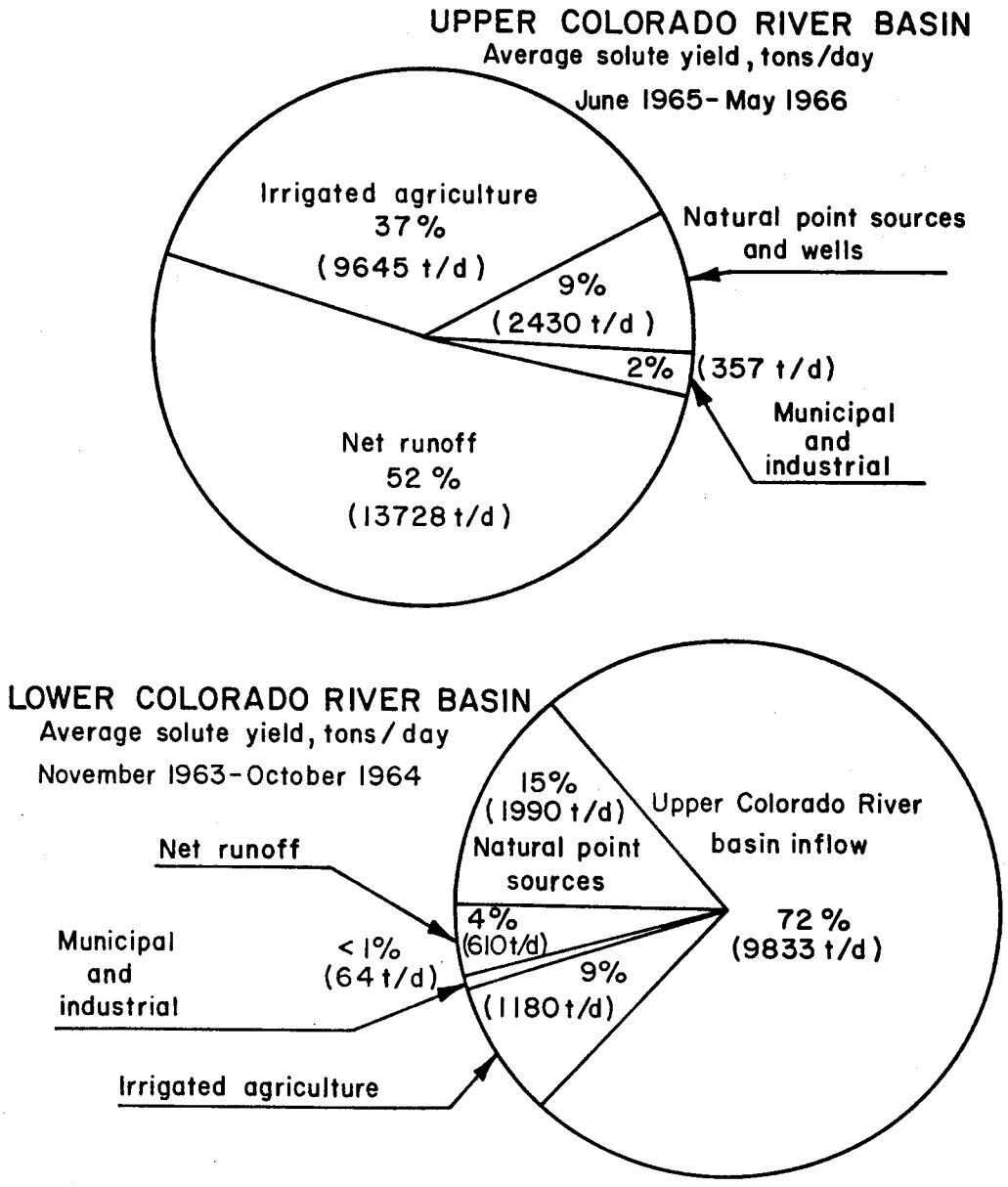

Figure 1.3. Contribution of solute loads from diffuse and point sources in the Colorado River Basin (after estimates made by EPA, 1971).

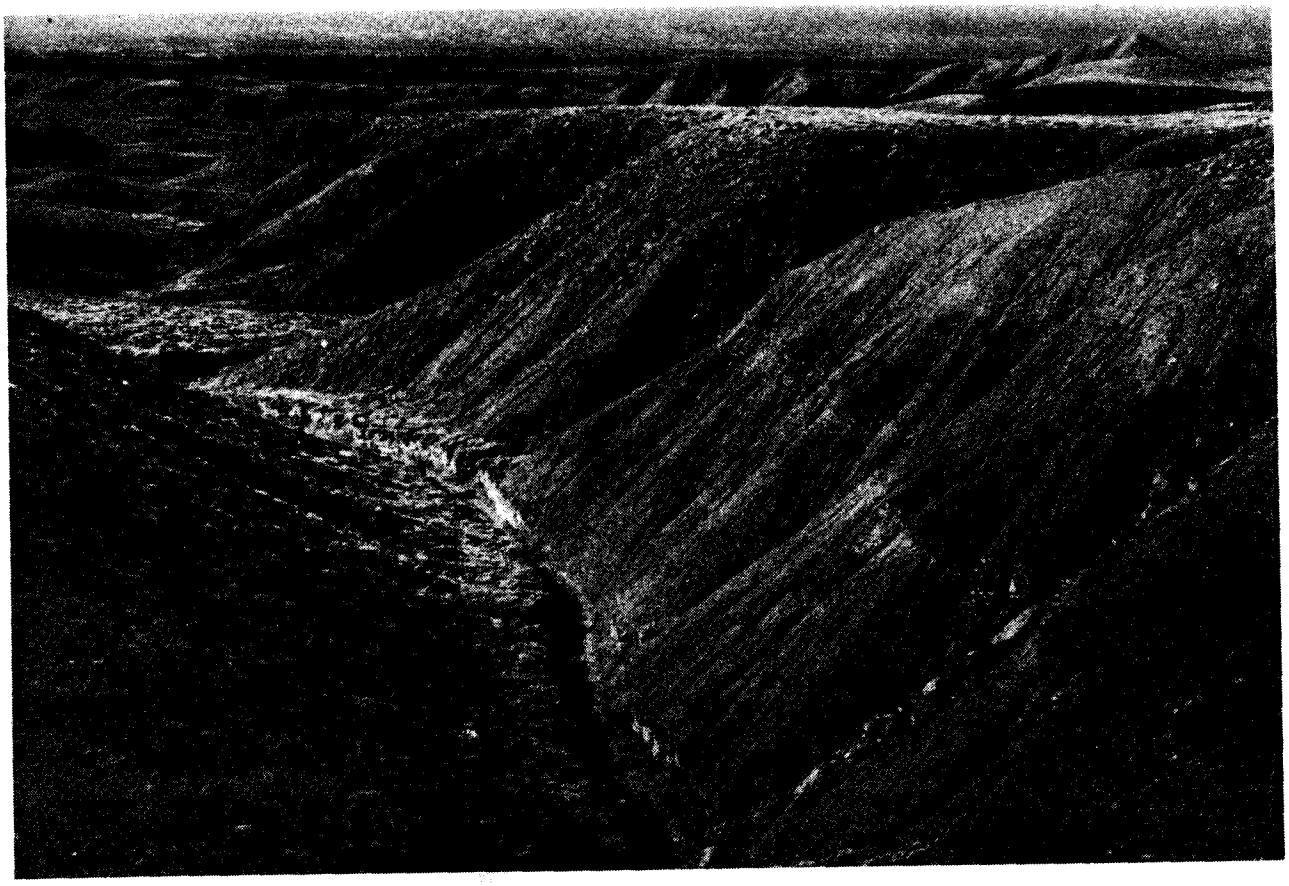

Figure 1.4. General view toward the southwest of the Mancos Shale terrain in the Grand Valley near Grand Junction, Colorado. Note the sparse vegetative cover, high hillslope inclinations, rilling and high drainage density in the foreground. The flat surfaces in the background are pediments capped by coarse alluvium.

from such strata below the Book Cliffs (between Grand Junction, Colorado and Price, Utah) may eventually reach the waters of the Colorado River. These areas are not only typified by an underlying material containing many diagenetic soluble minerals derived from the original contact with seawater, but they are also semiarid to arid in nature. Such climatic regions are by definition those of low annual precipitation and high evaporation (Fig. 1.5). The natural runoff of these regions becomes more concentrated with dissolved matter, or "salt-loaded", as evaporation occurs. The marine origin of these sediments, their shaly nature and salt loading are primary causes for the saline nature of the associated surficial materials, which are rich or enriched in calcium and magnesium carbonates and in soluble sulfates. The Bureau of Reclamation (1974) stated that:

> The major part of the dissolved constituents in the Colorado River water is made up of the cations: calcium, magnesium and sodium, and the anions: sulfate, chloride and bicarbonate. These, plus minor amounts of other dissolved constituents, are commonly referred to as salinity, "salt", dissolved solids, or dissolved mineral content.

A review of the occurrence of saline deposits within the Upper Colorado River Basin revealed that almost all of these outcrop in the arid-semiarid lowlands. Practically all the saline deposits are fine-grained and most are shales. The shales of the Colorado Plateaus were mostly deposited in shallow (epicontinental) seas that were often very saline; much calcium sulfate, if not sodium chloride and even potassium salts were, therefore, deposited contemporaneously with the sediments and subsequently remobilized and diagenetically altered. Among the variety of saline shales in the basin (Paradox, Moenkopi, Carmel, Summerville, parts of the Morrison, the

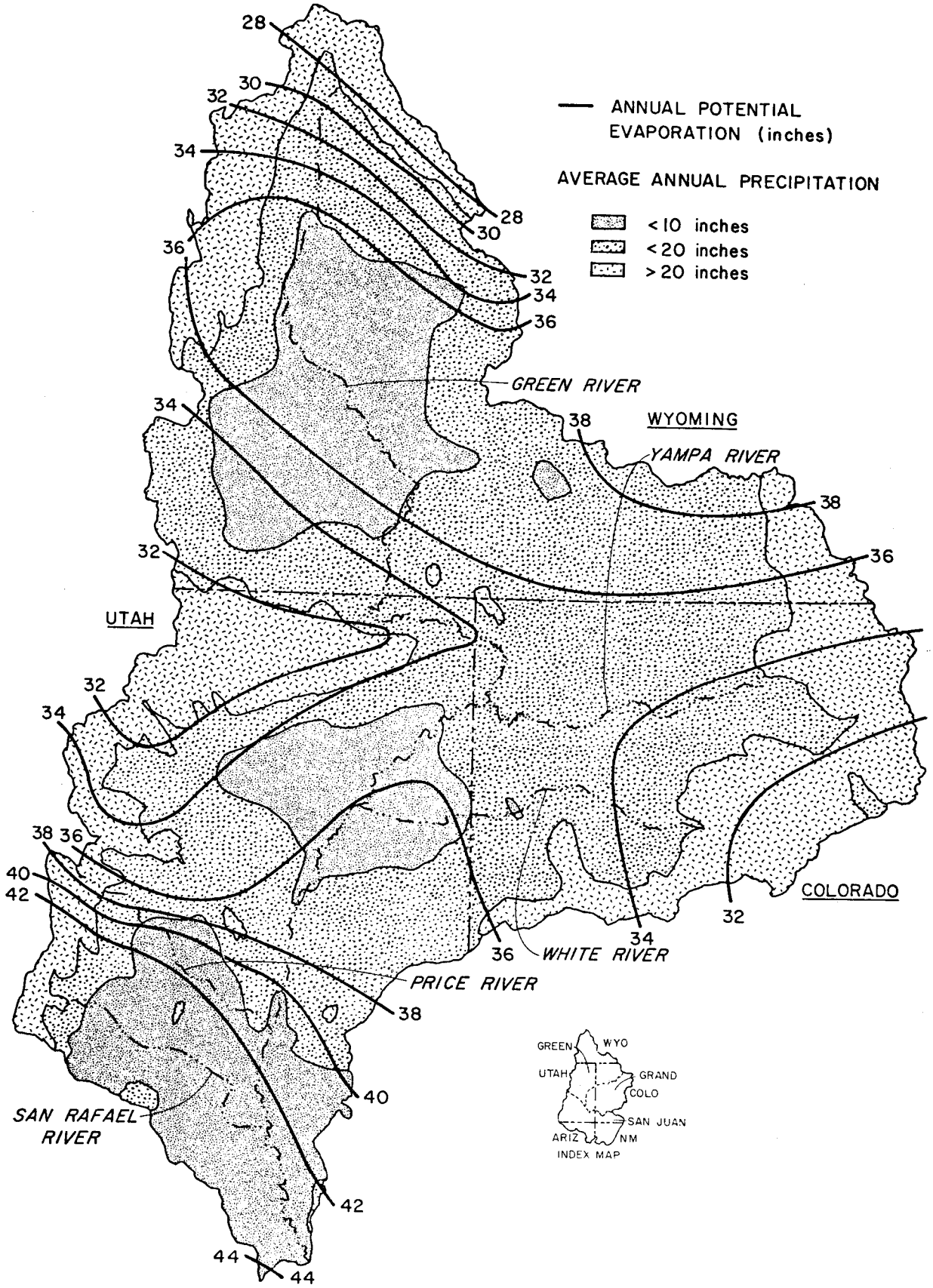

Figure 1.5a. Mean annual precipitation and potential evaporation in the Green River Basin (after Iorns, Hembree and Oakland, 1965).

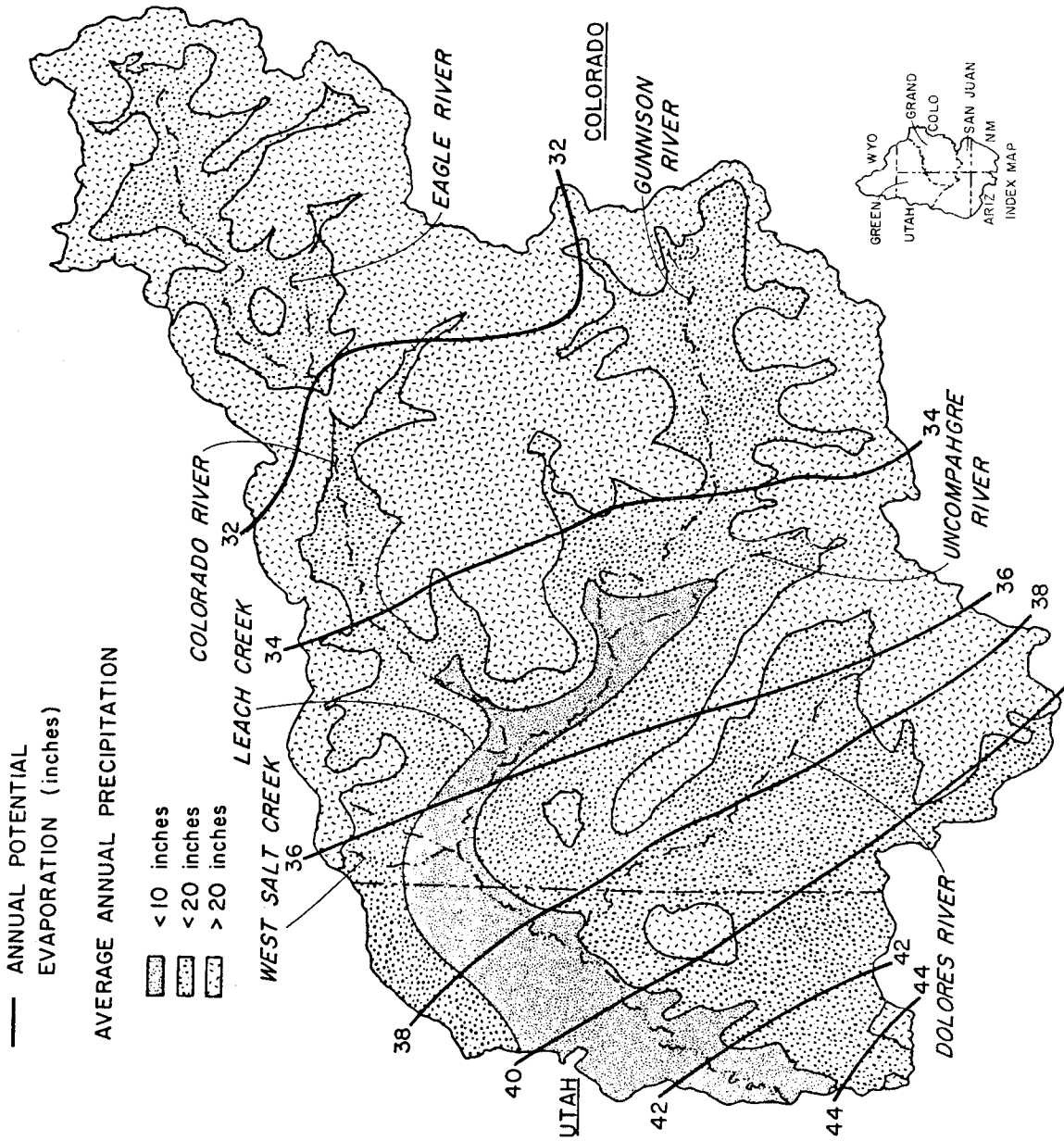

Figure 1.5b. Mean annual precipitation and potential evaporation in the Grand River Basin (after Ioms, Hembree and Oakland, 1965).

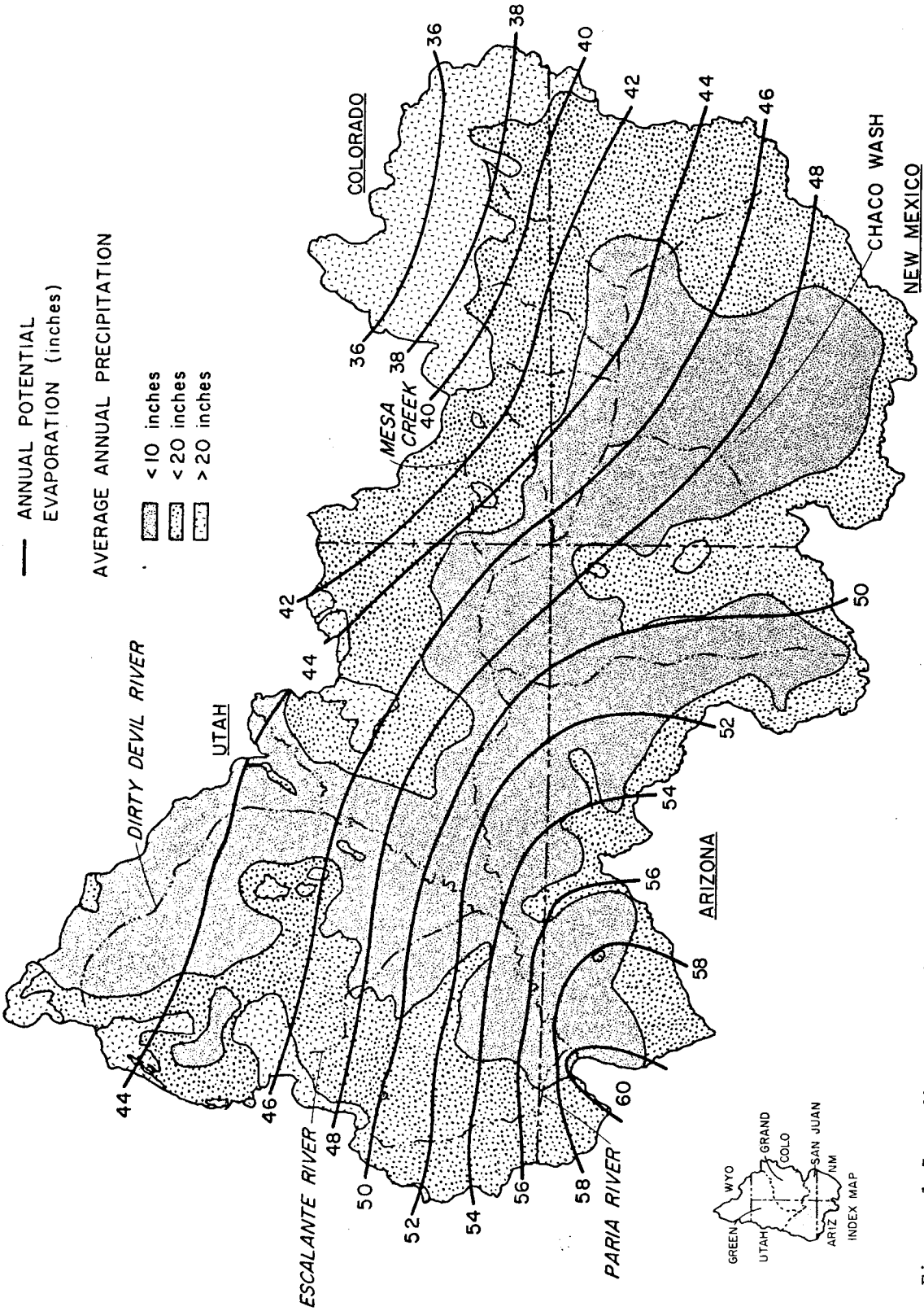

Figure 1.5c. Mean annual precipitation and potential evaporation in the San Juan River Basin (after Iorns, Hembree and Oakland, 1965).

Mancos-Mesa Verde and some shaly parts of the Green River Formations, herein mentioned in ascending stratigraphic sequence), the Upper Cretaceous Mancos and Mesa Verde Shales are the thickest in the succession, reaching a total thickness of 1000 m and covering bands 10-20 miles in width. Figure 1.6 is a map of a portion of the state of Colorado, showing the location of Mancos Shale outcrops.

The identification of specific soluble minerals by X-ray diffraction and chemical analyses, as well as the spatial trends in SMC are discussed in detail in the Appendix (A-1).

The occurence of Mancos Shale in this area is mostly restricted to the lowlands (e.g., Grand Valley and the Delta-Montrose area), which suggests that these low-lying semiarid areas are the largest potential contributors to the salinity of the Colorado River. In fact, the Environmental Protection Agency (1971) clearly identified these upper basin areas as being the Price, San Rafael, Dirty Devil, McElmo and Mancos River Basins, including the Grand Valley-Montrose region. In view of the preceding discussion on the simultaneous location of saline outcrops and semi-aridity, the Chaco Wash and Paria River Basins may also be included among the major contributors.

Figure 1.7, derived from Reir and Wadell's (1973) investigations, shows the quality of surface waters in the Upper Basin. It can be noted that the highest salinities are associated with low-lying semiarid areas where extensive outcrops of saline deposits occur. This map is useful in showing large-scale trends in water quality, mostly associated with the Green, Grand and San Juan main stems and their large tributaries. However, it is not useful for a precise delineation of those areas contributing mostly to the salinity of

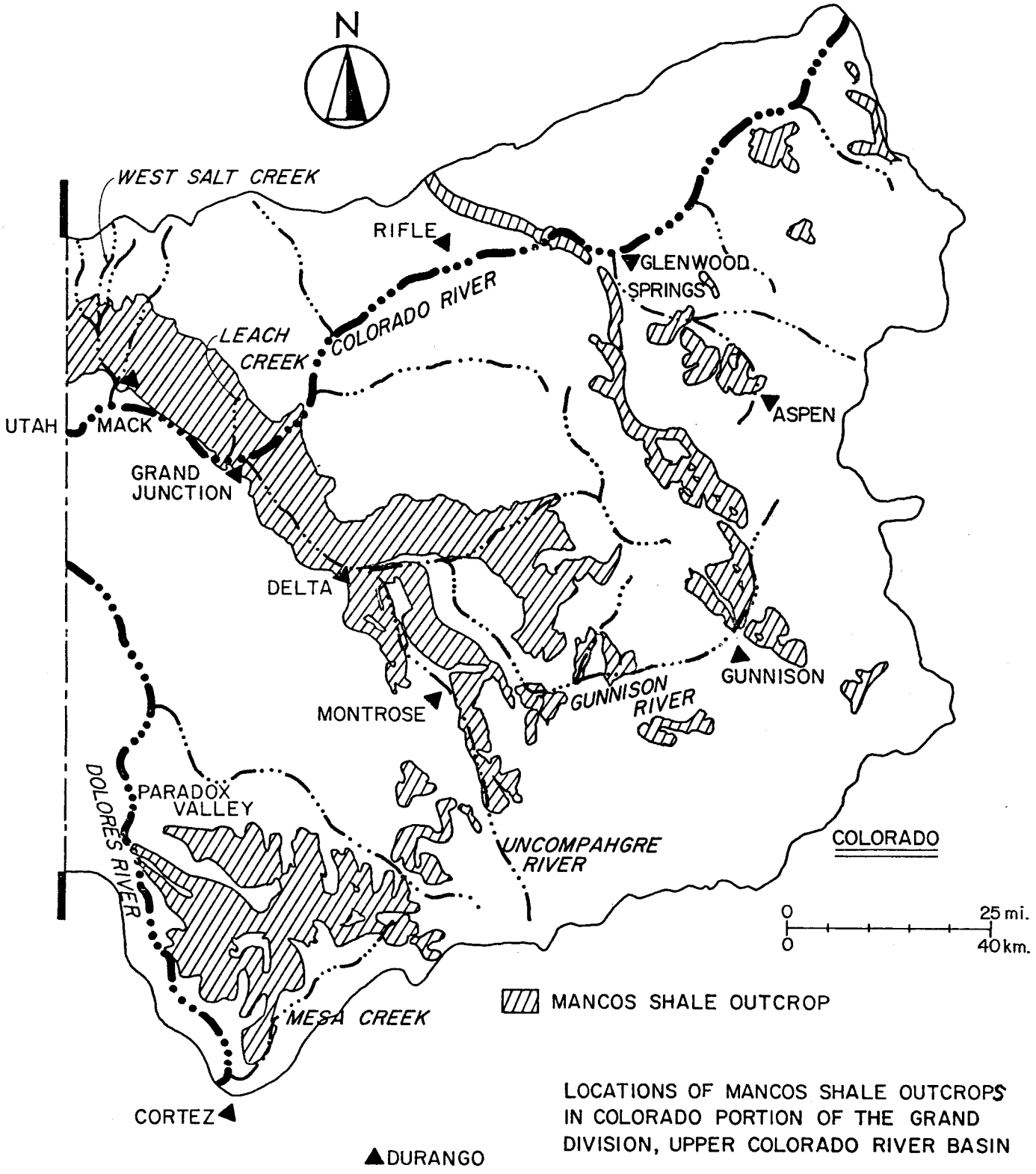

Figure 1.6. Mancos Shale outcrops in the Colorado portion of the Grand River Basin.

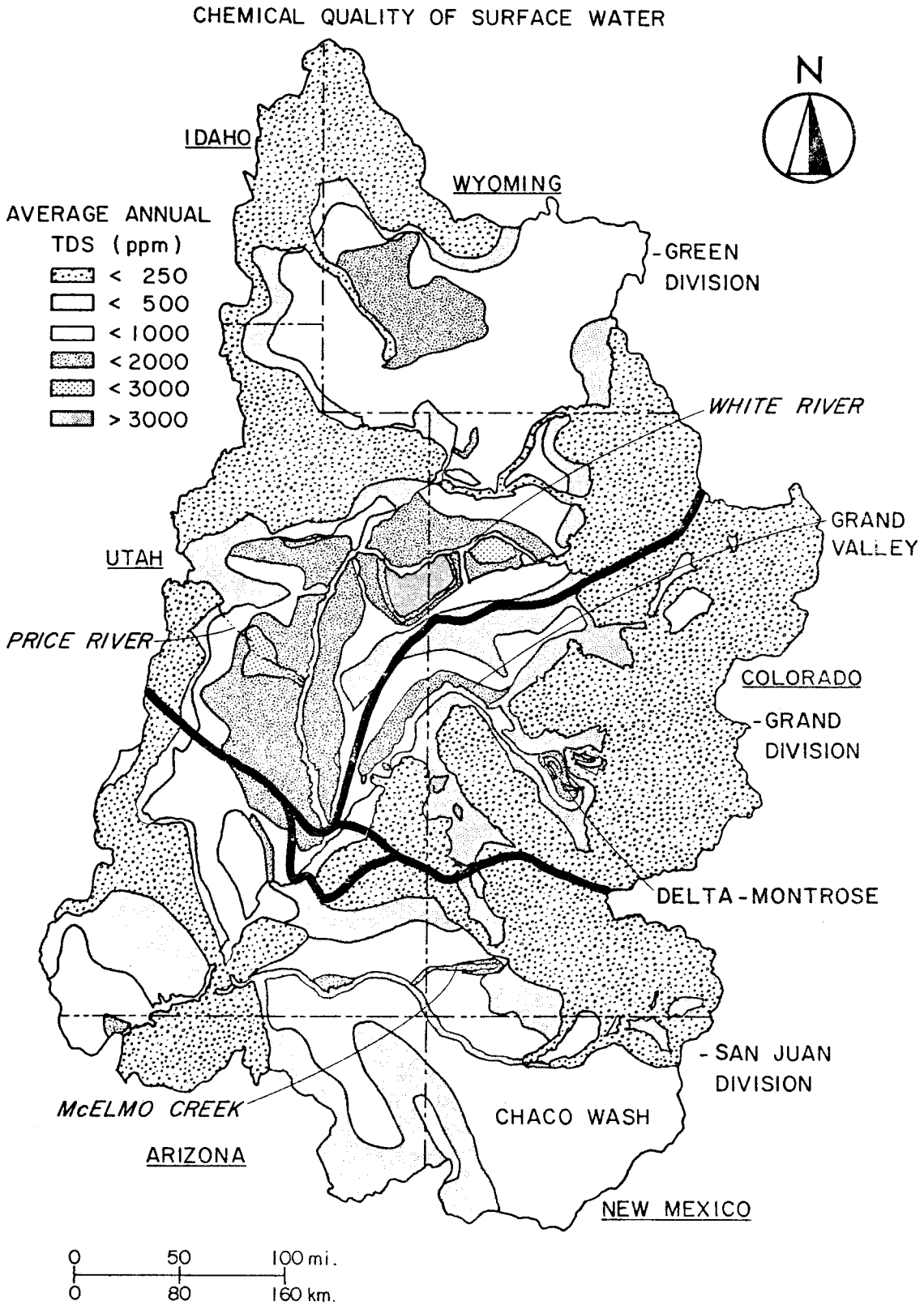

Figure 1.7. Quality of surface water in the Upper Colorado River Basin (after Reir and Wadell, 1973).

the Colorado River. For instance, the central to lower reach of the Dirty Devil River, from Hanksville to Lake Powell, carries low quality water, but the exact delineation of the areas contributing most of the dissolved constitutents is not specified. This generality in assigning a given salinity to a long channel reach and its immediate tributaries may be misleading to government officials whose duty it is to plan the reduction of salt yields from diffuse source areas. It is also very general because the water quality data upon which this and other similar maps (e.g., Iorns, Hembree and Oakland, 1965) are based is very meager. Most of it is derived from samples taken from main stems or main tributary basins (from which little can be concluded about the source areas) or from mountainous watersheds yielding very high quality runoff. Note, for example, that there are only four locations in the Utah section of the Upper Basin (Fig. 1.8) where both chemical quality and sediment discharges are recorded, and all are on large rivers; in addition, there are only nine sections, all in rivers draining more than 100 square miles, for which water quality data is available (for some, this includes merely two analyzed water samples per year). Also, note that all sites where data were obtained on the specific conductance of surface water (Fig. 1-8) are for large rivers or small mountain streams.

Although the identification of major source areas of salts is not sufficient to delineate potential salinity hazard areas, it is interesting to note that the watersheds within the Upper Basin with high sediment yields occupy the terrain of the major source areas of salts. This areal correspondence may point to a causal relationship between sediment transport and solute pickup.

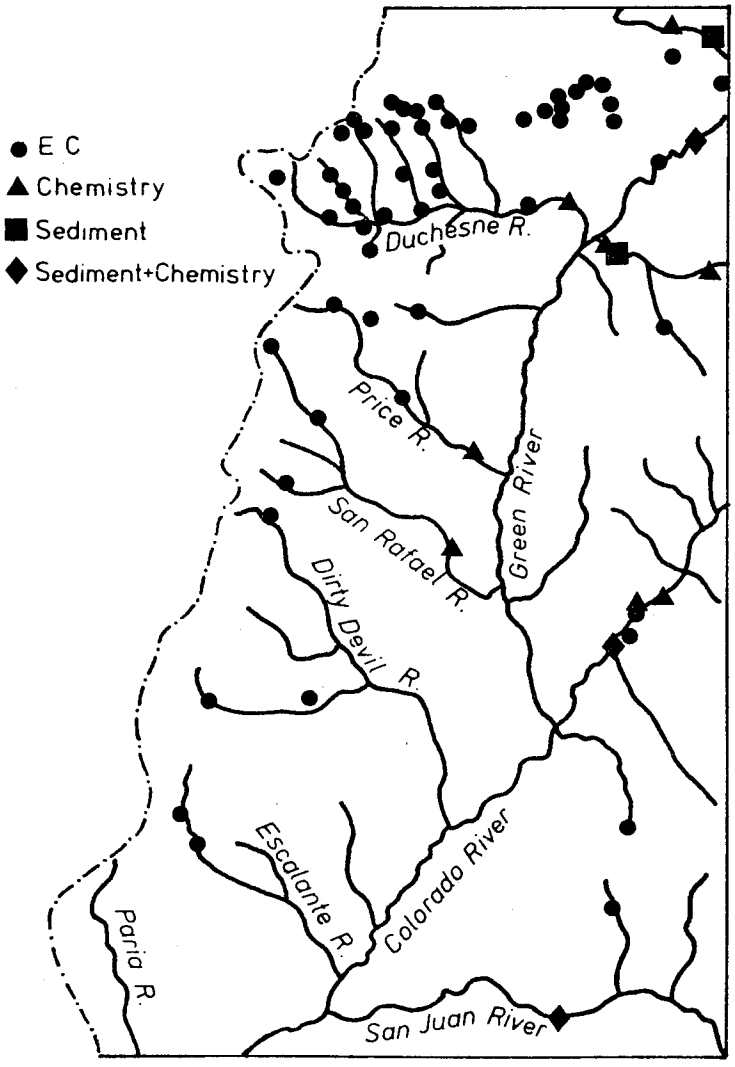

Figure 1.8. Map of the Utah section of the Upper Colorado River Basin showing location of water sampling stations.

1-4. The Research Team

The research project was jointly planned and executed by staff from Colorado State University and the University of California, Davis. These two teams have met at several times every year to closely coordinate efforts. The areas of expertise of the staff include hydraulics and sediment transport, soil physics and chemistry, mineralogy, water quality and geomorphology.

The Colorado State University team had primary responsibility for data collection in addition to planning, site selection, data analysis and the final report for this proposed project. The University of California team has provided support for the chemical, mineral and water quality analyses. They also provided field equipment for on-site filtration of water samples and assistance in field sampling.

1.5 Project Approach.

Following the processes of flow from hillslopes to streams, the investigations were divided into the following steps:

A. Laboratory Investigations (Chaper 2).

(1) Variation of dissolution rate of soluble minerals with flow velocity;

(2) Variation of dissolution rate of soluble minerals with intensity, duration and frequency of rainfall; and

(3) Effect of dilution, agitation and contact time between water and soil on dissolution rate.

B. Field Investigations

(1) Spatial variation of soluble mineral content (herein denoted SMC) and of soluble minerals in the region (Appendix A.1).

(2) Movement of water, sediment and solutes on hillslopes. Rill-flow as well as overland flow with raindrop splash were studied (Chapter 3). The prominent effect of rilling on solute yield has prompted the development of a computer simulation of rill pattern development (Appendix A.5).

(3) Mass transfer of sediment and solutes in a medium-sized drainage basin (Chapter 4), at a confluence (Appendix A.6) and in several large tributaries (Appendix A.7).

C. Determination of solute contribution and hazard areas

Based on results obtained from both field and laboratory analyses, estimates of solute contribution from diffuse sources and of general hazard regions in the Upper Colorado River Basin are given in Chapters 5 and 6, respectively.

CHAPTER 2

LABORATORY INVESTIGATIONS

Three laboratory tests were designed to isolate the effects of velocity, sediment concentration, dilution, exposed surface area, extended contact time and agitation on solute concentration in flow over Mancos Shale. In the first experiment, a specially designed apparatus was used to relate solute concentration to carefully controlled flow rates. The rate of dissolution was observed with standing water, a slow rate of flow (before incipient motion) and at rates which produced sediment transport. These conditions were repeated for weathered and unweathered samples. The unweathered shale was grouped into two sizes.

A second experiment using a simple jar test was conducted to observe the effects of dilution, agitation and contact time on EC values. For the third laboratory experiment, simulation was conducted over a bed of Mancos Shale using artificial rainfall in a tilting flume. Velocity, total solute concentration and total sediment concentration were measured for runoff over weathered Mancos Shale.

Soil description. The Mancos Shale used in all the experiments is from the Grand Valley near Fruita, Colorado. Two layers were removed. The upper weathered portion was approximately five inches deep. The second, unweathered sample of shale was taken from a depth of 5-12 inches below the surface. Table 2.1 lists the characteristics of the shale.

The shale samples were greatly disturbed in the removal process and in placement for the experiments. The shale was wet when removed from the field. It was dried before storage.

Table 2.1. Analysis of Mancos Shale samples used for laboratory tests

Saturation Extract - Not Corrected for Percent Moisture
(meq/l)

	Percent Moisture	EC (μmho/cm @ 25°C)	ph	Sand	Silt	Clay
				---Percent----		
Weathered	36	5667	7.65	19	52	29
Unweathered	33	13421	8.23	38	36	26

	Na	Ca	Mg	K	Cation Total
Weathered	27.10	27.00	27.00	1.00	82.10
Unweathered	128.00	18.00	29.00	1.00	176.00

	HCO_3	Cl	SO_4	Anion Total
Weathered	1.88	1.13	78.00	81.01
Unweathered	1.25	1.35	172.50	175.10

2.1 Experimental Measurement of Salt Pick-up at Varying Flow Rates (In a Cylinder)

The purpose of this experiment was to relate solute concentration to carefully controlled flow rates. The rate of dissolution was observed with standing water, a slow rate of flow (before incipient motion) and at rates which produced sediment transport. These conditions were repeated for two samples of Mancos Shale, weathered and unweathered. The unweathered shale was grouped into two sizes, small particles similar to the unweathered material and rock size particles.

2.1.1a Experimental Procedure

The cylinder for this study is shown in Figure 2.1. An electric motor mounted in the hollow inner cylinder produced circular flow

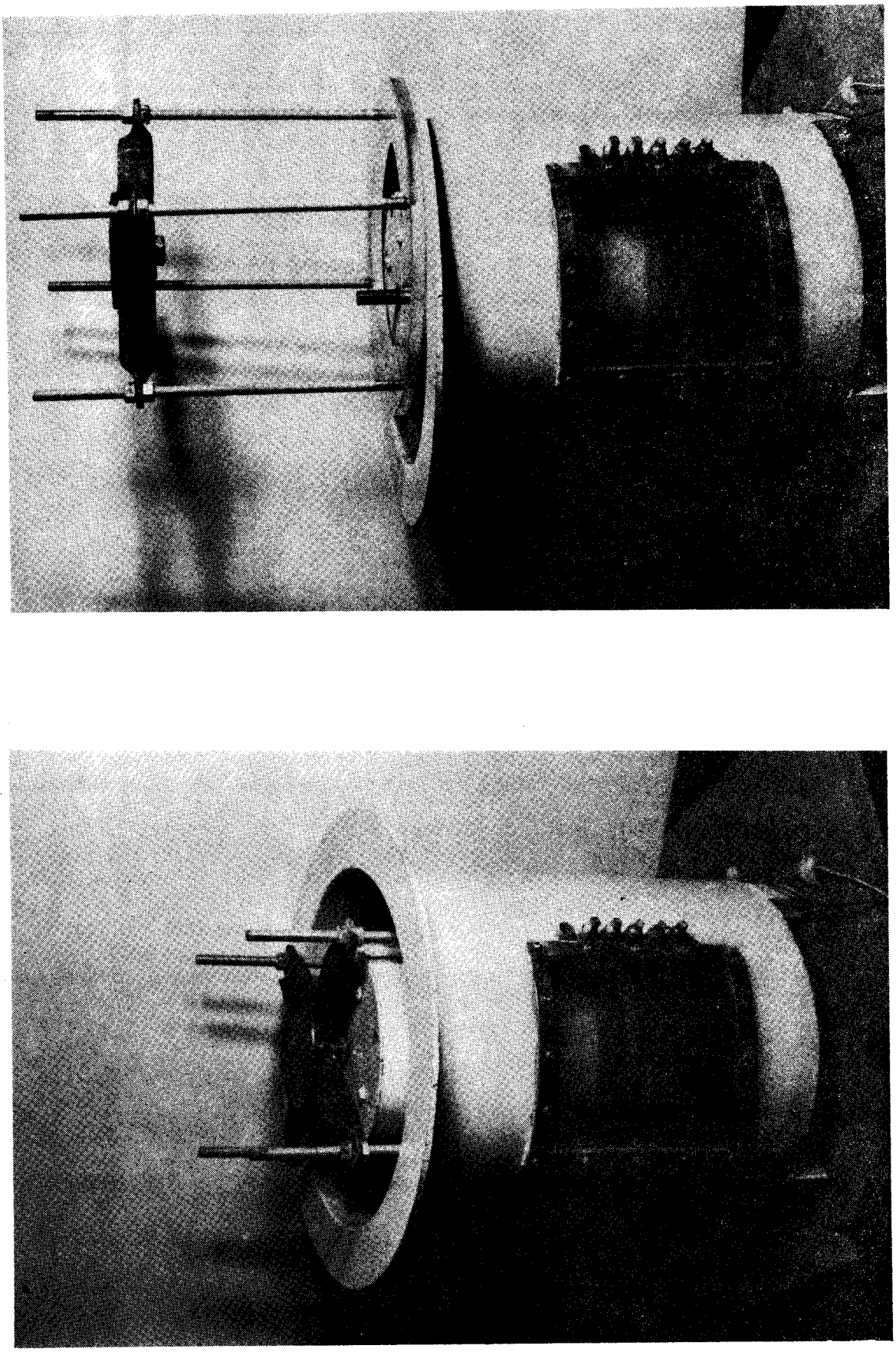

Figure 2.1. Flow cylinder designed to vary flow velocity over Mancos Shale samples.

required to fill the water sample. Timing of each of the runs started when water introduction was complete and the water surface was in contact with the rotating disc.

EC was measured by withdrawing a water sample from the lowest port (just above the bed) at specified time intervals. Samples were taken at 5, 10, 15, 20, 30, 40, 50, 60, 70, 80, 90, 105 and 120 minutes and their temperature was also recorded. They were returned to the flow cylinder by pouring over the disc as in the beginning of the run. The volume required for a measurement was approximately 0.5 liters or about 13% of the total water in the cylinder. Each sample took between thirty and forty-five seconds from the time the sample was removed (and the flow stopped) and returned. Losses during the sampling were generally insignificant. At the completion of the run, the soil surface was changed by as much as 20 mm from the original level. This was mostly the result of water introduction and returning of samples. A separate run (W-4b) with only one sample taken at completion (120 minutes) was done to check this effect. Repeatability was also checked by doing three runs at the same speed (W-3a, b, c). Between each EC sample, the motor speed was measured so that a consistent value could be maintained. The motor was connected to a variable-speed controller for this purpose.

2.1.1c Velocity Measurement

Average velocity for the depth of flow was measured by injecting dye through a port and timing its movement. The window in the side of the flow cylinder was adjacent to the upstream side of the injection point. The dye was viewed just as it completed one revolution.

The velocity dropped off very quickly with distance from the plate. The greatest mass of dye substantially trailed the leading edge which was just below the plate. This large mass was assumed to be representative of the average velocity.

Measurements were made with varying disc speeds. Measurements at medium speeds (30-60 rpm) were most accurate. At high speeds, the dye moved across the viewing window too quickly for accurate timing. At low speeds the dye diffused and clouded the viewing window before the leading edge could be detected.

It was assumed that the velocity of flow over the small size range of unweathered shale would not differ significantly from the velocity of flow over the weathered shale. A curve (Sunday, 1979) was used to determine the average velocity for both the 'U' runs and the 'W' runs. Separate dye measurements were made for the rock bed. The average velocity was slightly lower (0.47 ft/sec, Figure 2.2) than for the small size range of particles (0.50 ft/sec, Figure 2.3). This resulted from the higher roughness in the rock bed.

2.1.1d Calculation of Average EC

The measured EC values were weighted according to the time interval of sampling and averaged.

$$\overline{EC} = \frac{\Sigma(t_j EC_i)}{\Sigma\, t_i} \qquad (3.1)$$

where EC_i denotes the average of the EC values measured at t_{i-1}, and t_i is the time interval of sampling.

2.1.1e Varitation of Parameters

The experimental runs were divided between those using weathered shale (W-1 through W-6) and those using unweathered shale (U-1 through U-3 and R-1 through R-3). In W-1 there was no flow rotation. The water and samples were introduced in the described manner to contrast the runs with water movement over the sample. Next, a very low rate of flow (8 rpm) was used. The repeatability of the results was checked with a still higher rate (17 rpm) on W-3a, b and c. W-4a was sampled in exactly the same way but at 33 rpm. W-4b was run at 33 rpm but with only one sample taken at the end of two hours. This demonstrated the effect of sampling on the results. For the next run, W-5, the rate was increased to 60 rpm which was sufficient for bed motion. W-6 was at 82 rpm.

For the unweathered shale, U-1, U-2 and U-3 runs were performed at 9, 58 and 77 rpm. Bed motion was noted at a higher velocity (77 rpm) than on the weathered samples due to increased particle size.

Runs R-1, R-2 and R-3 also used unweathered shale using coarser material than in the U runs. Rocks with diameters in the range 12.7-76.2mm (0.5-3 inch) were placed in the cylinder as closely packed as possible. These runs were done to contrast the U runs where bed motion was an important factor.

2.1.2 Results

The changes in EC of the water as it was rotated over the various samples of shale are shown in Figures 2.2 through 2.4 and in Table 2.2. All the curves show that EC increases at a decreasing rate. The EC *vs* time curves of Figure 2.2 show that dissolution rate of weathered

Table 2.2 Summary of data for the cylinder experiment.

Run No.	Soil Density (pcf)	Motor Speed (RPM)	Avg. Vel. at top (ft sec^{-1})	Avg. Velocity (ft sec^{-1})	Water Temp (°C)	Avg. EC (μmho/cm @ 25°)	Final EC (at two hours) (μmho/cm @ 25°)
W-1	84	0	0.00		23	460	700
W-2	101	7.1	0.37	0.19	23	660	850
W-3a	85	16.2	0.85	0.43	22	920	1260
W-3b	65	17.5	0.92	0.46	21	950	1260
W-3c	83	17.7	0.93	0.47	23	1040	1500
W-4a	77	32.9	1.70	0.85	19	1030	1480
W-4b	87	33.4	1.75	0.88	20	Uninterrupted flow	1360
W-5	78	59.8	3.13	1.57	22	1570	2100
W-6		82.0	4.10	2.05	21	1760	2310
U-1	82	8.7	0.46	.23	20	1660	2400
U-2	89	58.6	3.07	1.54	24	2850	3820
U-3	87	77.0	4.03	2.02	18	3870	4080
R-1	63	45.4	2.27	1.07	22	1100	1460
R-2	56	79.8	3.99	1.88	21	1240	1540
R-3	63	103.6	5.18	2.43	21	1650	2220

Weathered Shale W-1 through W-6; Unweathered shale U-1 through U-3 (small size) and R-1 through R-3 (larger size)

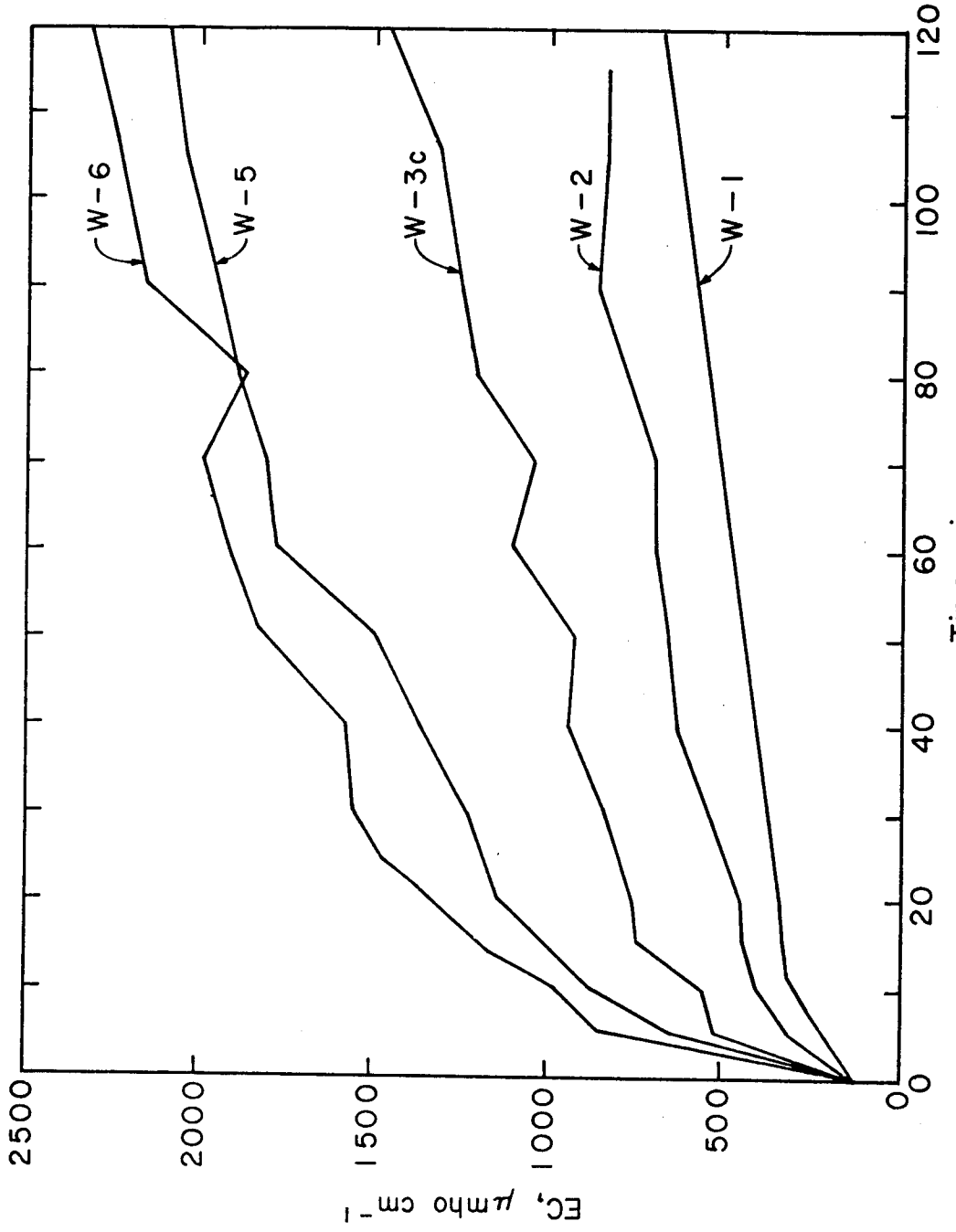

Figure 2.2. Temporal variation of EC for weathered Mancos Shale samples in cylinder experiment. See text for details.

shale increases with increase in velocity of flow. The same trend holds for unweathered crushed shale (Figure 2.3) and for unweathered shale rocks (Figure 2.4). These curves also demonstrate that the unweathered shale is richer in soluble minerals and that dissolution rate decreases with increase in size of dissolving mineral particles. The large impact of particle size on dissolution rate is demonstrated in Figure 2.5. Note that the unweathered large particles of shale dissolve slower than the finer weathered shale, although SMC is higher in the former.

2.1.3 Analysis of Results

Rate of dissolution is controlled by the solute concentration gradient between the bulk solution (the main body of flowing water) and the region near the surface of the dissolving mineral crystal. It is also inversely proportional to the thickness δ of this so-called double-layer. δ decreases as flow velocity increases and, therefore, dissolution rate increased with increase in velocity as depicted in Figures 2.2 - 2.5.

The rate of dissolution is also proportional to the surface area of the dissolving mineral that is in contact with the bulk solution. This surface area is per unit weight or per unit macro-surface area of mineral particles. Dissolution rates were, thus, larger for U runs than for R runs.

The shape of the EC-time curves for the lab experiment can also be explained. For a given run, the exposed surface area and δ are relatively constant. The only factor which affects the dissolution rate is the diffusion gradient between the δ layer and the rest of

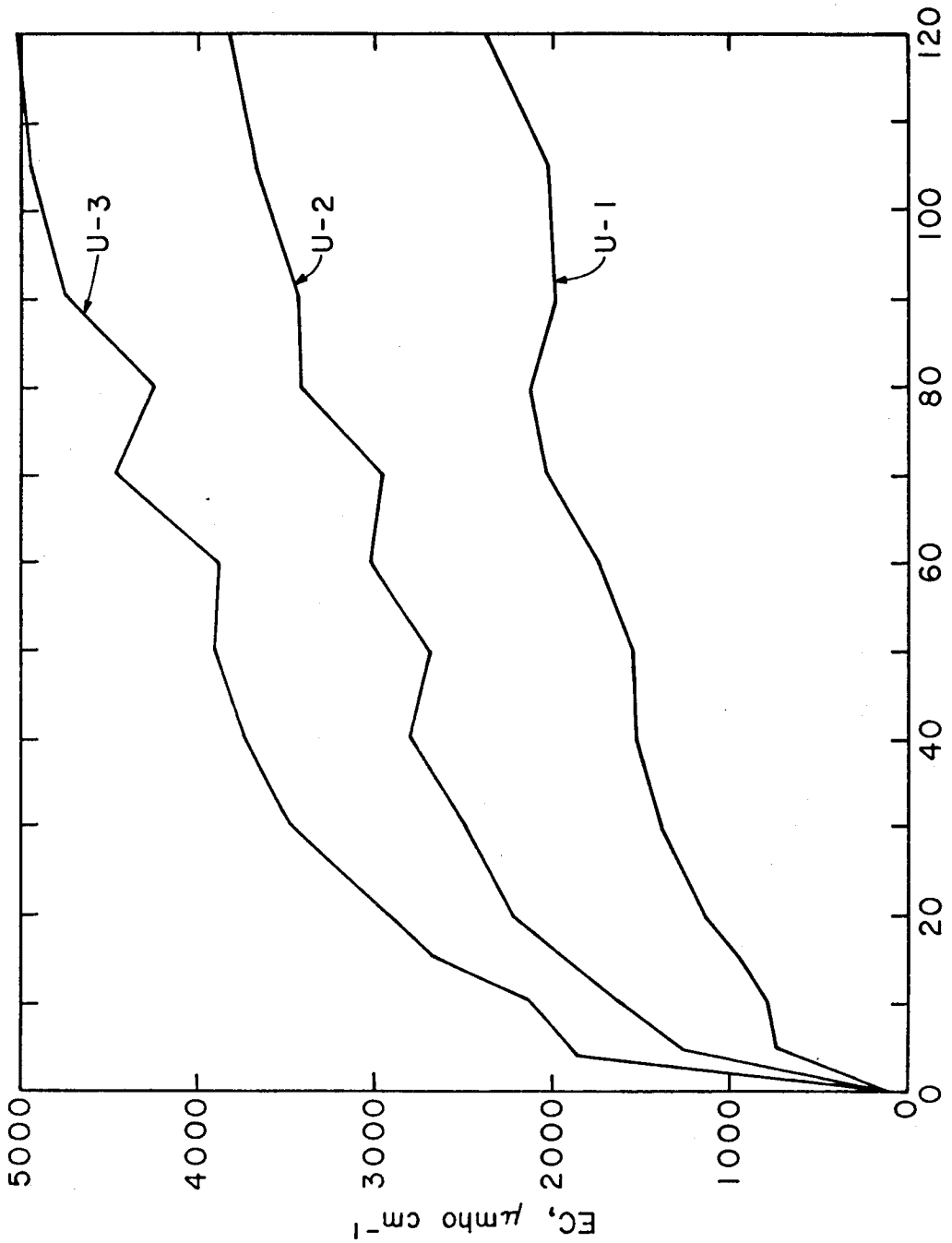

Figure 2.3. Temporal variation of EC for unweathered Mancos Shale samples in cylinder experiment. See text for details.

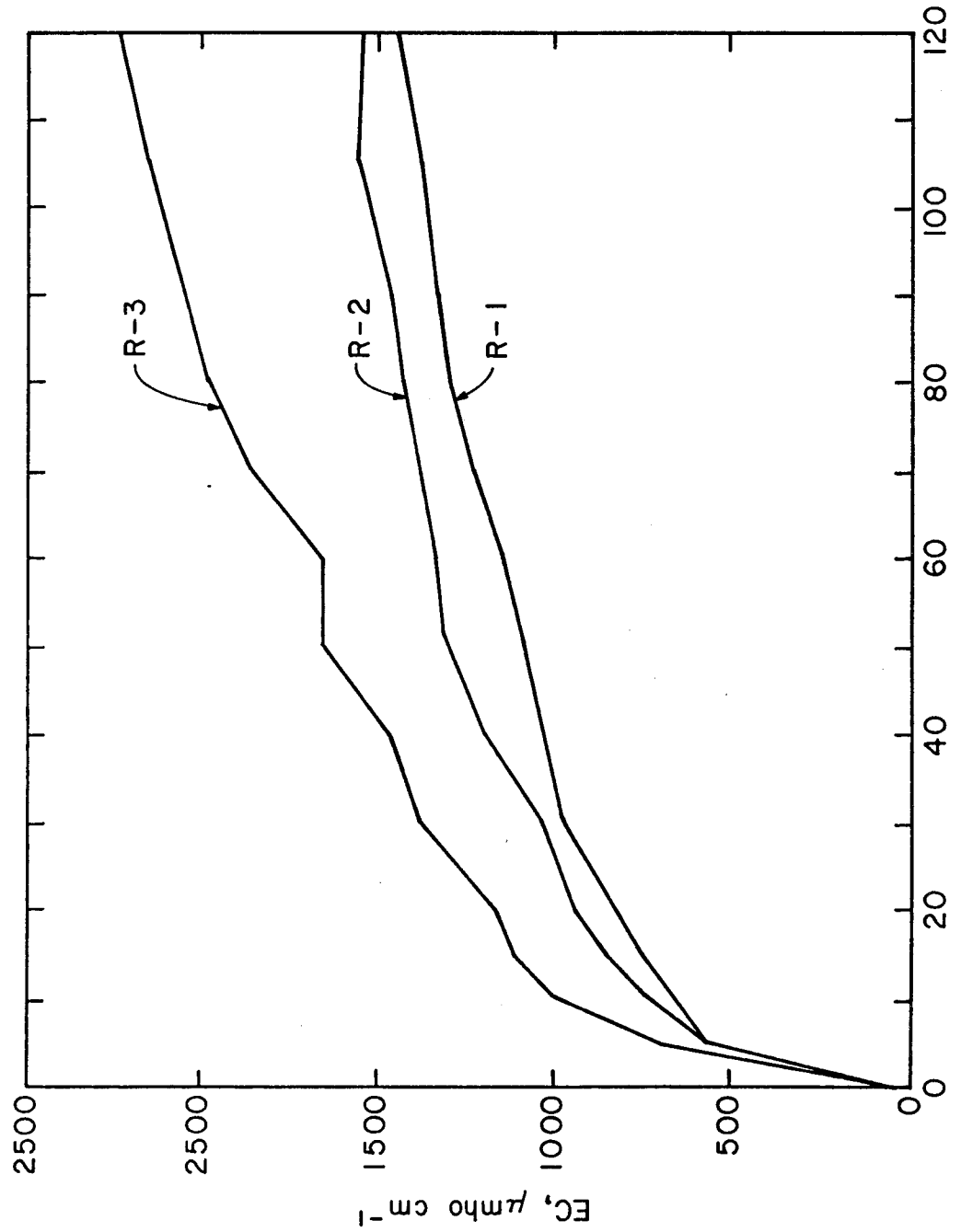

Figure 2.4. Temporal variation of EC for unweathered rocks of Mancos Shale in cylinder experiment. See text for details.

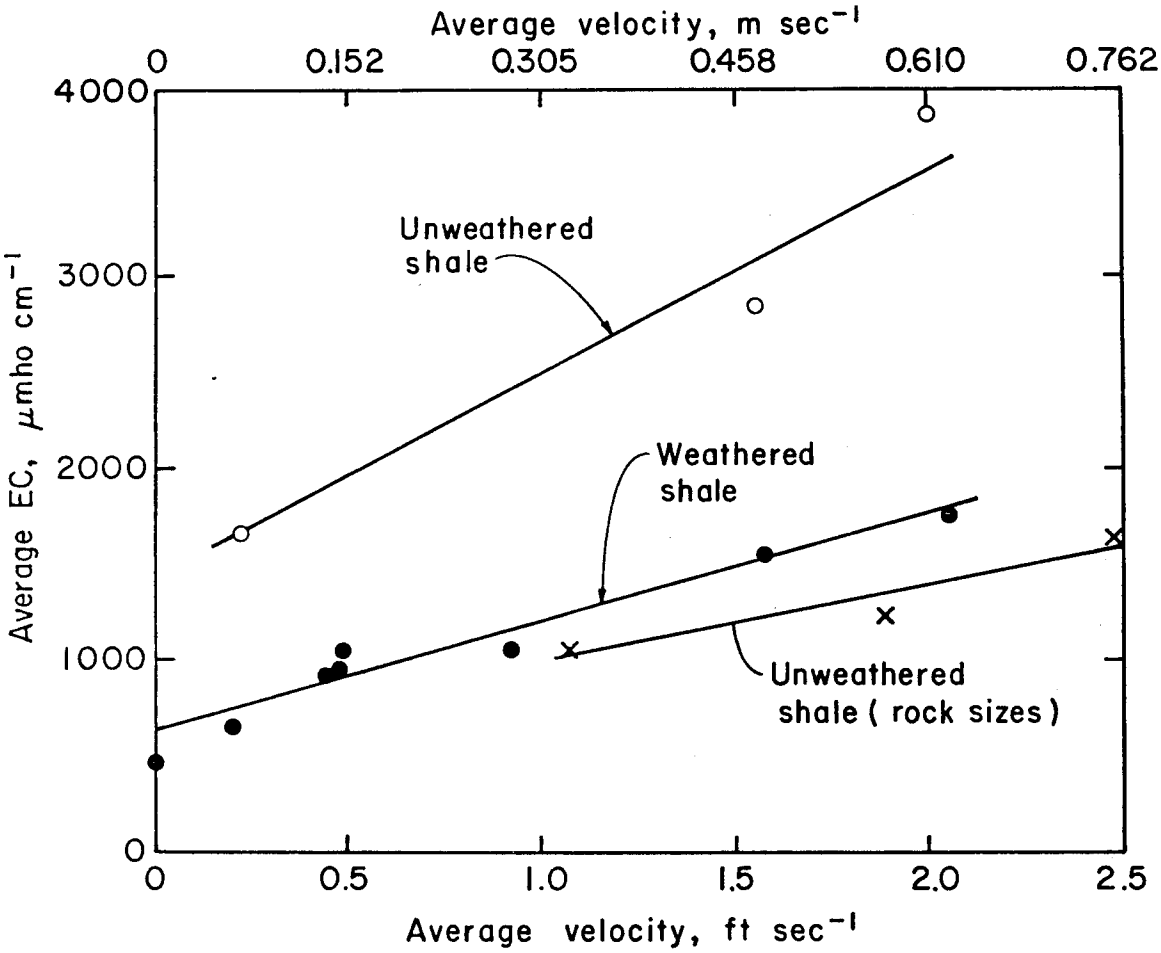

Figure 2.5. Variation of average EC with flow velocity for the cylinder experiments.

the solution. As the flow becomes increasingly saline, this gradient will decrease, causing a corresponding decrease in dissolution rate. In general, one-half the final value of flow EC (reached after two hours contact with the shale) was obtained prior to twenty minutes. The diffusion gradient explanation suggests that the lower velocities would reach the same equilibrium value in a longer time period than the high velocity flows.

2.2 Dissolution Changes with Agitation and Dilution

2.2.1 Procedure

A jar test using varying concentrations of Mancos Shale in water was designed to demonstrate the effects of agitation and extended contact time between water and sediment on solute concentration. Each sample of shale was exposed to three water samples of high quality to demonstrate the effect of dilution on high solute concentrations.

For jar test number one, 100 g of weathered Mancos Shale were added to 2000 ml of good quality water and agitated for 30 seconds. Measurements of EC were taken at 2, 4, 8, 12 minutes, 5 hours, and 43 hours after the agitation. The mixture was reagitated and sampled at one minute and 24 hours. This agitation cycle was repeated until the EC was not significantly increased by the agitation. At this point, 1500 ml of water in the mixture was replaced with 1500 ml of fresh water. Agitation and sampling were repeated until there were no increases in EC measured in the water-sediment mixture. A third

change in water was sampled in the same manner. The entire procedure was repeated twice using 250g and 500g of weathered Mancos Shale for jar tests two and three. The sampling intervals varied according to the changes in EC. Temperatures were recorded for all samples. EC of the fresh water was less than 10 μmho/cm at 25°C. The results are summarized in Figures 2.6 through 2.8.

2.2.2 Results and Discussion

EC increased with time as a step function with agitation; it increased immediately after agitation for the first three to four minutes. The EC of the sample then remained nearly constant until reagitated. The increases were most significant in the dilute solutions.

Replacing part of the high concentration water with clean water significantly reduced the initial EC of the sample. However, agitation increased the EC in the water more than in the original sample. Most of the second and third water samples approached the high EC levels of the initial sample with continued agitation. This suggests that the plateau level of EC attained by the runoff in hillslope studies represents incomplete dissolution (see Chapter 3). Mixing high concentration runoff with more dilute flow would most likely result in continued leaching of salt from the sediment. This substantiates results demonstrated by Laronne (1977) where dissolution of sediment was found to be more complete as sediment concentration decreased.

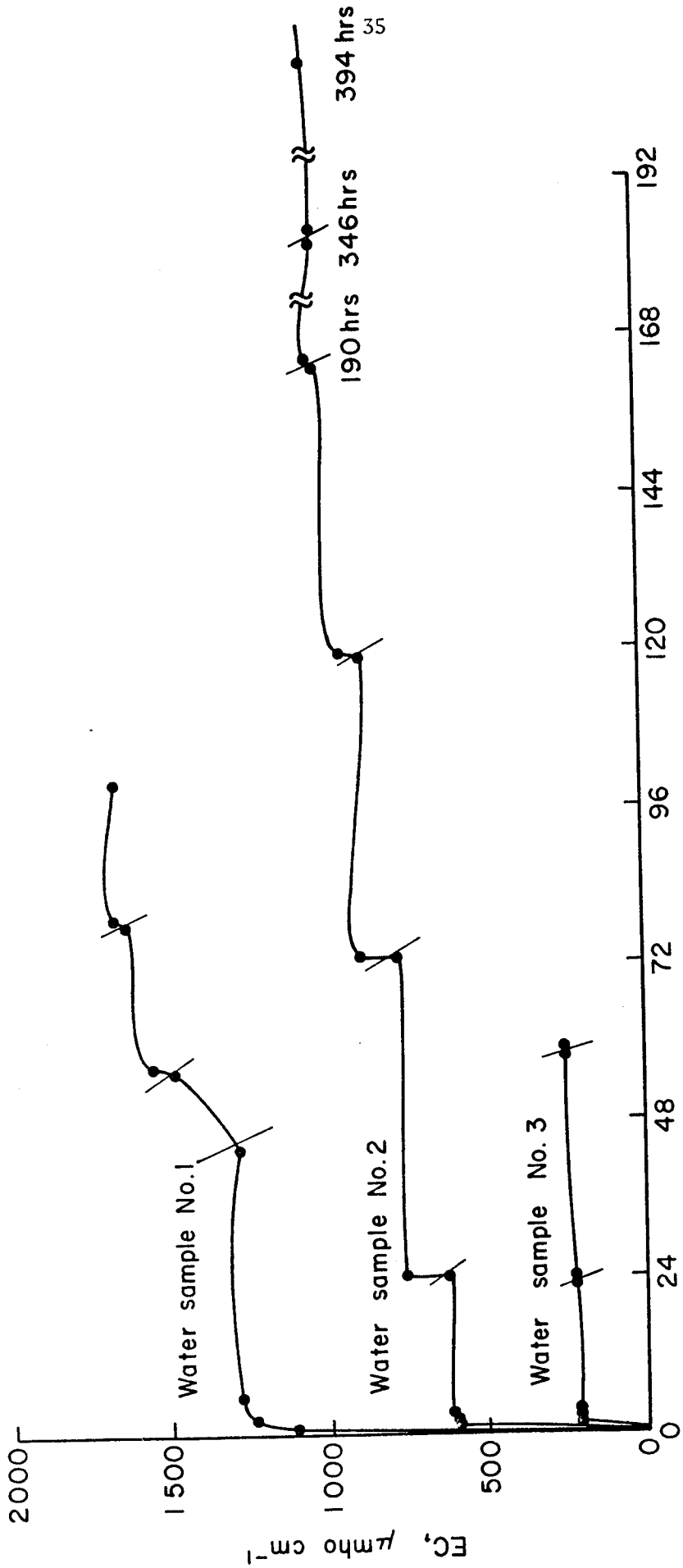

Figure 2.6. EC *vs* time at a 1:20 sediment/water ratio; jar no. 1.

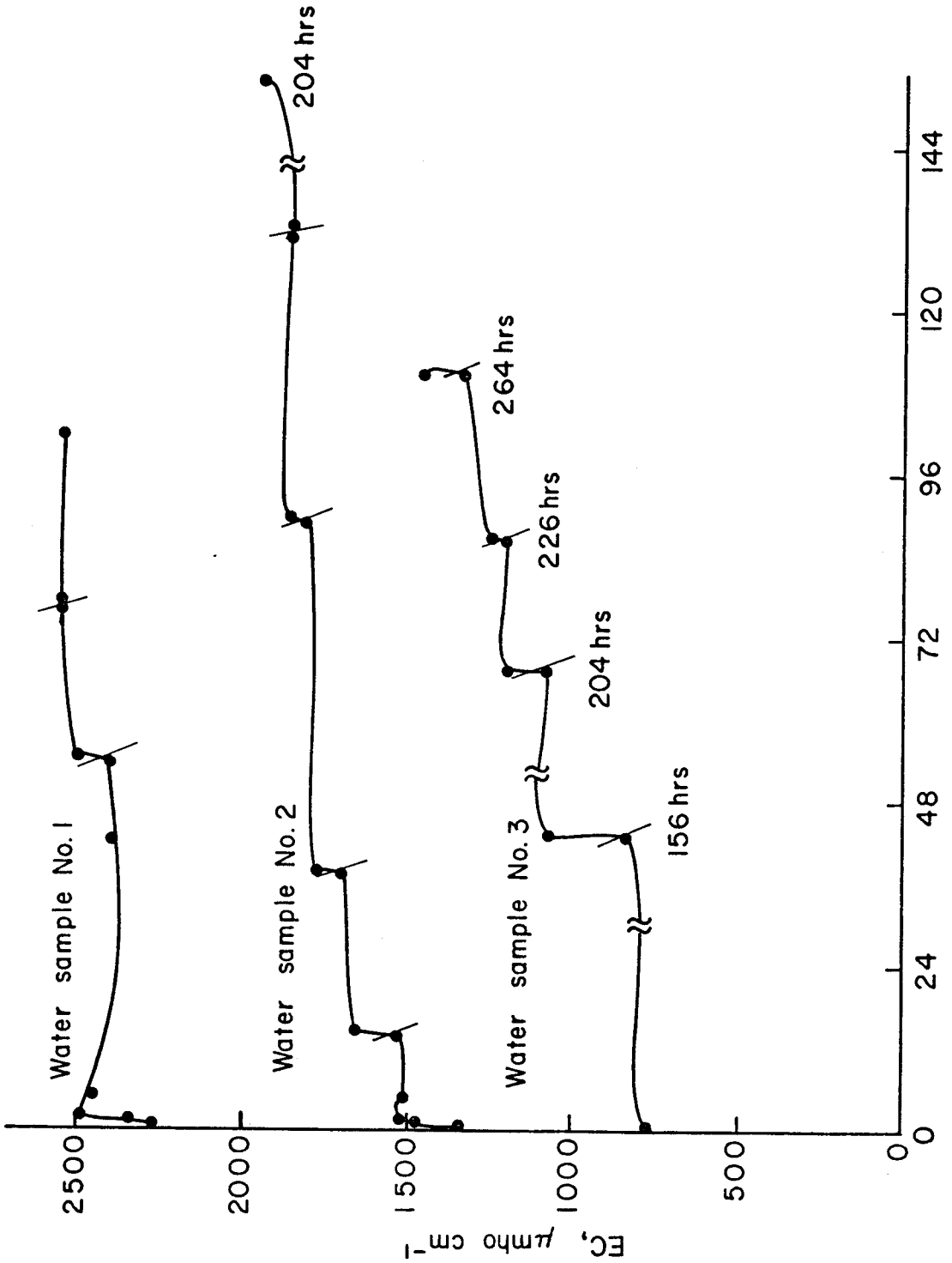

Figure 2.7. EC *vs* time at a 1:8 sediment/water ratio, jar test no. 2.

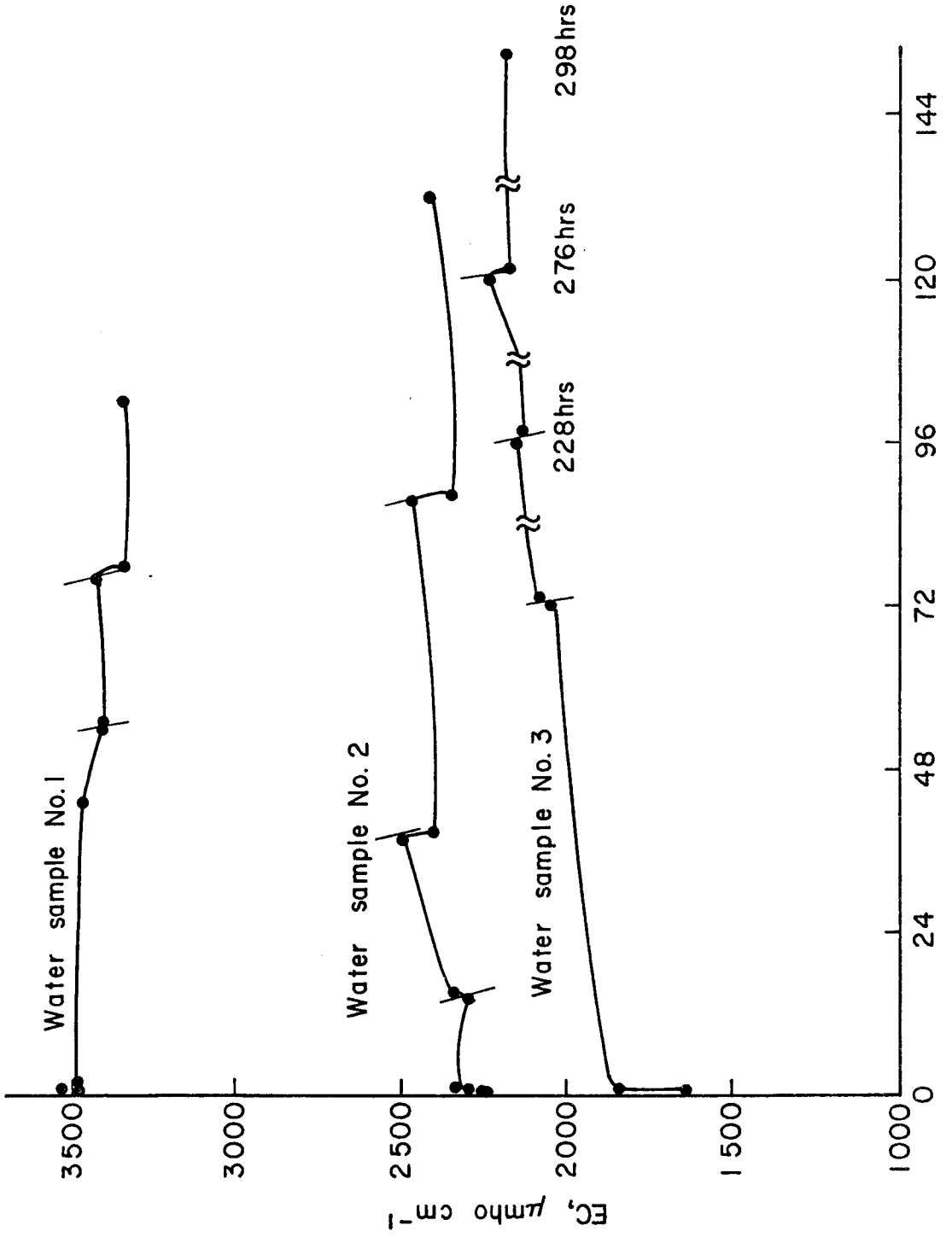

Figure 2.8. EC *vs* time at a 1:4 sediment/water ratio, jar test no. 3.

2.3 Simulation of Direct Runoff and Rainfall-Induced Runoff

Runoff over Mancos Shale from simulated rainfall in a flume with an adjustable slope was measured to determine changes in EC in the flow at three locations upslope of the outlet. The effect of initial soil conditions on salt pick-up, and the relationship between total sediment load and EC in the flow were also investigated.

2.3.1 Experimental Facility

The CSU Indoor Rainfall Facility was utilized as the base facility in this laboratory experiment. The rainfall facility consists of a 18.3 x 1.2 m metal and plexiglas flume with 40 plexiglas reservoirs (rainfall modules) suspended 2.82 meters above the floor of the flume. The rainfall modules are 61 x 61 cm, with 576 capillary spaced at 2.5 cm. There are over 23,000 capillary tubes, each with an inside diameter of 0.56 mm and which produce a mean drop diameter of 3.63 mm. The facility has the capability of producing either a uniform or a spatially varied rainfall over a 12.5 x 1.2 m basin with intensities varying from 2.5 cm/hr to 12.7 cm/hr. Slopes can be varied by mechanically altering the slope of the flume between 0 and 3-1/3 percent. The basin consists of a 12.7 cm thick layer of soil placed on the impermeable metal bottom of the flume. A soil suction system keeps the soil from becoming totally saturated during a rainfall event.

For the laboratory simulation in this phase of the study, a masonite flume was laid down the center of the rainfall facility so the actual study area was just 0.305 m wide. The narrower basin was used to conserve soil without drastically reducing slope length.

The soil profile in the laboratory basin consisted of three different soils. The bottom layer on the impervious flume bottom containing the soil suction system was a sandy loam from the area east of Ft. Collins. This layer was approximately 7.6 cm thick. A 2.5 cm layer of fractured unweathered Mancos Shale from the West Salt Creek basin was then packed in. The surface layer consisted of a 2.5 cm layer of weathered Mancos Shale, also from the West Salt Creek basin (see Figure 2.9).

2.3.2 Data Collection and Sampling

The facility is equipped with a critical depth measuring flume and stage recorder which allows for a continuous record of discharge at the end of the experimental area. Due to the constriction of the flow at the measuring flume, this location was used to take water and sediment samples. A vacuum bottle was used to take water samples of the overland flow on the basin without disturbing the bed. Flow velocity measurements were estimated from average travel times of Rhodamine WT dye. The dye was injected in a line source across the 30.5 cm width and the peak concentration was observed as it crossed a cross section some specified distance downflume.

Four separate data collection runs were made with this laboratory set-up.

2.3.2a Storm 1

Storm 1, on a 6.4m long 3-1/3 percent slope, occurred on a surface layer that was initially dry with a powdery consistency. A steady

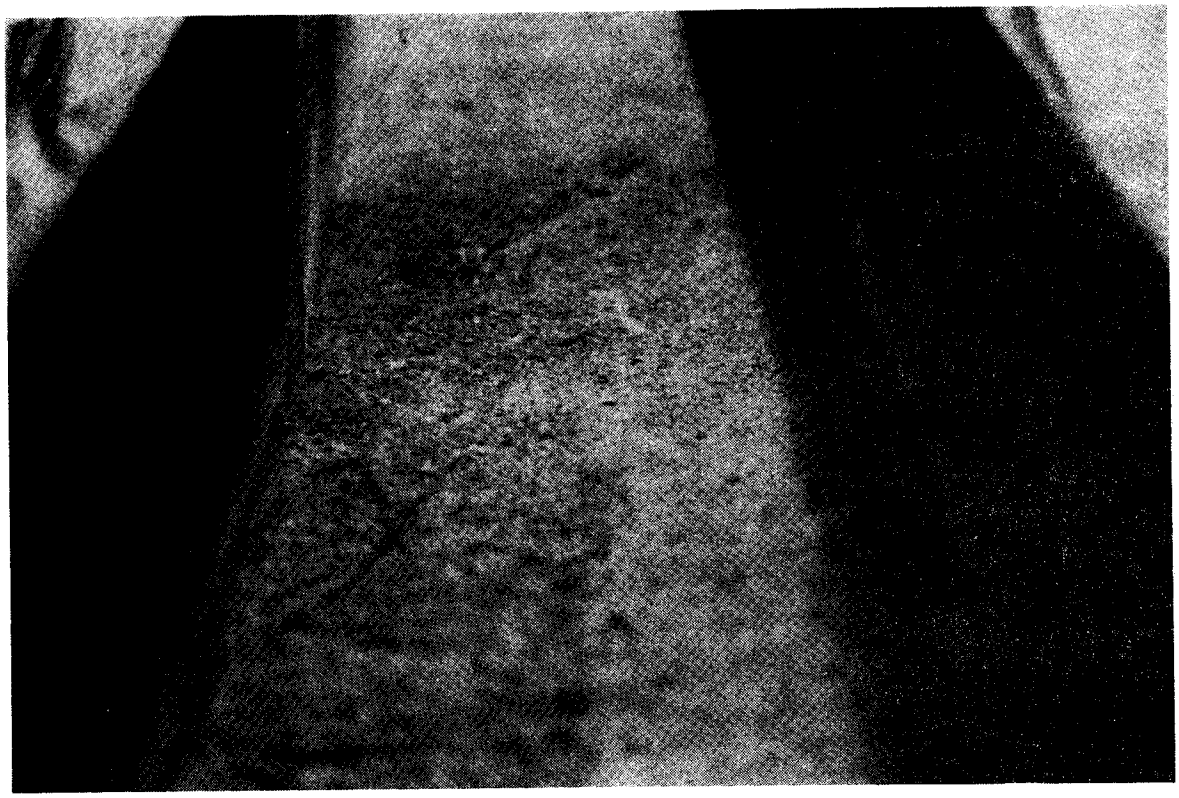

Figure 2.9. Initial Mancos Shale soil condition for storm 1.

Figure 2.10. Initial Mancos Shale soil condition for storm 3 and baseflow 1.

rainfall intensity of 12.4 cm/hr was applied for 70 minutes. Water quality samples were taken 2.1 m and 4.3 m from the top of the basin and at the end of the flume. Water discharge was also recorded.

2.3.2b Storm 2

This storm was generated on the same basin as Storm 1, 12 hours after drying. The soil surface was still wet and had a very sticky consistency. Steady rainfall of 13.1 cm/hr was applied to the study area for 130 minutes. Water discharge and travel time were also recorded.

2.3.2c Storm 3

Storm 3 took place on a 6.4 m slope at 3-1/3 percent. The surface was prepared with fresh weathered Mancos Shale placed into the flume with a dry and powdery consistency. The shale was then wetted and packed by walking on it. The surface was allowed to dry forming a cracked surface crust (Figure 2.10). The soil surface appeared to be similar to that observed in the West Salt Creek basin and to the Mancos Shale surfaces described by Laronne (1977). Rainfall was applied to the basin for 120 minutes. During this time water quality and sediment samples were taken at the end of the flume. Water quality samples were also taken of the overland flow at 2.1 m and 4.3 m from the top of the basin. Flow velocity data was taken and a continuous record of discharge was kept for this storm.

2.3.2.d Baseflow 1

For this data collection run, water was applied to the top of a

12.5 m slope at 3-1/3 percent. The application was made uniformly across the flume width with a head box. There was no rainfall in this study. The soil surface was prepared in a similar procedure as the soil in Storm 3. The resultant soil surface had the same cracked, crusty appearance as that used in Storm 3. A flow rate of 190.5 cm^3/sec was applied for 200 minutes. Discharge, water quality and sediment samples were collected at the end of the flume while flow velocity data was collected on the basin. Water quality samples were taken at 3.05, 6.10 and 9.14 m from the top of the basin.

2.3.3 Results

Figures 2.11 and 2.12 present the temporal variation of EC with distance downslope for storms 1 and 2. The runoff at the beginning of storm 1 was high in EC, but EC rapidly dropped to a rather unstable value not only for the water quality samples taken at the end of the flume, but also for those taken midslope. An initial high EC with a consistent asymptotic decrease characterized storm 2.

Figure 2.13 presents the EC versus time data for storm 3. The dry crusted surface produced a very high EC value relative to the initial value for storm 1 and 2 after 20 minutes. Once again EC decreased with time and with distance downslope. The compaction and drying of the surfaces only affected the EC in that the initial values were higher and the salt loading stabilized much faster than with a dry powdery initial soil condition.

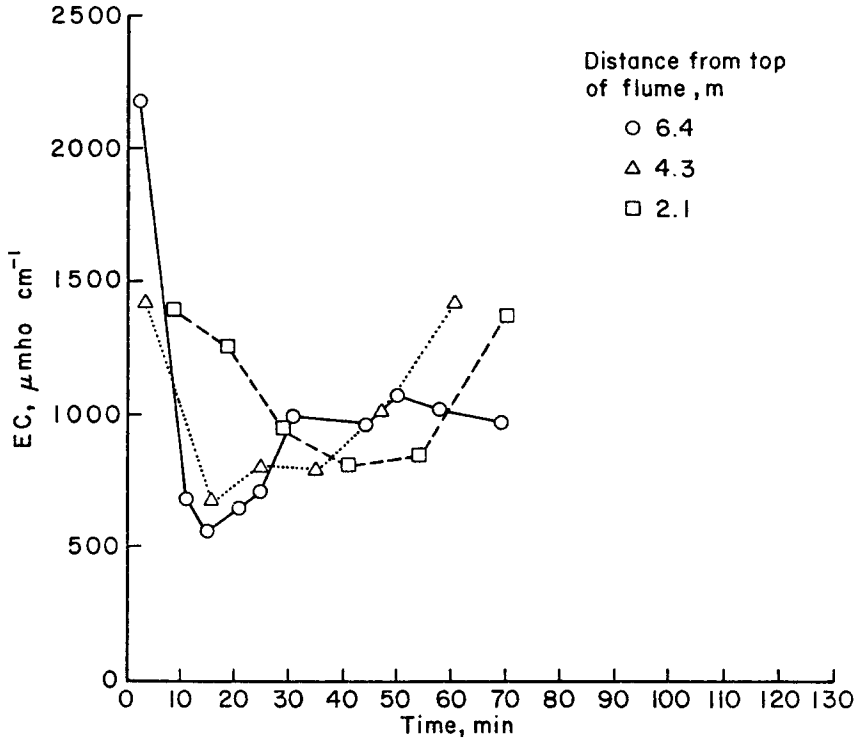

Figure 2.11. Temporal and downflume variation of EC, s torm 1.

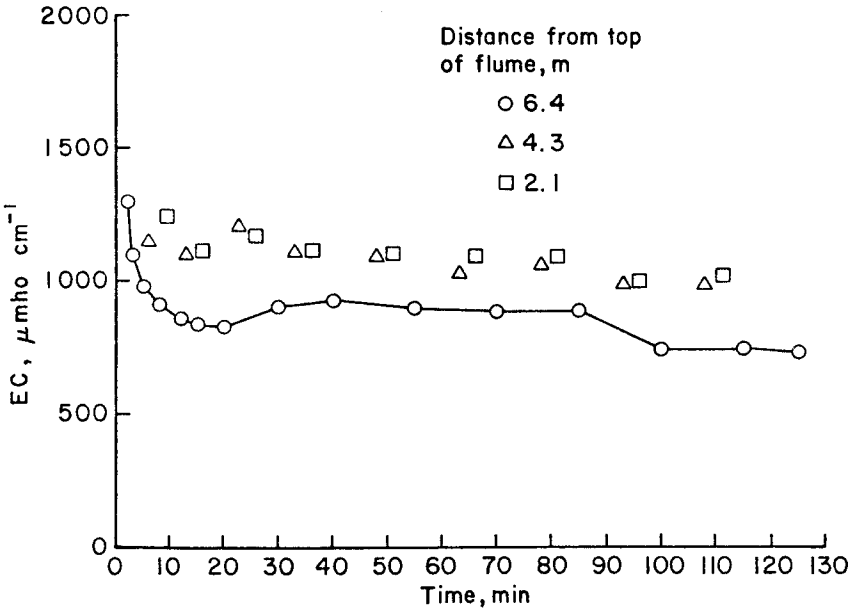

Figure 2.12. Temporal and downflume variation of EC, storm 2.

2.3.4 Analysis of Results

The temporal variation of solute concentration in rainfall-induced runoff (Figures 2.12 and 2.13) follows a general downward asymptotic path: EC is initially high due to the large concentration gradient between the bulk solution and the soil solution; it decreases with time because the soil is leached with a resultant decrease in the above-mentioned concentration gradient. Runoff EC did not appear to decrease asymptotically during run 1 (Figure 2.11), possibly because of induced upflume erosion and concommittant solute release at the head of the flume as the experiment progressed. The general shape of the EC *vs* time curve was, however, maintained in the direct runoff experiment (Figure 2.14).

The downflume increase in EC was maintained during the baseflow run due to 1) a downflume increase in sediment concentration and 2) a downflume increase in contact time between runoff and transported sediment. Runoff EC was highest at the head of the flume during runs 1-3 because erosion of the flume bed was restricted to the upper flume section (compare Figures 2.15 and 2.16) and because the runoff was diluted by rainfall in the central and lower sections of the flume (for further details consult Achterberg, 1981).

The effect of sediment transport on solute concentration is as important as that of contact time. Figure 2.17 depicts the temporal variation of water discharge, EC and sediment concentration during Run 3. Although sediment concentration rose 70 minutes into the run, the general downward asymptotic trend of EC with time may be assigned to the same trend in the concentration of soluble mineral bearing transported sediment.

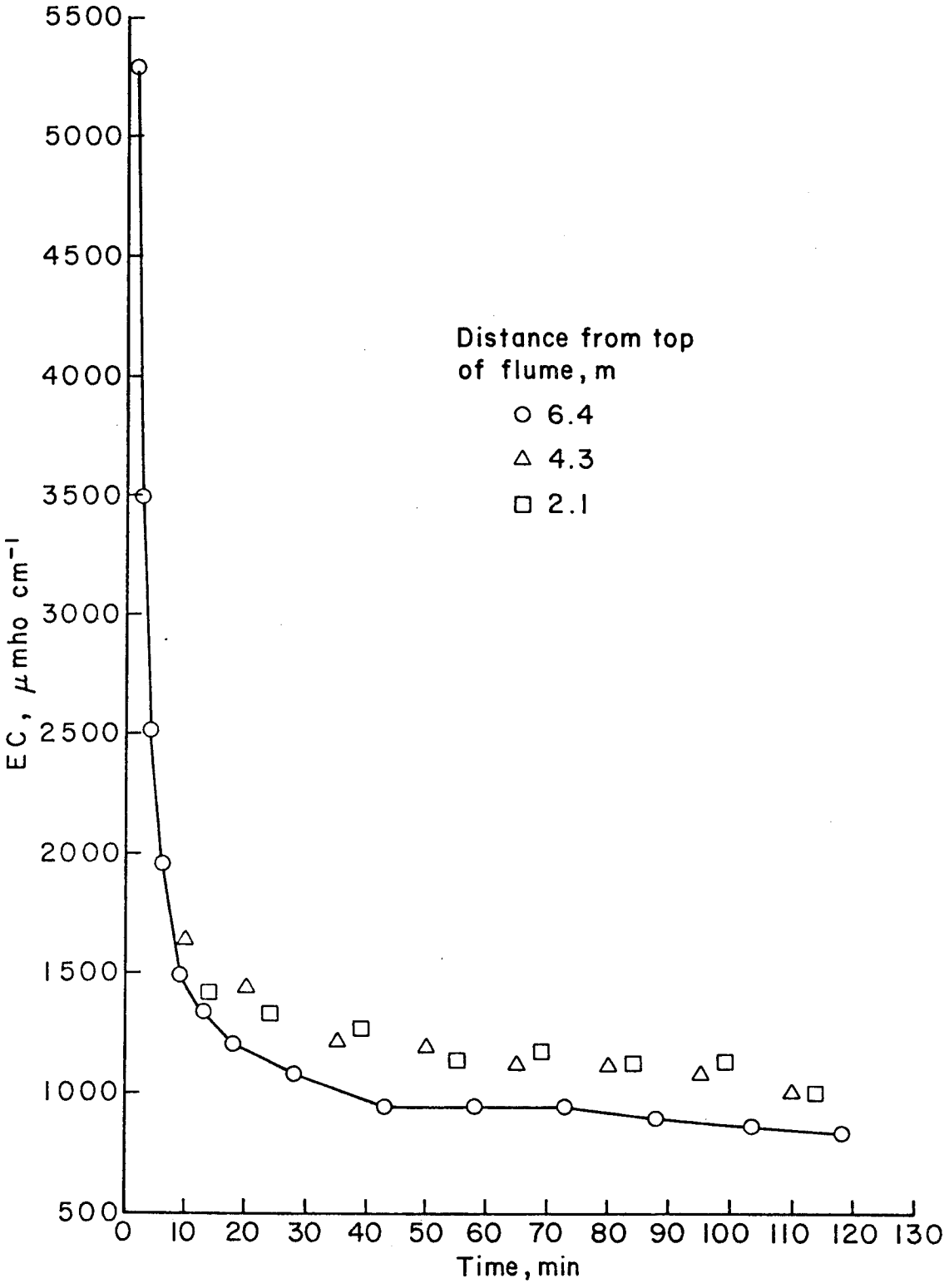

Figure 2.13. Temporal and downflume variation of EC, storm 3.

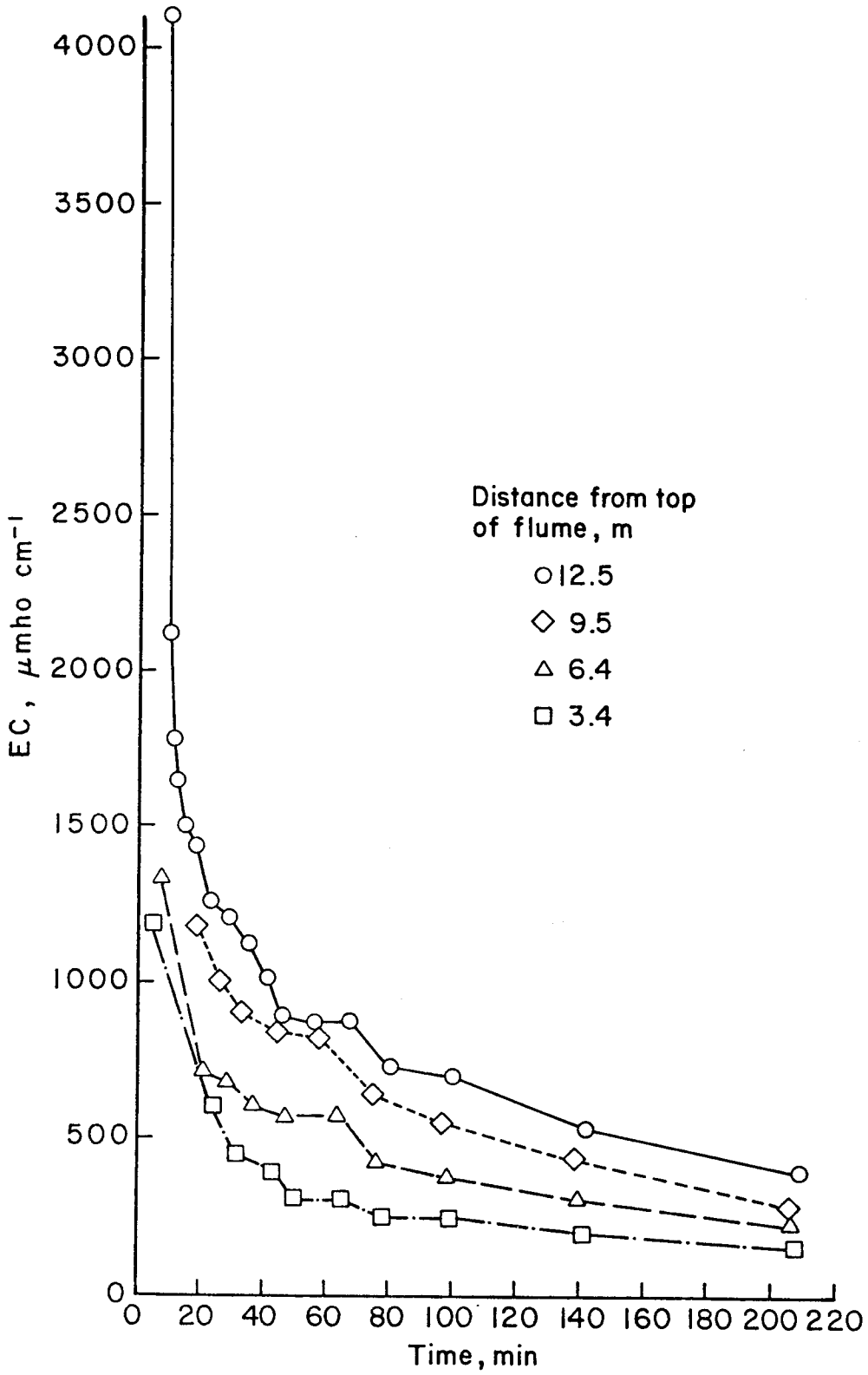

Figure 2.14. Temporal and downflume variation of EC, baseflow 1.

Figure 2.15. Rainfall impact and uniform sheetflow on Mancos Shale early in storm 3.

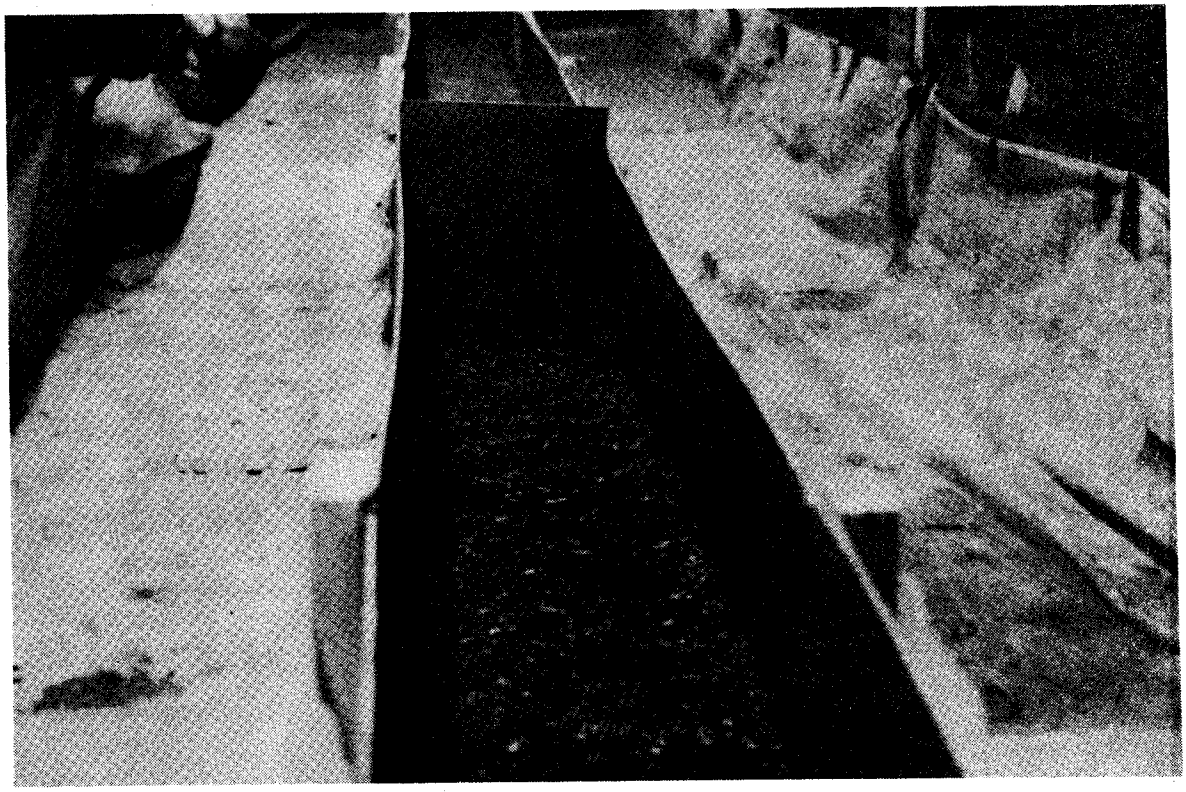

Figure 2.16. Eroded Mancos Shale at the upstream end of the flume for storm 3.

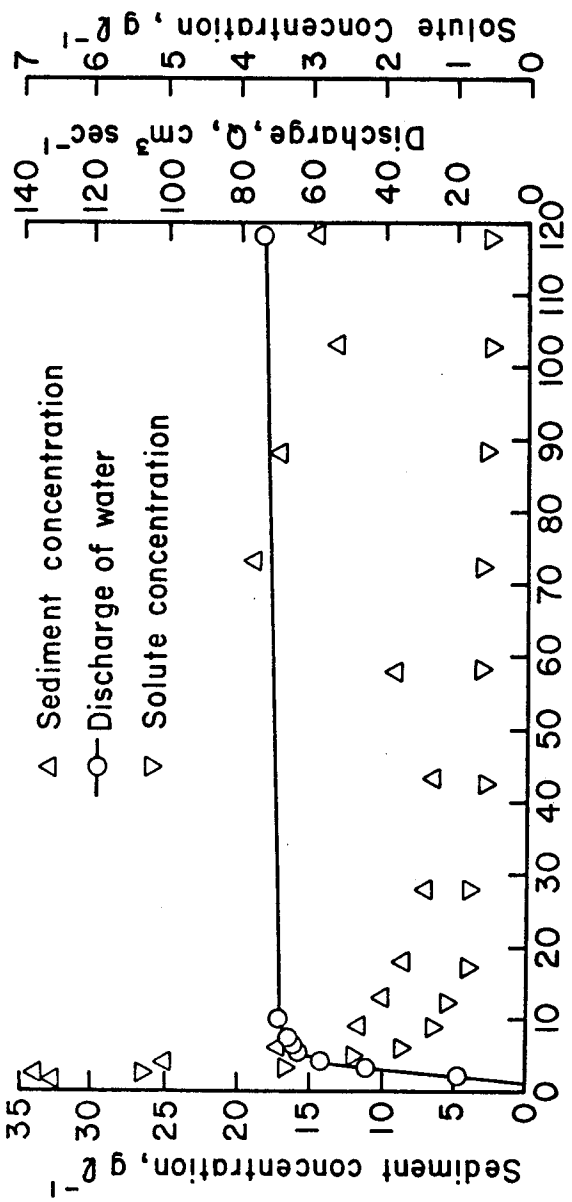

Figure 2.17. Temporal variation of flow discharge, EC and sediment concentration, storm 3.

CHAPTER 3

HILLSLOPE STUDIES

The objective of these studies is to trace salt loading through the movement of sediment and solutes in runoff from hillslopes. Two field studies were conducted in the Grand Valley, Colorado: 1) Application of direct runoff on hillslopes with a perforated pipe, and 2) generation of runoff with an artificial sprinkling system. Measurements were taken and data were analyzed to determine the effects of hillslope angle, types of flow (rills, overland flow, or a combination of both) and duration of flow events on the magnitude and spatial trend of solute yields.

3.1 Experimental Setups, Procedures and Observations

3.1.1 Hillslope Study 1

The first hillslope study (Hillslope Study 1) was conducted during June and July of 1977. The location of the study area is north of the Grand Junction airport, in the Indian and Leach Creek basins (see Figure 3.1). The chosen sites had a typically low vegetation cover and contours that developed into two, well-defined rills near the bottom of the slope. These were used to assess cross-slope variability. Hillslopes ranging from sixteen to seventy-one percent were studied (Figure 3.2). The total length of the runs was in the range 12.2-76m (40-225 ft.). The underlying bedrock material was gray or dark gray Mancos Shale. About half of the areas chosen were covered extensively by calcareous cemented sandstone. The selected hillslopes represent well the variation in slope angle, rill development, vegetation cover and soil crust appearance throughout the outcrop areas of Mancos Shale in the Upper Colorado River Basin (see Table 3.1).

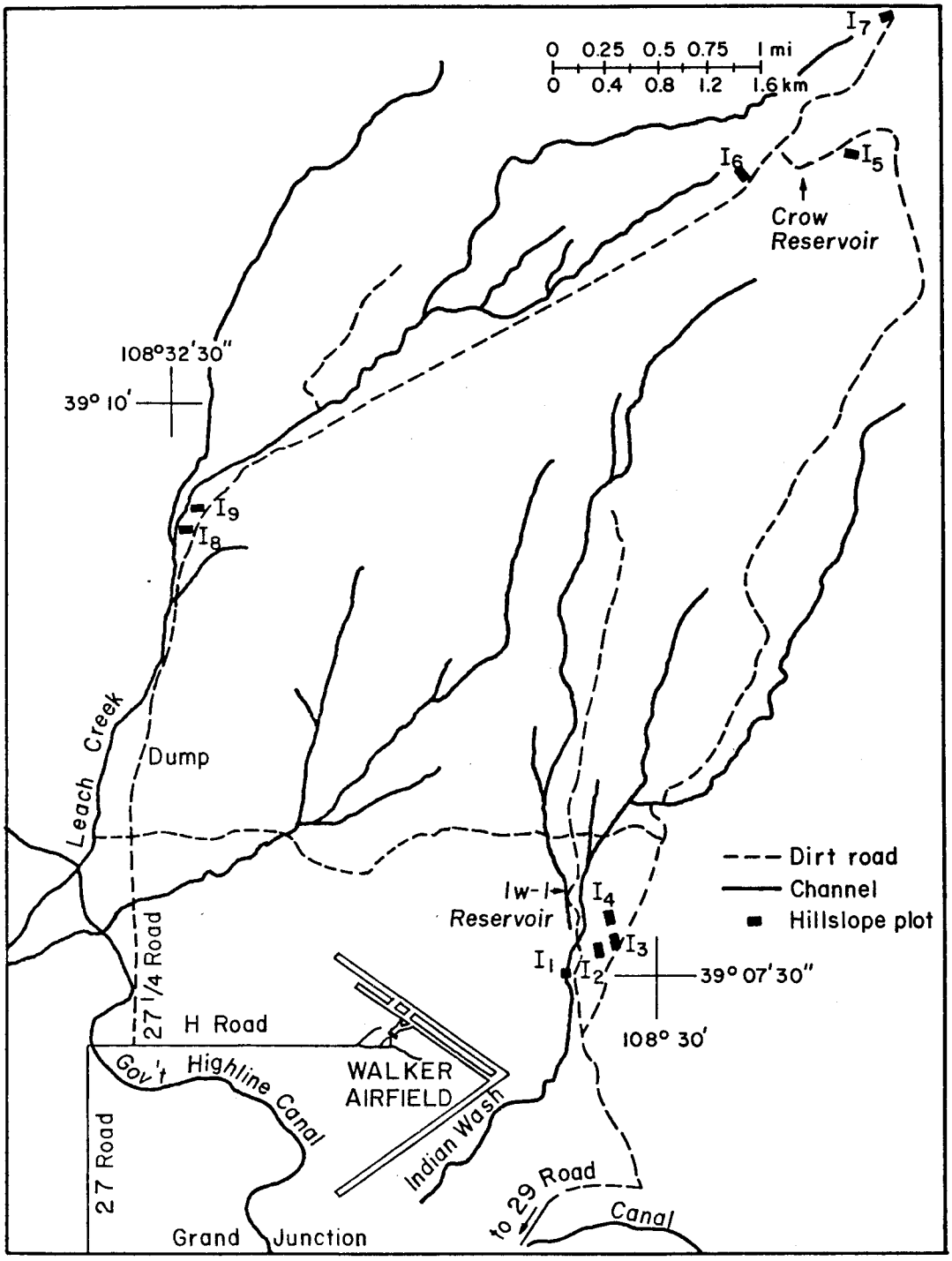

Figure 3.1. Map showing the location of Hillslope Study I sites.

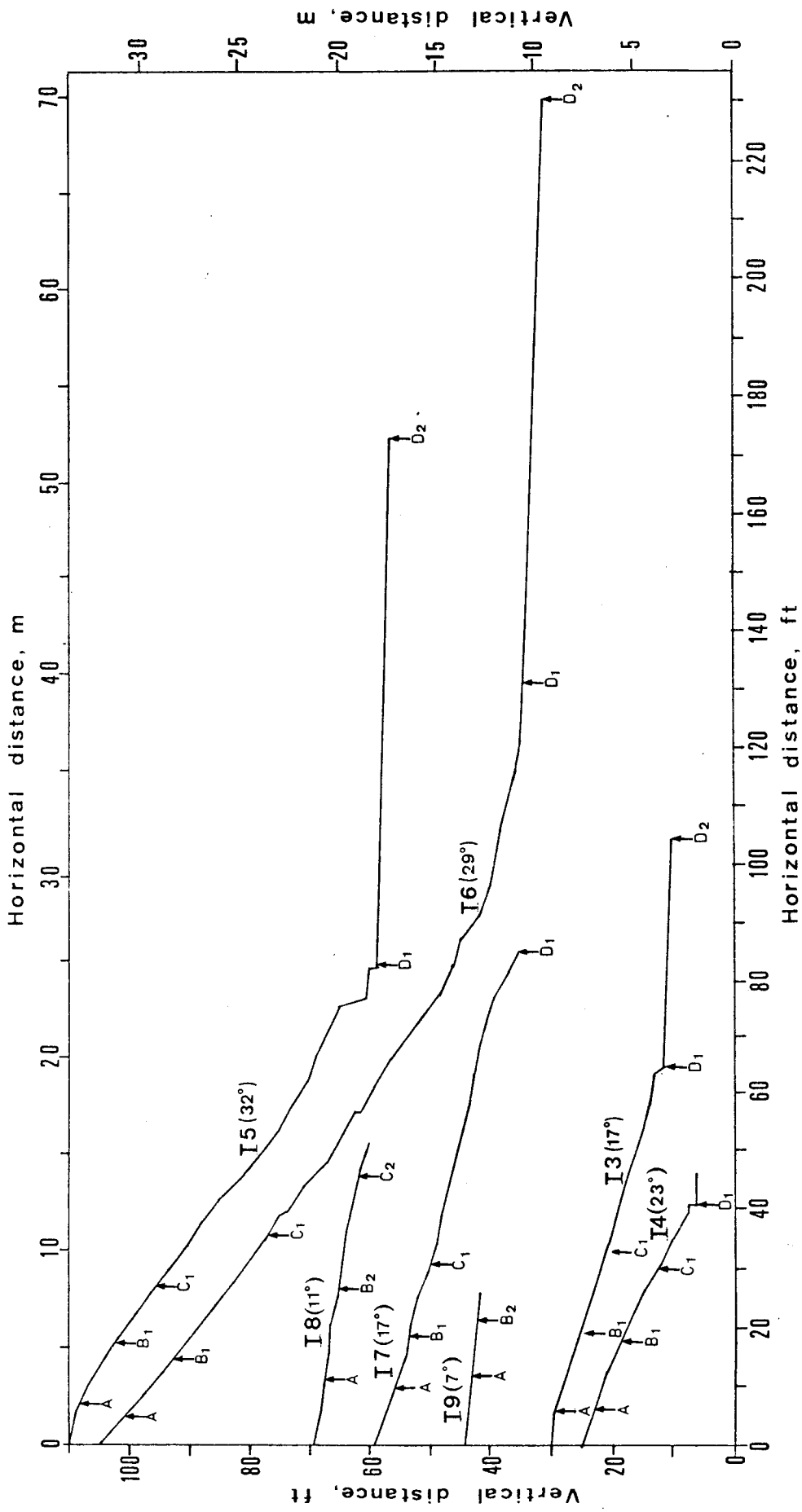

Figure 3.2. Longitudinal profiles of hillslopes showing location of measuring stations, Hillslope Study I.

TABLE 3.1 Generalized Description of Plots, Hillslope Study I

Plot Number	Experiment Date	Underlying Bedrock	Extent of Surface Covered by Calcareous Cemented Sandstone	Inclination From Station A to Station D_1	Hillslope Faces	Disturbance	Remarks
I-3	6/26	gray Mancos Shale	extensively	23°	S	1 off-road vehicle track at bottom	hummocky with few animal (gopher?) holes
I-4	6/26	gray Mancos Shale	extensively	17°	N	ibid at top and at bottom	ibid, more holes
I-5	6/27	dark-gray Mancos Shale	hardly at all	32°	E	undisturbed	two sandy stata rich in gypsum crystals
I-6	6/27	dark-gray Mancos Shale	hardly at all	29°	WSW	undisturbed	several holes between stations C_2 and D_1
I-7	6/28	dark-gray Mancos Shale	somewhat	17°	S	undisturbed	same as above, ~10% vegetative cover, very hummocky
I-8	6/28	gray Mancos Shale	extensively	11°	S	few Cattle footprints	footprints serve as miniature ponds
I-9	6/29	gray Mancos Shale	extensively	7°	WNW	few cattle footprints	footprints serve as miniature ponds

3.1.1a Experimental Set-up

Flow was supplied using a perforated four-inch PVC pipe and a constant head tank. Samples were taken approximately five, fifteen and thirty feet downslope (stations A, B and C, respectively) and also where the end of the slope entered a channel (as well as further down-channel, stations D_1 and D_2). Sampling was continued for up to three hours after the leading edge of the flow reached the sampling station. At the fifteen and thirty foot stations, samples were taken at two locations across the slope. Figure 3.3 shows a typical field set-up used during Hillslope Study 1; exact sample sites for data collection are shown in Figure 3.4. Relatively high quality water, 450 μmho/cm @ 25°C and 100 ppm suspended solids was supplied by a local artesian well service. The water was trucked to the site and fed as necessary into a 30-gallon constant head tank. A single 50.8cm valve was located at the bottom of this tank to regulate the outflow between the tank and outlet device. The outflow then passed through a 50.8 cm (2") 'tee' connected to two 25.4 cm (1") hoses. The two hoses led to the outlet device, which consisted of a 3.66 m (12 ft) long, 50.8 cm (2") piece of perforated (3.2 mm holes) PVC pipe. One hose was attached to each end of the PVC pipe and the pipe was laid across the top of the slope. Water was then applied to the slope at a nearly constant flow rate ranging from 0.51 to 0.57 l/sec (0.018 to 0.02 cfs). The flow of water from individual holes was dampened by wrapping a fabric around the pipe; this ensured a uniform flow which also minimized soil erosion at the outfall.

The direct application of water at the top of the slope determined the flow conditions. Due to the micro-topography of any

(a)

(b)

Figure 3.3. Photographs of field setup, Hillslope Study I: (a) general view and (b) dark surface indicating surface flow. Note the shallow, rilled and somewhat hummocky appearance of the surface.

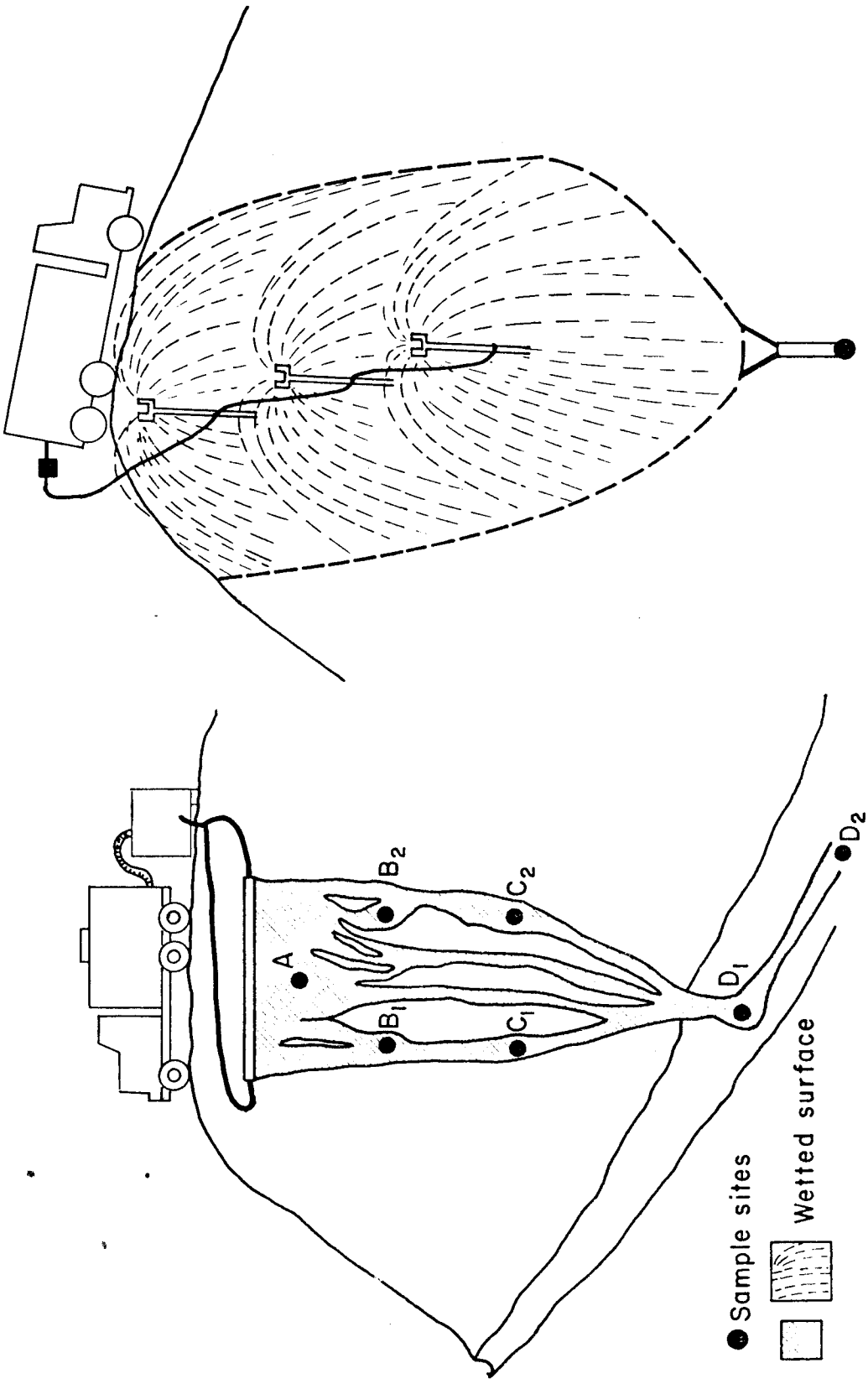

Figure 3.4. Typical field arrangements, Hillslope Studies I(a) and II(b).

particular slope, the water was concentrated into a small area, rather than uniformly wetting the hillslope surface. Anastomosing overland flow was generated downslope of the pipe on all hillslopes except those steeper than 30°. The steeper hillslopes were typically rilled before runoff was generated.

3.1.1b Experimental Procedure

Samples were collected at regular time intervals at various locations on the hillslope. Approximately half of the collected runoff samples were filtered to prevent further dissolution of the salt from the sediment into the water. Electrical conductivity measurements of the samples were taken in the field at the time of collection. For further analysis, the samples were shipped to the Natural Resources Lab at the University of California at Davis, where most underwent a complete analysis for: 1) total solute concentration, 2) suspended sediment concentration, 3) ion specie determination and 4) content of solutes in sediment.

An operator was located at stations A, B_1 and C_1. Each operator was supplied with a data sheet which instructed him to sample the leading edge of the overland and/or rill flow (zero minutes) and to collect additional samples at 2, 4, 6, 8, 10, 12, 15, 20, 30, 45 and 60 minutes after the leading edge. Operators were given a box of pre-marked half-quart sample bottles. One of the operators was required to note the time the leading edge reached each of the stations. When the sampling time intervals for station A became large enough (i.e., 15 minutes), the operator at station A moved to station D_1. In a

similar manner, the station B_1 operator transferred to station D_2, leaving operator B_1 to collect the remaining samples at stations A, B_1 and B_2.

The sample bottles were each marked with the station letter, the sample number (time) and the run number. All bottles numbered 0, 4, 8, 12, 20, 30, 45, 60... were immediately brought to the analysis station for EC determination. Samples 0, 8 and 30 were also filtered. Samples 2, 6, 10 and 15 (i.e., 2, 6, 10 and 15 minutes after the leading edge) were brought in for laboratory analysis only at the end of the run.

Much care was taken not to disturb the rill/overland flow, nor to cause erosion due to sampling. This was achieved by constantly changing the shape of especially prepared aluminum funnels to suit a given sampling situation. Broad flat funnel shapes were used for overland flow (also to decrease the sampling time) and narrow funnel shapes were used in rills.

Soil samples were taken before and after each run. Samples of both the crust and the underlying materials were collected at each of the sampling stations. Table 3.2 describes the numbering system for soil samples at two different plots.

Time-lapse movies were taken during each run. The film speed was set at either 1 or 1/2 frames per second.

3.1.1c Observations During Flow

Site I-1 was selected for preliminary testing with a short pipe runoff generator and results were, therefore, not analyzed. Site I-2 was performed with poor quality water. Results from plots I-3 through I-9 are given below.

Table 3.2 Description of numbering system of soil samples.

Plot Number	Dry Crust 0-5cm	Dry Material 5-25cm	Wet Surficial Material 0-5cm	Underlying Wet Material 5-25cm	Nearest Sampling Station
I-8	1	2	3(a)	4(b)	A
	5	6	7	8	B_2
	9	10	11	12	C_2
I-5	1	2	3	4	A
	5	6	7	8	B_1
	9	10	11	12	C_1
	13	14	15	16	D_1
	17	18	19	20	D_2

(a) The wet surficial material was collected from both rill and inter-rill areas.

(b) The sampled underlying material at times included at the bottom dry weathered bedrock into which the wetting front did not penetrate

Table 3.3 Timing of rill flow appearance and velocity of leading edge of flow.

Run	Slope (degrees)	Rills	Overland Flow	Time (min.) to Rill	Average Velocity (fps) of Leading Edge of Flow From Field Notes	From Movies
I-9	7		X		0.03	0.07
I-8	11	X	X	40	0.06	0.06
I-7	17	X	X	8	0.03	0.03
I-3	17	X	X	15-20	0.03	0.04
I-4	23	X	X	2-6	0.03	0.03
I-6	29	X		4-5	0.09	0.10
I-5	32	X		slope initially rilled		0.15

The timing of the rill formation listed in Table 3.3 should be carefully noted. The mildest slope never rilled. Rills formed on I-8, but after a much longer time than on the steeper slopes. Runs I-8 and I-7 had very shallow, surface rills only. Runs I-3 and I-4 formed noticeable concentrations of flow followed by rills which deepended for the next four to five minutes. The much steeper slope of I-6 had surface rills at four minutes and after five minutes there was no overland flow, only a few deep rills. Run I-5 was on a slope that was initially very rilled. The number of rills deepened substantially after eight minutes; the total depth was 17.8-25.4cm (4-10") at the end of the run. The two steepest runs had mud and slug flows in the rills.

Velocity of the leading edge of flow was calculated using time of arrival at known distances from field notes. Independent observation of timing using time-lapse movie films was in reasonable agreement with these results.

3.1.2c Hillslope Study II

Hillslope Study II was conducted in the West Salt Creek and East Salt Creek Basins, approximately nine miles northwest of Mack, Colorado (see Figure 3.5). Slope length varied from 11 to 22.6m (36-74ft). All slopes chosen were slightly concave so all of the water applied to the slope could be collected at one point. The angle of the slopes ranged from 15 to 41 percent. This study was conducted in order to reinforce the conclusions drawn from the first study by using an experimental set-up that more closely simulated a natural rainfall-runoff event.

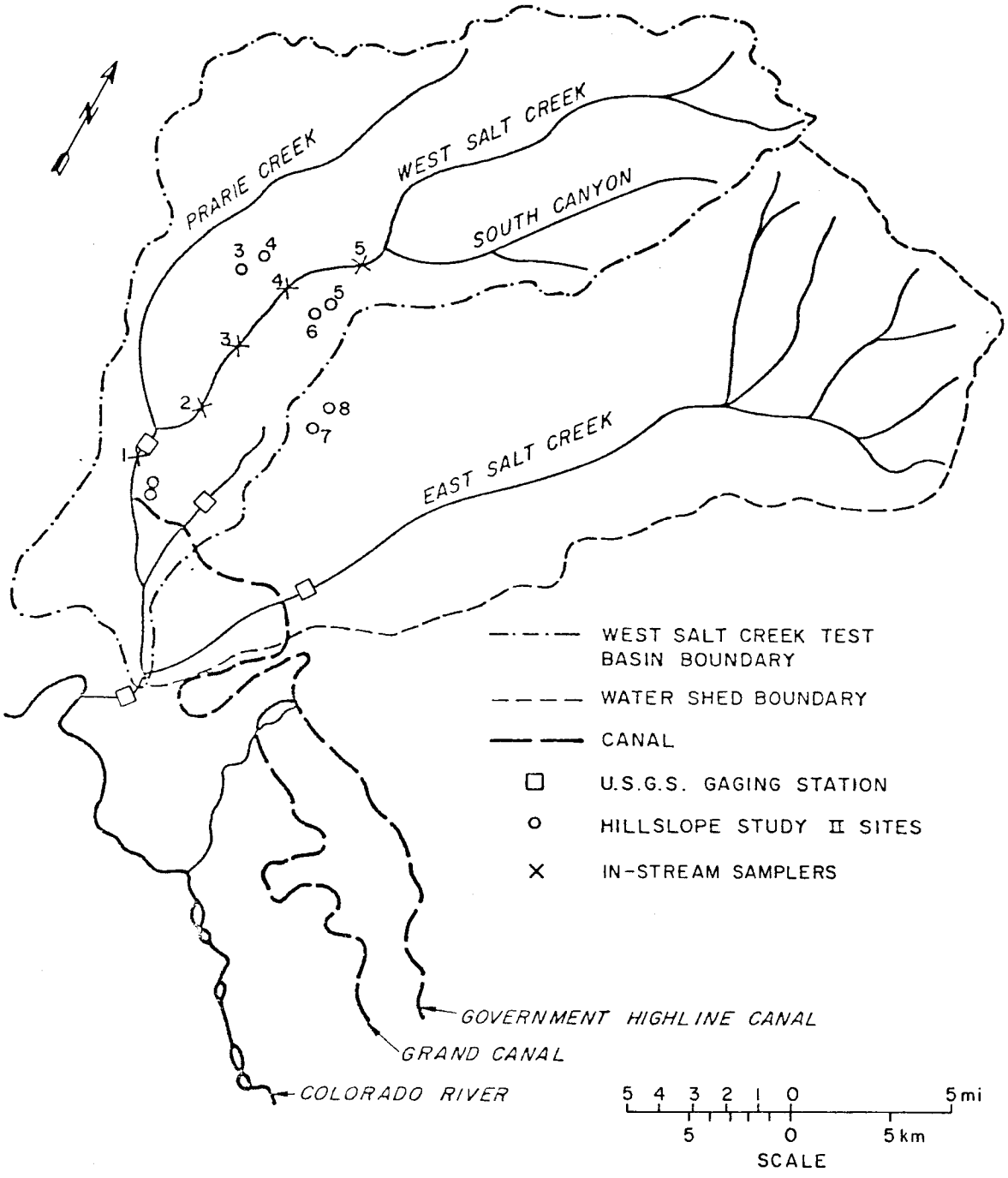

Figure 3.5. Map of West and East Salt Creek Basins showing the location of Hillslope Study II sites.

3.1.2.a Experimental Set-up

Water was supplied by the same artesian well service used for Hillslope Study I. The water was trucked to the sites with a 1600 gallon tank truck. The truck had been used exclusively for hauling water so there was no chance for contamination by foreign substances. It was equipped with a five-horsepower pump that supplied water to a series of three sprinkler risers. Each riser had two 25.4cm (1") brass sprinkler heads. The risers were connected in series using one-inch plastic line. Each riser had a flow regulator that was used to vary the flow to the sprinkler heads. This provided a reasonably uniform areal coverage for each sprinkler head. Three rainfall gages which were spread over the hillslope measured the rainfall distribution (Fig. 3.6).

The length and width of the wetted surface was measured after each run. The distance between the risers was carefully measured for use as a scale in the time-lapse movies.

A collection funnel was designed and built to collect all of the runoff at the bottom of the slope. A hole was dug below the weir and a bucket positioned in the hole to catch the flow. The flow rate was measured and all samples were taken below the weir. An EC monitoring station was set-up adjacent to the collection weir. Figures 3.4b and 3.6 show a typical experimental set-up.

3.1.2.b Experimental Procedure

One operator was assigned the job of foreman. His job was to coordinate all operations, take photographs and make general observations and notes. Three additional operators were stationed at the collection weir. The first operator measured the flow rates. The

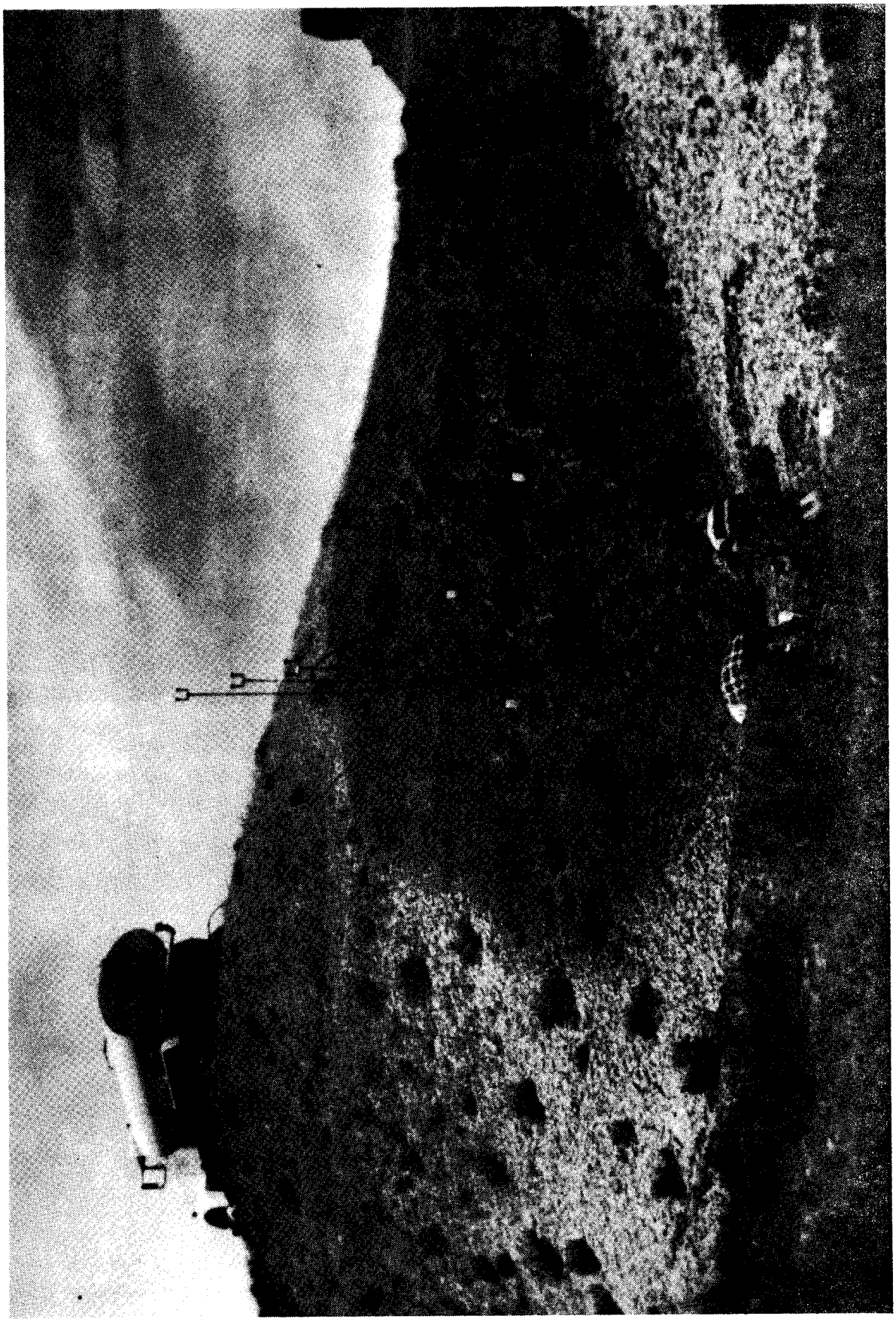

Figure 3.6. Photograph of typical field arrangement, Hillslope Study II. Note the spatial coverage of the sprinklers.

second operator collected samples at specified time intervals. The third operator immediately measured and recorded the EC values of the samples.

A number of soil samples were taken prior to each run, and all sample bottles were labelled with their collection time and run number. Time-lapse movies were taken during each run. The exposure rate was set at 0.5 frames per second.

3.1.2.c Observation During Flow

Unlike the generation of runoff at the top of the hillslope in Hillslope Study I, the entire sprinkled area was wetted and produced runoff in Hillslope Study II. Table 3.4 summarizes the types of encountered flow and the timing of rill flow appearance.

3.2 Results of Hillslope Data

3.2.1 Variation of Flow with Hillslope Inclination

Analysis of the data in Table 3.3 shows that overland flow and rill flow were generated on hillslopes with intermediate inclinations. The time to rilling was lengthened as hillslope inclination decreased. The mildest slope produced only overland flow and the two most steep slopes only rill flow; hillslope I-5 (32°) had an initially rilled surface.

The mild and intermediate inclined hillslopes in the second study (Table 3.4) produced both rill and overland flow. Hillslope II-2 (32°) produced only rill flow. Time to rilling did not correlate as well with hillslope inclination for the artificial rainfall runs as it did for the first set of runs.

Table 3.4. Types of encountered surface flow and timing of rill flow appearance, Hillslope Study II.

Run	Slope (degrees)	Rills	Overland Flow	Time (min.) to Rill
II-8	15	X	X	25
II-1	16	X	X	16
II-7	20	X	X	25
II-6	20	X	X	16
II-3	25	X	X	15
II-4	30		X	
II-2	35	X		immediate
II-5	41		X	

3.2.1 Electrical Conductance (EC) as a Measure of Solute Correlation (SC)

Detailed stoichiometric determinations of ion concentration are expensive and time consuming. However, specific electrical conductance (herein denoted EC) is a measure of the total positive (cationic) or negative (anionic) charge in electrolytes. Although the electrical charge of ions varies with ion species, it is quite constant for natural aqueous solutions containing typical solutes. Therefore, EC is a reliable measure of total solute concentration (herein denoted SC).

For high quality water it is customary to use the empirical relationship

$$SC = k\ EC \tag{3-1}$$

where k=0.65, concentration is expressed in mg/l and conductance in μmho/cm @ 25°C. Such a linear relationship breaks down when a wide range of solute concentrations are considered because of ionic pairing and the formation of ion complexes. Hence, k increases as SC and EC increase.

The relationship between EC and SC is shown in Figure 3.7 for our data. The regression curve is

$$SC = 5.3 \cdot 10^{-6}\ EC^2 + 1.05EC - 348.4 \tag{3-2}$$

A similar relationship was found by Laronne (1977).

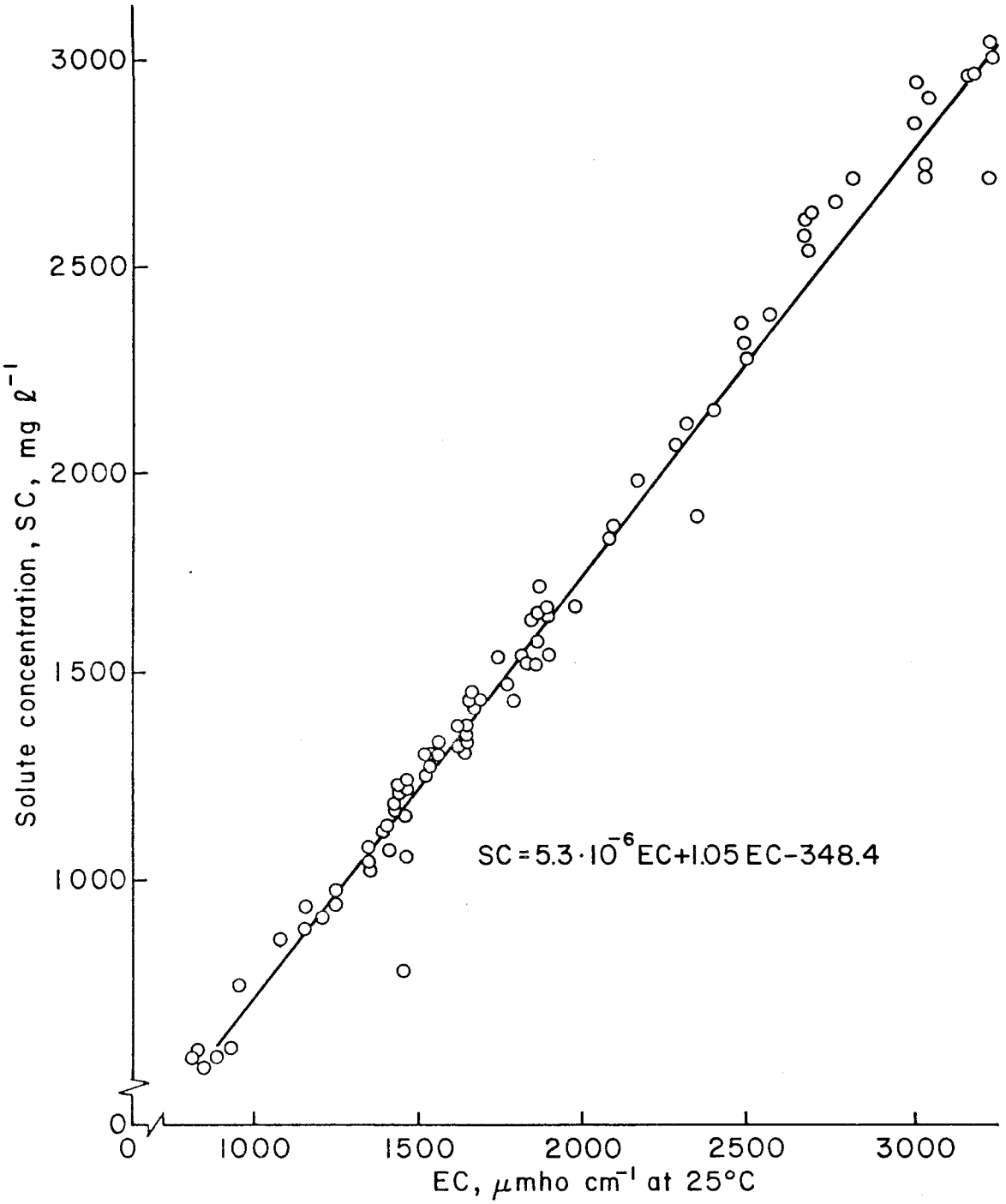

Figure 3.7. Quadratic fit of solute concentration, SC, *vs* EC.

3.2.3 EC *vs* Time

Figures 3.8 through 3.14 show the temporal variation of EC from the onset of water application at different stations for Hillslope Study I. Note that sample collection was initiated at each station with collection of the leading edge of flow and, therefore, the first data point for each station is gradually moved to the right along the abcissa from station A to station D_2.

The temporal variation of EC cannot be expected to be identical for all runs and stations because each has inherent characteristics of type of encountered flow, soluble mineral content and mineralology of soluble minerals.

All stations exhibited an initial high EC when compared to the EC of the applied water. The smallest increase, about 25% (550 μmho/ cm at station A, Figure 3.14), took place at the beginning of overland flow in the mildest hillslope. EC continued to increase for a few minutes at all stations in Figures 3.8-3.10 inclusive, or else reached a maximum value for the leading edge of flow. Thereafter, EC decreased exponentially in most stations.

The decrease in EC was not continous for all stations. Rather, a second EC maximum appeared later in the run at several stations. (e.g., at B_2, Figure 3.9; at B_1, Figure 3.11; B_1 and C_1, Figure 3.12; and most notably at all stations, Figure 3.13).

Figure 3.15 shows the temporal variation of EC from the onset of sprinkling for Hillslope Study II. The variation of EC with time also varies among these hillslopes. The quality of runoff generated in these runs also exhibits initial high EC values in comparison to the applied rainfall. Similarly, the temporal trends in

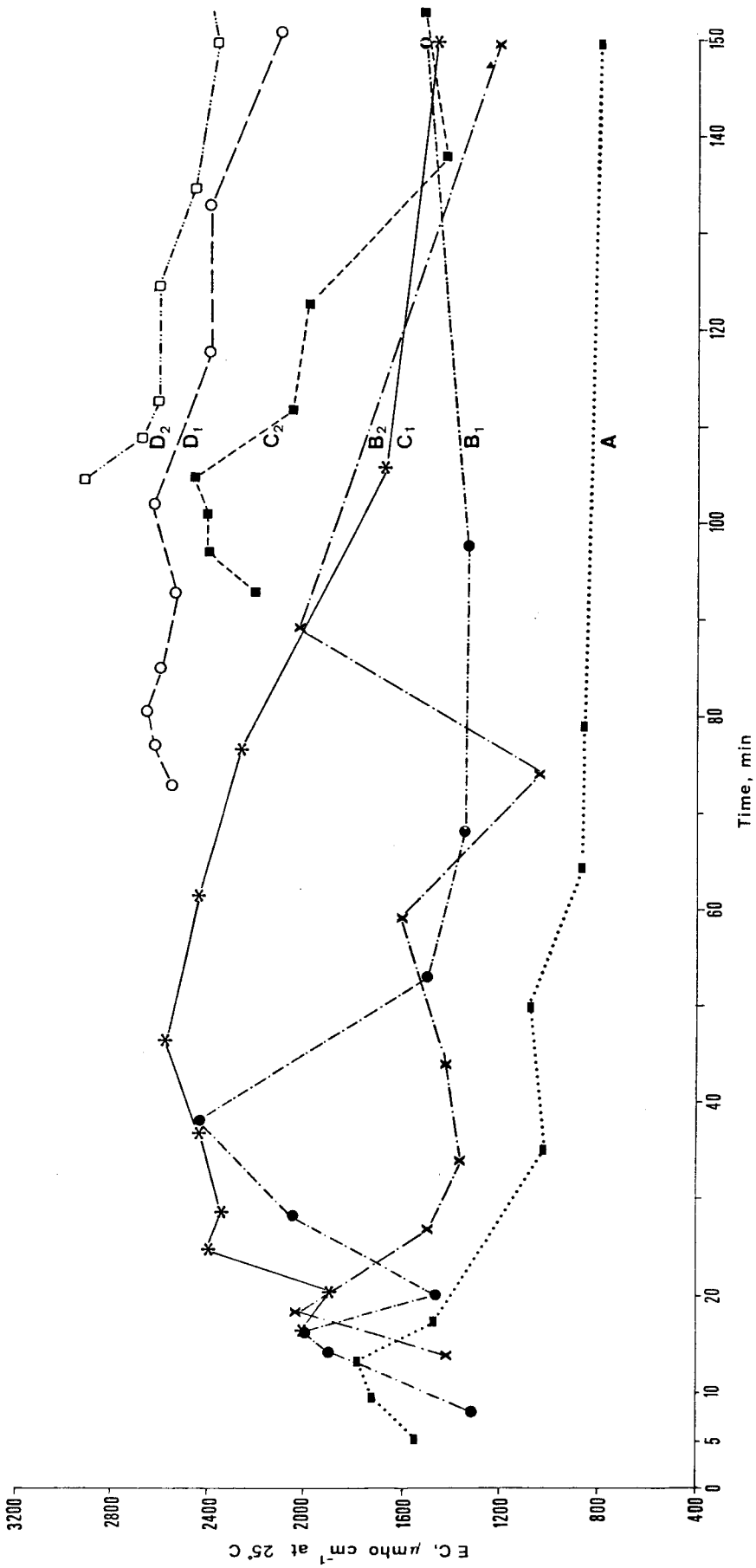

Figure 3.8. Temporal and spatial variation of EC, plot I-3.

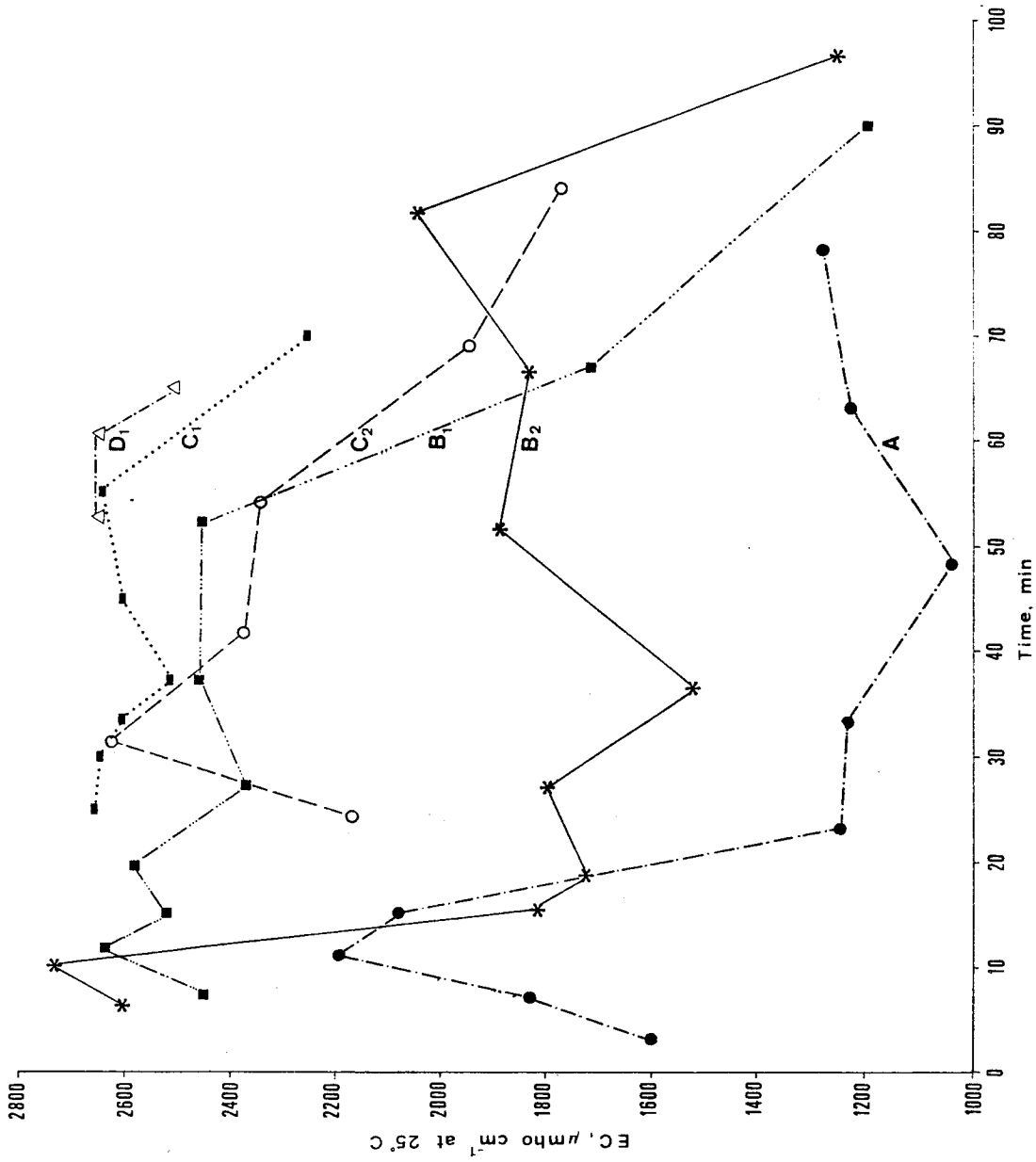

Figure 3.9. Temporal and spatial variation of EC, plot I-4.

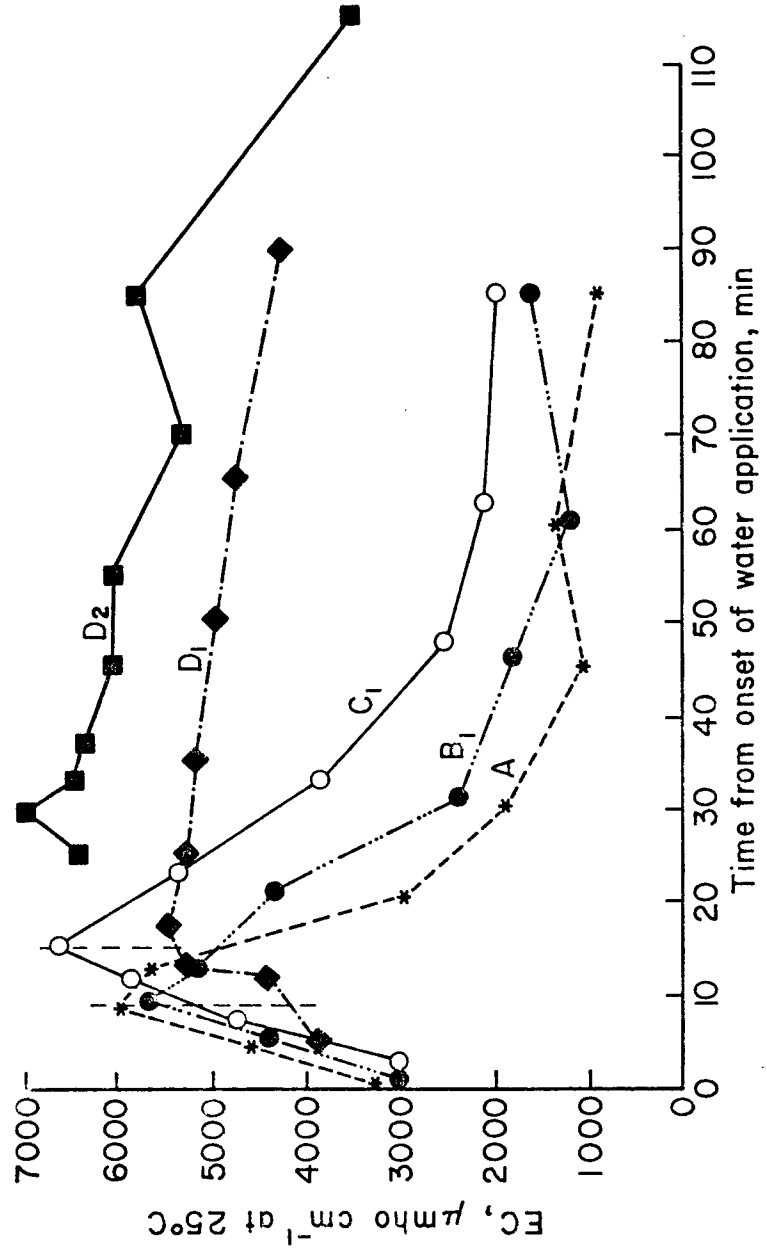

Figure 3.10. Temporal and spatial variation of EC, plot I-5. Dashed line indicates time of rill entrenchment.

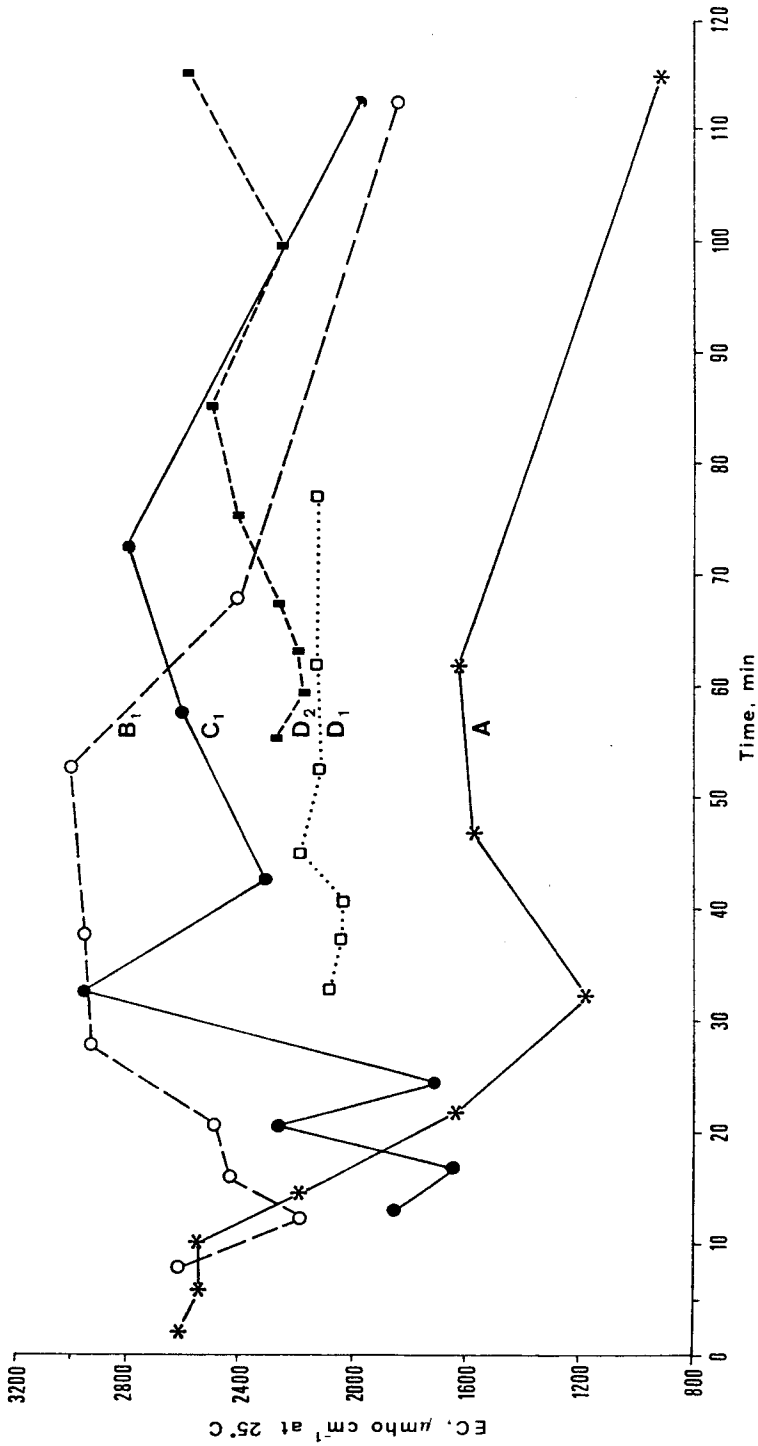

Figure 3.11. Temporal and spatial variation of EC, plot I-6.

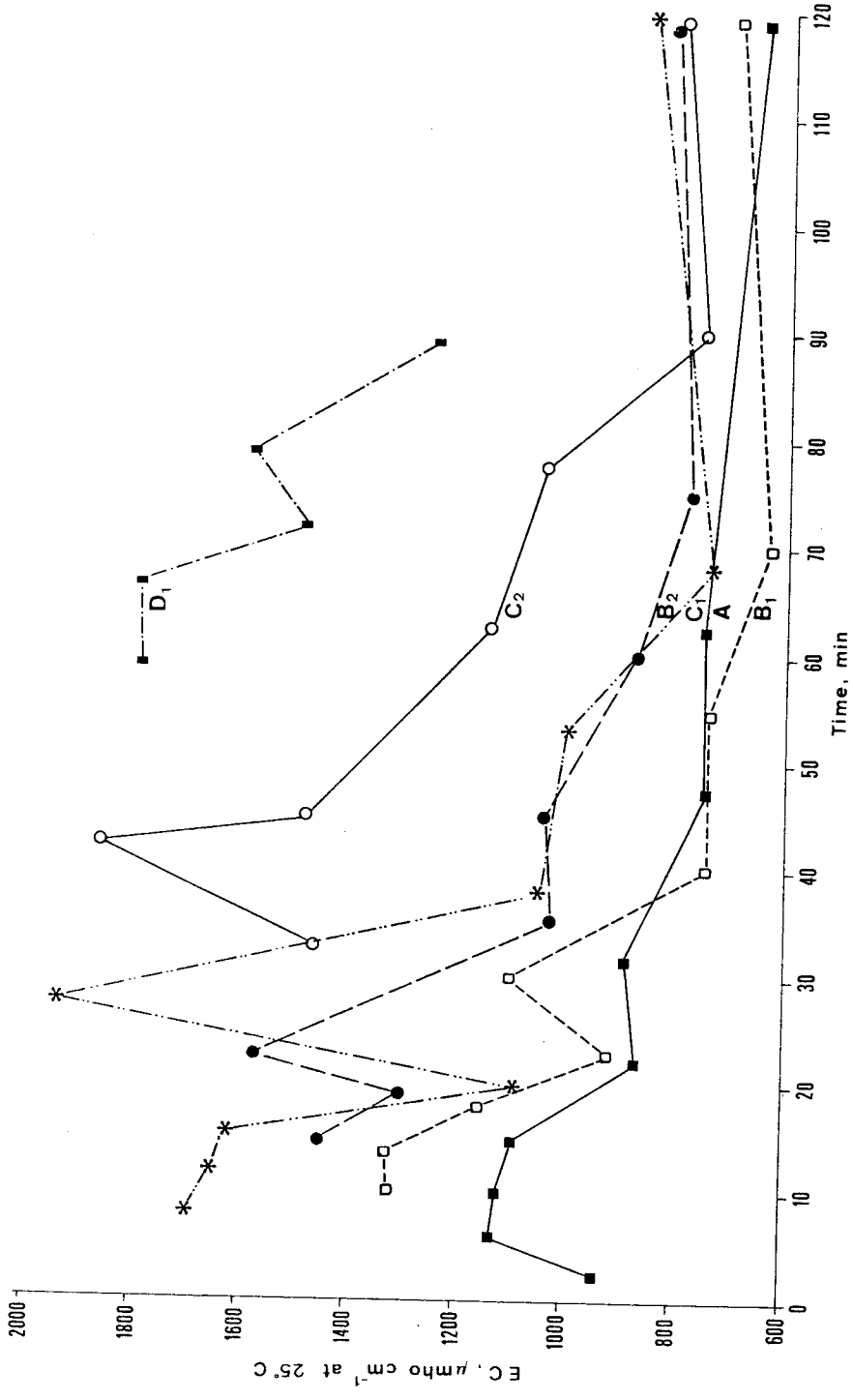

Figure 3.12. Temporal and spatial variation of EC, plot I-7.

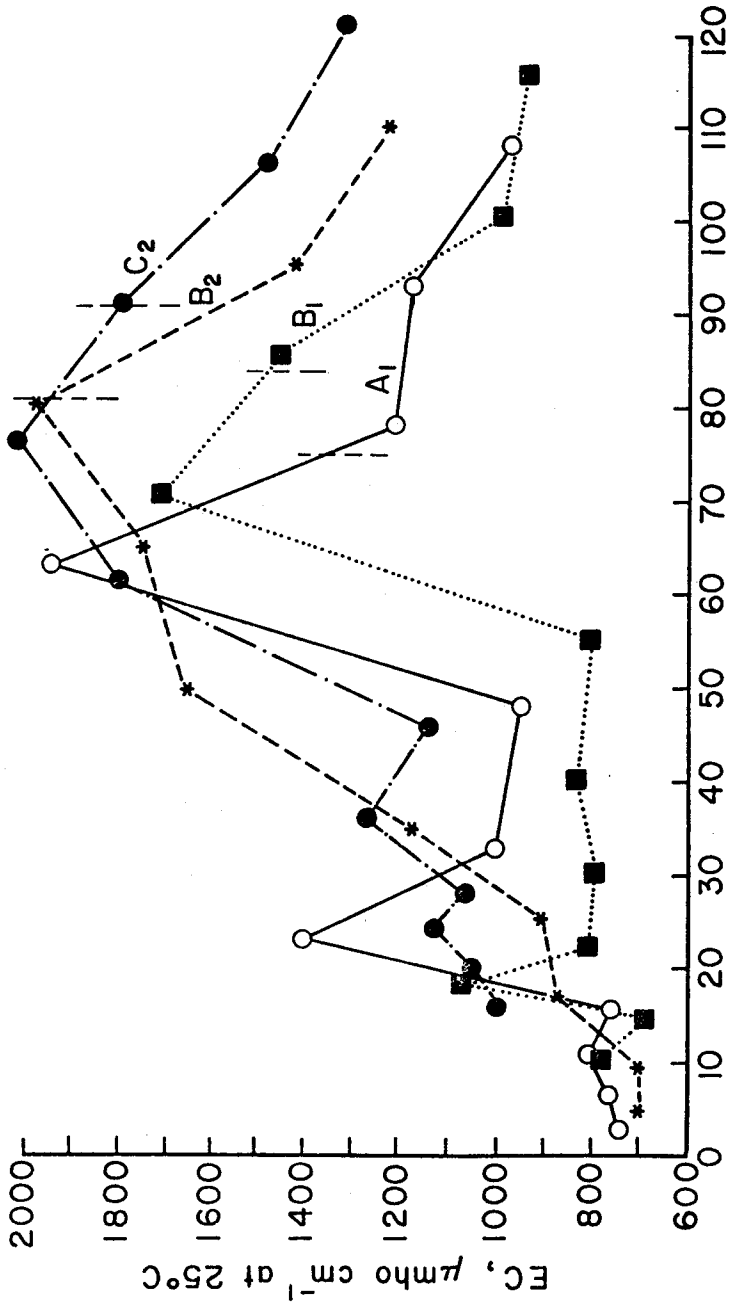

Figure 3.13. Temporal and spatial variation of EC, plot I-8. Dashed lines indicate time of rilling.

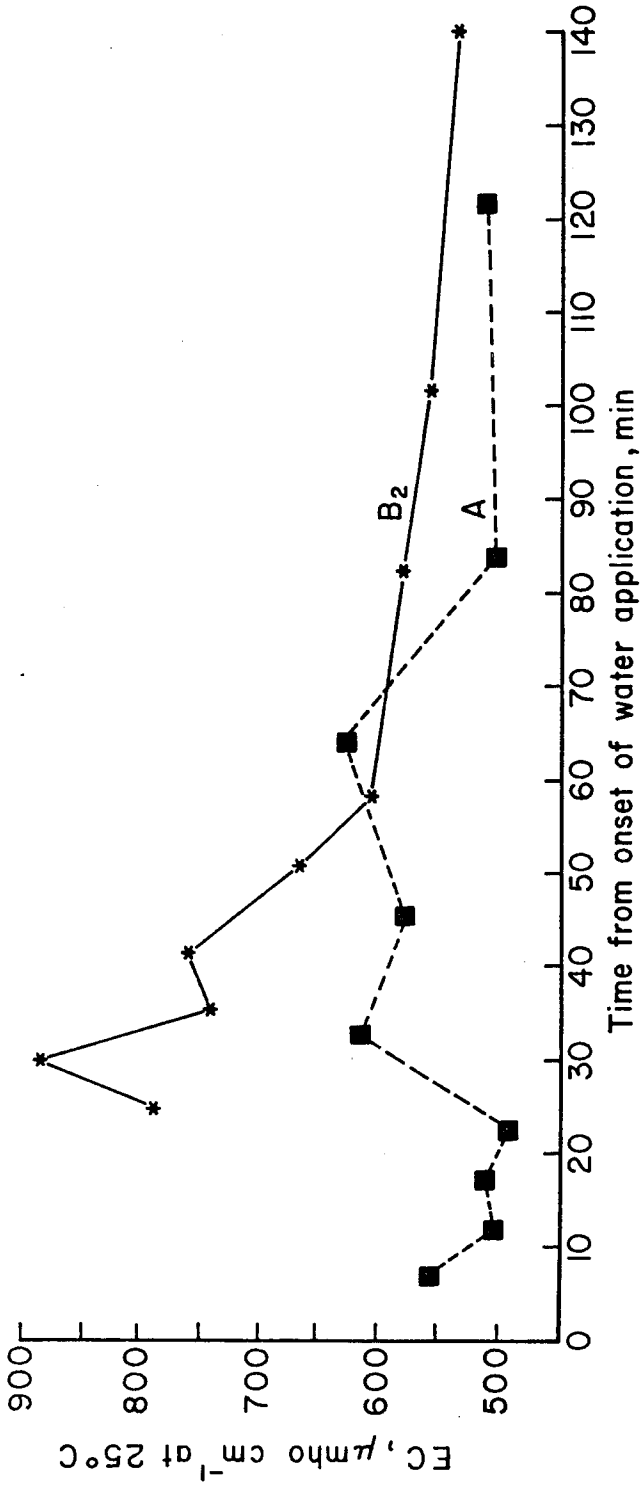

Figure 3.14. Temporal and spatial variation of EC, plot I-9.

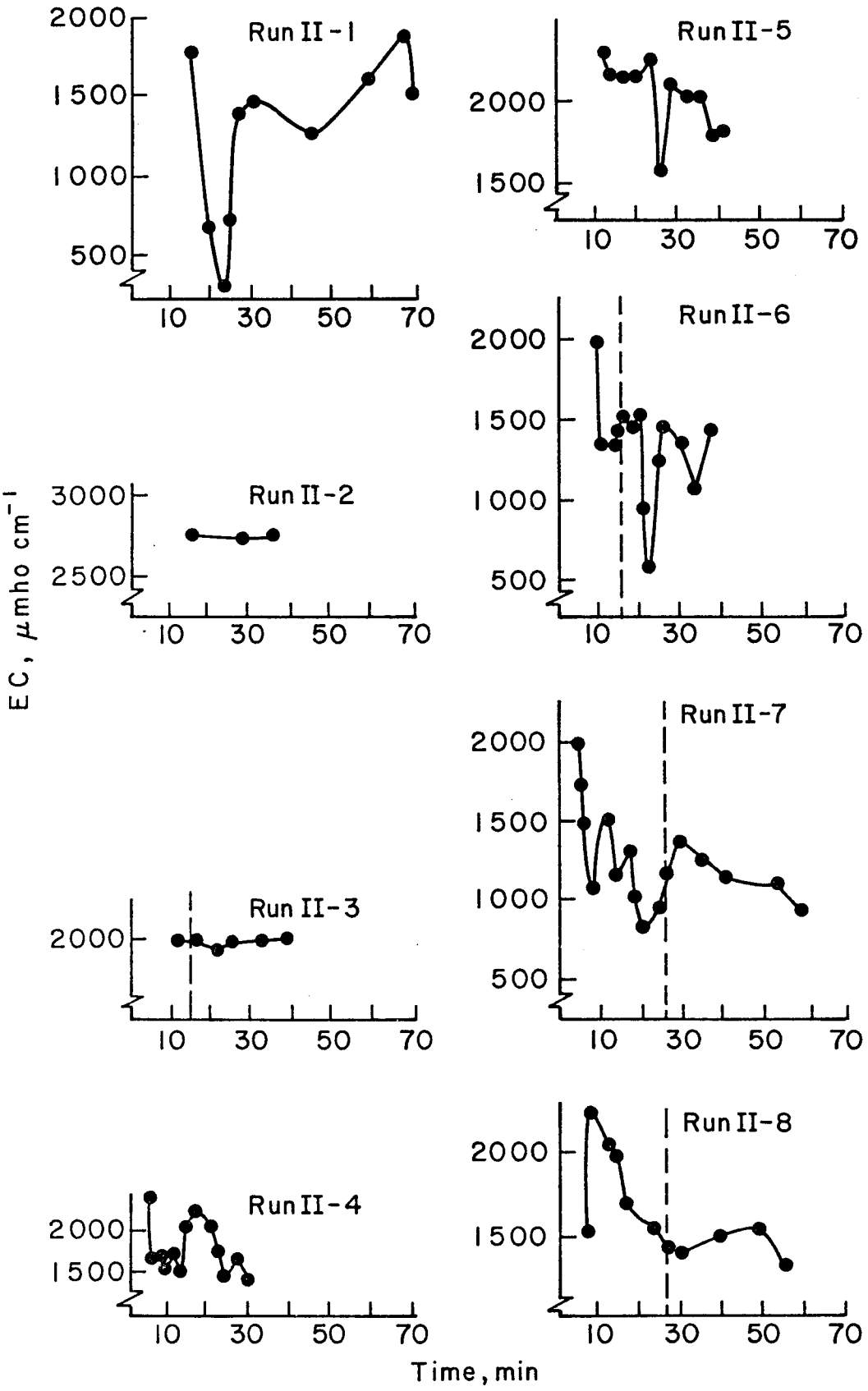

Figure 3.15. Temporal variations in EC, Hillslope Study II. Dashed lines indicate time of rilling.

EC exhibit either one or two maxima. No distinct decrease in EC with time was noted in runs II-2 and II-3 for which only few water samples were analyzed. Note that runoff was collected only at the bottom of the hillslope in this study.

3.2.4 Cross Slope and Downslope Variations in EC

Comparison of EC values across a hillslope (B_1 with B_2 and/or C_1 with C_2) shows a small spatial variation. This variation is particularly small, generally less than 10 percent, considering that comparable EC-time curves must be horizontally shifted, i.e., the comparison should be undertaken on an EC-time (from leading edge of flow) set of coordinate axes. For example, EC values at station C_2 (Figure 3.9) are considerably higher than C_1 at a given time, but they do not differ as much when both curves are horizontally shifted to the beginning of the abcissa.

Downslope variations in EC exhibit two distinct trends. EC increases downslope in all but few occasions. Also, the temporal maximum in EC flatten downslope considerably, a trend which is particularly noteworthy in Figures 3.8-3.10. The downslope increase in average EC during each run is shown in Figure 3.16.

3.2.5 EC *vs* Hillslope Inclination

Possibly the most important and useful result of the hillslope studies is the observed correlation between the steepness of a particular hillslope and the average EC values of the runoff from the hillslope. Table 3.5 shows hillslope steepness, flow velocity or rainfall rate, the maximum, minimum and average EC values of the runoff from each of the hillslope runs, as well as the respective flow types. The average EC values are plotted for the study in Figure 3.17.

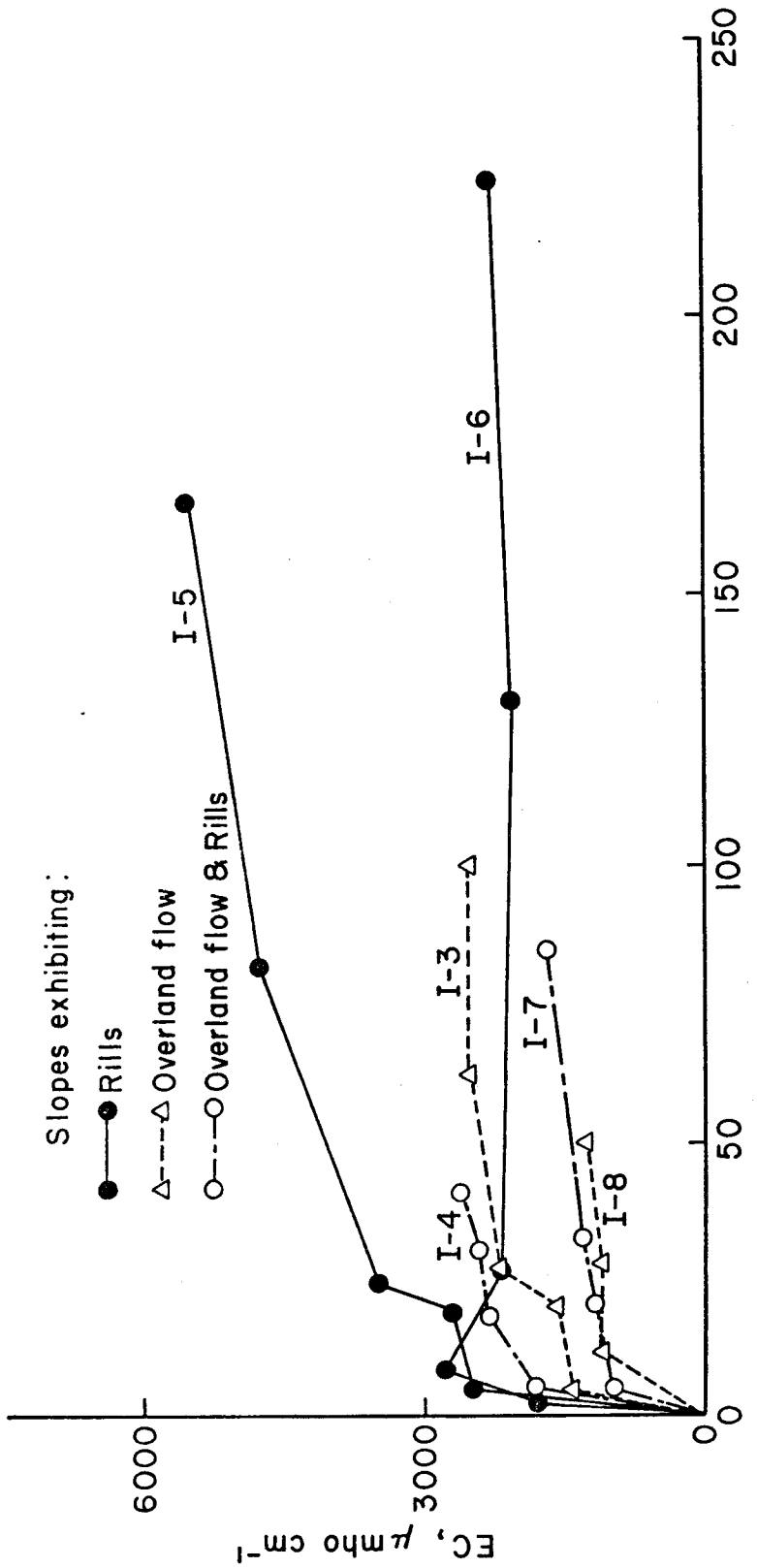

Figure 3.16. Downslope variation of the average EC of direct runoff, Hillslope Study I.

Table 3.5 Summary of Hillslope Study Data

A. Hillslope Study I (Q=0.02 ft^3/sec

Run No.	Slope (Degrees)	Estimated Flow Velocity (ft/sec)	EC (μmho/cm at 25°) Max.	Min.	Avg.	Remarks
I-9	7	0.03	900	500	600	Overland flow throughout run
I-8	11	0.06	2000	950	1490	Overland flow for 40 min., then rill flow
I-3	17	0.03	2500	1650	2190	Overland flow throughout run
I-7	17	0.03	1600	850	1115	Overland flow for 20 min., then rill flow
I-4	23	0.03	2700	2250	2500	Overland flow for 6 min., then rill flow
I-6	29	0.09	2900	1600	2388	Overland flow for 5 min., then rill flow
I-5	32	0.15	6000	2100	3800	Rill flow throughout run

B. Hillslope Study II

Run No.	Slope (Degrees)	Rainfall Rate (inches/hour)	EC (μmho/cm at 25° C) Max.	Min.	Avg.	Remarks
II-8	15	1.68	2500	1300	1585	Overland flow for 25 min., then rill flow
II-1	16	0.98	1900	300	1385	Overland flow for 16 min., then rill flow
II-7	20	0.58	2100	850	1225	Overland flow for 25 min., then rill flow
II-6	20	1.67	2000	700	1430	Overland flow for 16 min., then rill flow
II-3	25	1.50	2000	1950	1990	Overland flow for 15 min., then rill flow
II-4	30	2.68	1750	1250	1500	Overland flow throughout run
II-2	35	0.99	2750	2750	2750	Rill flow throughout run
II-5	41	0.82	2350	1600	2040	Overland flow throughout run

	Study I	Study II
Correlation coefficient (r) of EC *vs* slope	0.795	0.813

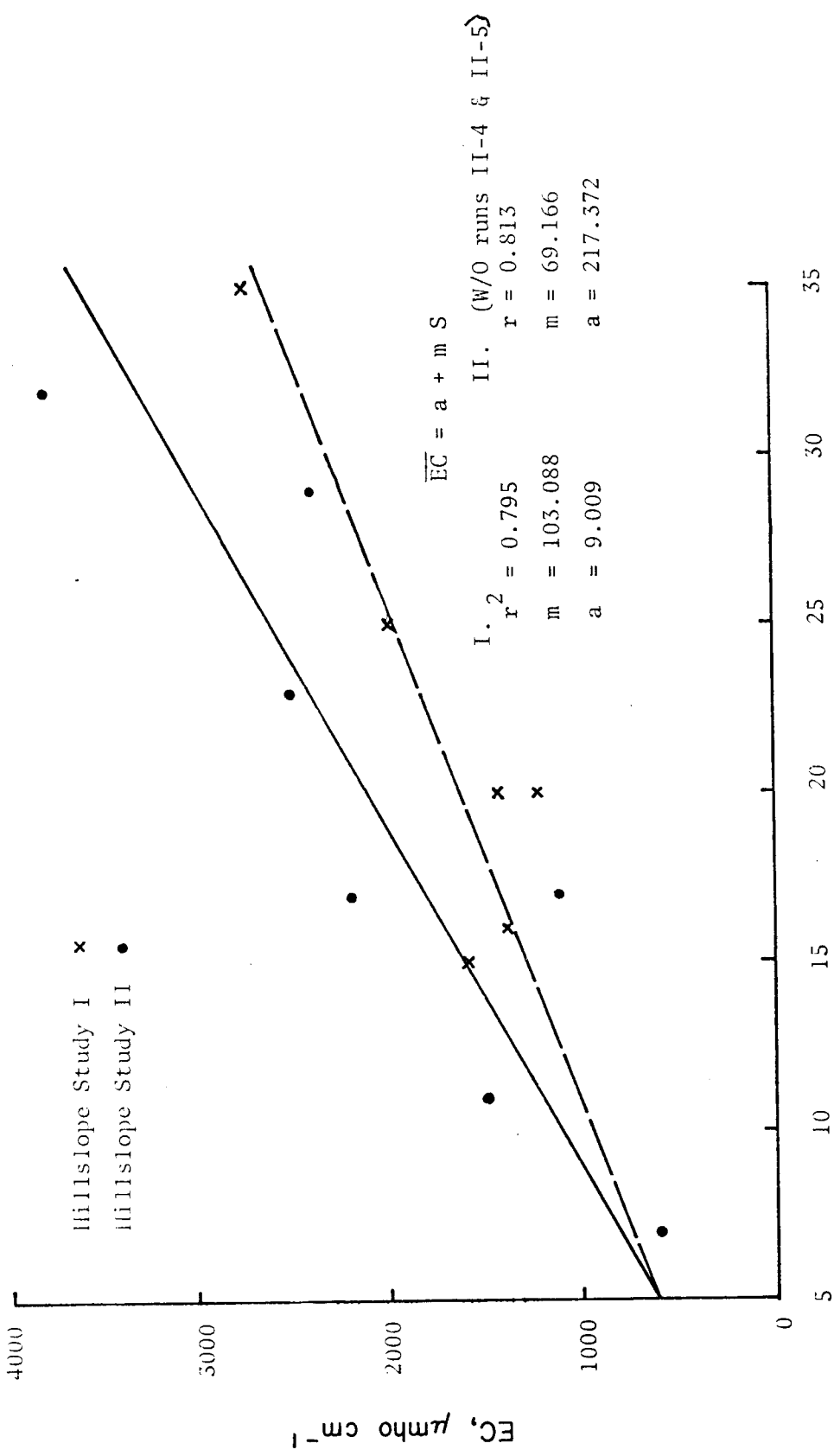

Figure 3.17. Average EC *vs* hillslope inclination for Hillslope Studies I and II.

A correlation coefficient (r) of 0.795 and 0.813 was found for Studies I and II, respectively. Runs 11-4 and 11-5 were located on alluvium. As would be expected, the runoff over these slopes had much lower EC values.

3.3 Discussion

3.3.1 Downslope Variation of EC

Solute concentration should consistantly increase according to principles of dissolution kinetics as long as the bulk solution (flowing water) is undersaturated with respect to any mineral specie. Dissolution rates typically decrease with time at a constant temperature, pressure and given size of dissolving particles. This explains the continous increase in EC in the downslope direction at a given time with few exceptions. Minor variations may be accounted for by measurement errors and by short-term variations in EC due to sampling of runoff at an upstream location. The downslope increase in EC is particularly noteworthy when comparing average EC of generated runoff for the two hillslope studies. Both overland and rill flow in the first study incorporate additional solutes as they move downslope due to 1) longer contact with dissolving minerals on the hillslope surface, 2) longer contact with transported sediment particles, and 3) increased concentration of sediment. EC must, therefore, increase downslope at a slower rate in runoff generated by rainfall that dilutes the runoff downslope and transports less sediment.

3.3.2 Flow Velocity and Flow Type

The primary objective of this study was to determine the role of sediment transport in solute pickup. Therefore, variables related to sediment transport were analyzed in light of the solute concentration data presented in sections 3.1 and 3.2.

Correspondence of higher flow velocities, more rilling and increased rill erosion on the steeper hillslpes with higher flow salinities is indicated by the data in Table 3.5 and Figure 3.1. Given the assumption of a nonvarying soil cover (in terms of infiltration characteristics, erodibility, SMC and minerology of soluble minerals), as hillslope gradient increases so does the power available for sediment transport increase. This may be illustrated by the following equation:

$$\Omega = q \rho g S \tag{3.3}$$

where Ω is the available stream power per unit width, q is discharge of surface flow per unit width and g, ρ and S denote mass density, acceleration due to gravity and hillslope gradient, respectively.

The limiting step for the rate of dissolution of minerals may be governed by primary chemical reactions, diffusion kinetics or by the rate of transport (i.e., the velocity, and associated turbulence) of the flow. Because both chemical and diffusional kinetic principles appear to governthe rate of solute release from Mancos Shale and alluvium (Jurinak, Whitmore and Wagenet; Laronne, 1981), it is evident that solute release should increase as more sediment is entrained and transported by the flow. This conclusion is based on higher solute gradients between transported sediment particles and the solvent (the main body of flowing water) than the respective gradient in soil water. These differences in gradient are due to differences in flow velocity.

Not only does Ω increase with S, but it increases sharply when rilling takes place. Therefore, rilling is conducive to high rates of soil erosion. This explains the positive correlation between solute concentration (EC in Figures 3.8-3.15) and slope inclination, flow velocity and rilling.

3.3.3 Temporal Variation of EC

The EC *vs* time curves consist of an initial maximum, at times with a subsequent second maximum, and thereafter an asymptotic type decrease. The initial maximum may be explained as a surface flushing effect. Highly erodible weathered particles and accumulations of soluble minerals account for this first stage. This may be seen by comparing the temporal variation of sediment concentration (Figures 3.18 and 3.19) with the EC *vs* time curves (Figures 3.10 and 3.13, respectively). Note the contemporaneous increase in both EC and sediment concentration for these hillslopes. These observations agree with the high correlation found by Ponce (1975) and White (1977) between EC and sediment concentration.

The statistical correlation between sediment concentration and EC is further manifested in Run I-8 (Figures 3.13 and 3.19) where a rilling late in the run accounts for increase in both sediment concentration and EC.

It should be noted that the initial increase in EC at a given location and the subsequent asymptotic decrease of EC could not take place if the flowing water had been equilibrated (saturated). Basic dissolution kinetics dependent on solute gradients account for much of the initial high EC values and their subsequent decrease.

3.3.4 Role of SMC in Solute Pickup

The second temporal peak in EC during run I-8 results not only due to the rilling and increase in sediment concentration, but particularly due to the high SMC of the underlying material. Table 3.6 shows the salinity potential of crust and underlying less weathered

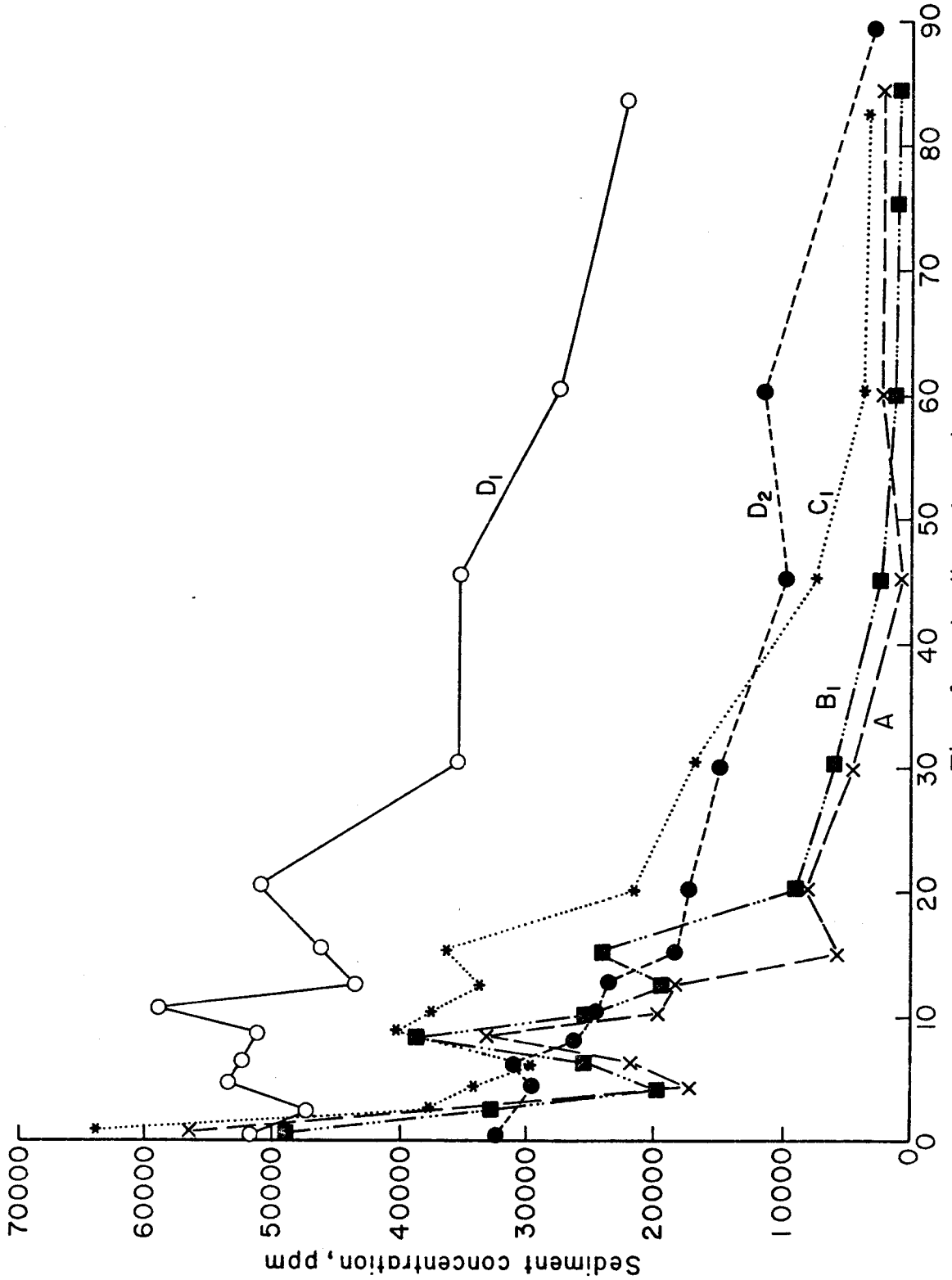

Figure 3.18. Temporal and spatial variation of sediment concentration, plot I-5. Note that sediment concentration is almost linearly related to sediment load due to low seepage losses.

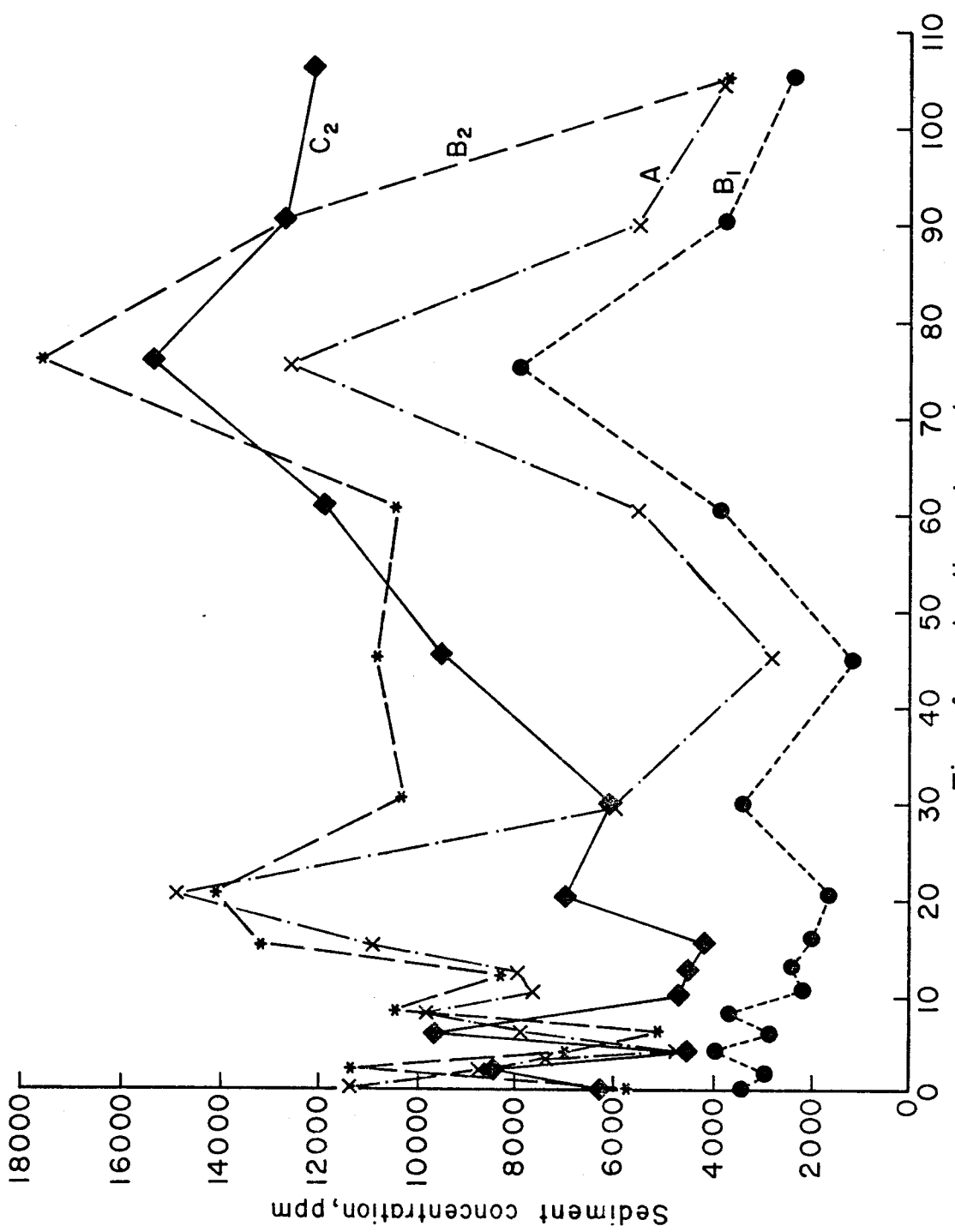

Figure 3.19. Temporal and spatial variations of sediment concentration, plot I-8. Seepage losses were larger than on plot I-5.

material of Mancos Shale. This potential is denoted by the EC of 1:99 soil:water extracts. Note the substantial higher SMC of underlying material in comparison to the crust, as discussed in detail in section A.1 of the Appendix.

Table 3.6. Salinity potential of the crust and underlying less weathered Mancos Shale in runs I-5 and I-8, Hillslope Study I.

RUN I-5			RUN I-8			
Distance Downslope (ft)	EC (μmho/cm) Crust	Underlying Material	Distance Downslope (ft)	EC (μmho/cm) Crust	Underlying Material	
					dry	wet
7	600	900			1700	
19	620	925	12	50		
28	760	925	28	350		
82		850	44	50	1600	875
190	800	625				

The role of SMC on solute concentration of generated runoff is minimized in comparison to the role of sediment transport. EC values as high as 2000 μmho/cm characterize the runoff in run I-8 during rilling (Figure 3.13), one hour after the beginning of runoff generation. In comparison, EC values are in the range 2000-5000 μmho/cm one hour into I-5 (Figure 3.10) because the hillslope inclination, flow velocity and resultant sediment concentration are higher in this run. This difference in solute yield took place even though the eroded material in run I-5 (i.e. the underlying material of Table 3.6) contained half as much soluble minerals.

3.3.5 Role of Sediment Transport in Solute Pickup

The discussion of the spatial and temporal variations of EC in sections 3.3.1-3.3.3 relies partly on basic theory of dissolution kinetics, but also on statistical relations between hydraulic, hydrologic and geomorphic processes and EC. The effect of increased flow velocity and turbulence (Chapter 2), in fact, also relies on dissolution kinetics theory.

A more straightforward, causal relationship between sediment transport and solute pickup is, however, necessary. The missing link prooving a causal relationship must necessarily rely on actual quantities of solutes released from sediment transport. This information is available in two forms. The sediment filtered from the runoff samples of Study II was analyzed for salt content and ion concentrations (Table 3.7). The average EC values of 1:5 soil-water extracts of these sediment samples for each of the runs indicate that substanial quantities of soluble minerals were still present in the sediment; these have the potential to increase the solute content of a higher quality diluting source (e.g., Colorado River water). Calcium and sulfate were the dominant ions in the sediment which indicates that Gypsum is the main source of salinity from sediment transported from these hillslopes.

Table 3.7. Average EC of 1:5 soil-water extracts of suspended sediment sampled from runoff, Hillslope Study II.

Run No.	1	2	3	4	5	6	7	8
Average EC (μmho/cm)	980	1700	1300	200	1500	1200	650	750

The above-mentioned filtration was undertaken in the laboratory and only indicates the potential for salt release from transported sediment. However, many runoff samples collected during runs of Hillslope Study I were immediately filtered in the field. Because of the large number of filtered samples and the actual time needed for filtration, the runoff samples were filtered approximately 5 minutes after collection (see Appendix 2 on extent of delay, t_d, of filtration). t_d was in the range 1-35 min; smaller t_d values would have necessarily brought about larger differences between EC of paired filtered and unfiltered runoff samples. Table A-3 of the Appendix summarizes EC data for filtered and unfiltered runoff samples. Analysis of this data shows that the increase in solute concentration due to continous dissolution of soluble minerals from the transported sediment averaged 32.3 percent, varied between 12.7 and 86.9 percent within each run and between 4.8 and 115.3 percent within each measuring station. Only two such comparisons between filtered and unfiltered samples yield a decrease larger than 3 percent, the latter value being a reasonable measurement error.

Figure 3.20 (a) depicts the mean measuring station increase in EC with distance downslope. Note that for all runs (except I-8) the increase in EC for unfiltered as compared to filtered runoff samples decreases downslope. This trend is explained by higher sediment concentrations associated with increase in distance downslope. A higher sediment concentration has been shown (Laronne, 1981) to increase the initial rate of dissolution. The actual increase in EC due to continuous dissolution from transported sediment decreases from 70 percent near the hillslope divide to 30 percent at the bottom of the hillslope.

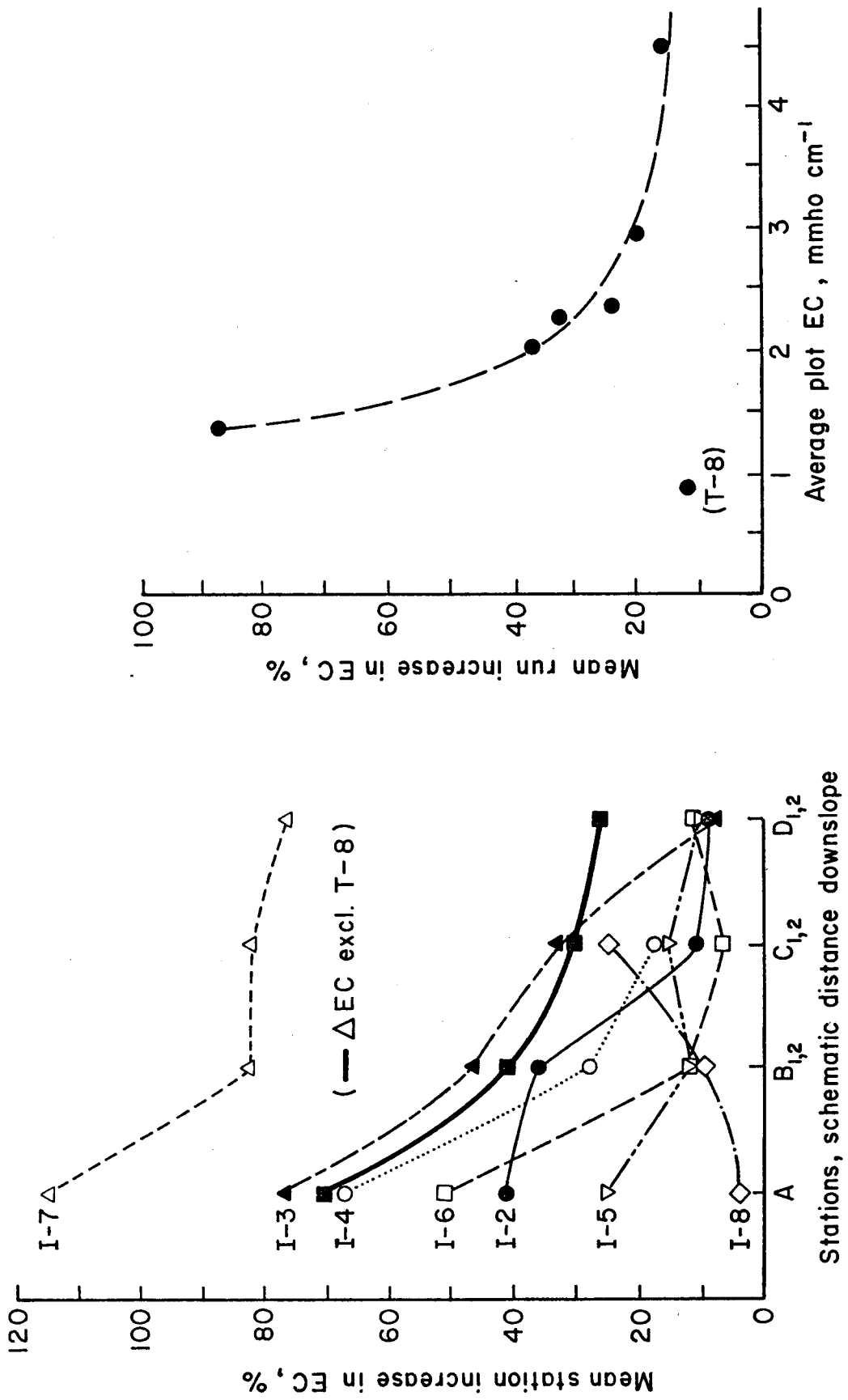

Figure 3.20. Increase in mean at-a-station EC with distance downslope (a), and increase in mean at-a-plot EC with average (runoff) plot EC (b).

The average solute concentration in runoff also affects the increase in EC (Figure 20.b). This trend also conforms to principles of dissolution kinetics (Laronne, 1981).

It cannot be overstressed that the data in Table A.3 shows the causal relationship between sediment transport and solute pickup. Additional quantities of solutes would have necessarily been added if t_d values were shorter; moreover, solute yields also increase upon dilution of such partially equilibrated runoff with higher quality river water.

The specific ion data (Table A.4 of the Appendix) of both filtered and unfiltered I-5 and I-9 runoff samples is of utmost importance. It not only proves that transported sediment contributes significantly to runoff salinity, but also clarifies which minerals contribute most significantly.

Comparison of ion specie concentrations (meq/l) for filtered and unfiltered run I-5 and run I-8 runoff samples shows the following temporal trends within the soluble transported sediments: $(SO_4)/(HCO_3)$, (Ca), and (Ca)/(Na) increase while (Na) stays approximately constant with contact time for I-8 samples. (Na) and (Mg) increase, (Ca) remains approximately constant and $(SO_4)/(HCO_3) \simeq 7$.

Comparing the temporal trends in ion specie concentrations between I-5 and I-8 samples shows that $[(Na)+(Mg)]/(Ca)_{I-5} >> [(Na)+(Mg)]/(Ca)_{I-8}$, and that $(Cl)_{I-5} \simeq 7(Cl)_{I-8}$.

These results indicate that due to the high salinity of I-5 runoff which is already saturated with respect to Gypsum at the hilltop, increase in salinity from dissolving sediment is achieved primarily by the dissolution of very soluble minerals - sodium-magnesium sulfates. The runoff of run I-8 has lower sediment concentrations and, therefore, continuing lower solute concentrations; the main salt enrichment mechanism is one of continued dissolution of Gypsum.

It may be concluded that the chemical quality of runoff, and not only its total solute concentration, is strongly controlled by sediment entrainment and, consequently, by sediment concentration. In this connection, it may be illustrated that the average sevenfold higher chloride concentration of I-5 runoff samples (relative to I-8 runoff samples) is a direct result of the average sevenfold higher sediment concentration (7000 ppm for I-8 *vs* 32250 ppm for I-5) involved. Being highly soluble, chloride salt (i.e., evaporite) concentrations would be expected to increase linearly with sediment concentration.

CHAPTER 4

SEDIMENT AND SOLUTES IN WEST SALT CREEK

Laboratory investigations and simulation of salt loading with particular emphasis on the role of sediment transport have clarified the pertinent processes operating on hillslopes. Similarly, understanding the temporal and spatial trends in sediment and solute yields from hillslopes is needed to explain the more complex variability of water quality in channels. The objectives of the watershed study were 1) to investigage the role of sediment transport in salt pickup 2) to develop a procedure for estimating expected flow peaks and volumes from West Salt Creek, and 3) to estimate the salt loading from the Grand Valley in general and from the test basin in particular (see Chapter 5). Section A.5 in the Appendix deals with the first objective in a river confluence study and Section A.6 in the Appendix summarizes relevent information on several large tributaries of the Green and Grand Rivers.

4.1 Description of Study Area

West Salt Creek, with a drainage area of 435 km^2 (170 mi^2), is located in the western-most extremity of the Grand Valley (Figure 4.1). Its headwater channels drain the southern face of the Book Cliffs (Green River siltstones and marls) and the mid reach drains sandstones and shales of the Mesa Verde Group.

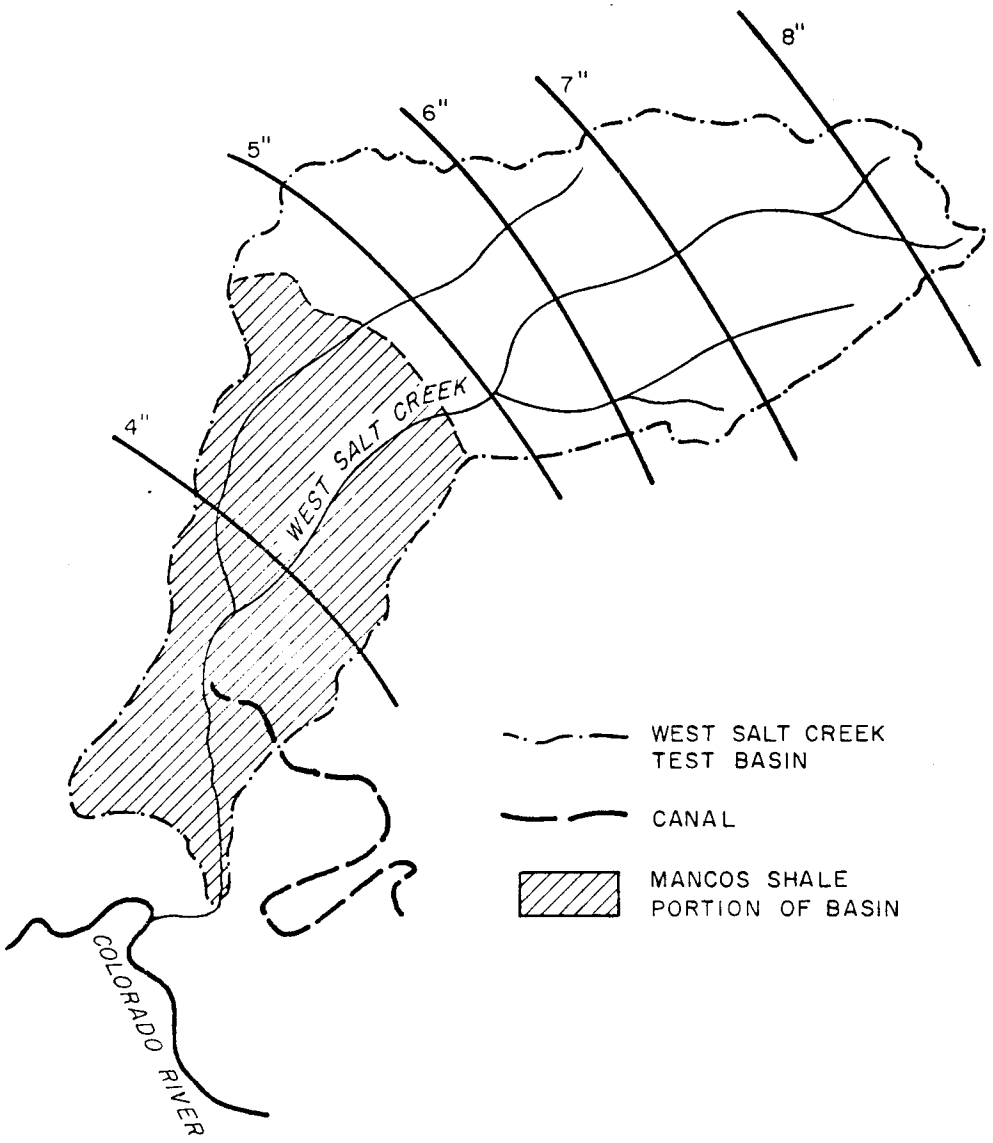

Figure 4.1. Map of West Salt Creek Basin showing the spatial distribution of mean annual precipitation with altitude.

The lower half of the basin is underlain by Mancos Shale (Figure 4.2). Elongated alluvial aprons that slope in the direction of the drainage cover parts of the shale, thereby limiting its exposure.

The channel of West Salt Creek is incised in alluvium throughout its length. The incision has formed a series of alluvial terraces (see Figure 4.3), the upper of which forms the flat valley bottom (Figure 4.2). The alluvium thickens downchannel, its thickness exceeding 50m at the U.S. Geological Survey gaging station (Laronne, 1977). This location is also the western extremity of irrigation, evidenced by the exit up the Government Highline Canal (Figure 4.1). A sweeping action of the sinuous channel has widened the valley and it has formed steep, arroyo-type banks. Saline seeps are found in some of these banks where the channel abbuts against Mancos Shale hillslopes. The channel bed is often covered by an efflorescent surface crust near the shale exposures.

The valley floor, where left unirrigated, is sparsely vegetated with pinyon-juniper (primarily on the alluvial aprons), shadscale and greasewood. The climate is semiarid with an annual potential evaporation of 750-1000 mm, a mean annual temperature of 12°C (records of -27°C in February and 40°C in July) and 175 frost-free days.

The valley floor annually receives 200-250 mm of precipitation while the headwaters receive 250-400 mm/year. Figure 4.1 shows the estimated average change in mean annual precipitation across the basin. It was constructed by averaging 30 years of precipitation records for stations in the vicinity of the Grand Valley and from precipitation records from gages installed as part of this study, and regressing

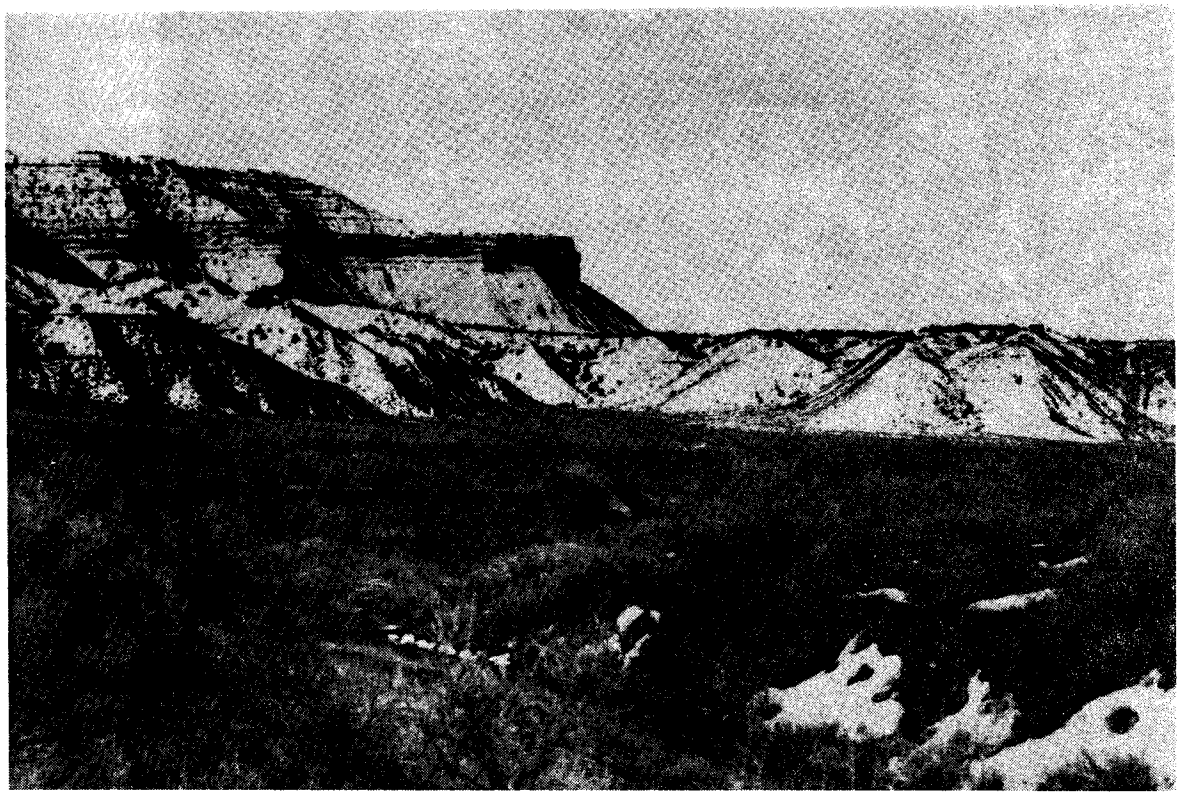

Figure 4.2. Photograph depicting the character of the lower West Salt Creek Basin.

Figure 4.3. Photograph of West Salt Creek showing an alluvial terrace in the foreground and Mancos Shale in the background.

these averages against the station elevation (for details consult Enck, 1981).

"Summer" (May - October) precipitation events are intense and of short duration. Winter precipitation may fall as snow which sublimates, evaporates or infiltrates without producing much runoff during most years.

4.2. Design and Installation of Samplers

Two types of samplers were installed in the bed of West Salt Creek. The samplers were required in order to collect water and sediment data related to hydrologic and geologic variables. One sediment sampler was designed according to Schick and Sharon (1974). Figure 4.4. shows the installed sampler in the bed of West Salt Creek, and its internal layout is exhibited in Figure 4.5.

Eleven samples of water and sediment may be collected by the sampler at the water surface while water stage rises. Upon entrance into the sampler, the water and sediment are collected in 1 liter bottles where they are stored until the sampler is serviced. Although this sampler has performed well, its initial cost is high and it does not separate the transported sediment from the water.

A new low-cost sampler that filters the sediment from the water during runoff events was specifically designed for this study in 1978. Its basic layout is depicted in Figure 4.6. The outside casing of the sampler is constructed from a recycled 30-gallon drum in order to reduce costs (Figure 4.7). This modified sampler was designed to be set into the channel bed so that the bottom of the door is flush with the channel bed. Unlike the original sampler, it can hold only four samples.

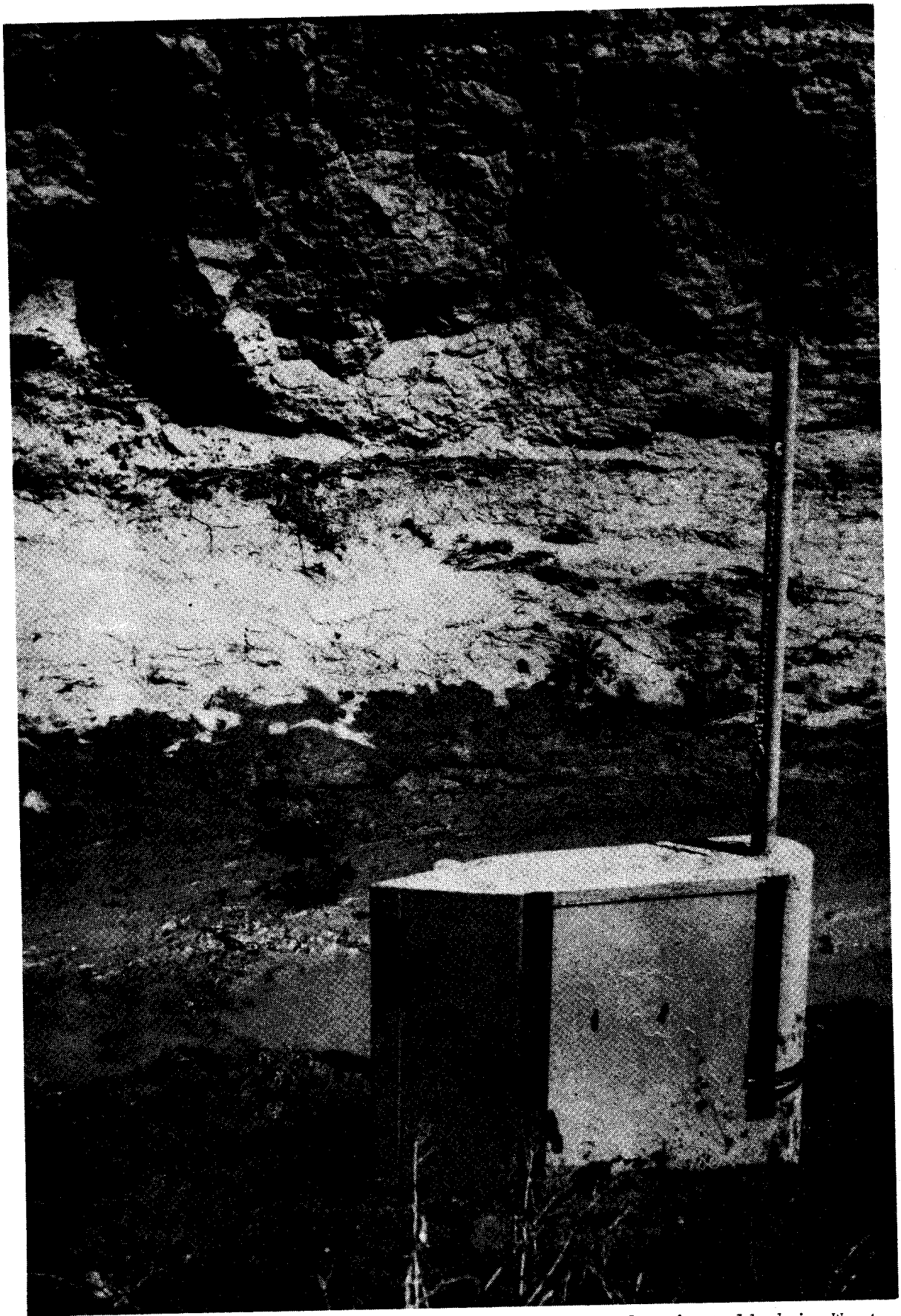

Figure 4.4. Photograph of the first sediment sampler installed in West Salt Creek. Notice the amount of fill around the sampler.

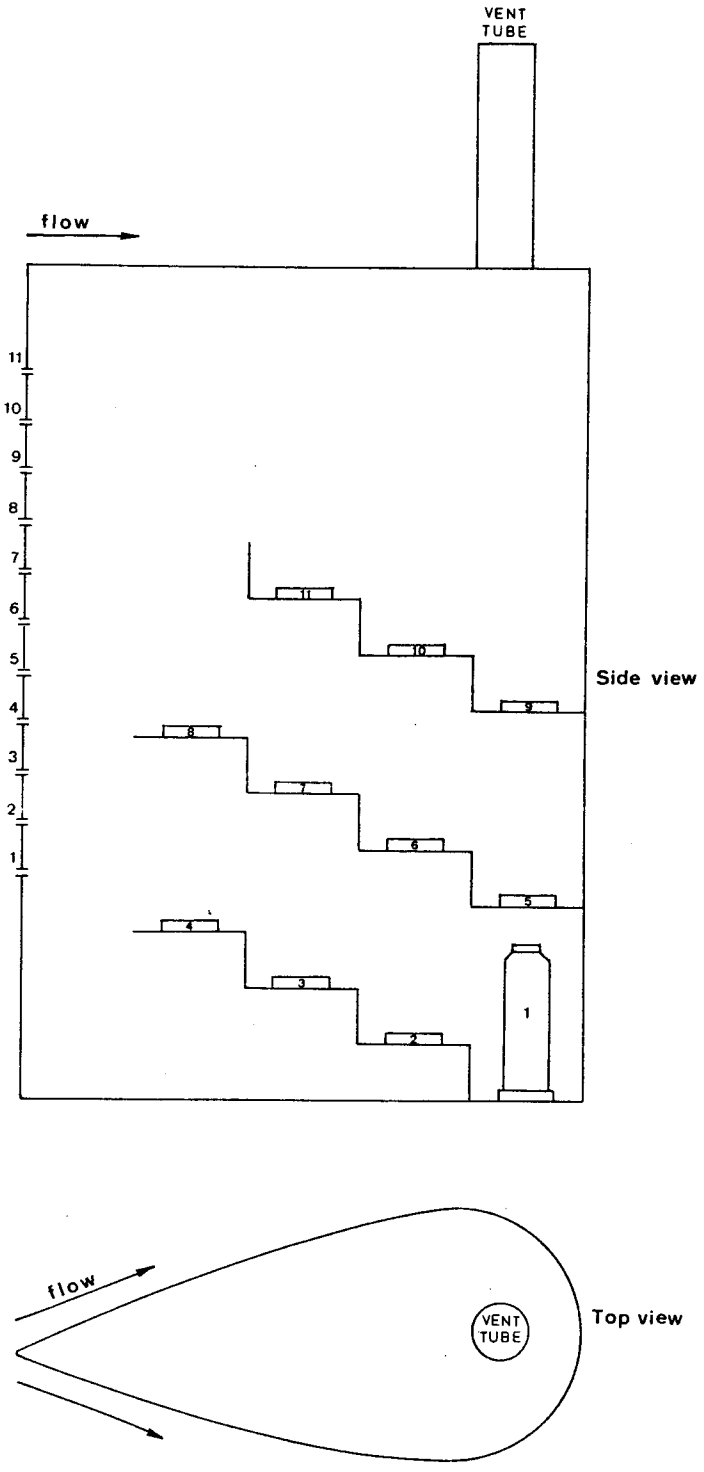

Figure 4.5. Design illustrating the internal layout of the first sediment sampler.

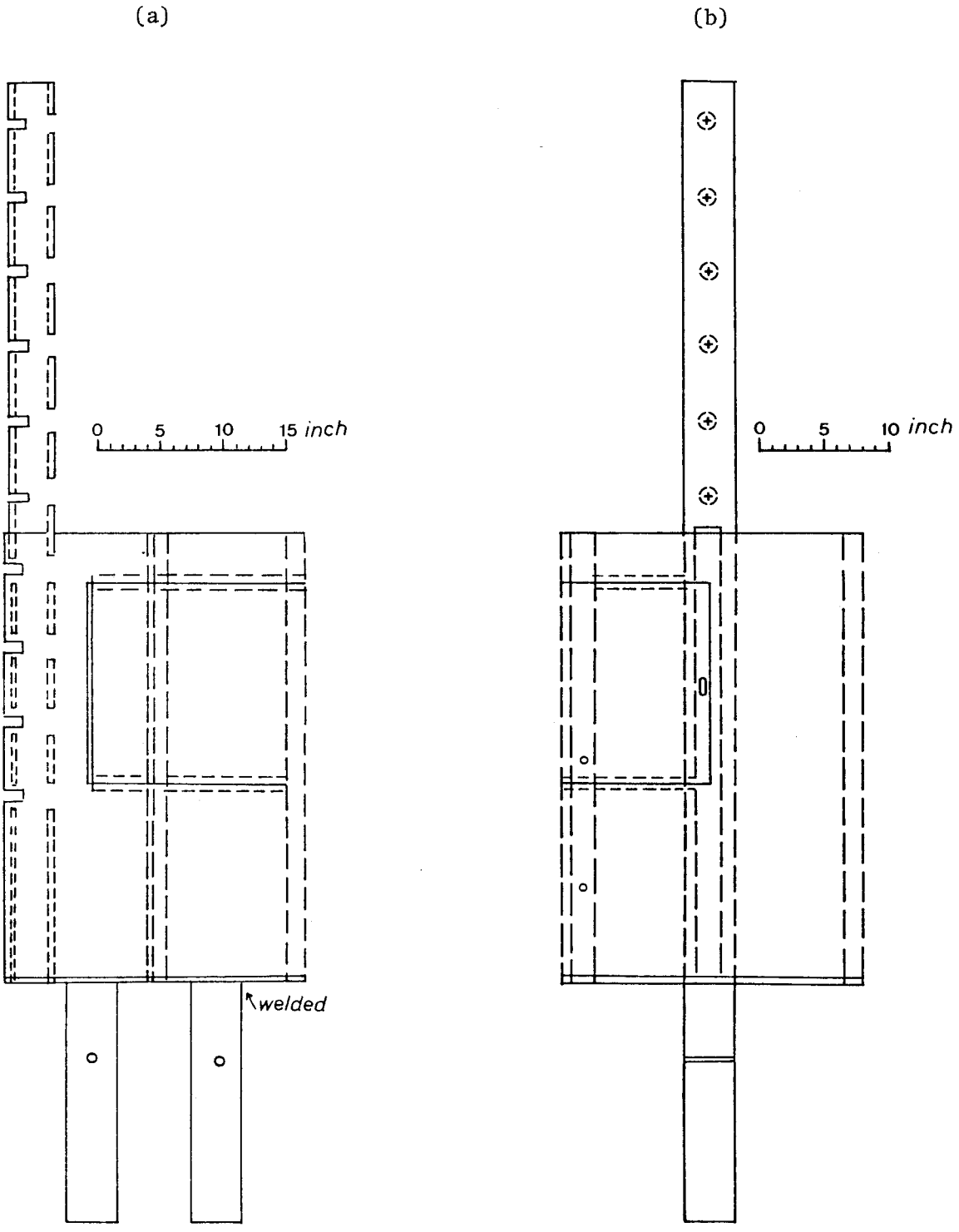

Figure 4.6. Side (a) and back (b) views of the newly-designed water and sediment sampler.

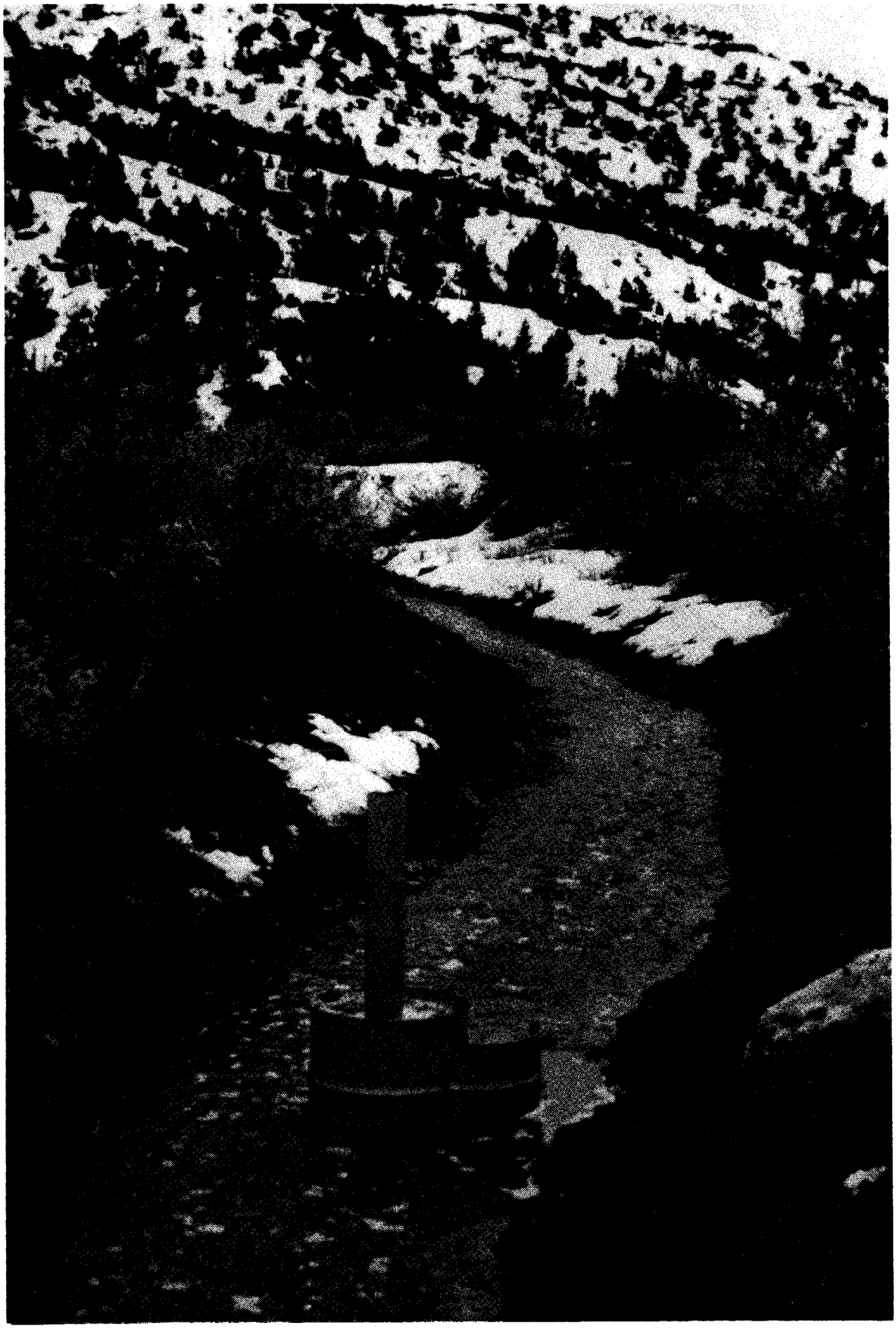

Figure 4.7. Photograph showing the newly-designed water and sediment sampler.

Samples are collected during the rising limb of a flow event at a depth of 2 inches below the water surface. The sample taken at the channel bed level is collected from the leading edge of flow. Each sample is carried from the opening to 1 liter sample bottles located inside the sampler. When a sample bottle is full a float valve shuts the supply of incoming water. The captured sample then filters through a built-in filter that separates the sediment from the aqueous phase to prevent a further increase in solute concentration by continued dissolution of soluble minerals.

Each sampler was carried by two people to the streambed and was set upright in a hole measuring 4x3x3.5 ft. It was then leveled and held right with guide wires while concrete was poured around the base. The hole was filled to the level of the bed and compacted after the concrete had cured. The sampler bottles were thereafter inserted, the sampler was loaded, and a profile of the streambed was surveyed.

The first sampler was positioned 1000 ft downstream of the gaging station and approximately 8 miles northwest of Mack. The site was ideal because of the availability of stage and EC data. Also, the channel reach was well defined so that incoming flows did not change location. Moreover, the sampler was easily accessible by vehicle, but not directly visible from the road. The other samplers were similarly installed further upstream (see Fig. 3.5).

4.3 Temporal Variation of EC

Figures 4.8 - 4.10 depict the temporal variation of EC and discharge (Q) during three thunderstorm-induced flow events. Note the initial rise in EC preceding the discharge peak in Figure 4.8. EC also

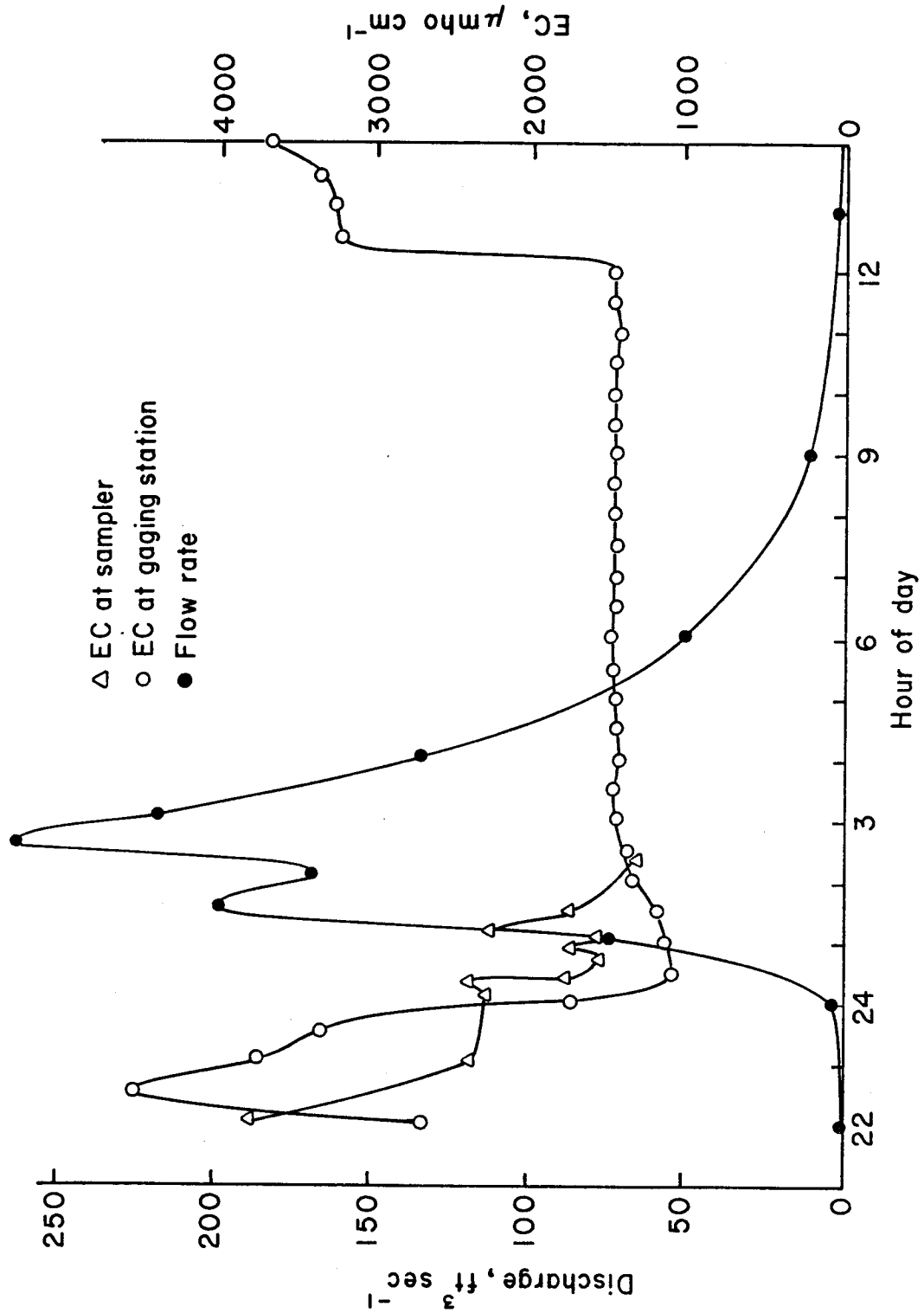

Figure 4.8. Temporal variation of EC and discharge during the March, 1977 flow event at West Salt Creek.

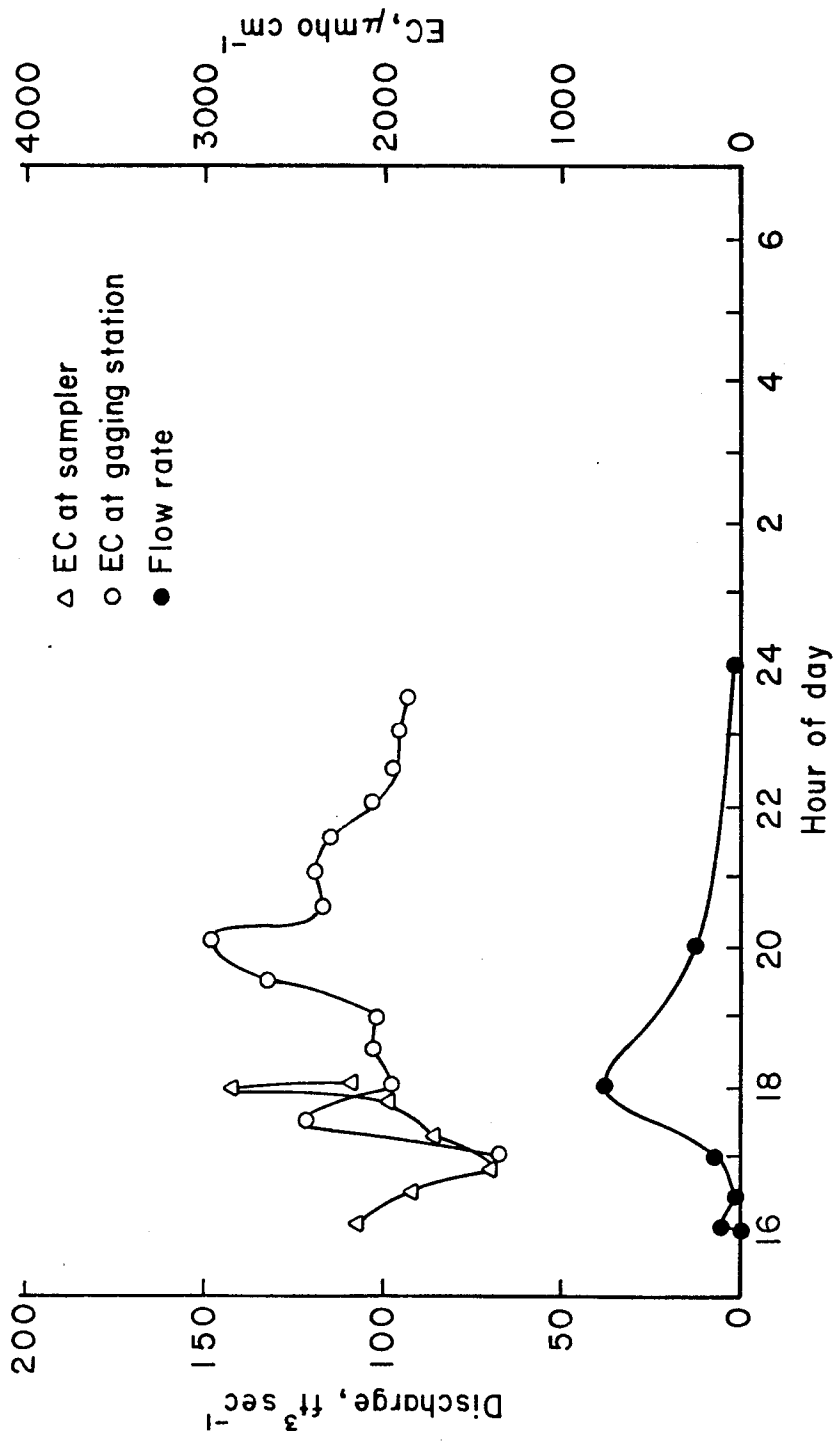

Figure 4.9. Temporal variation of EC and discharge during the November, 1977 flow event at West Salt Creek.

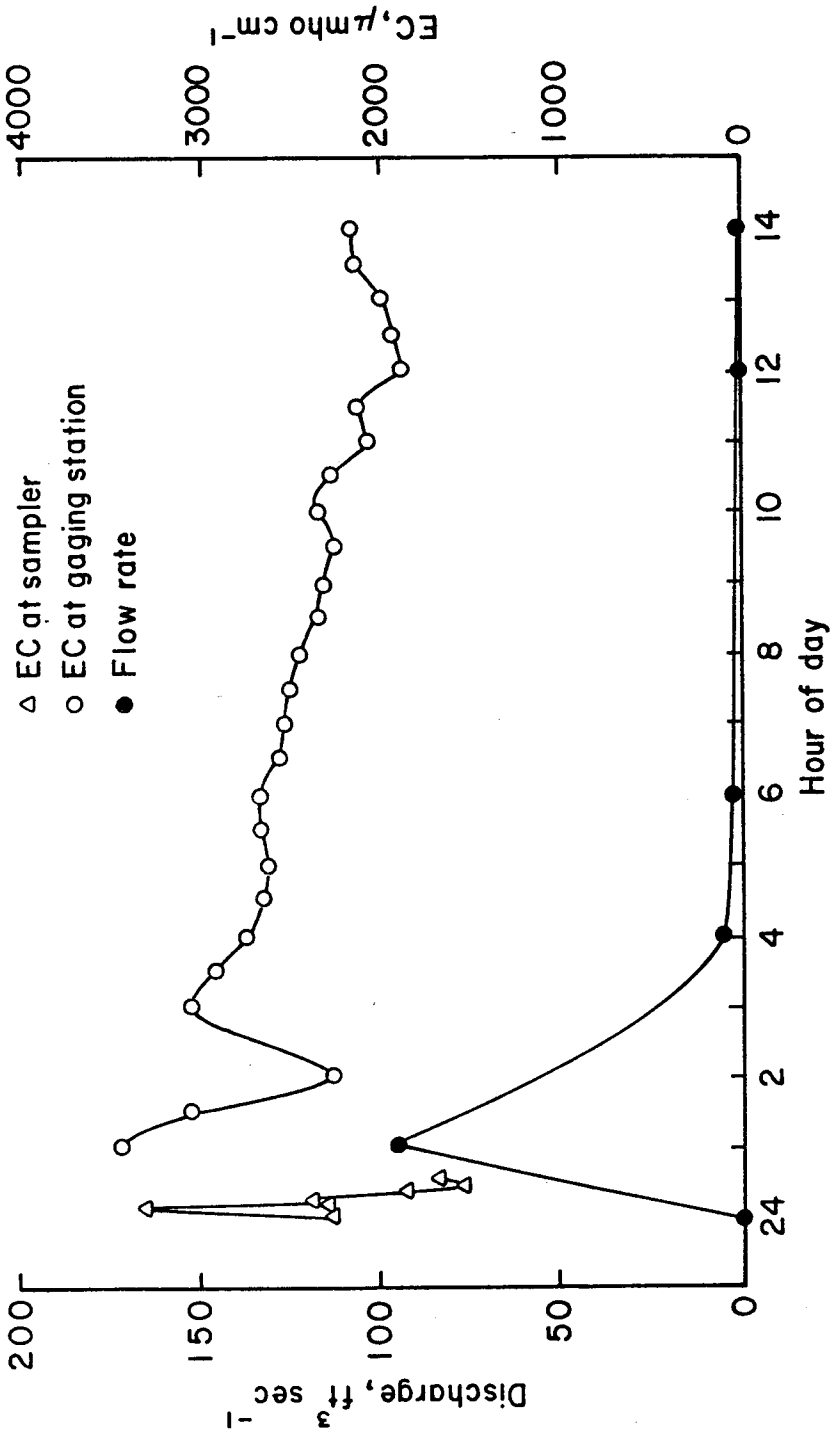

Figure 4.10. Temporal variation of EC and discharge during the May, 1978 flow event at West Salt Creek.

decreased with time during the latter part of the other flow events but the EC-Q relationship is less defined. In fact, it is not a straightforward dilution effect, as evidenced by low correlation coefficients between EC and flow rates (e.g., Figure 4.12).

Figure 4.11 shows the EC *vs* time curve for the leading edge of flow 7 miles upstream of the gaging station during snowmelt. This curve is similar to the ones derived in both hillslope studies and attests to a flushing phenomenon.

4.4 Spatial Variation of EC

During March 16-21 extensive field sampling of snowmelt runoff was undertaken in various tributaries of West Salt Creek. Each day as many locations along the channel as could be reached were sampled. For each flowing tributary these samples were taken from the main channel above the confluence with the tributary, from the tributary proper and from the channel downstream of the confluence at a location in which flow appeared to be well mixed. The EC data for these days are plotted in Figure 4.13. Mile 12 is the upstream and of the Mancos Shale outcrop area.

Interpretation of the data on the downstream variation of EC must be undertaken with care because the stream flowed intermittently depending on the inflow of ground water and daily snow melt variations. In general, the variation of EC along the channel was very large. Nevertheless, it can be seen that 1) overland flow that came directly from snowmelt was of high quality (100-300 μmho/cm), 2) there was a sudden increase in EC downstream of saline seeps and 3) a sudden decrease

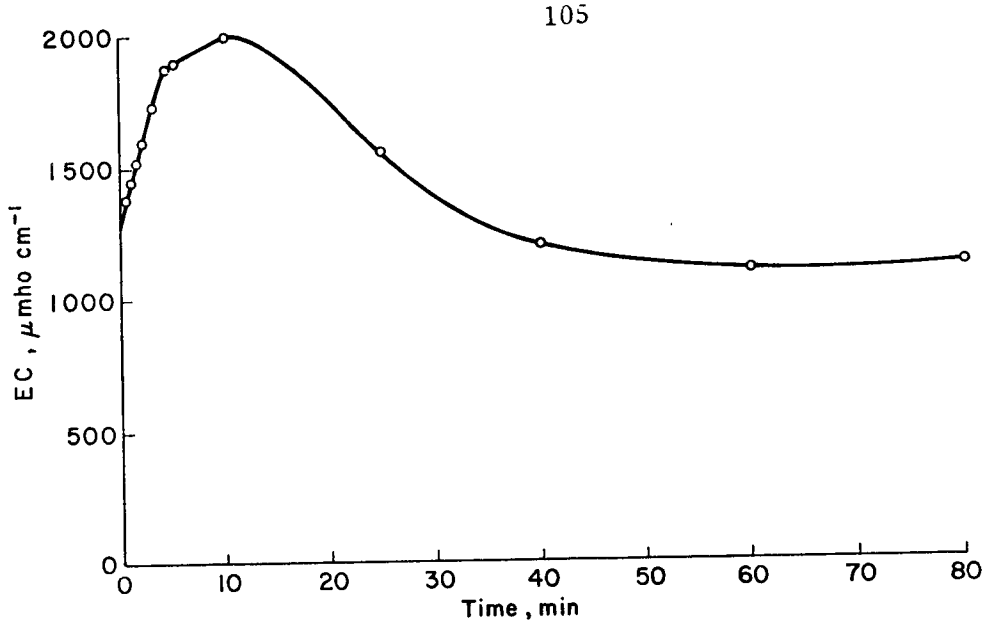

Figure 4.11. EC *vs* time for the leading edge of snowmelt runoff 7 miles upstream of the gaging station on West Salt Creek during March 16, 1979.

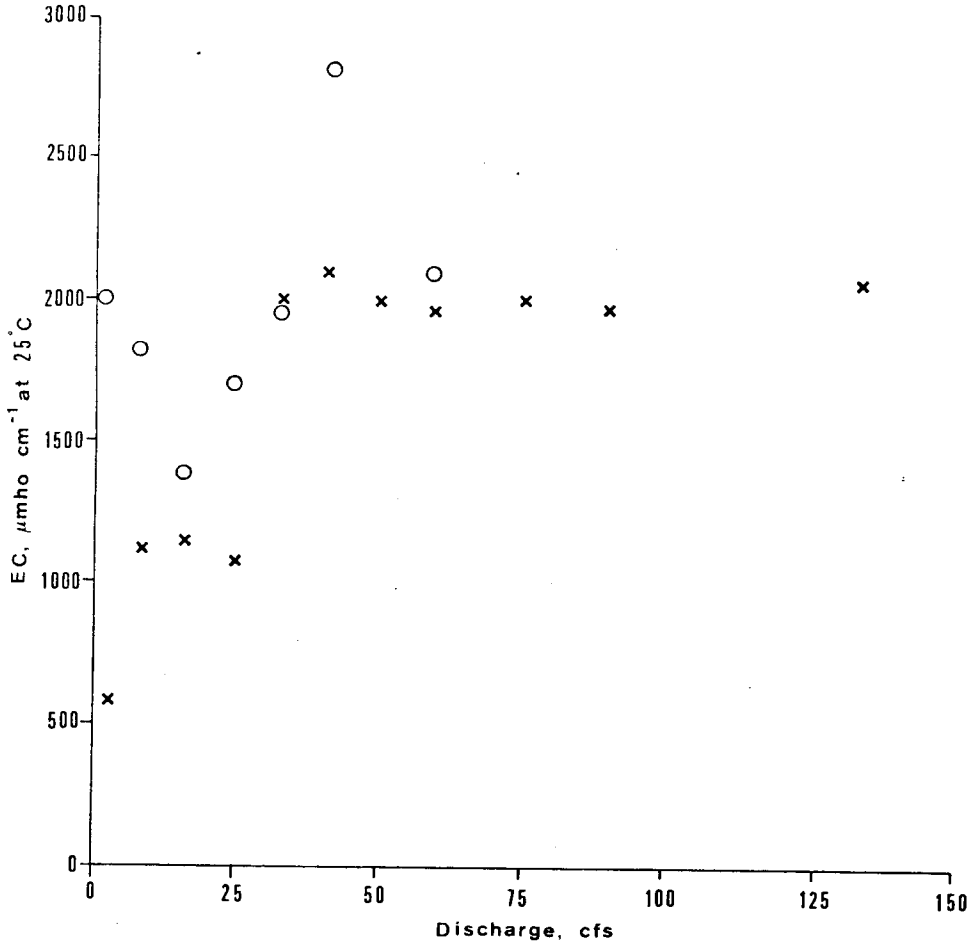

Figure 4.12. EC *vs* discharge during the rising limbs of flow events on October 6, 1977 (Qp=550 cfs) - crosses, and November 6, 1977 (Qp=50 cfs) - circles; West Salt Creek.

(a)

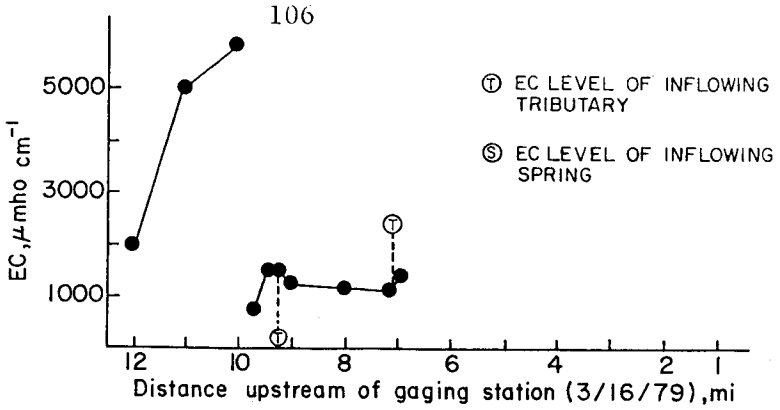

(b)

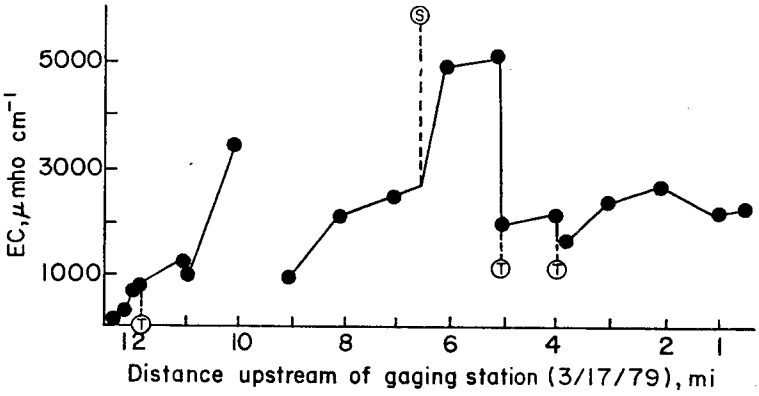

(c)

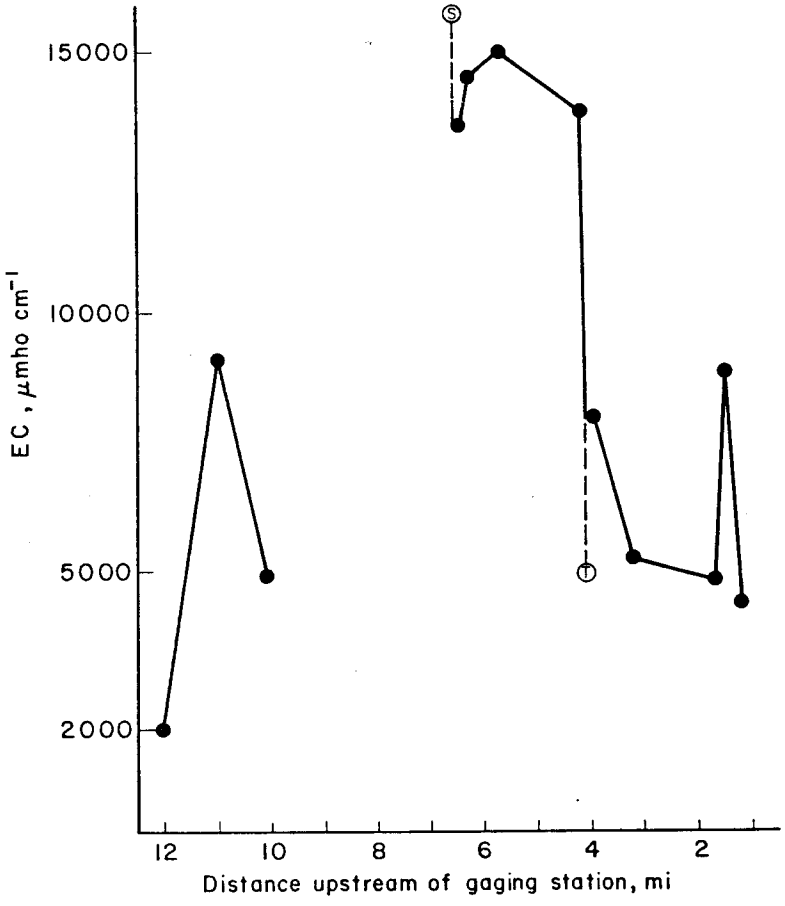

Figure 4.13. Spatial variation of flow EC during the March 16 (a) March 17 (b), and March 19 (c) snowmelt runoff period in West Salt Creek.

in EC downstream of tributaries carrying high quality snowmelt runoff, and 4) there was a general increase in EC as water flowed downstream with little or no influx of groundwater or tributary flow.

4.5 Mineralogy of Transported Sediment and Water Quality

Water samples collected from West Salt Creek underwent chemical analysis. Description of these samples is summarized in Table 4.1. Note that samples 145, 146 and 147 were obtained as grab samples during baseflow. Specific ion and sediment concentration data are summarized in Table 4.2.

Table 4.1. Description of water samples from West Salt Creek.

Sample No.	Sampling Date	Type of Sample and Location
145	7/29/76	Spring (large), Railroad Canyon
146	7/29/76	Spring (small), Railroad Canyon
147	7/29/76	Seep, bed of West Salt Creek near Mitchell Rd
10-6-1 to 10-6-11	10/6/77	Eleven water-stage height samples of a 550 cfs peak flow storm event
3-5-1 to 3-5-11	3/5/78	Eleven water-stage height samples of a 200 cfs peak flow storm event
5-2-1 to 5-2-5	5/2/78	Five water-stage height samples of a 90 cfs peak flow storm event

Note the high salinity of the springs and the saline seep (Table 4.2). This poor quality water derives from the dissolution of Gypsum and more soluble Na-Mg sulfates. The stoichiometric ion concentrations during the three sampled runoff events show that sulfate is the dominant

Table 4.2. Chemical Analyses of Water Samples from West Salt Creek.

Sample No.	pH	SS (mg/ℓ)	Turb. (JTU)	SC (mg/ℓ)	EC (μmho per cm)	Na	Ca	Mg	K	HCO_3	Cl	SO_4
						(meq/liter)						
145	8.1	25	8	2,000	2,370	10.0	7.2	10.8	0.12	6.6	0.41	22.0
146	8.2	18	2	1,880	2,630	18.0	5.5	5.2	0.15	7.6	0.35	22.0
147	7.9	3	<1	7,180	15,800	128.0	19.5	93.0	0.64	11.3	6.9	225.0
10-6-1	7.0				593	1.09	3.70	1.05	0.20	1.36	0.16	4.6
10-6-2	7.0				1,110	1.06	9.50	1.80	0.23	1.36	0.25	10.8
10-6-3	7.1				1,160	1.22	10.0	2.00	0.25	1.25	0.19	12.5
10-6-4	6.9				948	1.65	7.14	1.70	0.22	1.36	0.19	8.7
10-6-5	6.5				2,010	1.38	22.5	2.30	0.35	1.36	0.25	25.0
10-6-6	6.8				2,090	1.14	24.0	2.10	0.36	1.36	0.25	26.0
10-6-7	6.9				2,010	1.13	23.0	2.10	0.34	1.46	0.25	25.0
10-6-8	6.9				1,930	1.13	22.0	2.00	0.32	1.15	0.25	24.0
10-6-9	7.1				2,010	1.71	22.5	2.10	0.37	1.57	0.69	25.0
10-6-10	6.7				1,860	1.62	20.0	2.00	0.33	1.04	0.30	23.0
10-6-11	6.9				2,080	2.71	22.0	2.30	0.34	1.36	0.30	25.0
3-5-1	7.6	46,700		3,780	3,860	17.0	18.2	17.5	0.40	2.87	1.03	50.0
3-5-2	7.9	29,080		2,350	2,430	6.50	14.5	10.5	0.35	1.83	0.49	29.0
3-5-3	7.8	22,150		2,300	2,370	6.50	14.0	10.0	0.30	1.93	0.46	28.0
3-5-4	7.5	85,750		2,190	2,430	8.10	11.5	11.5	0.30	2.77	0.63	31.4
3-5-5					1,880	5.42	11.0	5.25	0.25			
3-5-6	7.8	27,290		1,380	1,594	5.18	7.75	5.75	0.25	1.93	0.44	16.5
3-5-7	7.7	29,480		1,530	1,820	5.42	9.50	5.25	0.20	1.98	0.52	18.5
3-5-8		30,020			1,530	4.72	8.00	5.00	0.20			
3-5-9					2,220							
3-5-10					1,720							
3-5-11					1,290							
5-2-1		1,261			2,273	13.7	6.5	8.25	0.18	4.33	0.65	24.5
5-2-2		2,382			3,333	21.0	7.5	13.12	0.23	3.24	0.93	37.0
5-2-3					2,381							
5-2-4		4,197			2,703	14.7	9.7	10.2	0.24	3.50	0.85	31.0
5-2-5		4,448			1,887	8.4	7.5	6.4	0.20	3.65	0.51	19.0

anion under all flow conditions. The ratios (Ca)/[(Na)+(Mg)] and $(SO_4)/(HCO_3)$ increase as discharge increases, implying that Calcite and even Gypsum precipitation ensue as the contact time of water with sediment (i.e., with time during baseflow) increases with contemporaneous increase in solute concentration.

Supernatants from the sediment water samples were decanted a few days after being collected in the samplers. EC values of mud and filtrates are compared in Table 4.3. Note the overall high EC values of the mud samples which are expected to yield more solutes when diluted. The lower values of the filtrate indicate that the runoff was kinetically unequilibrated during the flow event.

Table 4.3. Comparison of salinity (EC, in μmho/cm) of supernatant and mud-water samples.

Date of storm runoff	10/6/77	11/6/77	3/5/78
Estimated peak flow (cfs)	550	50	200
Date of chemical analyses	12/1/77	12/12/77	3/24/78

Stage levels	Estimated discharge (cfs)	Mud	Filtrate	Mud	Mud	Filtrate	
1	.1		593	2,170	3,885	3,795	
2	1.5	761	1,110	1,821	2,388	2,388	
3	5.2	1,085	1,159	1,397	2,510	2,277	
4	11	1,085	948	1,700	2,510	2,388	
5	21	2,615	2,006	1,962		1,883	
6	25	3,091	2,086	2,833	1,780	1,530	
7	52	2,488	2,006		1,998	1,748	
8	80	2,757	1,931	2,170		1,530	
9	170	2,318	2,006			2,225	
10	205	2,170	1,862			1,718	
11	264	2,757	2,086			1,288	Units

The dissolution of Calcite, Dolomite and Gypsum is evidenced by the detection of these minerals in the sampled sediment during the October, 1977 flow event (Table 4.4). The presence of more soluble minerals, particularly sulfates, is manifested by their identification, though only in trace quantities. Note that the trace amounts result from the dilution of this rare event. Samples from the bed of West Salt Creek below the USGS gaging station were also analyzed for mineral identification by X-ray diffraction. Sample location is shown in Figure 4.14. Gypsum and minor quantities of more soluble sulfates have been identified in the bed material (Table A.1.5). However, the data display no distinct spatial variation in Calcite (Figure 4.15) or in Dolomite (Figure 4.16) predominance neither along the channel nor with depth.

Table 4.4. X-ray diffraction data for the West Salt Creek sediment sampler. Samples are from the storm of 10/6/77. Scale used is 0-10; T - trace.

Sample #	$CaCO_3$	$CaMg(CO_3)_2$	$NaHCO_3$	$Na_2CO_3 \cdot 10H_2O$	$CaSO_4 \cdot 1/2H_2O$	$CaSO_4 \cdot 2H_2O$	Na_2SO_4	$Na_2SO_4 \cdot 10H_2O$	$Na_2Mg(SO_4) \cdot 4H_2O$	$MgSO_4 \cdot 6H_2O$	$MgSO_4 \cdot 7H_2O$
1	----------	----------	----------	----------	---	No Sample	---	----------	----------	----------	----------
2	2	3.5	T	T	T	T	T	T	T	0.5	T
3	2.5	3.5	T	T		T	T	T	T	0.5	T
4	2	3	T	T	T	T	T	T	T	0.5	T
5	2	3.5	T	T		T	T	T	0.5	0.5	T
6	2	5	T	T		T	T	T	T	T	T
7	2	3.5	T	T	T	T			0.5	T	T
8	2.5	3.5			T	T	T	T		1	T
9	8	4.5			T	T	T	T	0.5	1	T
10	2	5	T	T	T	T	T	T	T	T	T
11	2	5	T		T	0.5	T	T		T	T

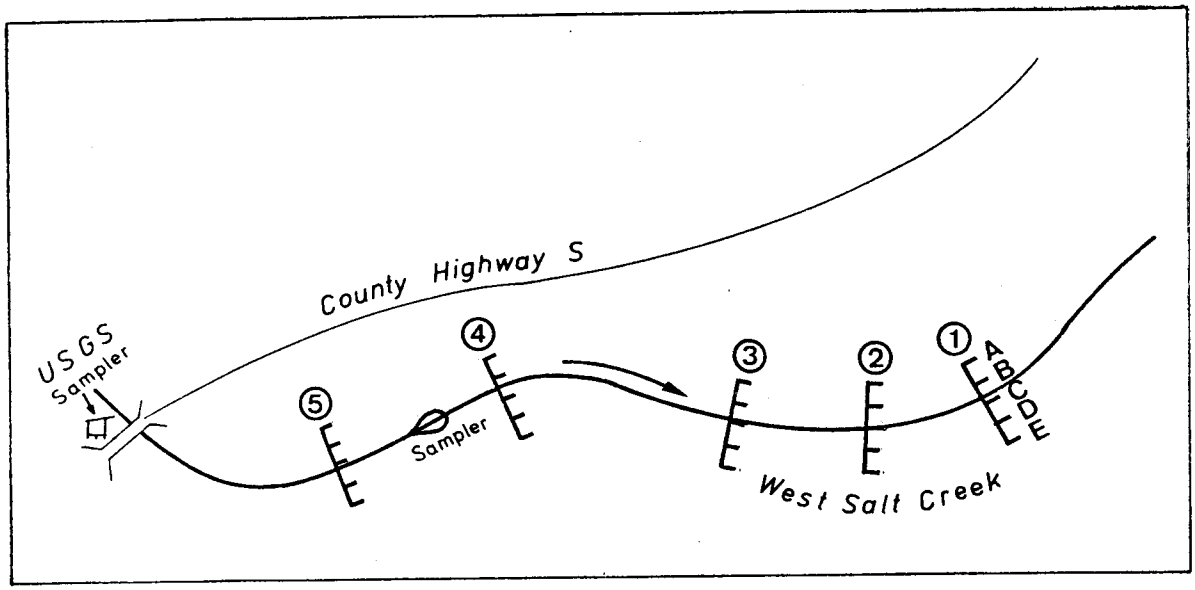

Figure 4.14. Location of samples collected from the bed of West Salt Creek.

4.6. Discussion

The temporal variation of EC of West Salt Creek runoff has an initial peak which precedes the water discharge peak. Thereafter, EC decreases asymptotically or else increases much later during base-flow. Such temporal trends may be explained by a surface phenomenon whereby weathered material in the surface and surficial accumulation of saline deposits are flushed.

The later increase in EC is attributed to flow from saline seeps. In fact, the increase in flow EC due to saline seeps is evidenced in Figures 4.10 and 4.11.

The chemical quality of West Salt Creek runoff is principally determined by the dissolution of Gypsum; it is affected by the dissolution of both less soluble minerals (Calcite and Dolomite) and of more soluble sulfates.

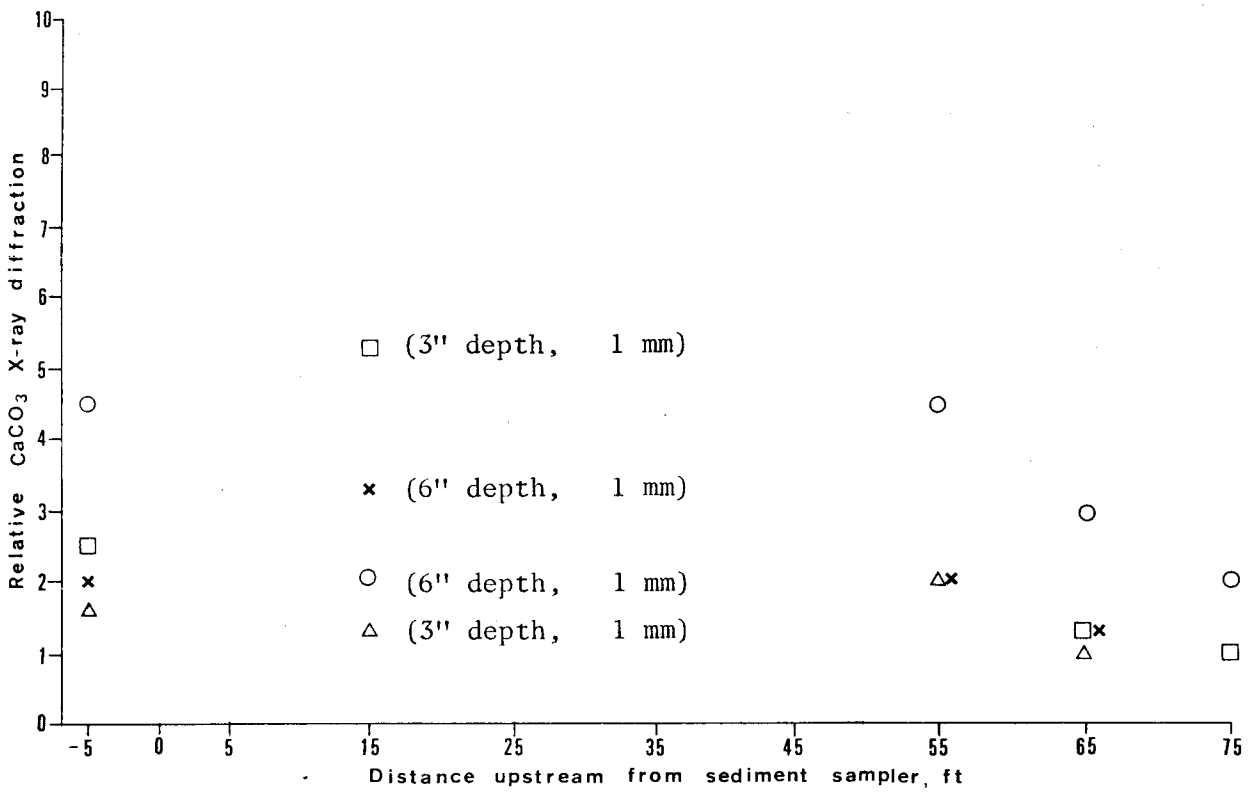

Figure 4.15. Spatial variation of relative Calcite X-ray diffraction in the West Salt Creek bed material.

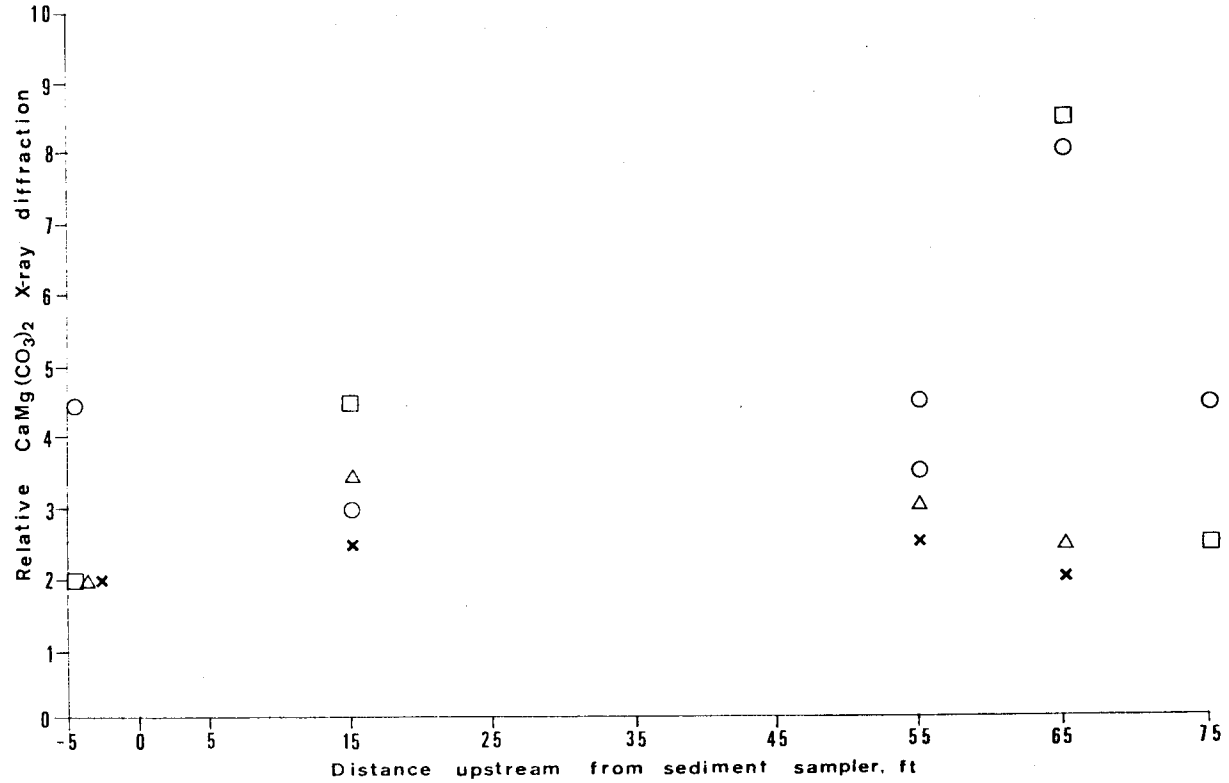

Figure 4.16. Spatial variation of relative Dolomite X-ray diffraction in the West Salt Creek bed material. Symbols denote sample depth and particle size as in Fig. 4.15.

Snowmelt runoff had a consistently low solute concentration, and it is, therefore, expected to add only minor quanitities of solutes to the yearly solute yield of West Salt Creek. Runoff is equilibrated with respect to carbonates and usually also with respect to Gypsum. Moreover, runoff is also kinetically undersaturated with respect to Gypsum and to more soluble sulfates. Hence, West Salt Creek runoff reaching the Colorado River is expected to yield considerably higher quantities of solutes than those determined solely from EC measurements.

CHAPTER 5

ESTIMATION OF SOLUTE YIELD FROM DIFFUSE SOURCES AND DELINEATION OF HAZARD AREAS

Calculation of the mass of solutes (M) transported from a given basin is essential in order to delineate hazard areas. The first part of this chapter deals with estimation of solute yields from natural diffuse sources in the whole Upper Colorado River Basin, in a selected small tributary (West Salt Creek) and in the Grand Valley. The second part deals with identification of hazard areas on a site specific case and on a larger scale.

5.1. Estimation of Solute Yield

5.1.1. Upper Colorado River Basin

Procedures to calculate M are described in this chapter. They are not based on a mass balance involving dissolution, transport and precipitation of solutes because there is insufficient data and information to undertake such a calculation. Rather, M is calculated from the volume of saline water discharged from diffuse sources (V) and its solute concentration (SC) as follows:

$$M = \gamma VSC \tag{5.1}$$

where γ denotes the specific weight of the bulk solution (i.e., water and solutes). Estimation of V is accomplished by examining the saline outflow from diffuse sources in the Grand, Green and San Juan Divisions obtained by superimposing hydrologic and salinity information (Figures 5.1-5.3) on a map of mean annual precipitation (Figures 1.5-1.7). Respective values for these three divisions are 25, 35, and 20 percent. Each of these percentages is weighted by its respective contribution to the total water discharge of the Colorado River at Lees Ferry, Arizona.

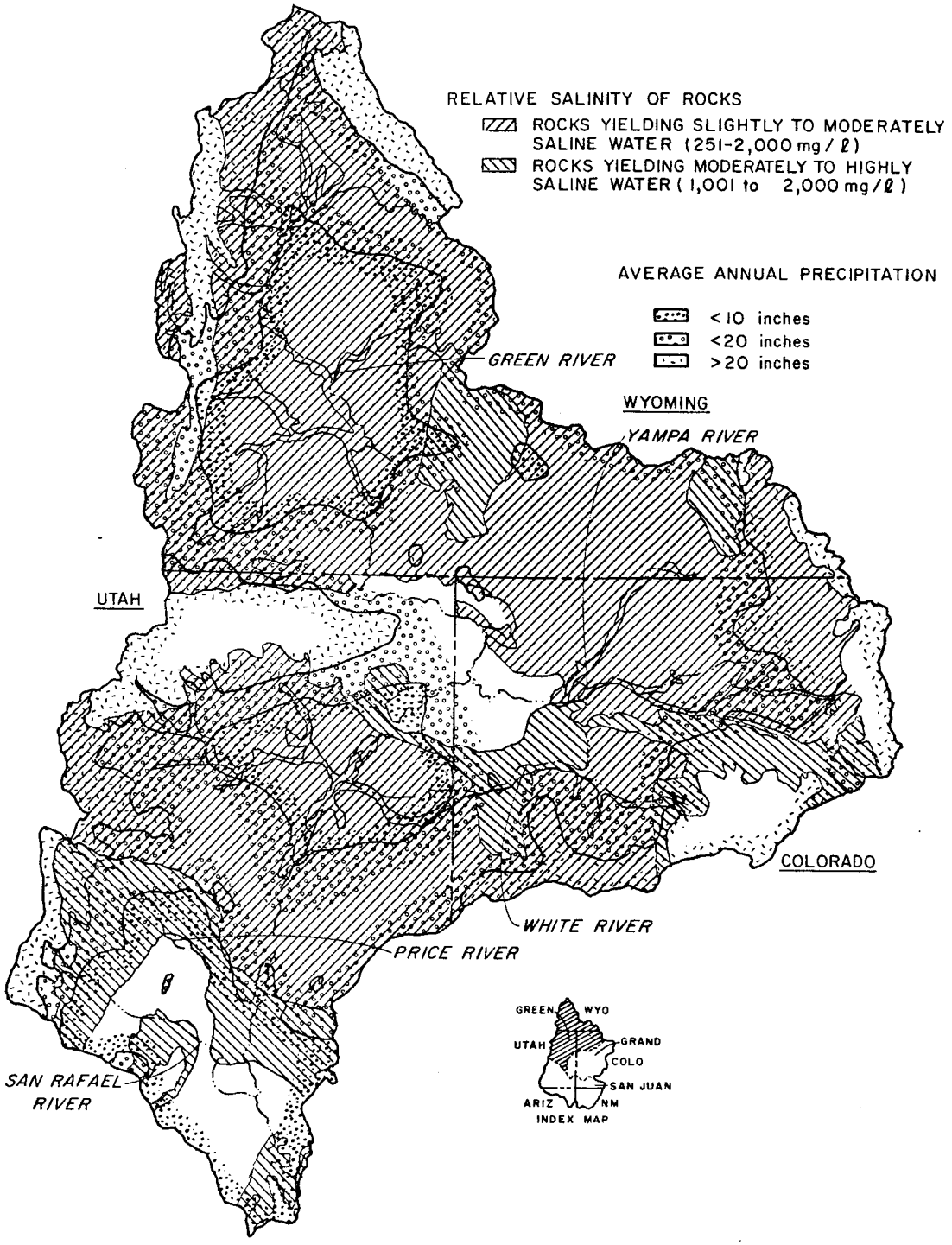

Figure 5.1. Relative salinity of rocks and mean annual precipitation in the Green River Basin.

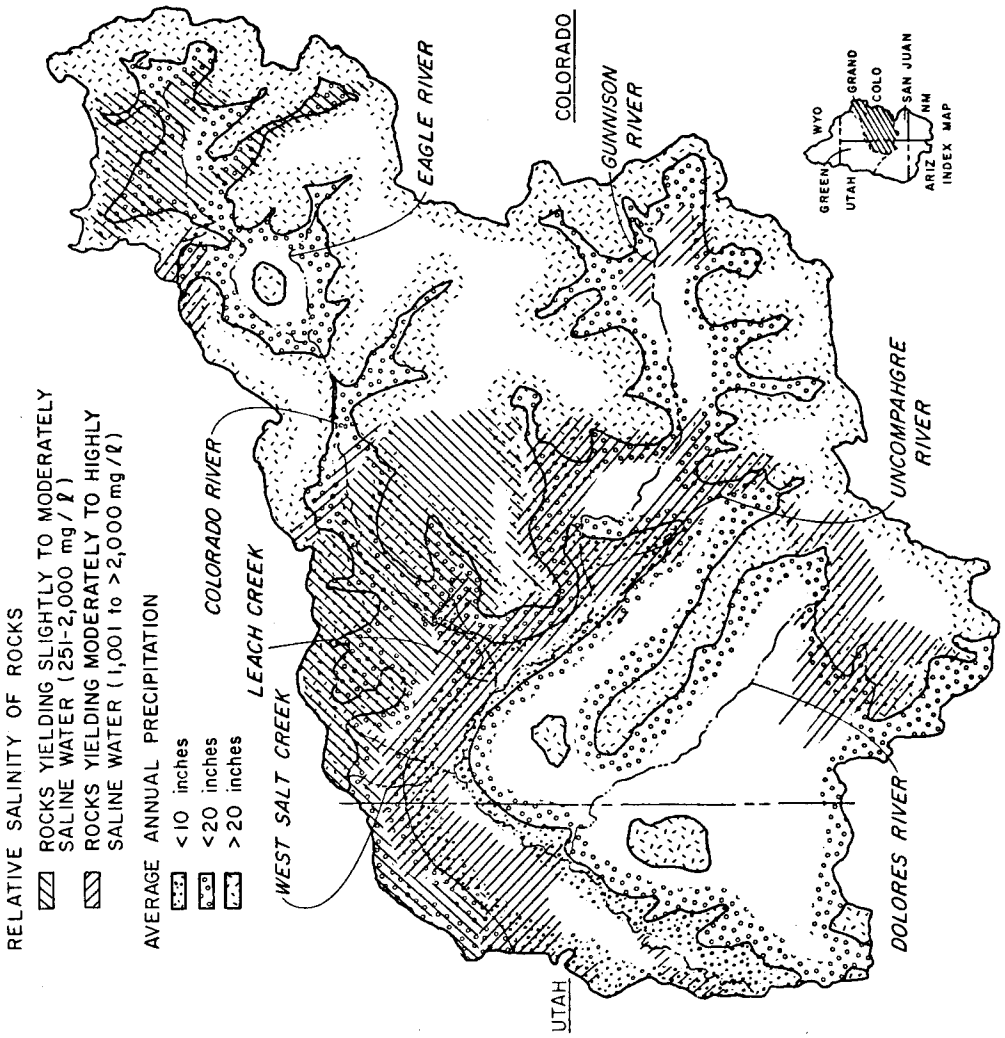

Figure 5.2. Relative salinity of rocks and mean annual precipitation in the Grand River Basin.

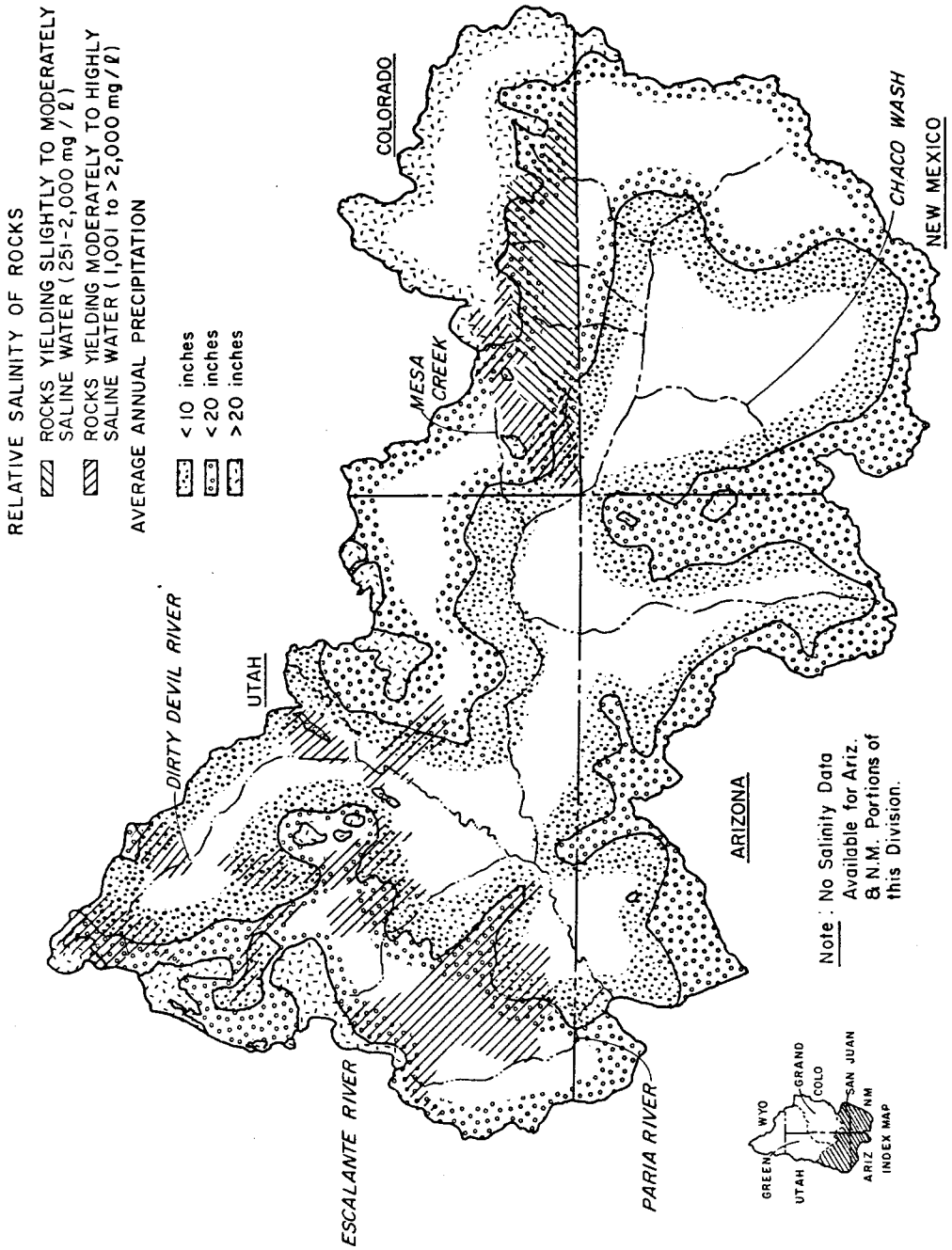

Figure 5.3. Relative salinity of rocks and mean annual precipitation in the San Juan River Basin.

Thus, the Grand River, which drains a smaller area of saline soils than the Green River, has a comparable effect on V because it yields 44 percent of the total flow at Lees Ferry, while the Green River contributes less, only 37 percent. The San Juan River contributes the rest, 19 percent.

Thus, the weighted average volume of saline outflow is equal to

$$V = .44\ (25\%) + .37(35\%) + 19\ (20\%) \qquad (5.2)$$

or 28% of the total volume of water passing Lees Ferry annually (i.e., 12,733,100 acre-feet).

Calculation of the weighted mean concentration of solutes (SC in mg/l) is based on the product of the weighted mean EC (in μmho/cm) times the constant K (equal to 0.65). Mean EC, the EC of overland and rill flow entering the channel from hillslopes, is derived from the regression of EC against slope inclination averaged over time (Figure 3.17).

Using an average value of 15 percent inclination of contributing hillslopes, EC is equal to 1400 μmho/cm and SC = 910 mg/l. For this assumption involving steep hillslopes, the mass of solutes from the entire Upper Colorado River Basin is $4.4 \cdot 10^6$ tons of solutes. This value is 51 percent of the total $8.64 \cdot 10^6$ tons/year of solutes passing Lees Ferry, assuming a non-varying basin-wide water yield.

Classification of the diffuse source areas according to weighted mean hillslope inclination, in fact, must also consider that the size of such drainage areas depends on S, their inclination. For instance, a region the area of which has been measured from a map to be 950 mi^2 sloping an average 18° is, in fact, 1000 mi^2 (an increase of 21 percent). Thus, as hillslope inclination increases so do EC as well as the actual contributing area increase.

A mean hillslope inclination of 15 percent may be too high. A more thorough analysis of mean inclination should be based on a modified version of Horton's (1926) determination of mean land slope. Changing mean inclination to 10 and 20 percent yields respective estimates of 44 and 58 percent of the total solutes contributed from Mancos Shale. While there is, admittedly, a wide range in these estimates, even the lowest is substantially larger than the 0.5 percent figure suggested by Ponce and Hawkins (1978).

Estimates of solute yield from diffuse sources in the Upper Colorado River Basin presented herein are preliminary. Discussion of a more detailed and accurate calculation procedure is given in Chapter 6.

5.1.2. West Salt Creek Basin

The first step in providing a rough estimate of the solute load of West Salt Creek is to determine the quantity of soluble minerals transported as particulate matter (suspension and traction load) that dissolve in the Colorado River. Such a late dissolution is brought about by dilution if the West Salt Creek flow is saturated with respect to any of the transported soluble minerals. In fact, samples of streamflow from West Salt Creek were saturated with respect to Gypsum at about 2000 μmho/cm, well undersaturated at 1200 μmho/cm and saturated or undersaturated between these values (Chapter 4). This means that West Salt Creek flow events with EC values above 2000 μmho/cm contribute additional solutes to the Colorado River when diluted by its water.

Furthermore, it has been shown (Laronne, 1977) that the time

necessary to reach 90 percent dissolution ranges from 0.5 to 24 hours for a suspended sediment concentration of 105 ppm to 0.25 - 10 hours at 10^4 ppm, which indicates that the sediment is initially kinetically unstable. Laronne (1977) estimated that soluble minerals (primarily Gypsum) transported as particulate matter can continue dissolving, thereby increasing the total solute load by as much as 500 percent over the solute load calculated from EC data obtained in the field. Assuming a mean velocity of flow of 5 ft/sec, the transported sediment can continue dissolving in a river stretch 1.4-131 km long from its source.

Unfortunately, it is beyond the scope of this study to incorporate the effect of all the sediment associated variables upon solute yield. Estimates of solute yield made hereafter exclude the affects of kinetic disequilibrium and dilution of undersaturated solutions.

5.1.2a. Standard Procedure of Estimation

Only three years of hourly records are complete for the period of record available (August 1973 - May 1978) to an extent whereby they may be used to calculate yearly solute production from West Salt Creek. These years include 1974, 1976 and 1977.

The stage strip charts from the USGS gaging station 09153400 at West Salt Creek were examined and average flow rates for appropriate time intervals were recorded. The EC values were read from the gaging station EC records and the average EC values were determined for the intervals of the recorded flow rate. Flow rate intervals were adjusted if large changes in EC occurred during periods of steady flow. The following equation was used to determine the solute load (pounds) for each time interval.

$$0.18\ I\ Q\ (EC) = \text{Solute Load} \qquad (5.3)$$

where, I is the length of the time interval used in hours, Q is the average flow rate during interval I in cubic feet per second, EC is the average value for the interval I in μmho/cm and 0.18 is a conversion factor that changes EC into pounds of dissolved solids per cubic foot of flow and I into seconds. The loads for each interval were summed to determine the total solute load for the year. Table 5.1 shows the values of Q, EC and I used to determine the load for each day of the 1977 water year. Mean annual yields are summarized in Table 5.3.

Analysis of available discharge and EC data for West Salt Creek has shown that monthly solute loads may be closely approximated by a simplified method (see Table 5.3). The appropriate equation is

$$SL = K\ (\overline{EC})\ V \qquad (5.4)$$

where the monthly solute load (SL) is equal to the product of K (= 2.32 for $(\overline{EC})$ < 2000 μmho/cm; = 2.69 for $(\overline{EC})$ > 2,000 μmho/cm), which converts EC to pounds per acre-feet, and V is the monthly flow volume reported in acre-feet. The variable $(\overline{EC})$ is the monthly flow weighted average EC in μmho/cm, and is determined according to

$$(\overline{EC}) = (\Sigma_{i=1}^{m}\ EC_i\ Q_i)/\Sigma_{i=1}^{m} Q_i \qquad (5.5)$$

where EC_i and Q_i are the daily average EC (in μmho/cm) and discharge (in cfs) respectively, as reported by the USGS publication Water Publication Data for Colorado.

5.1.2b. Estimation Based on Hillslope Study II

The following procedure was developed in order to estimate the annual solute load of West Salt Creek based on the results of Hillslope Study II (Chapter 3). For each plot a solute load (mass of solutes per

Table 5.1. Data from U.S.G.S. gaging station 09153400 used to determine salt load for the 1977 water year.

DATE	(hrs)	Q (cfs)	EC (mho/cm)	LOAD (lb)
10/2	1.5	35	1325	12521
	1	26	1400	6552
				19073
10/3				
	.25	26	1450	1670
	.50	157	1450	20488
	.75	81	1400	15309
	1	78	1300	18252
	1	102	1330	24419
	1.5	82	1375	30442
	4	40	1200	34560
	4	14	1100	11088
	6	4	1250	5400
	3.5	.52	950	1729
				163357
10/4	6	.31	900	301
	6	.07	900	68
				369
7/21	.5	4.75	2650	1133
	.75	1.48	2710	752
	.50	3.75	2900	979
	1.25	2.33	2700	7864
	2.00	.66	1900	451
	3.00	.17	1800	918
				12097
8/18	0.50	.04	2100	8
	0.50	.04	2200	9
	0.25	20.25	2200	2005
	1.00	43.0	2250	17415
	1.75	25.38	2200	17588
	3.25	12.19	1900	13549
	2.25	2.18	1900	1678
	1.25	3.44	1900	1471
	4.25	5.57	1950	8309
	6.0	.60	1880	1218
	3.0	.15	1400	113
				63362
8/24	8.0	.03	1300	56
	3.0	6.05	1350	4410
	6.0	.97	1350	1414
	3.0	.10	1350	73
				5953
8/25	11	.94	1250	2326
	1	.90	1350	219
	2	.88	800	253
8/27	3	1.14	1000	616
	3	11.25	1370	8323
	6	.66	1400	998
	6	.73	1600	1348
	6	1.04	1600	1797
				15880
8/28				
	8	.06	1600	138
	2	.06	1250	27
	6	.06	1000	65
				230
9/11	3	1.05	2200	1247
	14	1.05	1550	4101
				5348
9/15	1	1.0	1100	198
	7	1.0	1270	1600
	1	1.0	1350	243
	3	1.0	1400	756
	1	1.0	1250	225
	1	1.0	1185	213
				3235

inch rainfall per plot wetted surface area) was determined. These values are plotted on Figure 5.4 against the gradient of the plot. This presentation of solutes derived from each plot provides an estimate of the quantity of solutes produced per square mile per inch of applied rainfall. In Figure 5.4 these values are plotted against hillslope inclination.

The second step of this estimation procedure involves the determination of the percent of the total area for each slope interval. A standard topographic quad map was used as a base and the lower West Salt Creek basin was sectioned into squares (0.25 mi^2). Average contour pattern and number of contours were used to tabulate this data (Table 5.2). The percent of the lower basin area covered by shale badlands was estimated using a recent SCS (1978) survey.

Table 5.2. Percent of lower West Salt Creek Basin with varying hillslope inclinations.

Slope interval (degrees)	0-5	5.1-10	10.1-15	15.1-20	20.1-25	25.1-30	30.1+
% of lower basin area	56	26	10	7	0.9	0.2	0.1

The information from Figure 5.4 and Table 5.2 was used to derive the following solute load (SL, short tons) equation:

$$SL = 491\ P\ B \qquad (5.6)$$

where P is total precipitation during the "summer" months and B is a runoff coefficient similar to the one used in the rational formula. The constant 491 was determined from soil type and hillslope inclination as detailed by Enck (Appendix D, 1981).

Annual solute loads for West Salt Creek using both procedures are summarized in Table 5.3. It is realized that this procedure is an

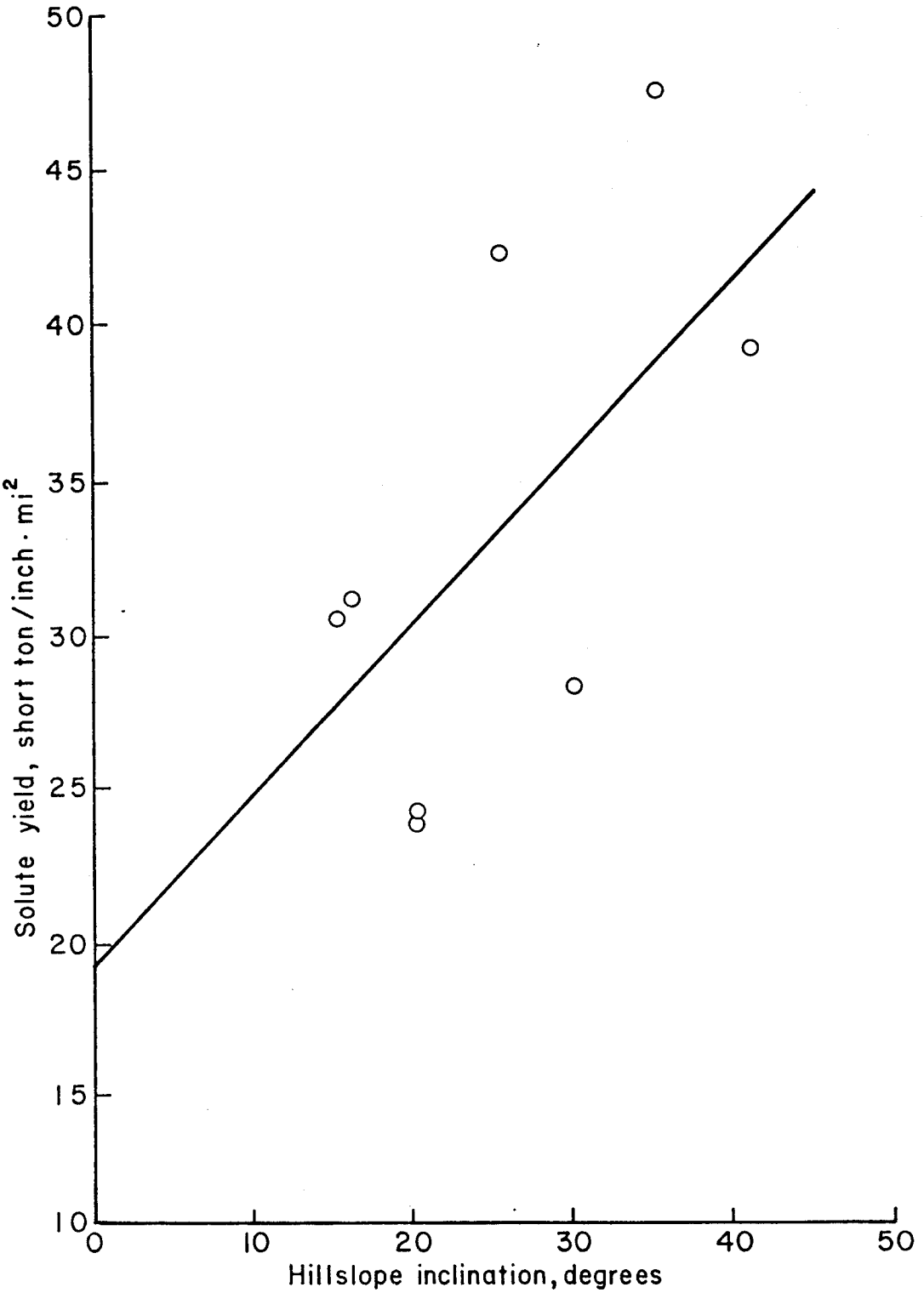

Figure 5.4. Variation of solute yield with hillslope inclination based on Hillslope Study II. The metric equivalent ($t/100mm \cdot Km^2$) of sediment yield values is calculated by dividing ordinate values by 1.72.

oversimplification of the dissolution-salt loading process. The major problem is that rainfall is not linearly related to runoff; one must ideally consider intensity, duration, frequency and antecedent conditions in order to determine runoff volumes.

Table 5.3. Annual solute loads from West Salt Creek calculated by different procedures.

Year	"Summer" Precipitation (in)	Solute Load (short tons) Standard Procedure	Simplified Procedure	Hillslope II Procedure
1974	2.08	702	717	508
1975	2.87	-	-	701
1976	4.98	1700	2092	1217
1977	3.13	144		765

It can be seen in Table 5.3 that the annual loads do not vary directly with summer precipitation; therefore, the estimation equation can overestimate or underestimate the loads for any given year. All in all, this is a quick inexpensive methodology; however, it is not a very accurate method to determine short term loads for ungaged watersheds.

5.1.2c. Long Term Frequency Analysis of Solute Load

By using the flow-duration curve that has been derived from long term precipitation records (see Enck, 1981), the expected long term solute load from the West Salt Creek can be estimated. From this curve the duration of expected flows can be determined. Flow rates, when combined with an average EC value, produce an estimate of the long term load. An average EC value of 3068 μmho/cm was determined using a flow weighted average of all of the available EC records for West Salt Creek. (As noted in Chapter 3, an attempt to correlate EC and flow rate was unsuccessful).

The procedure used to estimate a 50 year solute load is outlined in Table 5.4. The calculations show that if climatic conditions have been similar for the past 50 years, $3.6 \cdot 10^8$ lb or $1.8 \cdot 10^5$ short tons of salt may have been produced by West Salt Creek.

Table 5.4 Estimation of 50 year solute load of West Salt Creek

(1) Discharge (cfs)	(2) Time exceeded (adjusted with precip. data) (%)	(3) time column(1) flow expected (%)	(4) time column(1) flow expected (hr)	(5) V, water volume (ft)	(6) dissolved mineral load (lb)*
.1	5.9	.6	2628	9.5×10^5	$1.6 \cdot 10^5$
1.0	5.3	.3	1314	4.7×10^6	$8.4 \cdot 10^5$
5.0	5.0	.2	876	1.6×10^7	$2.8 \cdot 10^6$
10	4.8	1.8	8760	3.2×10^8	$5.6 \cdot 10^7$
25	3.0	.1	438	3.9×10^7	$7.0 \cdot 10^6$
50	2.9	.7	3066	5.5×10^8	$9.8 \cdot 10^7$
100	2.2	.2	876	3.2×10^8	$5.6 \cdot 10^7$
250	2.0	.2	876	7.9×10^8	$1.4 \cdot 10^8$
					$3.6 \cdot 10^8$

*Solute load = $(0.0000053\ \overline{EC}^2 + 1.05\ \overline{EC} - 348.4).000062V$

5.1.3 Grand Valley and Selected Tributaries

The simplified procedure was adopted in order to estimate the relative contribution of solutes from natural and man-affected diffuse source areas in the Grand Valley and its vicinity. 1976 data were used to calculate the annual or seasonal solute concentrations for nine tributaries of the Colorado River and four of its reaches (denoted A-D, see Figure 5.5). The calculated annual solute load was divided by the annual volume of flow. An average value of 600,000 acre-feet of water diverted from the Colorado River for irrigation was used in this calculation (Leathers and Young, 1976).

Calculated mean annual solute loads are summarized in Table 5.5. Note that the highest loads derive from baseflow during the non-irrigation period (November-March), and that natural diffuse sources contribute appreciably more solutes than irrigation return flow and tailwater during irrigation months. This statement is particularly true when considering solute loads (equal to the product of solute yields times the respective drainage areas).

5.2 Delineation of Hazard Areas

Salt loading from wildland areas appears to be an unmanageable problem because of the diffuse nature of the solute pickup process; vast areas of exposed saline soils are located throughout the Upper Colorado River Basin. However, the quality of runoff is highly variable. Areas that potentially contribute large quantities of solutes and specifically large quantities of saline water can be defined and delineated by isolating those factors that control high salt loads and yields, respectively. Delineating areas that produce high solute yields is the essence of the salinity management problem. High solute loads (expressed as weight per unit time) are not problematic as long as solute concentrations, equivalent to solute yields, remain low. The feasability of effective mitigation measures could be greatly increased if relatively small, well-defined areas producing high solute yields can be identified as salinity hazard areas.

Table 5.5 Mean annual (1976 water year) solute yields and relative hazard, selected tributaries and Colorado River reaches in the Grand Valley region.

Stream or Reach	Solute Yield (tons/acre-foot)	Comments on the origin of flow (U.S.G.S., 1976)	Relative hazard of source area*
Reed Wash	6.9	Base flow from irrigation returns during non-irrigation months (November through March).	1 (5.0+)
Adobe Creek	6.4		
Leach Creek	6.1		
Big Salt Wash	5.4		
San Rafael River and Price River	4.8	Mean annual of returns from natural sources and 42,000 acres (4% of drainage basin) and 18,000 acres (2%) of irrigated land for the San Rafael and Price Rivers, respectively.	
West Salt Creek	4.7	Yearly average of returns from snowmelt and precipitation nduced runoff from natural sources induced.	2 (3-4.9)
East Salt Creek	3.6		
Reach B (The Grand Valley)	3.5		
Big Salt Wash	2.3	Base flow from irrigation return and tailwater during irrigating months (April through October).	
Reed Wash	2.1		
Adobe Creek	1.9		
Leach Creek	1.9		
Reach D (Colorado River above the Colorado-Utah Border)	1.31	All types of flow entering the Colorado River above Cisco, Utah.	3 (1-2.9)
Reach C (Colorado River above the Colorado-Utah border)	1.25	All types of flow entering the Colorado River above the Utah-Colorado border.	
Gunnison River above confluence with the Colorado River	.99	All types of flow entering the Gunnison River above its confluence with the Colorado River.	4 (0-0.9)
Reach A (Colorado River above Cameo, Colorado)	0.73	All types of flow entering the Colorado River above Cameo, Colorado.	

*range of respective solute yields in parenthesis

Solute yields depend on the following three criteria: 1) availability of soluble minerals, 2) availability of runoff, and 3) availability of potential energy. The first criterion listed above is synonymous with soluble mineral content and in general corresponds to the solute concentration of subsurface water. Areas that meet this first criterion (i.e., saline exposures) may be mapped using existing data. High (surface and subsurface) water yields may be related to precipitation, although it is realized that evaporative losses vary such that the rainfall-runoff relationship is non-linear. Areas meeting this requirement of high precipitation may also be delineated using existing data. The last criterion, high transport capacity, is indicated by hillslope steepness, which can be traced from existing topographic maps.

5.2.1. Upper Colorado River Basin

Areas that meet the first two criteria have been delineated using existing maps of rock salinity and precipitation (Figures 5.1 - 5.3 and 1.5a - 1.5c) from which areas were identified as follows: Hazard I areas (Figure 5.6) include regions that receive more than twenty inches of mean annual precipitation and Hazard II areas receive less precipitation; both areas, however, yield moderately to highly saline surface and groundwater flow (see Figures 5.6 - 5.8). The delineated hazard areas can be further reduced in size by examining relief maps of the relevant subbasins. Results of field studies (chapter 3) and indirect implications from laboratory experiments (chapter 2) show

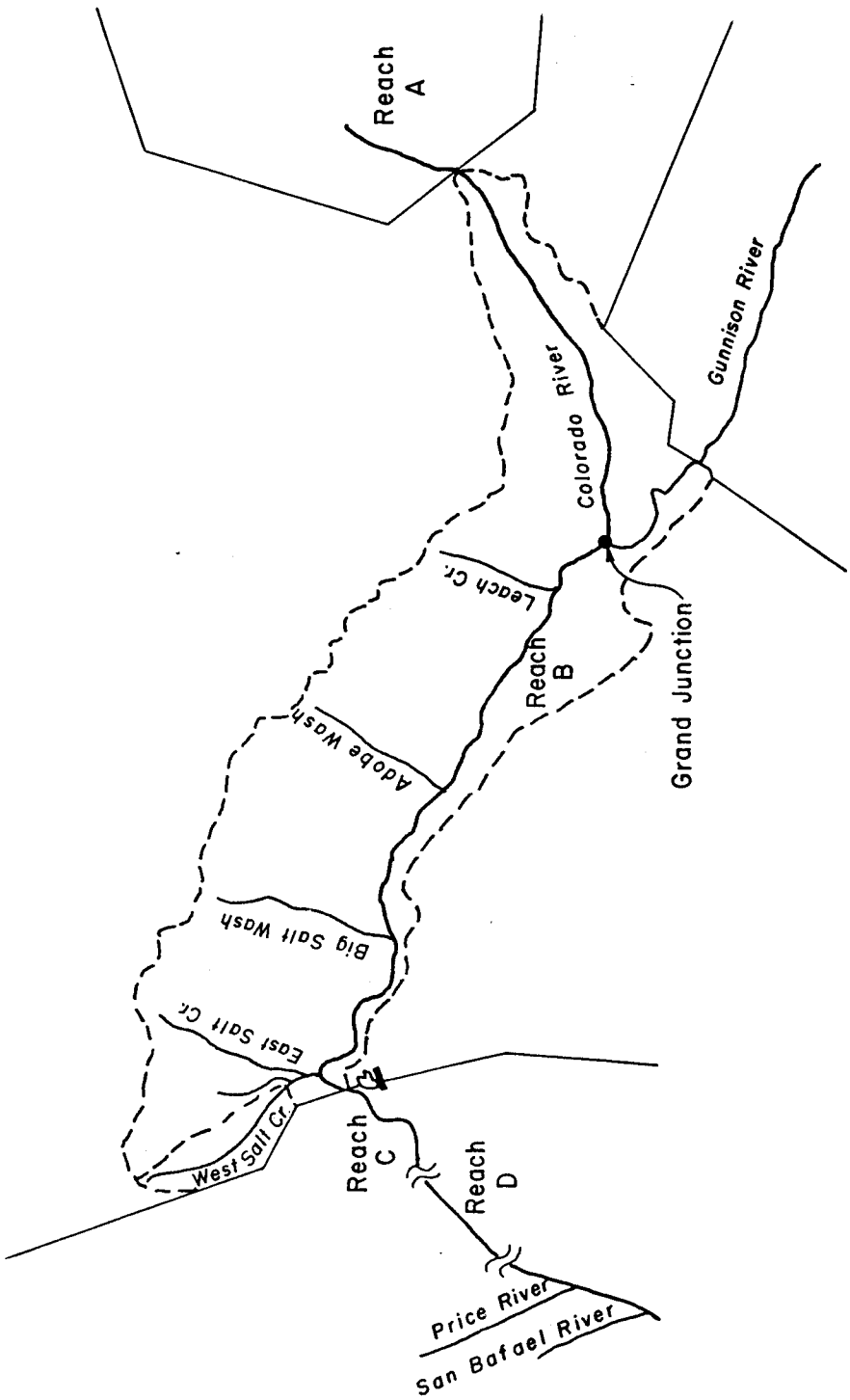

Figure 5.5. Schematic map of the Grand Valley and vicinity showing the location of selected tributaries and channel reaches.

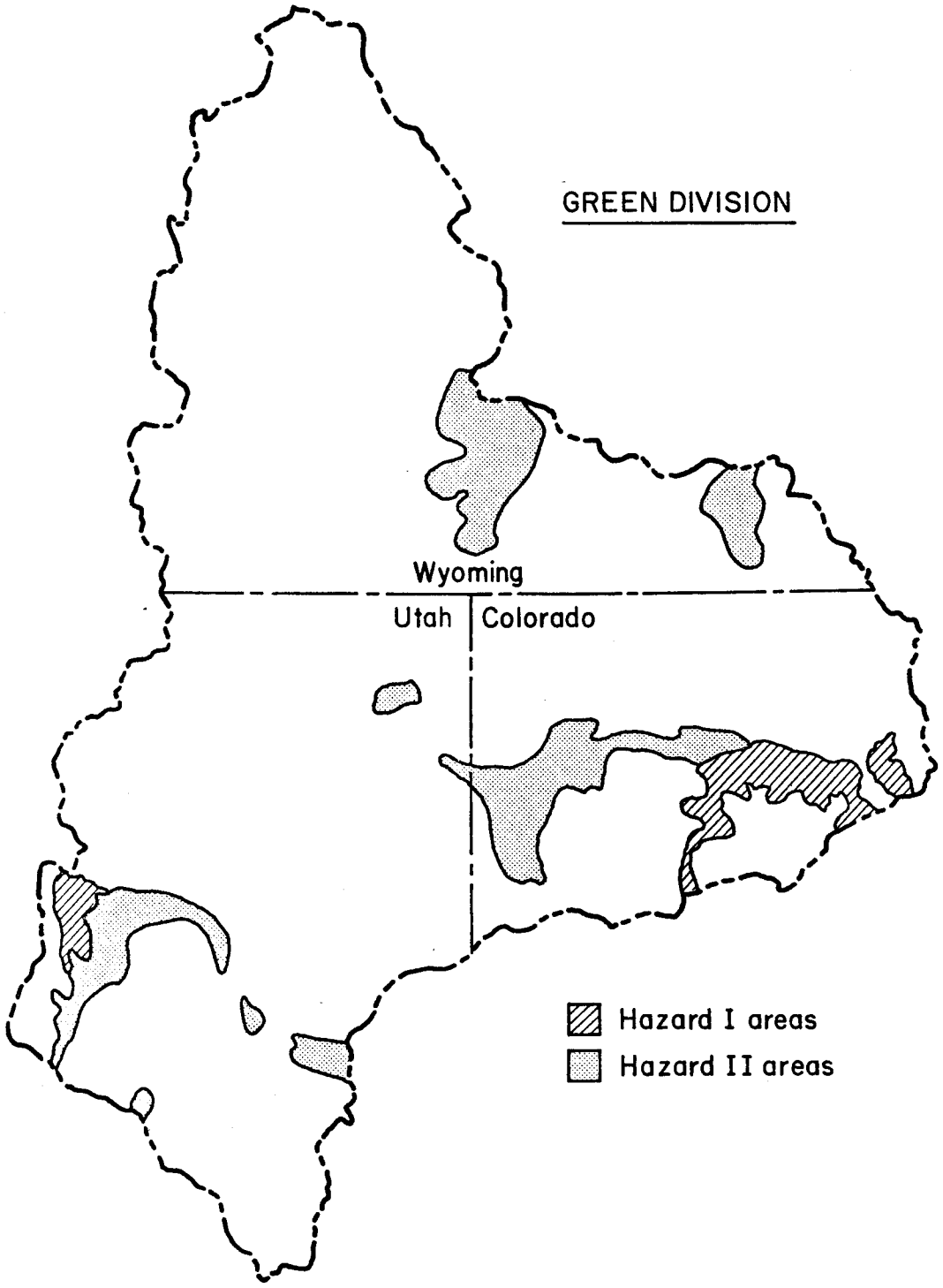

Figure 5.6. Salinity hazard areas in the Green River Basin; preliminary delineation.

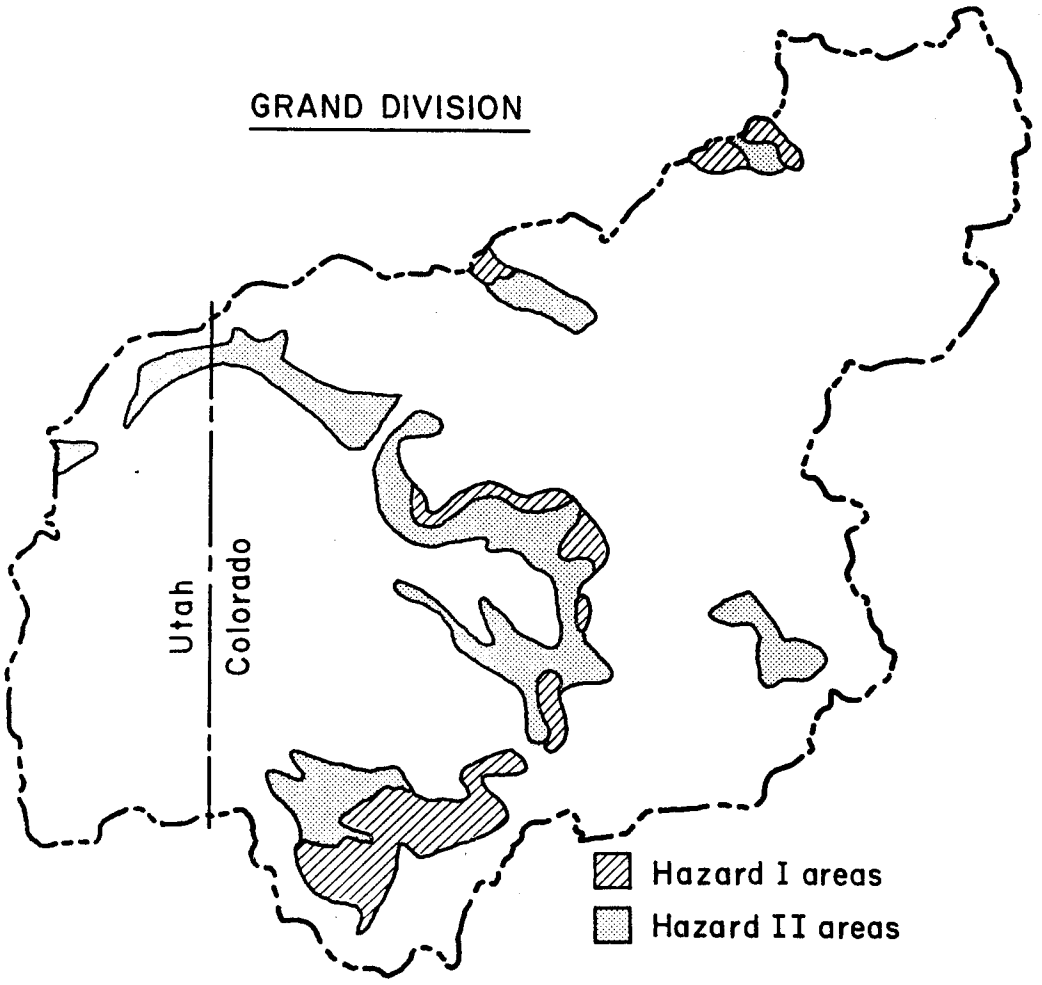

Figure 5.7. Salinity hazard areas in the Grand River Basin; preliminary delineation.

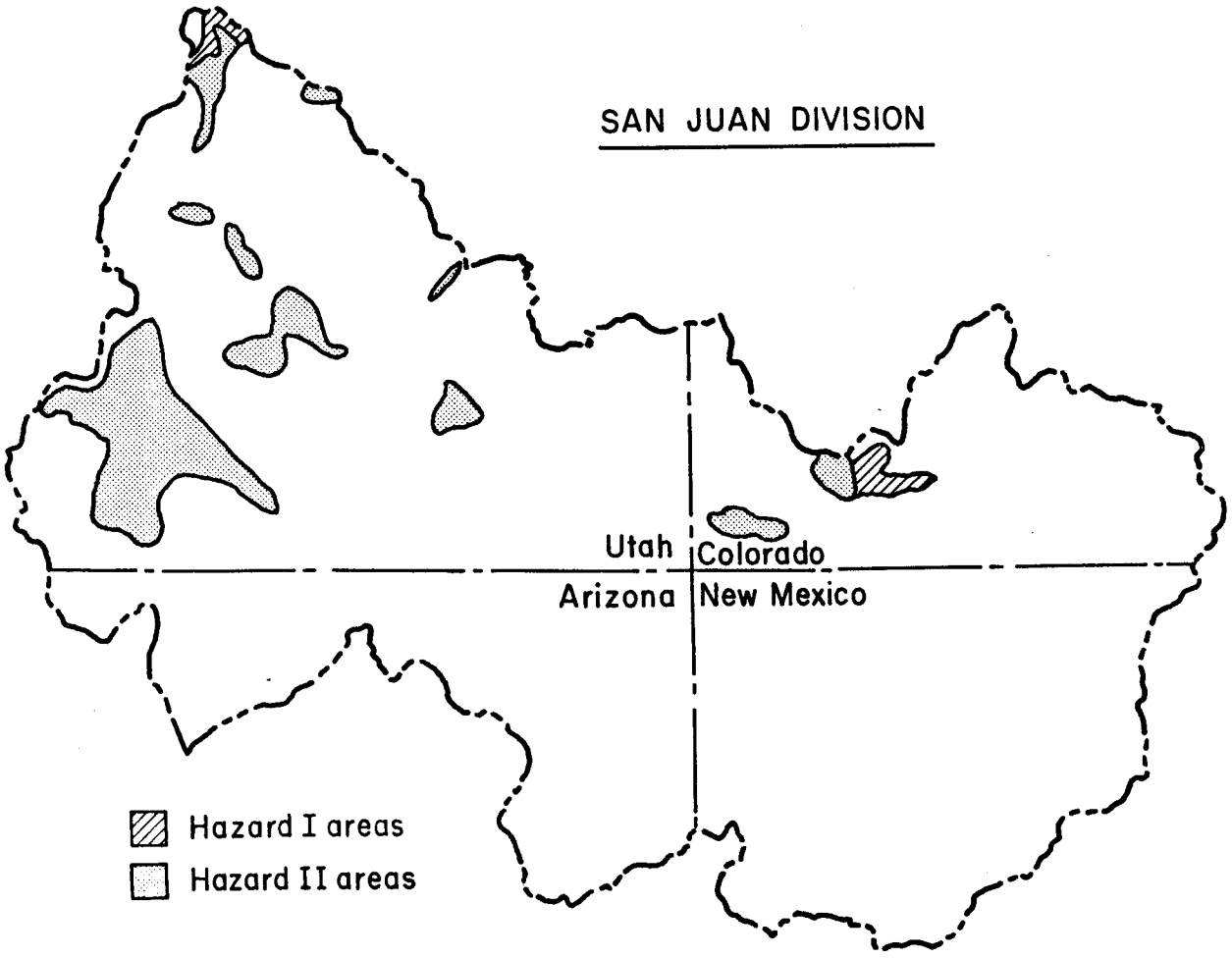

Figure 5.8. Salinity hazard areas in the San Juan River Basin; preliminary delineation.

that solute yields are directly correlated with hillslope inclination. Therefore, structural or land use mitigation measures could most effectively be used in the portions of the basin with steep slopes in basins with saline rock and high precipitation.

This type of problem analysis, identification of hazard areas by parameters known to affect high salt loading, is presented here on a very large scale, i.e. the entire Upper Colorado River Basin. However, a similar, more detailed analysis of non-point source salt loading in a smaller basin could produce very detailed maps of hazard areas. The procedure can be refined according to the type and accuracy of available data in a basin. For example, some tributary basins to the Colorado River have very detailed mapping of soils and bedrock. This information could be used as input to a water and sediment routing model, which would also utilize accurate climatic and watershed data to develop water and sediment hydrographs. This type of hydrologic analysis is, of course, much more informative than using only high precipitation as an indicator of high runoff.

Additional accuracy can be obtained by comparison of high salinity predictions with actual measurements of SMC in the basin. Temporal and spatial variations in SMC are good indicators of contributing factors. This data can also be used to calibrate any hydrologic analysis, whether be it a standard hydrograph technique or a complete watershed model.

In summary, effective planning of structural and nonstructural measures to reduce salt loading from non-point sources should succeed the identification of major contributing areas. This should be undertaken with predictive procedures, as discussed in this section, and with a verification program that includes field data collection and analysis.

5.2.2. Grand Valley and Vicinity

The relative hazard of source areas in the vicinity of the Grand Valley is summarized in Table 5.5. Note that the extent of total chemical pollution has been defined arbitrarily by solute yields and relative hazard ranges. However, it should be realized that extent of hazard also depends on the cost of measures to reduce salinity.

For instance, Anderson and Kleinman (1978) have estimated that the opportunity cost of water directed from the Upper Colorado River Basin is $15/acre-ft. At 455 acre-ft of water and 1700 tons of dissolved matter produced by West Salt Creek during the 1976 water year, it becomes apparent tnat the water supplied by this stream is worth considerably less than the damages incurred by the solutes it carries. If this total volume of water had been diverted, the avoided damages would have totalled $28,521 and the value of the lost water would have equalled $6,832. The cost and effectiveness of measures aimed at the reduction of solute concentration must be estimated. Such proposed measures are discussed in the next chapter.

CHAPTER 6

SUMMARY, CONCLUSIONS AND RECOMMENDATIONS

The studies and results reported herein involve three laboratory experiments (cylinder, jar and flume), two computer simulations (the first of specific ion concentrations of solutions derived from dissolution of minerals from Mancos Shale - soon to be reported in detail by Fujii, K. Tanji, Pers. Comm., the second of rill pattern formation), as well as fieldwork that included two hillslope studies and a watershed, tributary and confluence study. Several of these research efforts have been written as theses (for details consult Sunday, 1979, Achterberg, 1981, and Enck, 1981), and parts thereof have already been published (Shen, et al., 1979, and Laronne and Shen, 1981).

6.1. Summary

The following is a summary of the results obtained from this research project.

1. Dissolution kinetics experiments, soluble mineral and specific ion determinations, and X-ray diffraction diagrams reveal the following:
   a. Dissolution rate of minerals from Mancos Shale is initially rapid but slows down considerably as determined by Laronne (1977) and Jurinak, Whitmore and Wagenet (1977); the rate is not necessarily diffusion controlled.
   b. Surface crusts of Mancos Shale are leached, containing about half as much soluble minerals as underlying material.
   c. The main soluble mineral in Mancos Shale is Gypsum; varying amounts of less soluble carbonates and more soluble sodium-magnesium sulfates have also been detected.

d. Sulfate minerals are particularly enriched in efflorescent crusts.

e. Calcite and Dolomite are present in Mancos Shale but they do not contribute significantly to the solute load.

f. A computer simulation of specific ion concentrations in aqueous solutions derived from contact of water and Mancos Shale agrees well with stoichiometric data.

2. Laboratory experiments were designed to identify the effects of various parameters on the rate of solute pickup. It has been shown that solute pickup rate

a. increases linearly with flow velocity;

b. is larger for unweathered shale than for weathered shale;

c. increases as the size of the shale particles decreases according to kinetic principles and as shown by Laronne (1977);

d. increases with agitation or increased turbulence;

e. increases initially with increase in sediment concentration;

f. increases as erosion and sediment concentration increase in flume studies;

g. is higher at the upper end of a simulated surface flow event (i.e., flume) rather than at the bottom end due to upflume erosion and downflume dilution; and

h. increases downflume under 'baseflow' (i.e., direct runoff generation) conditions.

3. Solute pickup during field experiments on hillslopes

a. is initially very high but decreases asymptotically after an early maximum is reached due to:

I. a surface flushing effect

II. decrease in erosion rate (i.e., sediment concentration), and

III. decrease in solute concentration gradient between the bulk solution and the 'soil' solution;

b. may reach a second, later maximum, due to:

I. rilling or downcutting of rills with concommittant increase in sediment production, and

II. erosion and transport of deeper-lying, more saline Mancos Shale material;

c. is higher during direct runoff generation than during rainfall induced runoff generation due to:

I. downslope dilution by rainfall, and

II. larger water losses and resultant less channelized flow associated with rainfall-induced runoff;

d. has been shown to be strongly dependent on sediment transport. This is based on

I. correspondence in temporal trends of sediment and solute concentration,

II. correspondence in time of rilling and time to EC maxima, and

III. increase of solute concentration in unfiltered runoff samples;

e. increases downslope and downchannel during direct runoff generation, but does not vary appreciably across-slope;

f. increases when underlying shale material that contains a high SMC is eroded; and

g. increases with increase in hillslope inclination.

4. The chemical character of runoff from Mancos Shale hillslopes

   a. is generally of the Ca-Na-Mg-SO_4-HCO_3 type;

   b. changes with increase in hillslope inclination as follows:

      I. [(Na)+(Mg)]/(Ca) increases and

      II. (SO_4/(HCO_3) increases;

   c. changes temporally during an event as follows:

      I. (SO_4)/(HCO_3), (Ca) and (Ca)/(Na) increase on mild hillslopes, and

      II. [(Na)+(Mg)]/(Ca) increases on steeper hillslopes

      Note that ion concentrations are in meq/l.

5. Under natural conditions (West Salt Creek), solute concentration in runoff

   a. does not vary systematically with discharge,

   b. is high such that saturation with respect to Gypsum is ordinarily attained,

   c. is typically very low when contributed directly from snowmelt runoff,

   d. increases initially due to surface flushing and decreases thereafter, and

   e. varies spatially to a large extent due to inflow from saline springs and seeps and with the SMC of the contributing surface.

6. Mixing of water at a large confluence is

   a. complete only several miles downstream of the confluence, and

   b. continues for several hours during which soluble minerals continue to dissolve because of kinetic disequilibium and/or saturation.

7. The quality of runoff from natural diffuse source areas in the San Rafel, Dirty Devil and Price Rivers is low.
8. The solute yield from diffuse source areas in the Upper Colorado River Basin
   a. may be roughly estimated using
      I. the standard procedure
      II. monthly averages, or
      III. the relationship between mean EC and hillslope inclination, and
   b. accounts for approximately half the solute load transported by the Colorado River at Lees Ferry.
9. Salinity hazard areas in the Colorado River Basin and in specific, smaller basins thereof can be delineated quite accurately by superimposing available geologic, precipitation and topographic information on a map showing spatial trends in SMC. Data on SMC requires additional field investigations.

6.2. Conclusions

The results of the studies summarized in the previous section prove that entrainment and transport of sediment by overland and channelized flow are crucial factors affecting the salinity of runoff from diffuse source areas. Increased concentration of transported sediment increases the availability of soluble minerals. Moreover, transported sediment may continue dissolving due to kinetic disequilibrium and/or when mixed with a more dilute aqueous solution such as water of the Colorado River.

An increase in either flow velocity or agitation increased solute release rate. However, the magnitude of the increase due to agitation was very small. The laboratory results also suggest that high velocities of flow are not the direct primary contributor to high solute concentrations and solute yields. The velocities obtained in the experimental apparatus are not directly comparable to those under natural runoff because of the different bed conditions. Moreover, the variation in velocity of flow on a natural mild hillslope and a steep one (in the range 0.9-4.6 cm/sec, or 0.03-0.15 ft/sec) are too small to account for the large effect of hillslope inclination on solute yield.

The effect of transported sediment on solute yield is shown by several parts of this study. Sediment yield increases during rilling with a contemporaneous increase in solute yield. Rills form faster and are undercut to a greater extent by direct runoff than by rainfall-induced runoff. In fact, the importantce of rill flow (which has a higher power per unit width than overland flow) to erosion and solute yield is so overwhelming that a computer simulation of rill pattern and its variation with hillslope inclination has been developed (Chapter A.5 of the Appendix). The effect of rilling and rill downcutting on solute yield is manifested by the correspondence of a) time to rilling and time to EC maxima, b) sediment and solute concentrations, and by c) high sediment concentrations giving rise to higher temporal increases in solute content in unfiltered runoff samples. The most practical conclusion arising from the rilling effect is the indirect dependence of solute yield on hillslope inclination. The regression of solute yield against slope may be used as a reliable procedure to estimate solute yield under varying climatic conditions from diffuse source areas that are comparable in terms of their SMC and erodibility.

The extent of dissolution of soluble minerals transported as suspended load and bedload is difficult to determine quantitatively. For instance, results from the confluence study show that an increase of merely 1-3 ppm of solutes may have taken place in the Green River. However, that such continuous dissolution does occur is shown by the agitation and dilution experiments (see also Laronne, 1977), by the saturation with respect to Gypsum of runoff from various tributaries, and by the increase in solute concentration of unfiltered runoff samples. This latter increase decreases downslope due to the increase in contact time between runoff and transported sediment; it also decreases as the average SMC of the contributing area (or else, the SC of the runoff) increases according to principles of dissolution kinetics.

Erosion and transport of sediment not only increases total solute yield, but it also affects the chemical composition of runoff. Ionic derivatives of more soluble minerals are more common as sediment load increases.

6.3. Recommendations

At first hand it may appear economically unfeasible to decrease solute yields from diffuse sources because of the large expanses of area involved. However, areas contributing high solute yields are invariably drained by channels. Therefore, the ultimate goal of specific structural or nonstructural measures is an optimization study that would determine the best location, size and type of treatment. Delineation of salinity hazard must be undertaken to determine location. Certainly, it is unfeasible to treat first order basins because of the large number involved, and it is inappropriate to treat the water

at a location downstream from the confluence of a tributary discharging saline water. In fact, evaluation of solute yields must preempt the determination of the size of treated area.

The following, recommendations, based on results presented in this report, should apply in order to access optimal measures to decrease solute yields:

1) Monitor water quality of runoff from medium and small sized channels that drain Mancos Shale and other saline outcrops. The monitoring program should include EC metering as well as collection of water samples to determine sediment concentration and detailed water chemistry.

2) Delineate salinity hazard from natural diffuse source areas by undertaking extensive field determinations of SMC in Mancos Shale and similar saline deposits;

3) Locate saline seeps and springs by identifying efflorescent crusts and saline water in channels with the aid of aerial photography and other remote sensing techniques.

4) Construct a primarily deterministic mathematical model of the mass balance of soluble minerals, solutes, sediment and water based on further research. Such a required additional research effort would determine the path of soluble minerals and their dissolution from the origin, the diffuse source area, into and through the channel system.

REFERENCES

Achterberg, D.G., 1981, Laboratory study: runoff, sediment, transport and salt loading under simulated rainfall: M.Sc., Colorado State University, Ft. Collins.

Anderson, J.C., and Kleimman, A.P., 1978, Salinity management options for the Colorado River - damage estimate and control program impacts. Utah Water Research Laboratory, Utah State University, Logan.

Cook, C.W., 1974, Surface rehabilitation of land disturbances resulting from oil shale development. Final Rpt. Phase I, to Colorado Dept. of Natural Resources, Env. Res. Center, Colorado State University, Ft. Collins, Colorado.

Enck, E.D., 1981, Non-point salt loading from West Salt Creek near Mack, Colorado: M.Sc., Colorado State University, Ft. Collins.

Horton, R.E., 1926, Discussion of paper--Flood plain characteristics by C.S. Jarvis: Trans., Am. Soc. Civ. Eng., 89.

Horton, R. E., 1945, Erosional development of streams and their drainage basins-hydrophysical approach to quantitative morphology: Geol. Soc. of Am. Bull, 56, 275-370.

Howard, A.D., 1971, Simulation of stream networks by headward growth and branching: Geol. Anal., 3(1).

Iorns, W.V., Hembree, C.H., and Oakland, G.L., 1965, Water Resources of the Upper Colorado River Basin - Tech. Rpt.: U.S. Geol. Survey, Prof. Paper 441, 370 p.

Jurinak, J.J., Whitmore, J.C., and Wagenet, R.J., 1977, Kinetics of salt release from a saline soil: Soil Sci. Soc. of Am. Jour., 41(4), 721-724.

Laronne, J.B., 1977, Dissolution potential of surficial Mancos Shale and alluvium - Ph.D., Colorado State University, Ft. Collins.

Laronne, J.B., 1981, Sediment and solute yield from Mancos Shale hillslopes, Colorado and Utah: *in* Bryan, R.B., and Yair, A. (eds), Badland Geomorphology and Pipe Erosion, Geoabstracts, Norwich.

Laronne, J.B., and Schumm, S.A., 1977, Evaluation of the storage of diffuse sources of salinity in the Upper Colorado River Basin: Colorado State University, Env. Res. Center Compl. Rpt. Series No. 79.

Laronne, J.B., and Shen, H.W., 1981, Temporal and spatial variations of solute pickup during runoff generation in saline hillslopes. Proc. Internat'l, Symp. on Rainfall-Runoff Modeling, Mississippi State Univ., 238-9, (soon to be released as a contributer paper in Singh, V.P., Rainfall-Runoff Modelling).

Leathers, K.L., and Young, R.A., 1976, Evaluation of economic impacts of programs for control of saline return flows: A case study of the Grand Valley, Colorado: EPA Region VIII, Denver.

Leopold, L.B. and Langbein, W.B., 1962, The concept of entropy in landscape evolution: U.S. Geol. Survey Prof. Paper 500-A.

Maletic, J.T., 1973, Colorado River Water Quality Improvement Program: Presented in Seminar on Agriculturally Related Pollution, unpubl., Colorado State University, Ft. Collins.

Mosley, M.P., 1972, An experimental study of rill erosion: M.Sc., Colorado State University, Ft. Collins.

Parker, R.S., 1977, Experimental study of basin evolution and its hydrologic implications: Ph.D., Colorado State University, Ft. Collins.

Ponce, S.L. II, 1975, Examination of a non-point source loading function for the Mancos Shale wildlands of the Price River Basin, Utah: Ph.D., Utah State University, Logan.

Ponce, S.L. II, and Hawkins, R.H., 1978, Salt pickup by overland flow in the Price River Basin, Utah: Water Resources Bull., 14(5), 1187-1200.

Price, Don, and Waddell, K.M., 1973, Selected hydrologic data in the Upper Colorado River Basin: U.S. Geol. Survey Hydrol. Atlas, Investig. HA-477, 2p.

Schick, A.P. and Sharon, David, 1974, Geomorphology and Climatology of Arid watersheds. Final Bi-annual Tech. Rpt. No. DA JA-72-C-3874, U.S. European Resources Office, p.161.

Schmehl, W.R., and McCaslin, B.D., 1973, Some properties of spent oil shale signifcant to plant growth: *in*: Hutnik and Davis (eds), Ecology and Reclamation of Devastated Land, V.I, Gordon and Breach, London, 27-43.

Schumm, S.A., 1956, Evolution of drainage systems and slopes in badlands at Perth Amboy, New Jersey: Geol. Soc. of Am. Bull., 67, 597-646.

Shen, H.W., Enck, E., Sunday, G.K. and Laronne, J.B., 1979, Salt loading from hillslopes: Internat'l Assoc. of Hydraulic Research Proc., 5, 99-105.

Smart, J.S., 1972 Channel networks: *in* Chow, V.T., (ed), Advances in Hydroscience, 81, 305-343.

Smart, J.S., and Moruzzi, 1971, Random-walk model of stream network development: IBM Jour. Res. Dev., 14(3).

Strahler, A.N., 1957, Quantitative analysis of watershed geomorphology: Trans. Am. Geophys. Union, 38, 913-920.

Sunday, G.K., 1979, Role of rill development in salt loading from hillslopes: M.Sc., Colorado State University, Ft. Collins.

Tanji, K.K., 1969, Solubility of Gypsum in aqueous electrolytes as affected by ion association and ionic strengths up to 0.15M at 25°C: Environmental Science and Technology, 3(7), 656-661.

U.S. Bureau of Land Management, 1978, The effects of surface disturbance on the salinity of Public Land in the Upper Colorado River Basin U.S.D.I., Denver.

U.S. Bureau of Reclamation, 1972, Colorado River Water Quality Improvement Program: USDI, 88 p.

U.S. Bureau of Reclamation, 1974, as above, 125 p.

U. S. Dept. of Agriculture, 1975, Erosion, sediment and related salt problems and treatment opportunities: Soil Conserv. Service Special Projects Div., Golden, Colorado, 152 p.

U.S. Environmental Protection Agency, 1971, The mineral quality problem in the Colorado River Basin - Appendeces A and B and summary rpt., regions 8 and 9. U.S. Government Printing Office, Washington, D.C.

U.S. Geol. Survey, 1969 - Water Resources data for Colorado: Prepared in cooperation with the State of Colorado and with other agencies.

White, R.B., 1977, Salt production from microchannels in the Price River basin, Utah: M.Sc., Utah State University, Logan.

Whitmore, J.C., 1976, Some aspects of the salinity of Mancos Shale and Mancos derived soils: M.Sc., Utah State University, Logan.

Zernitz, E.R., 1932, Drainage patterns and their significance: Jour. of Geology, 40, 498-521.

APPENDIX

A.1 MINERAL AND SALT CONTENT

The solute yield which eventually reaches a given downstream point in a river is transported from its source either completely in the aqueous phase or it may move partly in the solid phase (i.e., particulate sediment which partly/totally dissolves while in transport). Considering only transport processes acting upon the land surface (i.e., excluding interflow and ground water flow), the yield of solutes per unit watershed area is a function of: (1) the salt content and type (mineral species) within the surficial minerals, (2) the dominant mechanisms by which the dissolved and particulate matter is transported (i.e., aqueous dissolution upon contact with surficial materials, and/or aqueous dissolution from particulate sediment in transport), (3) the duration, magnitude and frequency of flow events, and (4) the rate of weathering of surficial materials and storage of soluble minerals in horizons (i.e., vertically) and locations (i.e., horizontally), including aeolian transport and mass wasting of sediment between runoff events. The material dealt with in this section belongs to the first category--the quantity and quality of soluble salts within surficial geologic materials.

A.1.1 Salt Content

Salt content determinations of saline formations within the Upper Colorado River Basin were first undertaken by Ponce (1975). His work was limited to the Price River Basin in east central Utah and although the values reported by him are not equivalent to salt content (e.g., weight-soluble salts per weight soil) as will be explained later, they may be used as indicators. Ponce reported the EC of solutions derived

from 1:10 soil:water ratios* which were allowed to remain in contact a fixed period of time. He found that the salinity of non-Mancos Shale members and of several shale members was much lower that that of the Blue Gate member, and especially the Mancos Undivided. In his dissertation (Ponce, 1975), and in its more available version (Ponce and Hawkins, 1978), an emphasis is laid on the large inherent variability of salt content. This variability, related to shale crust samples within several small (28 m^2 and 167 m^2) grids, was manifested by a difference of one order of magnitude between the lowest and highest values and by coefficients of variation in the range 0.25-0.41 (calculated from Ponce and Hawkins, 1978, Fig. 4) for the microgrids.

An intentional emphasis on salt content variability led Wagenet and Jurinak (1979) to conclude, based on 35 samples - each at three depths - from various locations within the Price River Basin, that a large number of samples must be collected to determine the mean salt content with reasonable accuracy of estimation. They demonstrated that the point of diminishing returns for their data occurred at 50-100 collected samples (of a given soil or sediment), increasing as the accuracy of estimation is increased. They and Laronne and Schumm (1981) concluded that care must be taken to avoid using salt content values based on few measurements. Additionally, having found that the salt content values (determined from 1:1 and saturated extract solutions in a manner similar to Ponce) are lognormally distributed about the mean, Wagenet and Jurinak (1979) concluded that the salt content

---

*A 1:10 mixture is a one part soil to ten parts water (by weight), and is equivalent to a sediment concentration of 1/11=90,909 ppm, or 100,000 mg/1.

variation in Mancos Shale is typified by "hot spots", i.e., few locations with very high salinities and most of the area typified by much lower salinities.

Laronne and Schumm's (1977) report in conjunction with the present report contain extensive data on over 800 samples of Mancos Shale and associated alluvium. The samples were divided into morphological groups, most of which are characterized by salt contents significantly different (determined by the same analysis of variance used by Wagenet and Jurinak) from those of other groups. Among the important morphological groups were several crust types and alluvial materials either in close proximity to Mancos Shale or far removed from it.

Unlike Wagenet and Jurinak's (1979) conclusions, Laronne and Schumm (1981) showed that significant (mostly at the 5 percent confidence level) differences in salt content can be determined with relatively few samples. This apparent discrepancy is explained by the non-random nested sampling program in the latter study, in which samples were collected from specific morpho-geologic units (e.g., crust of lower part of shale gully wall or underlying alluvial bed materials at specified depths) with extensive notation on the characteristics of the sampling locality. Hence, the variability in salt content can be reduced significantly by referring to natural morphologic, pedologic and geologic units. In fact, being as thick as it is and covering such extensive and variable terrain, one should expect Mancos Shale or other surficial materials to show not only variations with depth, but also variations with locale. A similar statement also holds for soils as evidenced by the need and wide use of soil classification schemes and maps by agronomists and soil scientists. It might herein be

stressed that salt content, like any other physical or chemical property of natural materials, varies considerably in space and time. The use of statistical moments (such as the mean value) necessitates knowledge of deviations about that moment.

Surficial materials are normally leached such that salt content increases with depth. This also holds for semiarid and arid areas (high evaporation rates and resulting considerable upward capillary transport) where the surficial material has a high infiltration capacity. Characteristic of this situation is coarse alluvium (most dry washes and their terraces) removed sufficiently from Mancos Shale outcrops (Laronne and Schumm, 1977). Under these circumstances much more water moves downward than upward and the net result is either a high degree of leaching throughout the whole profile to great depths, or else a similar trend with a relatively small saline accumulation at the surface proper due to the last precipitation-evaporation event.

Significant surface accumulations of salts appear whenever downward percolation is strongly inhibited and relatively large moisture contents prevail near the surface after a precipitation event. Such is the case with shallow (fine and coarse) channel bed alluvium overlying Mancos Shale, associated steep alluvial gully walls and bedrock (Mancos Shale) channels.

The surficial accumulation of salts where slow downward percolation takes place will not be effective, however, if the surface is not saucer-shaped, serving as a temporary water-storing depression or water conveyance conduit in which the processes of downward water movement and subsequent evaporation are of long duration. Mancos Shale hillslopes are an example of such a situation wherein downward

percolation of water is so inhibited that after all but the most intense and long rainstorms, the wetting front merely advances 5 cm. The advance and retreat of these wetting fronts is evidenced by the formation of slightly (clay-) lithified crusts, the thickness of which varies but is usually less than 2 cm. To determine salt content variations with depth within the Mancos Shale, it is, therefore, necessary to sample undisturbed crusts separately from the underlying material. Laronne and Schumm (1977) found these crusts contained less than half the salt content of underlying material. Additional samples analyzed within this reported project confirm this statement. Figures A.1.1a - A.1.1e (consult Table 3.2 for description of these samples) depict results from dissolution kinetic experiments wherein the EC of aqueous mixtures varies with contact time. With undersaturation with respect to the major soluble salts, the equilibrium (horizontal) parts of the scatter diagrams invariably show higher salinities in underlying materials and lower salinities in shale crusts. This holds for the following paired samples: T5-1 and 2 (Figure A.1.1a), T5-5 and 6 (Figures A.1.1a, A.1.1b), T5-9 and 10 (Figure A.1.1b), T8-1 and 2 (Figure 2.1.1d), and T8,9 and 10 (Figure A.1.1e). Also, the wetting of material underlying a rill apparently also leached it (T8-12, Figure) A.1.1e). Unlike Mancos Shale, the crust of the alluvium (T5-17) has slightly accumulated salts relative to the underlying alluvium (T5-18, Figure A.1.1c).

Dissolution experiments such as these are necessary in order to determine salt content, proving by chemical analyses that the mixtures are undersaturated. A straightforward use of EC data from saturated extracts, 1:1 or even 1:10 soil:water mixtures in contact during a

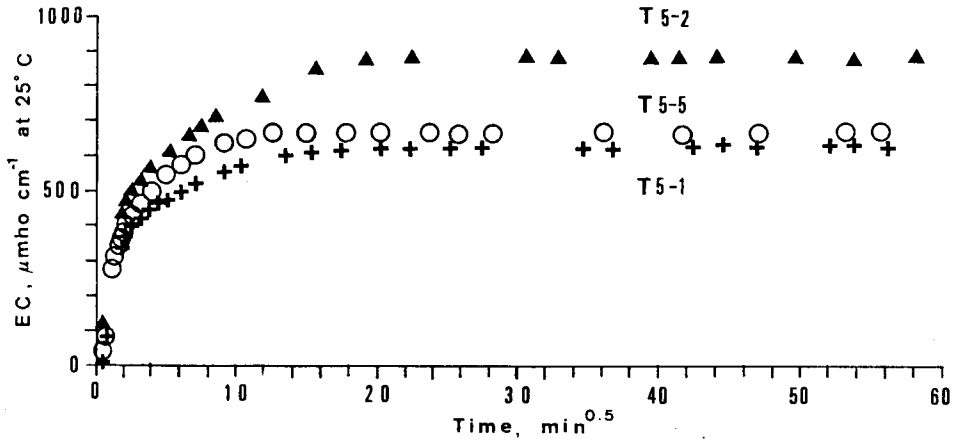

(a)

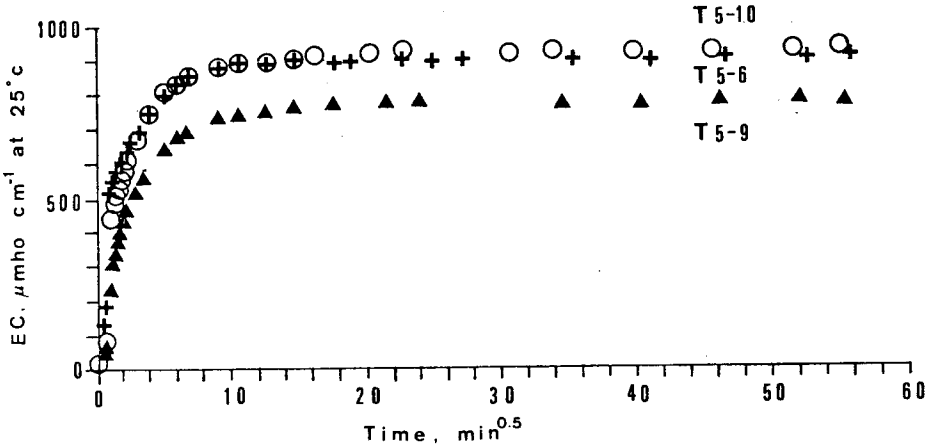

(b)

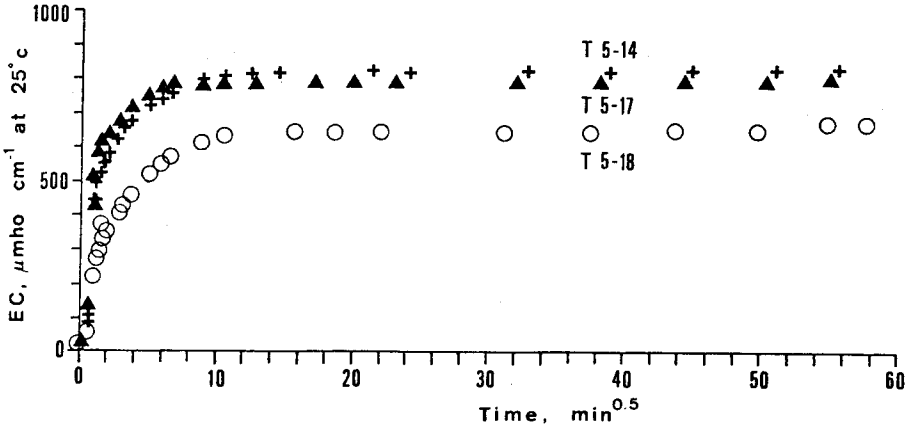

(c)

Figure A.1. Dissolution kinetics of selected 1:99 soil/water mixtures. Equilibrium EC values transposed to SC (mg/ℓ) and divided by 100 are equivalent to SMC in percent. Refer to Table 3.2 for description of soil samples.

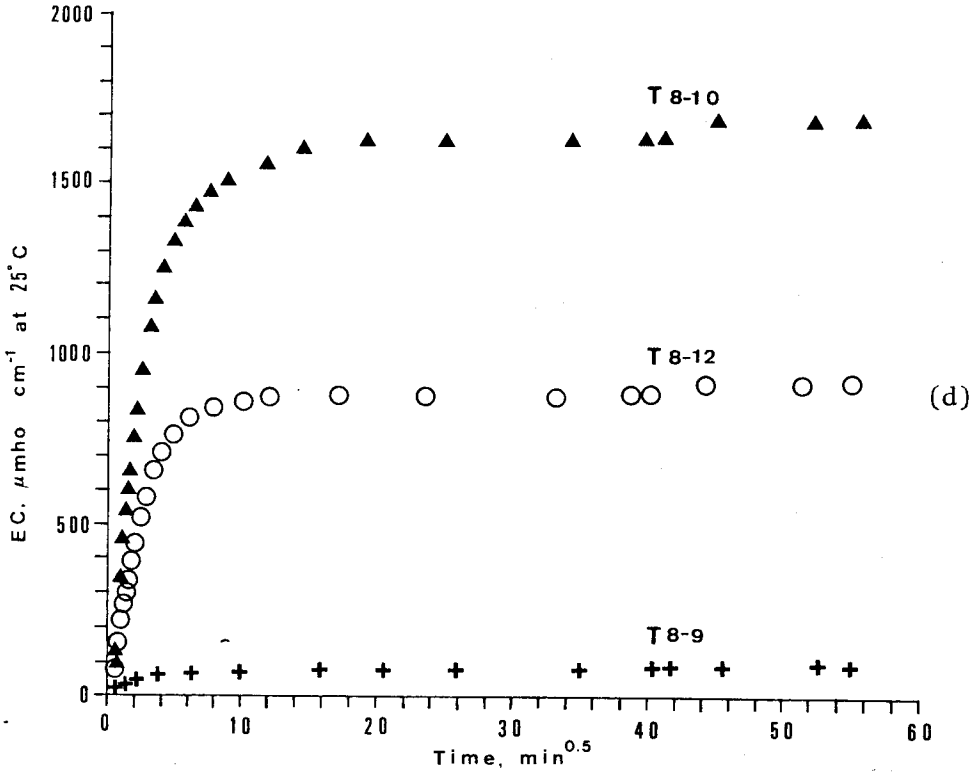

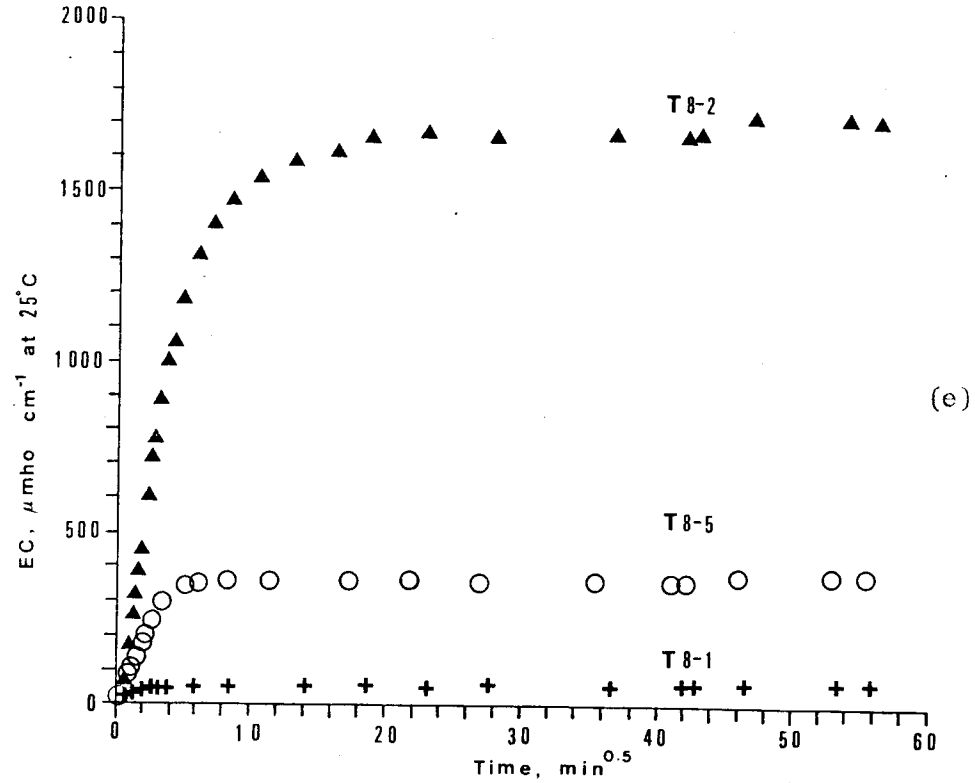

Figure A.1. continued.

fixed period of time, may be very misleading. A minimum contact period (which varies with the soil:water ratio and with the actual salt content) is necessary to insure an asymptotic closeness to equilibrium, undersaturation must be assured and a realistic sediment:water ratio should be used if sediment transport (rather than soil water movement) is studied.

A.1.2 Identification of Chemical and Mineral Species

SMC and EC data are used throughout this and other reports dealing with the salinity problem in the Colorado River Basin. Such data provide the necessary information to calculate solute loads and yields. However, it is insufficiently intricate to provide a means to understand the dissolution process nor the spatial and temporal variations of salt content and salt loads. Chemical analyses are tools by which cations and anions are determined, thereby forming a necessary backbone to water quality studies. For instance, a high concentration of SO_4^{2-} is more harmful than the same dosage of HCO_3^{1-} for drinking purposes. The acquisition of specific ion data is time-consuming and expensive, but an inquiry into the actual minerals (i.e., salts) which dissolve and thereby dissociate is ultimately needed to fully comprehend the specific chemical nature of the water and the chemical reactions which led to its present character. For example, sodium and bicarbonate may be identified in water samples, but their origin need not be the mineral Nahcolite ($NaHCO_3$) nor its more soluble hydrates; they may have originated separately from Thenardite (Na_2SO_4) and Calcite ($CaCO_3$), or from very slightly soluble minerals.

The identification of soluble minerals is, however, the only information necessary to chemically characterize, by common thermodynamic laws, the contact solution (provided equilibrium is reached and that the ionic strength - a measure of the salinity of the aqueous solution - is not too high). Furthermore, the identification, though only on a relative scale, of mineral species is a useful tool in explaining variations in solute loads.

Soluble ion and mineralogical analyses were performed on a wide range of earth materials sampled throughout the study area in conjunction with water quality studies. Mineral identification analyses were performed on corresponding dry, powdered samples by means of X-ray diffraction on a bakelite mount. In mineralogical analysis, attention was directed toward evaporite or precipitate mineral species which might contribute significantly to soluble ion concentrations of natural waters. In all, thirteen different relatively soluble mineral species have been identified within the study area by X-ray diffraction. For reference, these mineral species with their chemical compositions are listed in Table A.1.1.

Chemical analyses, Gypsum determinations and kinetics experiments were perfromed on six samples of Mancos Shale and bed crusts from West Salt Creek and from the Green River below the confluence of the Price River. Four of the samples were examined by X-ray diffraction and of these, three were used to test a computer simulation analysis (Table A.1.2). If in sample 164 the Hemihydrate ($CaSO_4 \cdot 1/2H_20$) identified by X-ray diffraction is combined with Gypsum ($CaSO_4 \cdot 2H_20$) for the purpose of comparison, then there is a very good correlation between the Gypsum identification by chemical analysis and that by X-ray diffraction. This is justified because the chemical analysis is unable to differentiate between the various hydrate forms of $CaSO_4$ and the solubilities are of the same magnitude (Anhydrite 0.463 moles/l, Hemihydrate 0.0521 moles/l, and Gypsum 0.0154 moles/l). The data summarized in Table A.1.2 show the potential of solute release from these soil materials. Most of the increase in solute content is attributed to Calcite, Dolomite, Gypsum and Aragonite with minor contributions to sulfates.

Table A.1.1. Salt mineral species identified in earth materials by X-ray diffraction analysis.

Mineral	Composition
Calcite	$CaCO_3$
Dolomite	$CaMg(CO_3)_2$
Nahcolite	$NaHCO_3$
Soda (Natron)	$Na_2CO_3 \cdot 2H_2O$
Trona	$Na_2CO_3 \cdot 10H_2O$
Gypsum	$CaSO_4 \cdot 2H_2O$
Hemihydrate	$CaSO_4 \cdot 1/2H_2O$
Epsomite	$MgSO_4 \cdot 7H_2O$
Hexahydrate	$MgSO_4 \cdot 6H_2O$
Mirabilite	$Na_2SO_4 \cdot 10H_2O$
Thenardite	Na_2SO_4
Bloedite	$Na_2Mg(SO_4)_2 \cdot 4H_2O$
Halite (detected once in trace amount)	NaCl

The X-ray diffraction (Table A.1.3) patterns also indicate large amounts of Calcite and Dolomite in samples 164, 165 and 169, and a moderate amount in sample 156. Other minerals detected by X-ray diffraction were Thernardite (Na_2SO_4, samples 156, 164 and 175), Bloedite ($Na_2Mg(SO_4)_2 \cdot 4H_2O$, sample 156), and Hexahydrite ($MgSO_4 \cdot 6H_2O$, samples 156 and 164). The presence of these soluble minerals may explain the discrepancies between the computer analysis and the chemical analyses.

Table A.1.2. A comparison of X-ray diffraction data, saturation extract analysis, a kinetics experiment and computer simulation. See table A.1.3 for description of samples.

Sample #	Calcite	Dolomite	Hemyhydrate	Gypsum	Thenardite	Bloedite	Hexahydrate
156	2	2		0.5	1	1	T
169	10+	7		T			
164	5	4	1	T	0.5		T
165	5	5		T	T		

Scale is 0-10, T = trace

Saturation Extract, meq/100g of soil

Sample #	HCO_3	Cl	SO_4	Na	Ca	Mg	K
156	0.93	2.53	109.25	63.84	0.76	47.31	0.76
169	0.10	0.02	0.13	0.02	0.16	0.03	0.02
164	0.14	0.13	4.72	3.28	1.03	0.64	0.06
165	0.16	0.17	2.69	2.70	0.15	0.17	0.05

Kinetics Experiment-1:100 dilution, meq/100g of soil

156	15.70	6.20	130.00	85.00	17.50	53.80	1.20
169	14.60	0.60	0.40	7.50	5.50	2.30	0.80
164	8.40	5.10	38.00	10.40	34.00	5.50	0.80
165	21.90	0.60	2.80	12.80	4.50	3.80	1.20

Computer Simulation *vs* Measured Data-1:100 dilution, meq/ℓ

156 meas	1.57	0.62	13.00	8.50	1.75	5.38	0.12
156 sim	1.80	0.665	29.06	16.80	2.10	12.46	0.20
169 meas	1.46	0.06	0.04	0.75	0.55	0.23	0.08
169 sim	0.229	0.0052	0.039	0.005	0.249	0.008	0.007
164 meas	0.84	0.51	3.80	1.04	3.40	0.55	0.08
164 sim	1.133	0.033	1.152	0.40	1.365	0.155	0.015

Table A.1.3. Minerals detected by X-ray diffraction in samples from the Upper Colorado River Basin.

			mineral													
	Sample	Particle size (mm)	$CaCO_3$	$CaMg(CO_3)_2$	$NaHCO_3$	$Na_2CO_3 \cdot 10H_2O$	$Na_2CO_3 \cdot NaHCO_3 \cdot 2H_2O$	$CaSO_4 \cdot 1/2H_2O$	$CaSO_4 \cdot 2H_2O$	Na_2SO_4	$Na_2SO_4 \cdot 10H_2O$	$Na_2Mg(SO_4)_4 \cdot 4H_2O$	$MgSO_4 \cdot 6H_2O$	$MgSO_4 \cdot 7H_2O$	NaCl	Unknown Peaks
West Salt Creek																
Bed crust	156		2	1					0.5	1		1	T			✓
Bank crust	158		1.5	5.5								0.5				✓
Soil under bank crust	159		0.5	1.5					0.5							
Mancos shale, weathered talus	169		10+	7					T							
Soil, from Mancos Shale	173		1	4					10+	T		T				
Bed of channel	G7A1S	>1	1	3					0.5	T		T				
Bed of channel	G7A1S	<1	3	3.5					0.5	T		0.5				
Efflorescence, channel bed	G8B1	>1	1	3					T	1		5	0.5			
Efflorescence, channel bed	G8B1	<1	1	1.5					T	0.5		2.5	1			
Salt seep (air dry)	G8			T						10+	0.5	10+		T		
Salt seep (field moist)	G8			1		0.5				3	10+			3		✓
Salt from creek bed	X2		T	1			T	T	0.5	3.5	0.5	10+	1	0.5	T	
South Canyon, West Salt Creek																
Bank crust, Mesa Verde Frm.	162		0.5	4.5					T				T			✓
Prairie Canyon, West Salt Creek																
Bed crust	175		2	2.5		0.5			T	T						
Bed crust	176		2	2												
Badger Wash																
Soil Mancos Shale surface	X6		1.5	7		T	T	T	T	0.5			1	T		

Note: Samples U5C4A and U5M2A are from a Mancos Shale bedrock channel.

Table A.1.3. Continued.

	Sample	Particle size (mm)	mineral													
			$CaCO_3$	$CaMg(CO_3)_2$	$NaHCO_3$	$Na_2CO_3 \cdot 10H_2O$	$Na_2CO_3 \cdot NaHCO_3 \cdot 2H_2O$	$CaSO_4 \cdot 1/2H_2O$	$CaSO_4 \cdot 2H_2O$	Na_2SO_4	$Na_2SO_4 \cdot 10H_2O$	$Na_2Mg(SO_4) \cdot 4H_2O$	$MgSO_4 \cdot 6H_2O$	$MgSO_4 \cdot 7H_2O$	NaCl	Unknown Peaks
Leach Creek																
Efflorescence, Mancos Shale	X3		T	1					1							
Weathered Mancos Shale	X5		T	2	0.5		T		2.5		T	T				
Bed Crust (0-2 cm), alluvium	G1B1	>1	2	3.5					1							
Bed crust (0-2 cm), alluvium	G1B1	<1	2	4.5					0.5							
Mancos Shale, hillslope	G1E3	>1	2.5	7.5					5							
Mancos Shale, hillslope	G1E3	<1	2	7.5					5							✓
Bed of channel, alluvium	G2A1	>1	2.5	8					6	T						
Bed of channel, alluvium	G2A1	<1	3.5	7					7.5				1			✓
Crust, Mesa Verde shale	G20A	>1	T	3					6							
Crust, Mesa Verde shale	G20A	<1		1.5					0.5							
Green River																
Weathered Mancos Shale	164		5	4				1	T	0.5			T			
Unweathered Mancos Shale	165		5	5					T	T						
Fresh Mancos Shale	X1		3.5	4.5		T		T	T				T	T		
Sandy shale, bedrock	167		3.5	7												
Exposed salt layer	168		10+	3					10+				T	T		
Evaporite Mancos Shale	X4								10+							
North Miller Creek																
Channel bed efflorescence	U5C4A	>1	5.5	5.5					0.5	T			1			
Channel bed efflorescence	U5C4A	<1	4	6					1	T		T				
Channel bed efflorescence	U5M2A	>1	3.5	8.5		T	T	T					T	1		
Channel bed efflorescence	U5M2A	<1	2	2					T	T		0.5				
Mancos Shale mass wasted	U5IJ	>1	4.5	8					2.5	T		T				
Mancos Shale mass wasted	U5IJ	<1	2.5	3					1.5	0.5		0.5				
Channel bed Mancos Shale crust	U6F1	>1	3	3.5					0.5			T				
Channel bed Mancos Shale Crust	U6F1	<1	3	4.5					1	0.5		T				

The coating of more soluble minerals by less soluble minerals may also cause discrepancies between X-ray diffraction and chemical analyses. If a soluble mineral is coated by a mineral of lower solubility, then its rate of dissolution and, more importantly, whether it dissolves at all, will depend on the behavior of the coating.

While the lithification of clays and the formation of iron oxide coatings must be measured by a geologic time scale, the formation of a less soluble salt coating could be quite rapid in soils and on channel beds by the following mechanism. As the soil solution becomes concentrated as a result of evaporation, two things occur: the solution boundary moves from the larger pores towards the smaller pores, keeping the small pores full of liquid while the large pores empty; and at the same time, the less soluble salts start to precipitate and form around the edge of the boundary, thus enclosing or partially enclosing the more soluble salts still in solution.

Data supportive to a coating or other dissolution limiting theory are supplied in the last column of Table A.1.4. Denoting solute concentration of a 1:X sediment:water mixture by $SC_{1:X}$, the ratio $SC_{1:99}/SC_{1:9}$ is an indicator of additional dissolution upon dilution even when the more sediment laden mixture is undersaturated with respect to the major dissolving minerals (Laronne, 1977). Note that all except two 1:9 mixtures (G8B1 and U5M2A) of Table A.1.4 were undersaturated with respect to Gypsum.

A.1.3 Soluble Mineral Species Available in Study Area

Numerous soil samples have been collected from locations throughout the potentially saline areas of the Upper Colorado River Basin. The

Table A.1.4 EC and total solute concentration data for selected soil samples from West Salt Creek (G7 and G8), Leach Creek (G1 and G2) and North Miller Creek in the Price Basin (U5 and U6).

Sample No.	EC* µmhos/cm at 25°C			SC mg/ℓ		
	1:1	1:9	1:99	1:9	1:99	$11\frac{SC_{1:99}}{SC_{1:9}}$
G7A1S	2000	435	61	294	30.6	1.14
G8B1	71600	12500	2130	14131	1836.9	1.43
G1B1	1915		181		107.1	
G1E3	3220		760		599.8	
G2A1	2140		670		484.1	
G20A	1975	1050	222	812	135.5	1.83
U5C4A	6500	1420	242	1151	149.6	1.43
U5M2A	38700	6700	1230	6885	975.3	1.56
U51J	4300	1660	450	1378	305.9	2.44
U6F1	2400	682	121	494	67.3	1.50

*Particle size separation was not used in EC or SC analyses.

samples consist mainly of grab samples from the streambed crust, underlying streambed materials and stream banks and from various Mancos Shale outcrops. The samples were taken to identify soluble mineral species (Table A.1.3) and to observe the variations in saline mineral concentrations (on a relative scale of 1 to 10) throughout the study area.

Selected samples of earth materials from seven regions within the study area have been analyzed for salt mineral species and for soluble salt content. The sampling locations included areas in or near the Green River at the confluence with the Price River and North Miller Creek in Utah, and Leach Creek, Badger Wash, Prairie Canyon, South Canyon, and West Salt Creek in Colorado.

Although the principal bedrock in each of these areas is shale of the Mancos Formation, there are differences in relative quantities and types of salts among these locations. Differences are due to the type of samples taken at a particular location (rock formation, soils, stream bed material, stream transported sediment, efflorescent crusts or crystal deposits at evaporative surfaces). Differences in soluble minerals among locations may also be due in part to different sections of sampled shale which represent different geologic time spans as well as varying conditions of marine sedimentation during formation.

In general, the less soluble minerals (Calcite and Dolomite) were dominant in soil materials, as was the more soluble Gypsum. The highly soluble minerals (Nahcolite, Soda, Hemihydrate, Epsomite, Hexahydrate, Thenardite, Mirabilitie and Bloedite, as well as Gypsum) were more concentrated in efflorescent crusts in dry stream beds and near seeps where evaporative concentration has occurred. The single occurrence of

Halite was in an efflorescent crust from the dry channel bed of West Salt Creek. Gypsum was commonly found in pure crystalline form within voids and on surfaces of bedding and fracture plains in the Mancos Shale formation. Relatively large (1-20 mm) Gypsum crystals were distributed on the surface of weathered shale in some locations. The presence of more soluble minerals in the shale proper is inferred from soluble ion analyses and also by the low or trace concentrations detected by X-ray diffraction.

A.1.4 Soluble Mineral Variations on a Selected Hillslope and a Channel

Leach Creek Erosion Study: Earth materials from this area were taken in conjunction with slope erosion studies (see Chapter 3). The samples, as collected and reported herein, were not materials transported during the erosion study itself, but rather were undisturbed samples taken at various positions along the hillslope (Run I-5). The parent material on the slope was dark gray Mancos Shale. The soil on the slope and over the shale was of shallow depth (<20 cm).

All but one of the samples were subdivided by dry sieving into greater than 1 mm and less than 1 mm fractions prior to X-ray diffraction analysis. Calcite and Gypsum were most concentrated in coarse fractions, whereas Dolomite was most concentrated in finer fractions (Table A.1.5). At the upper slope positions, Gypsum was most concentrated near the surface at each sampling location. This did not appear to hold for Gypsum near the base of the slope, nor was there an evident relationship between Calcite or Dolomite content and soil depth. All samples contained relatively large amounts of these minerals. Gypsum was dominant throughout. Identification of other possible mineral species in these samples is still being studied.

Table A.1.5. Results from X-ray diffraction measurements for Hillslope Study I on run (plot) I-5. Scale used is 0-10; T = trace

	Station	Sample #	Depth (cm)	Particle size (mm)	$CaCO_3$	$CaMg(CO_3)_2$	$CaSO_4 \cdot 2H_2O$	Unknown peaks
Dry soil	A	T5-1	0-5	>1	2	2	10+	✓
Dry soil				<1	1	3	3.5	✓
Dry soil		T5-2	5-25	>1	1	1.5	2.5	
Dry soil				<1	1	3.0	3	
Dry soil	B_1	T5-5	0-5	>1	1	2.5	5.5	
Dry soil				<1	0.5	2.0	3.5	
Dry soil		T5-6	5-25	>1	1	2.0	5	✓
Dry soil				<1	0.5	1.5	2	
Dry soil	C_1	T5-9	0-5	>1	1	2.5	5	✓
Dry soil				<1	1	2	3.5	
Dry soil		T5-10	5-25	>1	1.5	2	4.5	✓
Dry soil				<1	0.5	2	2.5	✓
Dry soil	D_1	T5-13	0-5	>1	1	1.5	1.5	✓
Dry soil				<1	0.5	2	2	✓
Dry soil		T5-14	5-25	>1	0.5	2	4	
Dry soil				<1	T	2.5	2	
Dry soil	D_2	T5-17	0-5	>1	0.5	1.5	2	
Dry soil				<1	T	2.5	1.5	
Dry soil		T5-18	5-25	>1	0.5	2	2.5	
Dry soil				<1	0.5	5.5	3	
	B_1	T5-8	5-25		0.5	3	5.5	

West Salt Creek Stream Sampling Study: Selected samples, taken in conjunction with flow and water quality studies following a storm event, were examined for presence of saline minerals. Samples at this location were taken under two different situations. The first set of samples represent suspended sediment collected by sediment sampler No. 1 during a storm event on October 6, 1977 (Chapter 4). The second set of samples represented stream bed sediments collected 12 days after flow from the storm event had subsided.

The twelve stream bed samples selected for analysis were taken from depths of 3 and 6 inches. All samples contained Calcite, Dolomite and Gypsum (Table A.1.6). Calcite and Dolomite were most concentrated in sediments greater than 1 mm diameter. Gypsum was randomly distributed between the coarse and finer fractions and there was no consistent difference in relative amounts of Calcite, Dolomite or Gypsum between the two depths of sampling. Note that sample G8B was collected from the bed crust near a saline seep; sample G20 characterizes Mesa Verde Shale in contact with the channel in the upper part of the basin.

Table A.1.6. X-ray diffraction data from West Salt Creek bed samples.

Scale used is 0-10; T = trace.

Particle size (mm)	Station	Depth (in)	Sample #	$CaCO_3$	$CaMg(CO_3)_2$	$Na_2CO_3 \cdot 10H_2O$	$Na_2CO \cdot NaHCO_3 \cdot 2H_2O$	$CaSO_4 \cdot 1/2H_2O$	$CaSO_4 \cdot 2H_2O$	Na_2SO_4	$Na_2SO_4 \cdot 10H_2O$	$NaMg(SO_4)_2 \cdot 4H_2O$	$MgSO_4 \cdot 6H_2O$	$MgSO_4 \cdot 7H_2O$
	1	3	1B3	1	2.5				T					
	1	6	1B6	2	3.5				T					
>1	2	3	2B3	1.5	8.5				4					T
<1	2	3	2B3	1	2.5				2.5					
>1	2	6	2B6	3	8				T		0.5		0.5	
<1	2	6	2B6	1.5	2				T				T	T
>1	3	3	3B3	10	3.5				T					
<1	3	3	3B3	2	3				T					
>1	3	6	3B6	4.5	4.5				T				T	
<1	3	6	3B6	2	2.5				T			0.5	T	
>1	4	3	4B3	5.5	4.5									
<1	4	3	4B3	1.5	3.5				1			T		
>1	4	6	4B6	2	3	3	T		T				0.5	T
<1	4	6	4B6	3.5	2.5				T		0.5		T	T
>1	5	3	5B3	2.5	2				T					
<1	5	3	5B3	1.5	2				T					
>1	5	6	5B6	4.5	4.5									
<1	5	6	5B6	2	2				T					
>1	1	3	1D3	7.5	8.5				T	T				
<1	3	3	ID3	3	4.5			T	T					
>1	1	6	1D6	3	10				T					
<1	1	6	1D6	4	5.5				0.5					T
>1		0.5	G7A	1	3				0.5	T		T		
<1		0.5	G7A	3	3.5				0.5	T		0.5		
>1		0.1	G8B	1	3				T	1		5	0.5	
<1		0.1	G8B	1	1.5				T	0.5		2.5	1.0	
>1		1	G20	T	3				6					
<1		1	G20		1.5				0.5					

Table A. 2. Data on extent of delay (time from collection of runoff sample to its filtration) for Hillslope Study I. Note: an asterisk, usually denoting the odd numbered samples which were not measured immediately, means that the data were excluded from the determination of the average delay.

RUN 1-3

Sample #	1	2	3	4	5	6	7	8	9	10	11	12	13	14	15	Average
Station A			5	184*	2	181*	2	182*	4	2	1	2	9	14		4.6
B1				1	2	180*	3	174*	4	3	1	2	1	1		2.0
B2	6		6	175*		4	4	167*	5	5	1	2	12	8		5.3
C1	5		5	178*	3	176*	5	171*	4	9	2	1	1	3		3.7
C2	6		9		7		7	99*	7	4	4	7				6.4
D1	4	157*	3	154*	3	150*	2	146*	1	5	5	3	3			3.2
D2	7	117*	6	115*	5	113*	4	110*	5	10	5	8				6.3

RUN 1-4

Station A	6	192*	5	190*	4	188*	6	184*	8	5	9	6	19			6.7
B1	2	196*	6	194*	7	191*	11	187*	8	8	10	7	10			7.7
B2	12		9	201*	12		10	185*	10	11	9	7	1	7		9.1
C1	10		9		9	185*	11		13	10	10					9.0
C2	10				10				12	11	9	19				11.8

RUN 1-5

Station A	2	160*	4	157*	10	156*	12	152*	13	20	17	25	8			12.5
B1	3	106*	9	104*	11	101*	14	97*	16	24	18	25	9			14.9
C1	3	168*	8	166*	11	164*	14	160*	18	27	18	26	12			12.2
D1	7		8	169*	11	167*	15	164*	17	26		26	11			15.1
D2	6		9	155*	11	152*	9	148*	10	24	11	14	1			10.6

RUN 1-6

Station A	3		3	88*	2	85*	1	81*	3	2	5	5	4			3.1
B1	1	91*	2	89*	3	86*	4	98*	3	5	7	3	7			3.9
C1	4		3	122*	6		4	114*	2	6	9	10	11			6.0
D1	4	88*	8	86*	20	84*	19	74*	13	13	4					11.8
D2	6	91*	12	88*	10	87*	12	82*	11	35	27	14				15.5

RUN 1-7

Station A	2		1	97*	1	95*	1	91*	5	11	5	5	4			3.9
B1	2	97*	2	95*	5	91*	6	88*	8	8	7	4	4			5.1
B2	10		8	125*	9	122*	17		18	2	10	2	6			9.0
C1	6	127*	10	130*	10	9		122*	10	20	19	26	50			17.7
C2	20					113*	46			13	15	4	27			20.5
D1	6	96*			13	81*	8	78*	8	9						8.8

RUN 1-8

Station A	3		1	105*	1	103*	1		9	12	3	1	2	3	1	2.6
B1	4	115*	6	118*	5	115*	15	112*	6	10	6	9	3	3	6	6.7
B2	5	132*	5	129*	8		19	122*	1	11	9	9	13	5	1	9.2
C2	14		11	121*	18	119*	15	115*	12	9	12	6	4	3	4	9.8

RUN 1-9

Station A	2		1	36*	1	33*	1	30*	7	3	6	1	1	1	1	2.3
B2	4		5	37*	3	35*	10	31*	3	4	3	3	1	6	3	4.1

Table A.3. EC data (in μmho/cm-1 at 25°C) for filtered (Column 2) and unfiltered (column 3) runoff samples collected in Hillslope Study I. Column 4 shows the increase in EC, in percent. Column 5 shows the average increase in EC for each station, in percent. Note: the increase in EC took place over a 60 day period. The increase in EC for runs 1-5 and 1-8 are based on unfiltered samples for both the immediate and the late EC reading.

RUN I-2

(1) No.	(2) EC_f (29.8.77)	(3) EC_{uf} (26.8.77)	(4) $\frac{\{(8)-(2)\}100}{(2)}$	(5) Average (4)
A-1	1160	1434	23.7	
5	1360	1818	33.7	41.6
10	1940	3260	68.0	
B_1-1	2100	3090	47.1	
5	2430	3160	30.0	
10	2890	3190	10.4	
B_2-1	1620	2480	53.1	30.7
5	1570	2160	37.7	
10	2880	3060	06.0	
C_1-1	2780	3110	11.8	
5	2810	3140	11.4	11.8
10	2890	3240	12.1	
D_1-5	2940	3120	6.1	
10	2790	3130	12.2	
D_2-1	2800	3160	12.9	10.2
5	2640	2920	10.6	
10	2430	2680	10.3	
Average:	2355		23.2	

RUN I-3

(1) No.	(2) EC_f 30.8.77	(3) EC_{uf} 29 & 30/.8/77	(4) {(3)-(2)}100 (2)	(5) Average (4)
A-1	1390	2660	90.6	
5	1940	2660	37.1	76.4
10	940	1950	107.4	
B_1-1	1050	1680	60.5	
5	2090	2790	34.0	
10	2310	2810	21.4	
B_2-1	2350	2770	17.9	46.9
5	1730			
10	1300	2610	100.9	
C_1-1	2000	2780	39.0	
5	2240	2830	26.3	
10	2450	2860	16.7	33.1
C_2-1	1870	2730	46.0	
5	2080	2620	26.0	
10	1860	2710	45.0	
D_1-1	2480	2870	11.0	
5	2560	2740	7.0	
10	2480	2720	9.7	9.0
D_2-1	2630	2820	7.2	
5	2390	2630	10.0	
10	2140	2230	8.9	
Average:	2016		36.1	

RUN I-4

(1) No.	(2) EC_f (1.9.77)	(3) EC_{uf} (31.8.77)	(4) {(3)-(2)}100 (2)	(5) Average (4)
A-1	1520	2770	83.3	
5	2410	2710	12.4	67.9
10	1230	2560	108.1	
B_1-1	2600	3160	21.5	
5	2550	2760	8.2	
10	2520	2740	8.7	28.6
B_2-1	2470	2820	14.2	
5	1800	2690	49.4	
10	1550	2630	69.7	
C_1-1	2580	2770	7.4	
5	2660	2880	8.3	
10	2640	2880	8.3	16.7
C_2-1	2080	2740	31.4	
5	2760	3330	20.7	
10	2420	3020	24.8	
D_1-1		2960		
5				
Average:	2253	2950	31.7	

RUN I-5

(1) No.	(2) EC "immed"-uf much shaking	(3) EC_{uf} later	(4) {(3)-(2)}100 / (2)	(5) Average (4)
A-1	3200	2958	-7.5	25.4
5	5950	5949	0.0	
10	1910	3513	83.7	
B_1-1	2980	3232	8.4	12.7
5	5620	6087	8.2	
10	2400	3610	50.4	
B_2-1	3700	3467	-6.2	
C_1-1	3000	3399	13.3	15.1
5	5800	6627	14.3	
10	3850	4513	17.6	
D_1-1	3800	4674	23.0	11.1
5	5200	7271	39.8	
10	5150	5569	8.1	
D_2-1	6350	6888	8.5	
5	6450	6423	-0.4	
10	6000	5235	-12.7	
Average:	4460		15.5	

RUN I-6

(1) No.	(2) EC_f (2.9.77)	(3) EC_{uf} (2.9.77)	(4) {(3)-(2)}100 / (2)	(5) Average (4)
A-1	2530	2930	15.8	52.7
5	2550	2680	6.0	
10	1210	2660	136.2	
B_1-1	2560	2780	8.6	14.4
5	2560	3100	21.1	
10	3160	3590	13.6	
C_1-1	2640	2810	6.4	8.7
5	3620	3790	4.7	
10	3560	4090	14.9	
D_1-1	3850	4270	70.9	13.6
5	3020	3520	16.5	
10	2890	3590	24.2	
D_2-1	3170	3790	19.6	
5	3260	3470	6.4	
10	3140	3260	3.8	
Average:	2915		20.6	

RUN I-7

(1) No.	(2) EC_f (2.9.77)	(3) EC_{uf} (2.9.77) +(6.9.77)	(4) $\frac{\{(3)-(2)\}100}{(2)}$	(5) Average (4)
A-1	1060	2620	147.2	115.3
5	1320	2520	90.9	
10	1030	2140	707.7	
B_1-1	1530	2950	92.8	
5	1260	2500	98.4	82.3
10	720	1210	68.1	
B_2-1	1790	2950	64.8	
5	2020	3020	49.5	
10	1090	2290	110.1	
C_1-1	1630	2850	74.2	
5	1660	2780	67.5	
10	820	1380	68.3	83.5
C_2-1	1380	2880	102.9	
10	1060	2170	104.7	
D_1-1	1740	3060	75.8	
5	1630	2810	72.4	76.9
10	1190	2170	82.4	
Average:	1349		86.9	

RUN I-8

(1) No.	(2) EC "immed"-uf	(3) EC_{uf} 2 months later	(4) $\frac{\{(3)-(2)\}100}{(2)}$	(5) Average
A-1	708	709	0.0	
5	802	844	4.7	4.8
10	1002	1097	9.7	
B_1-1	778	806	3.6	
5	1060	967	-8.8	
10	830	806	-2.9	10.3
B_2-1	605	641	5.9	
5	788	1064	35.1	
10	1164	1499	28.8	
C_2-1	990	1182	19.3	
5	1124	1612	34.5	25.5
10	1140	1400	22.8	
Average:	830		12.7	

Table A.4. EC (in μmho/cm at 25°C) and ion specie concentrations (in meq l^{-1}) for I-5 and I-8 runoff samples of Hillslope Study I. Note: All sample numbers denoted by "F" refer to on-site filtered samples.

Sample No.	EC	HCO_3	Cl	SO_4	Total	Na	Ca	Mg	K	Total	pH
T8 A-1	709	5.32	0.53	2.29	8.14	3.60	3.55	0.55	0.22	7.92	7.7
3	729	5.01	0.36	3.12	8.49	3.50	4.05	0.55	0.20	8.30	7.6
4	831	4.91	0.37	4.68	9.96	3.40	5.30	0.70	0.19	9.59	7.7
5	844	4.59	0.34	4.95	9.88	3.50	5.50	0.50	0.19	9.69	7.8
6	806	4.70	0.34	4.30	9.34	3.30	5.20	0.50	0.17	9.17	7.7
7	917	4.80	0.57	5.40	10.77	3.30	6.50	0.70	0.17	10.67	7.8
8	1267	4.96	1.02	9.75	15.73	3.60	10.50	0.70	0.20	15.00	7.6
9	1637	5.22	0.88	18.00	24.10	3.50	18.50	0.90	0.25	23.15	7.5
10	1097	4.44	1.44	7.60	13.48	3.30	8.80	0.70	0.16	12.96	7.9
11	1013	4.44	0.52	7.20	12.16	3.30	7.40	0.50	0.15	11.35	7.8
12	2217	5.48	0.74	26.00	32.22	3.05	27.50	0.75	0.20	31.50	7.3
13	2264	3.65	0.43	29.00	33.08	3.25	28.75	0.50	0.18	32.68	7.9
14	1637	4.18	0.28	18.50	22.96	3.50	18.00	0.50	0.17	22.17	7.8
15	1520	4.02	0.20	15.50	19.72	3.40	15.00	0.50	0.15	19.05	7.9
T8 B-1	806	4.49	0.34	3.90	8.73	3.50	4.50	0.50	0.21	8.71	7.8
2	657	4.75	0.20	2.55	7.50	3.40	3.50	0.55	0.15	7.60	7.7
3	649	4.91	0.17	2.50	7.58	3.40	3.45	0.65	0.16	7.66	7.7
4	673	4.38	0.20	3.10	7.68	3.40	3.70	0.50	0.14	7.74	7.7
5	967	3.45	0.26	7.50	11.41	3.40	7.00	0.70	0.16	11.26	7.9
6	771	4.18	0.20	4.30	8.68	3.35	4.50	0.50	0.15	8.50	7.8
7	739	4.33	0.23	3.90	8.46	3.35	4.25	0.55	0.14	8.29	7.8
8	749	4.18	0.20	3.70	8.08	3.20	4.25	0.55	0.13	8.13	7.9
9	729	4.07	0.14	3.70	7.91	3.25	4.10	0.55	0.12	8.02	7.8
10	806	3.86	0.20	5.20	9.26	3.20	4.90	0.55	0.12	8.77	7.9
11	749	4.23	0.26	4.10	8.59	3.25	4.40	0.55	0.12	8.32	7.7
12	1716	4.02	0.23	18.50	22.75	3.50	17.50	0.90	0.18	22.08	7.6
13	1834	3.65	0.26	19.50	23.41	3.50	18.50	0.70	0.16	22.86	7.9
14	1132	4.12	0.20	8.75	13.07	3.50	9.20	0.70	0.12	13.50	7.7
15	985	4.07	0.23	7.00	11.30	3.20	7.30	0.50	0.10	11.10	.78
T8 B_2- 1	641	4.96	0.31	1.75	7.02	3.45	2.80	0.50	0.22	6.97	7.9
2	641	5.01	0.17	1.95	7.13	3.40	3.05	0.55	0.16	7.16	7.6
3	641	4.59	0.20	2.40	7.19	3.40	3.00	0.55	0.16	7.11	7.7
4	818	4.33	0.20	4.40	8.93	3.45	4.60	0.75	0.17	8.97	7.7
5	1064	4.12	0.20	8.00	12.30	3.40	7.60	0.90	0.15	12.05	7.5
7	902	4.28	0.20	5.60	10.08	3.40	5.90	0.70	0.14	10.14	7.7
8	1023	3.97	0.17	7.50	11.64	3.30	7.20	0.90	0.16	11.56	7.8
9	1064	4.23	0.23	8.00	12.46	3.30	8.20	0.70	0.15	12.35	7.7
10	1499	3.39	0.26	15.00	18.65	3.30	14.00	0.90	0.16	18.36	7.8
11	2128	4.02	0.20	26.00	30.22	3.25	25.00	1.25	0.19	29.69	7.6
12	2046	3.92	0.23	26.00	30.15	3.25	24.50	1.25	0.20	29.20	7.7
13	2264	3.86	0.26	30.00	34.12	3.05	29.00	1.00	0.21	33.26	7.7
14	1834	3.97	0.31	22.25	26.53	3.50	21.00	1.00	0.16	25.66	7.8
15	1237	2.92	0.28	11.00	14.90	3.40	9.80	0.70	0.14	14.04	7.7

Sample No.	EC	HCO_3	Cl	SO_4	Total	Na	Ca	Mg	K	Total	pH
T8 C_2-1	1182	4.18	0.26	9.75	14.19	3.60	9.20	0.70	0.22	13.72	7.7
2	1612	3.76	0.26	16.50	20.52	3.50	15.00	0.90	0.24	19.64	7.8
3	985	3.97	0.26	7.00	11.23	3.50	6.80	0.70	0.21	11.21	7.8
4	1298	4.23	0.28	10.75	15.26	3.50	10.50	0.50	0.24	14.74	7.5
6	985	4.18	0.20	6.60	10.98	3.50	7.00	0.50	0.18	11.18	7.7
7	1330	3.76	0.23	12.50	16.49	3.50	12.00	0.70	0.18	16.13	7.9
8	1298	3.81	0.28	12.00	16.09	3.40	12.50	0.50	0.16	16.56	7.8
9	1520	3.97	0.26	14.75	18.98	3.60	13.50	0.90	0.18	18.18	7.8
10	1400	3.39	0.26	11.50	15.15	3.30	11.00	0.70	0.17	15.17	8.0
11	1834	3.97	0.28	19.00	23.25	3.60	18.00	0.70	0.21	22.51	7.7
12	2217	4.33	0.23	28.00	32.56	3.85	26.25	1.25	0.23	31.88	7.8
13	1970	3.13	0.26	21.50	24.89	3.75	21.00	1.00	0.19	25.44	7.9
14	1803	3.50	0.28	18.50	22.28	3.50	17.50	0.70	0.18	21.88	8.0
15	1773	4.33	0.26	24.00	28.59	3.50	24.50	1.00	0.14	29.14	7.8
T8 A_1 - F	633	4.33	0.31	2.20	6.84	3.70	2.70	0.50	0.24	7.14	8.4
A_5 - F	739	3.71	0.23	3.90	7.84	3.50	4.00	0.55	0.20	8.25	8.1
A10- F	967	3.97	0.20	6.60	10.77	3.30	6.80	0.70	0.16	10.91	8.2
$B_1$1- F	673	3.97	0.28	2.80	7.05	3.50	3.25	0.50	0.22	7.47	8.2
$B_1$5- F	950	3.65	0.17	6.60	10.42	3.40	6.40	0.90	0.17	10.87	8.2
$B_1$10-F	739	3.71	0.17	4.10	7.98	3.35	4.05	0.55	0.13	8.08	8.2
$B_2$1- F	578	3.97	0.31	2.15	6.43	3.45	2.35	0.45	0.25	6.50	8.3
$B_2$5- F	739	3.13	0.20	4.10	7.43	3.20	3.90	0.50	0.16	7.76	8.1
$B_2$10-F	1004	2.71	0.20	7.60	10.51	3.20	6.90	0.70	0.15	10.90	8.1
$C_2$1- F	818	3.65	0.68	5.00	9.33	3.20	4.80	0.50	0.20	8.70	8.1
$C_2$5- F	985	2.82	0.17	8.00	10.99	3.40	6.70	0.70	0.23	11.03	8.1
$C_2$10-F	1108	2.61	0.17	9.25	12.03	3.30	8.20	0.70	0.14	12.34	7.9
T5 A_1 - F	2980	3.76	0.45	39.00	43.21	3.35	29.50	10.00	0.88	43.73	8.1
A_5 - F	5668	3.76	3.10	82.50	89.36	11.75	22.00	59.00	0.50	93.25	8.1
A_{10}- F	1931	4.18	1.24	19.50	25.03	5.88	4.50	14.75	0.26	25.39	8.1
$B_1$1- F	3068	4.04	0.88	40.00	45.03	4.50	28.00	11.50	0.50	44.50	8.1
$B_1$5- F	5926	3.71	2.43	92.75	98.89	13.10	22.50	63.00	0.50	99.10	8.0
$B_1$10-F	2370	3.97	0.74	26.00	30.82	6.10	10.50	14.00	0.44	31.04	8.2
$B_2$1- F	3259	3.92	0.88	45.00	49.91	4.50	27.50	16.50	0.50	49.00	8.0
$C_1$1- F	3259	3.65	1.58	45.00	50.31	4.50	29.50	16.50	1.00	51.50	8.2
$C_1$5- F	6360	3.71	1.92	98.00	103.74	15.50	21.50	69.50	1.00	107.50	8.1
$C_1$10-F	3524	3.86	1.07	48.00	53.03	10.85	15.00	27.00	0.68	53.53	8.1
$D_1$1- F	4741	3.65	2.43	66.50	72.69	11.75	29.00	32.00	2.00	73.75	8.1
$D_1$5- F	6432	3.65	3.14	100.00	105.79	18.00	21.50	67.50	1.00	108.00	8.1
$D_1$10-F	5321	3.65	2.14	78.00	83.90	15.00	23.00	45.00	0.50	83.50	8.1
$D_2$1- F	6773	3.92	3.83	100.04	111.75	20.00	23.50	67.50	1.00	112.00	8.2
$D_2$5- F	6208	3.39	2.43	90.30	96.12	19.00	22.50	55.00	1.00	97.50	7.8
$D_2$10-F	5113	3.65	1.86	80.00	85.51	19.00	23.00	41.50	1.00	84.50	8.1

Sample No.	EC	HCO_3	Cl	SO_4	Total	Na	Ca	Mg	K	Total	pH
T5 A-1	2958	6.53	2.14	35.00	43.67	3.35	28.00	10.50	0.85	42.70	7.6
2	3467	4.83	1.58	46.00	52.41	3.70	27.50	19.50	1.04	51.74	7.8
3	4695	4.18	2.00	74.00	80.16	7.70	24.00	48.50	1.06	81.26	7.9
4	5288	3.65	1.86	86.00	91.51	9.45	22.50	59.00	1.00	91.95	7.9
5	5949	4.44	3.83	97.50	105.77	13.10	23.50	69.50	1.28	107.38	7.8
6	6755	3.78	2.28	115.00	121.06	15.50	21.00	85.00	0.98	122.48	7.9
7	6270	3.92	2.00	109.00	114.92	14.50	22.00	78.00	0.90	115.40	8.0
8	5107	4.05	1.86	80.00	85.91	9.00	22.00	55.00	0.78	86.78	8.0
9	3466	4.31	2.00	56.00	62.31	7.70	21.00	32.00	0.57	61.27	7.9
10	3513	3.26	2.00	52.00	57.26	5.30	22.50	28.00	0.40	56.20	8.1
11	1370	3.13	0.74	12.00	15.87	2.85	6.25	6.00	0.18	15.28	8.2
12	1722	3.65	0.62	17.50	21.77	3.65	8.25	8.50	0.21	20.61	8.3
13	2727	3.39	0.96	36.25	40.60	4.50	21.50	13.50	0.23	39.73	8.1
$T5B_1$ -1	3232	6.26	2.71	39.00	47.97	3.70	30.00	12.50	0.87	47.07	7.7
2	3537	6.00	1.86	46.00	53.86	4.50	28.00	20.50	1.00	54.00	7.8
3	4633	4.70	1.58	69.00	75.28	8.10	24.00	43.00	1.14	76.24	7.8
4	5540	4.70	1.72	90.00	96.42	11.52	22.00	61.00	1.12	95.64	7.9
5	6087	4.18	2.43	104.00	110.61	13.32	21.00	74.00	1.14	109.46	7.9
6	7322	4.18	2.57	135.00	141.75	18.00	20.00	102.50	1.16	141.66	8.0
7	6017	4.05	2.85	104.00	110.90	13.55	22.00	75.00	0.95	111.50	8.0
8	7322	4.18	2.00	135.00	141.18	17.50	21.00	101.25	1.16	140.91	7.9
9	5034	4.18	2.14	80.00	86.32	9.90	22.50	53.50	0.72	86.62	7.9
10	3610	4.31	1.02	49.00	54.33	4.90	24.50	24.00	0.57	53.97	8.0
11	2991	4.18	1.16	37.00	42.34	4.90	23.00	13.50	0.40	41.80	8.0
12	1315	3.18	0.40	11.50	15.08	3.65	6.00	5.75	0.16	15.56	8.3
13	2657	3.86	0.79	33.00	37.65	4.05	19.25	13.50	0.37	37.17	8.0
B_2 -1	3467	4.96	1.58	46.00	52.54	3.35	29.50	18.50	0.95	52.30	7.6
2	3713	7.31	3.27	54.00	64.58	7.30	27.50	29.50	0.90	65.20	7.7
C_1 -1	3399	6.79	2.71	45.00	54.50	4.95	29.00	19.00	0.98	53.93	7.5
2	4222	5.87	1.44	58.00	65.31	6.90	26.50	31.00	1.16	65.56	7.7
3	5183	5.35	2.00	78.00	85.35	10.85	25.00	49.25	1.24	86.34	7.7
4	5660	4.57	2.14	90.00	96.71	12.20	23.00	61.00	1.20	97.40	7.8
5	6627	4.70	2.43	109.00	116.13	15.50	22.00	78.00	1.34	116.84	7.8
6	7699	3.92	2.71	135.00	141.63	20.00	21.00	100.00	1.42	142.42	7.8
7	7813	3.92	2.28	135.00	141.20	21.00	20.00	100.00	1.36	142.36	7.8
8	7992	4.57	2.43	135.00	142.00	19.00	20.00	102.50	1.40	142.90	7.8
9	5949	4.31	2.00	95.00	101.31	15.00	21.00	65.00	1.06	102.06	7.8
10	4513	3.92	1.44	65.00	70.36	9.45	23.00	36.50	0.74	69.69	8.0
11	3422	3.24	0.85	46.00	50.09	5.88	23.75	20.00	0.60	50.23	7.9
12	2925	3.86	1.02	36.00	40.88	4.73	23.50	11.50	0.44	40.17	7.8
13	3061	3.71	0.79	41.00	45.50	4.95	22.50	17.50	0.45	45.40	8.0
D_1 -1	4674	8.87	3.27	58.00	70.14	10.35	25.00	33.50	1.28	70.13	7.6
2	5315	6.79	2.71	76.00	85.50	10.85	24.00	48.50	1.24	84.59	7.7
3	6159	7.83	2.43	95.00	105.26	15.50	23.00	65.00	1.30	104.80	7.8
4	7221	7.31	2.99	113.75	124.05	19.00	21.50	82.50	1.38	124.38	7.6
5	7271	8.87	3.27	107.50	119.64	19.00	20.00	80.50	1.36	120.86	7.6
6	6799	7.31	4.40	104.50	116.21	18.00	22.00	76.00	1.38	117.38	7.6
7	6980	6.53	3.27	112.50	122.30	20.00	21.00	80.50	1.40	122.90	7.6
8	6843	6.26	4.13	104.00	114.39	19.50	21.50	71.50	1.40	113.90	7.7
9	6384	5.74	3.27	95.00	104.01	19.00	22.00	61.00	1.36	103.36	7.7
10	5569	6.79	1.86	74.00	82.65	15.00	21.00	46.50	1.20	83.70	7.7
11	5288	5.35	1.86	74.00	81.21	15.50	22.00	43.00	0.94	81.44	7.7

Sample No.	EXC10^6	HCO_3	Cl	SO_4	Total	Na	Ca	Mg	K	Total	pH
T5 D_7-1	4513	4.70	2.28	63.00	69.98	9.90	23.00	35.00	0.88	68.78	7.6
3	4363	6.13	1.58	55.00	62.71	9.00	23.50	31.00	0.76	64.26	7.6
4	6888	7.57	3.27	100.00	110.84	19.50	22.00	67.50	1.40	110.40	7.6
6	7027	6.39	2.57	104.00	112.96	21.00	22.00	67.50	1.46	111.96	7.6
7	6503	5.35	2.43	98.00	105.78	20.00	22.00	63.00	1.48	106.48	7.6
8	6423	6.39	2.99	95.00	104.38	19.00	22.50	61.00	1.42	103.92	7.6
9	6159	5.35	2.00	92.50	99.85	19.00	22.50	56.00	1.36	98.86	7.7
10	6181	5.87	2.43	90.00	98.30	19.00	23.00	55.00	1.36	98.36	7.8
11	6017	5.35	2.71	85.00	93.06	18.00	22.00	51.50	1.30	92.80	7.9
12	5540	5.09	2.14	82.00	89.23	16.00	22.50	48.50	1.14	88.14	7.8
13	5235	5.09	2.00	74.00	81.09	14.50	22.00	43.00	1.10	80.60	7.9
14	4695	4.44	2.00	66.00	72.44	13.55	22.50	35.00	0.96	72.01	
15	5235	4.83	2.00	76.00	82.83	16.50	23.00	43.00	0.98	83.48	
16	3212	3.55	0.90	39.00	43.45	7.25	18.75	16.00	0.50	42.50	

A.5 FEASIBILITY OF USING COMPUTER SIMULATION TO STUDY RILL PATTERNS

Introduction

Drainage basin form has been qualitatively described by Zernitz (1932), who identified patterns controlled by slope and structure. It has been suggested that drainage basin characteristics include topographic, soil, geologic or structural and vegetational factors. In a classic paper, Horton (1945) made a comprehensive analysis of many of the variables included in these categories, and introduced the concept of stream ordering as a measure of basin size and shape. He presented data that linked stream length, stream slope, and number of streams to order. Strahler (1957) improved the ordering system and validated the relationships. Schumm (1956) proposed the law of drainage areas which also used stream ordering and emphasized drainage density (total stream length divided by drainage area) as an indication of the deterministic factors in drainage basin development. Using physical models, Parker (1977) and Mosley (1973) showed that stream length and drainage density are related to changes in slope.

A more recent development in the study of drainage patterns is the use of random walk computer simulation. Leopold and Langbein (1962) proposed a random walk model to simulate the development of drainage patterns in areas of uniform lithology. This model was programmed and used as a basis for subsequent work (e.g., Smart, 1967). Discussion by Howard (1971) indicates that the similarities between simulation models and actual systems may result because the models produce topologically random networks and common link length distributions that are representative of regions with uniform lithology and no pronounced regional slope. Smart and Moruzzi (1971) moved closer to natural conditions with a

headward growth model in which channel growth is dependent on the amount of undissected area upslope of the stream tip. The uphill direction is made favorable to horizontal moves through decision rules.

The purpose of this study is to use physical assumptions to simulate reasonable dendritic and parallel rill patterns. The effect of slope on drainage patterns and drainage basin form has not been studied quantitatively because it is difficult to isolate the effects of a single variable in field studies. A conceptually simple model is proposed to determine if assumptions based on a single variable such as slope can produce results that will aid the study of rill pattern and rill formation.

Model Description

A drainage basin of fixed shape is modelled with various topographic conditions with assumed no structural controls. Main slope and cross-slope are the major parameters. The channels are formed sequentially by moving from a fixed set of sources, which define the drainage area and shape, to either an exit boundary or to a junction with a preexisting channel. This approach is one of many that could be used to simulate drainage patterns. The input values are relative numbers and have no connection to real data.

The hypothetical drainage area is represented by a square (100x100) matrix. At any location, the channel can move to one of five adjacent matrix points. It can move horizontally in either direction, straight downslope, or downslope at 45° in either direction. The direction of each move is chosen by a set of probabilities assigned to the move and a random number chosen from a uniform distribution between 0.0 and 1.0.

The adjustment of these move probabilities is the method by which the parameters affect the channel formation. After each of the rills is completed, an area of influence is defined on both sides of the rill. The move probabilities of later channels are adjusted in this region to encourage moves in the cross-slope direction toward the existing channel. The network is complete when all the predefined source points have been used in forming a channel.

The fixed sources are a limiting condition because, for the purpose of this preliminary study, we are only interested in the effect of the topographic assumptions. The first set of sources follows part of the evolution of a drainage area in a simplified manner by blocking out the area with main streams and then filling in with interior tributaries. Because the sources were chosen arbitrarily, two independent fixed sets were used so the effects of symmetry and shape would not dominate the resulting patterns (Figures A.5.1 and A.5.2). A third set of sources is generated randomly. Each set contains twelve simulations, four variations of slope and three variations of cross-slope, all with the same sources.

The main slope parameter determines the relative weight of the probability of moving downslope with respect to other possible moves. Using the main slope, default move probabilities are calculated. These are assigned to the five moves if the rill is not in the area of influence of a pre-existing rill. A mild slope has a smaller chance to move straight downslope than a steeper one. The default move probabilities for each value of main slope are shown in Figure A.5.3.

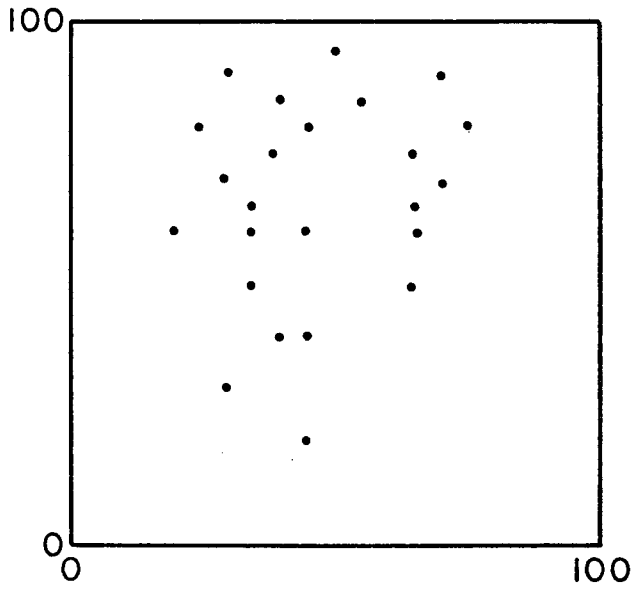

Figure A.5.1. Source points for first set of runs.

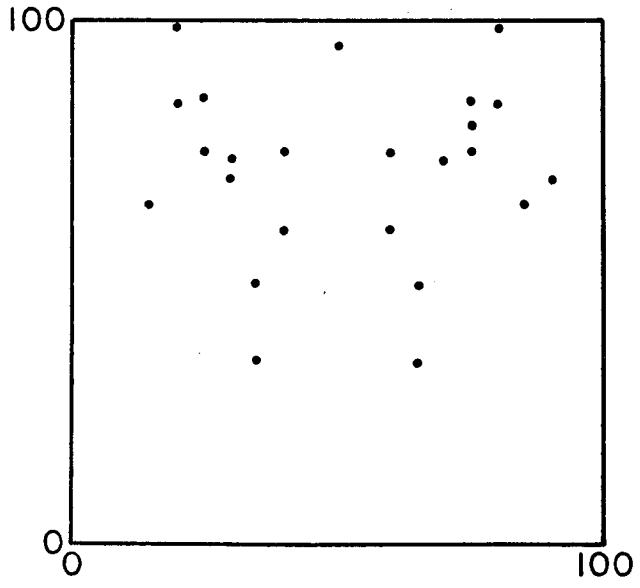

Figure A.5.2. Source points for second set of runs.

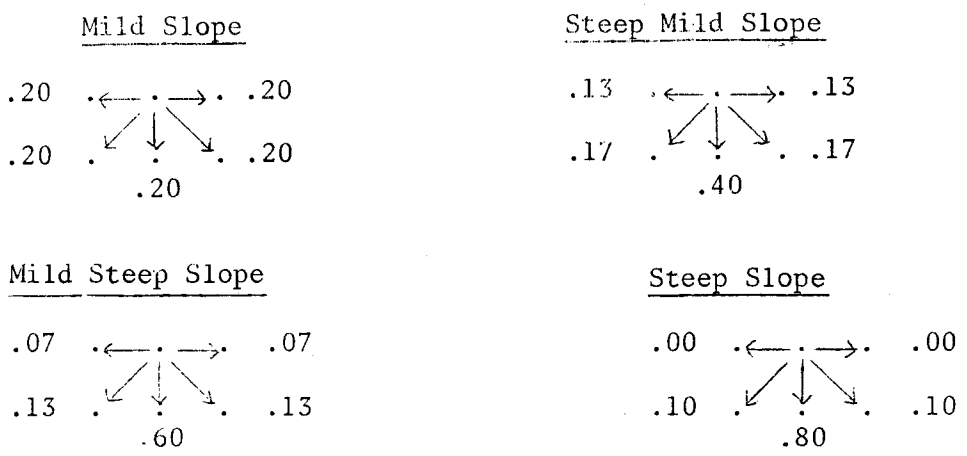

Figure A.5.3. Default move probabilities

The other function of slope is to determine the width of the cross-slope influence. The move probabilities of later rills which originate or venture into this cross-slope area are redistributed. The width of influence is also a function of the rill length, a longer one having a wider area. This assumes that a rill formed on a steep slope will not be affected by cross-grading as much and that a longer rill has degraded the hillslope more than a short one.

Although they are not simultaneously generated, as in natural systems, the channels do not form independently. For any potential move, consideration is given to the cross-slope as a function of distance from preexisting rills and the length of the preexisting rill (for details see Sunday, 1979). This is a stream capture process. After the default move probabilities are calculated as a function of slope, the location of the channels with respect to preexisting channels is checked. If the channel being generated is within the area of influence of another channel, its default move probabilities are adjusted accoring to the distance from the first channel to encourage the flow in this direction. The total amount the default move probabilities

change as the channel moves from outside the area of influence to a point adjacent to the first rill, is the value of the cross-slope. Channels are encouraged to join more quickly with a steep cross-slope. The move probabilities at various distances from a channel are shown in A.5.4. Note that the cross-slope extends symmetrically on both sides of the channel. The manner in which the probabilities are redistributed using the cross-slope is this: Number the move probabilities, as shown (Figure A.5.4) X marks the location from which the move will be made;

Figure A.5.4. Numbering of move probabilities.

PR1 is reduced according to its distance from the existing channel and the value of cross-slope (mild, medium or steep). With a mild cross-slope (Figure A.5.5), the value of PR1 outside the area of influence (its default value) and its value two moves away from the existing rill differ by 6.4 percent. In a medium cross-slope simulation the difference is 12.8 percent. A steep cross-slope would change these arbitrarily chosen values to 19.2 percent. The values of PR1 between the default area and the area adjacent to the rill vary linearly with the distance from the rill. After PR1 is reduced, half the reduction is added to PR2 and half to PR4 (as labelled in Figure A.5.5).

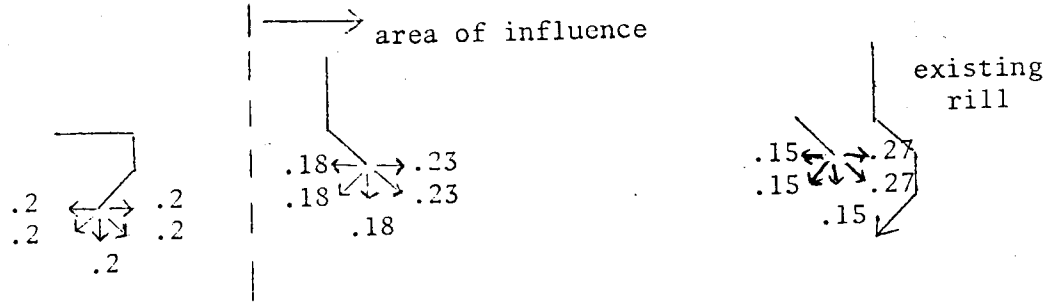

Figure A.5.5 Change in Default Probabilities on a Mild Slope Due to a Steep Cross-slope

PR5 and PR3 are reduced an equal percentage as PR1. The amount by which PR5 is reduced is added to PR4. The amount by which PR3 is reduced is added to PR2. The assumption of the cross-slope parameter is that, as a channel moves closer to an existing channel, the cross-grading will increase the likelihood of a move toward the existing channel.

Thus, the move probabilities at any given point are a function of: slope, cross-slope (as a function of distance from an existing channel) and a random element which takes into account local resistance and irregularities.

Results

The flattest slope produced a dentritic pattern (Figure A,5.6). As the slope steepened, the network became parallel. According to Zernitz (1932), as slope becomes the controlling factor, the pattern departs from the true dendritic type. Parallel drainage is the result of a pronounced regional slope or parallel geologic controls.

For comparison purposes, the bifurcation ratio, defined by Horton to be the relationship between rill order and number of rills, was calculated for all thirty-six of the generated drainage patterns. The length ratio, or relationship between rill order and average rill length, was also calculated. For one set of fixed runs (twelve patterns) Strahler ordering was also utilized to calculate the bifurcation and length ratios. The results are listed below:

	Bifurcation Ratio		Length Ratio	
	Horton	Strahler	Horton	Strahler
First set of fixed sources	2.05-4.61	2.71-5.60	1.82-4.23	0.63-2.49
Second set of fixed sources	2.02-4.16		1.35-3.25	
Random sources	2.00-5.67		1.32-5.38	
Horton (field data)	2.22-3.91		1.84-2.74	
Strahler (field data)		3.00-5.00		1.50-3.50

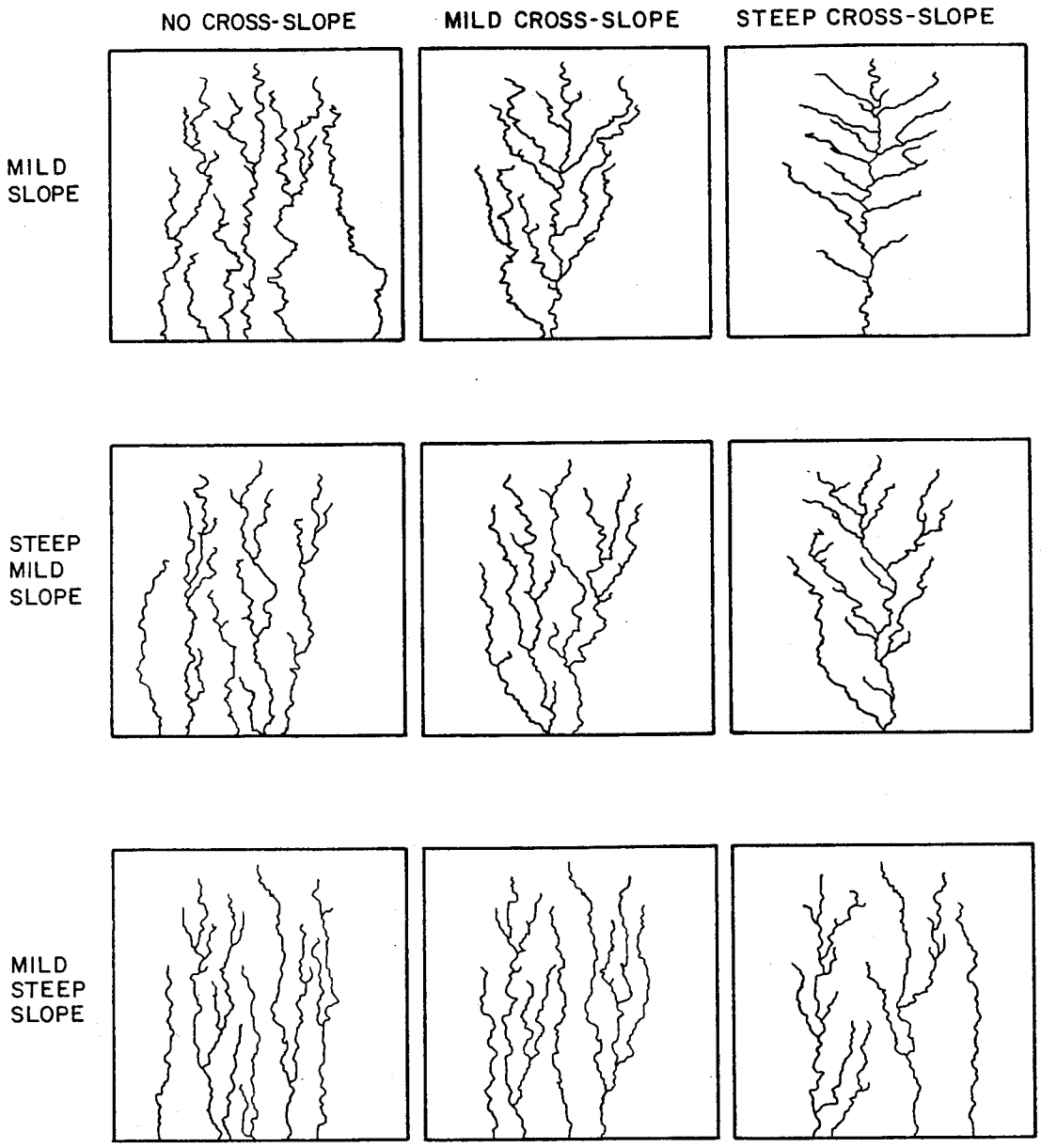

Figure A.5.6. Generated rill patterns using the first set of fixed sources.

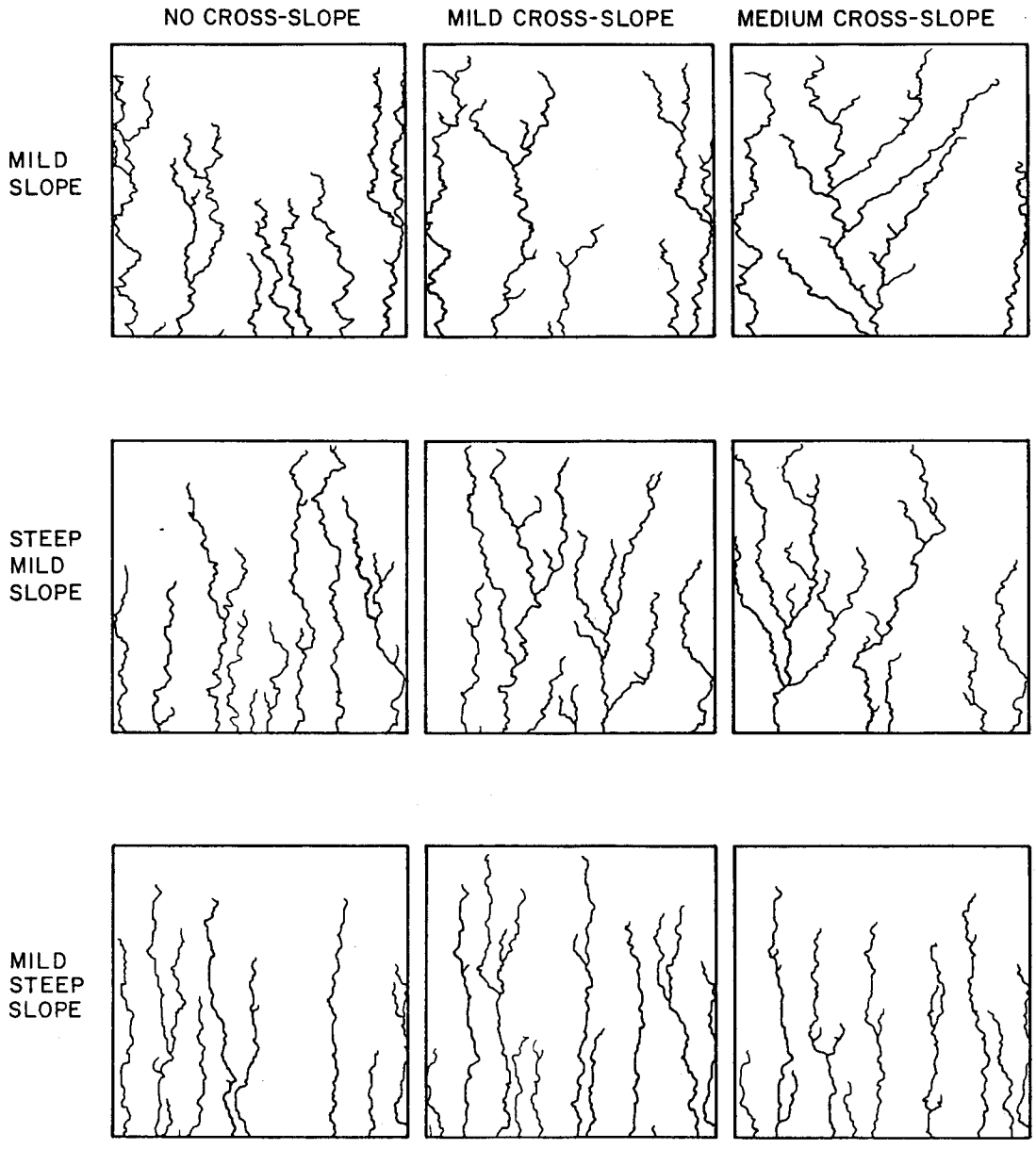

Figure A.5.7. Generated rill patterns using the random set of fixed sources.

The computer patterns are in reasonable agreement with the range of values of bifuraction ratio and length ratio noted in field observations. The fixed number of streams may constrain the results. The number of rill sources used, 21 to 24, is small in comparison to Horton who reported his values of bifurcation and length ratio for networks which contained 24 to 472 sources. The total length of the rills produced by the computer runs is limited by the size of the hillslope matrix. However, the large size (100x100) discretizes the moves so the distance between points does not control the derived channel lengths.

Several observations can be made with respect to the data from the generated rill patterns. As the main slope is increased, keeping the cross-slope constant:

1. Longer total rill lengths are noted (Figure A.5.6, A.5.7, and A.5.8). The numbers have no physical meaning but are relative values. For the slope, 10 corresponds to a mild slope, 30 is a steep mild slope and 50 is a mild steep slope. This is related to increased outlet density. The rills produced by the steeper slopes follow a fairly direct path to the exit boundary. More rills extend the length directly from their source to the exit rather than the shorter path to adjacent rills. This can be related to experimental results by Mosley (1972) for which drainage density was found to increase linearly with slope. Drainage density is total channel length divided by drainage area. In the computer simulation, the drainage area was relatively constant so changes in drainage density are mostly related to changes in channel length.

2. There is a tendency toward longer first-order and second-order rills (Figures A.5.8b and A.5.8c). An increase in length of first-order rills with an increasing slope was also noted by Parker (1977) in laboratory simulation of basin evolution.

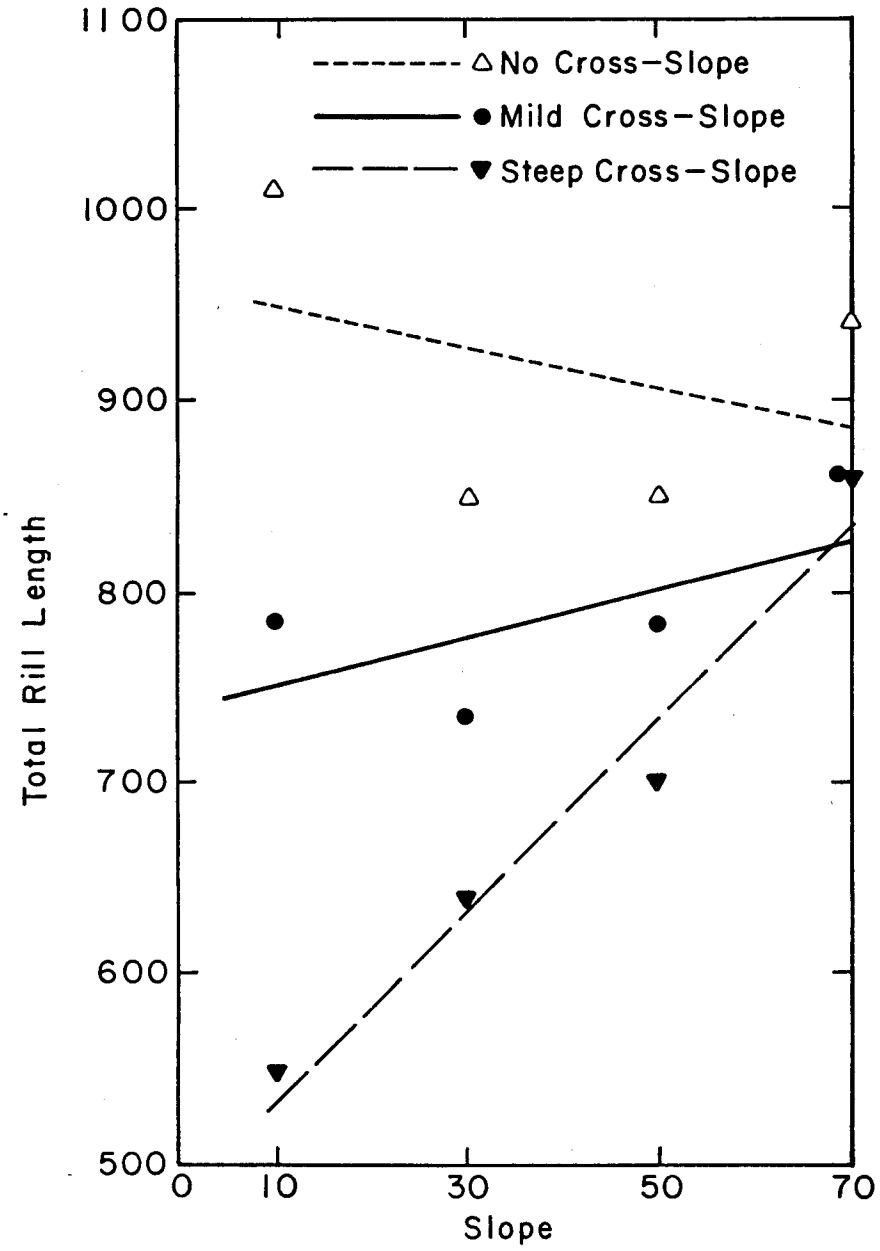

Figure A.5.8a. Variation of total rill length with hillslope inclination.

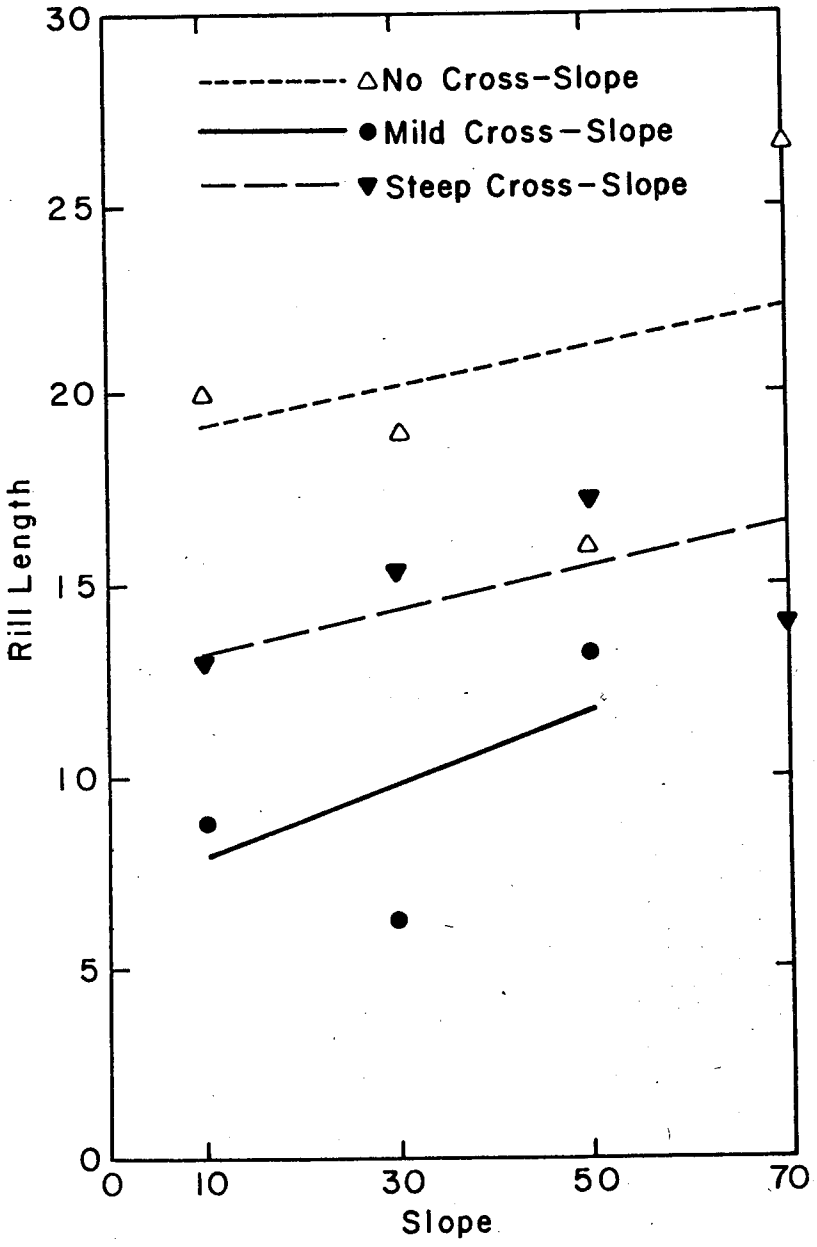

Figure A.5.8b. Variation of first order rill length with hillslope inclination.

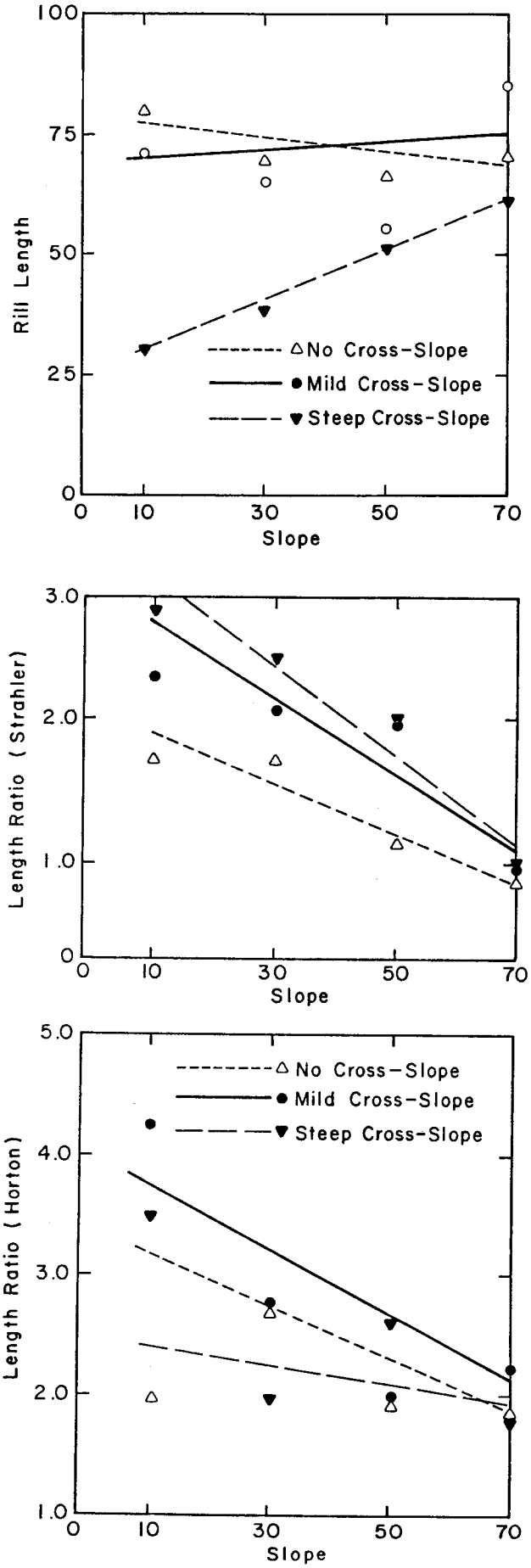

Figure A.5.8 (continued). Variation of average second order rill length (c), and length ratio according to Strahler (d) and Horton (e) with hillslope inclination.

3. A related result is a decrease in length ratio (Figures A.5.8d and A.5.8c). The average first and second-order rill lengths increase with slope more quickly than the higher-order rills. As the cross-slope is increased, keeping the main slope constant:

1. A smaller total rill length results from reduced outlet density. The steeper main slopes with greater outlet density are less affected. This is partly a result of the assumption that a steep slope has a smaller area of influence.

2. Shorter second-order rills result from a more direct path to the main channel. The number of junctions on the main channel down the center of the area are fewer with a mild cross-slope. With a mild cross-slope, there are more likely to be two main channels which compete for tributaries. Thus, the rills have a shorter distance to traverse before joining. There is no corresponding decrease in first-order streams.

The total length of rills produced by the random sources depends mostly on the location of the source point with respect to the exit boundary. However, longer first-order rills are produced in the steeper slopes just as in the fixed source runs. A corresponding decrease in length ratio with increasing slope is noted. As shown in Figures A.5.8a and A.5.8c, the runs without the cross-slope parameter do not demonstrate the same results.

Conclusions

It appears to be feasible to evaluate the deterministic factors in drainage basin form and specifically in rill pattern formation with computer simulation. Dendritic and parallel patterns have been produced with conditions of slope similar to those observed in natural systems. The results are in reasonable agreement with Horton's laws of drainage composition. Some of the network changes resulting from varying topographic conditions are similar to experimental results by Parker (1977) and Mosley (1972). Using computer simulation methods, large quantities of data may be obtained more readily than with field studies. It is also possible to determine the effect of certain variables such as slope on drainage basin form and rill formation.

In this preliminary study, increases in hillslope gradient are shown to increase total channel length in drainage patterns. A more interesting result is decreasing length ratios with increasing slope, indicating that first and second-order rill lengths may increase with a steeper slope more than higher-order streams. Increasing the cross-slope parameter decreases the total rill length by reducing the outlet density. Shorter second-order rill lengths are produced with increasing cross-slope.

A.6 CONFLUENCE STUDY

An intensive sampling program was undertaken on the confluence of the Price River with the Green River, upstream of Green River, Utah, during May, 1976. The objectives of this study were twofold:

1) to study the dispersion of a plume and determine the mixing length for two dissimilar water bodies, and

2) to determine the role of sediment release.

This confluence is of particular interest because the Price River conveys high concentrations of both solutes and sediment into the main stem of the Green River. The dimensions and characteristics of the plume formed in the Green River downstream of its confluence with the Price River depend on the relative flow rates of these two streams. Because of the effect and expense involved with an intensive sampling program, additional sampling solely included a few grab samples collected under different relative flow rate conditions.

A.6.1 Intensive 1976 Sampling Program

Figure A.6.1 shows the location of sampling stations for the intensive sampling program. The inset table summarizes the characteristics of flow, and the type of samples obtained at each cross section. Pertinent information on EC, SC, turbidity and suspended sediment concentration (herein denoted SS) is shown in Table A.6.1. EC values at varying cross-sectional locations for each cross section are summarized in Table A.6.2.

During the sampling period the water discharge in the Green and Price Rivers was 13,800 $\pm$ 250 cfs and 52 $\pm$ 6 cfs (USGS Water Resources Division, Salt Lake City), respectively. From the concentration of

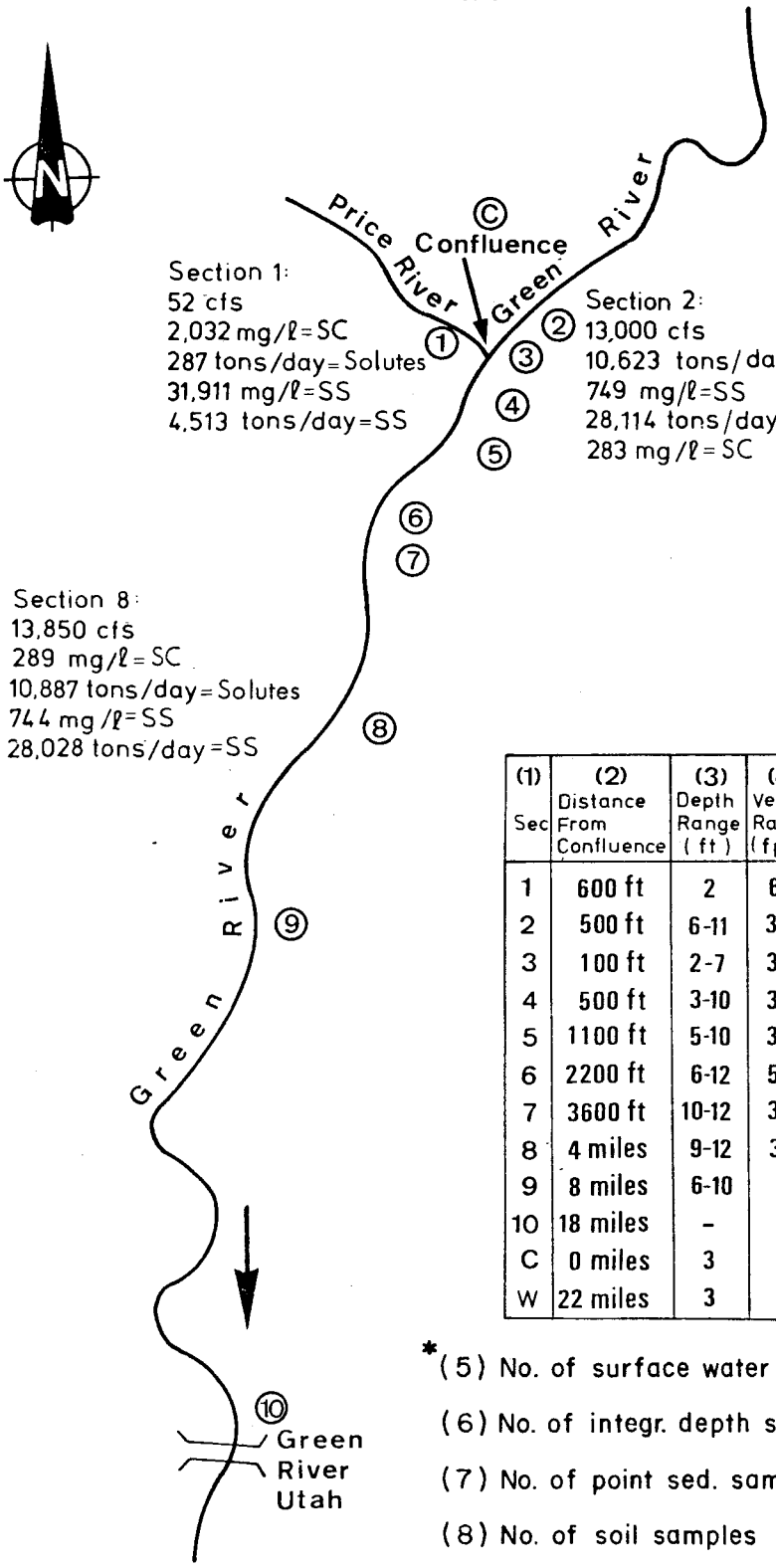

(1) Sec	(2) Distance From Confluence	(3) Depth Range (ft)	(4) Vel Range (fps)	(5) *	(6) *	(7) *	(8) *
1	600 ft	2	6-1	1	0	2	0
2	500 ft	6-11	3-5	4	3	0	3
3	100 ft	2-7	3-6	5	4	2	7
4	500 ft	3-10	3-7	3	3	5	3
5	1100 ft	5-10	3-5	3	3	6	2
6	2200 ft	6-12	5-7	3	3	5	2
7	3600 ft	10-12	3-6	3	3	6	1
8	4 miles	9-12	3-5	3	3	6	1
9	8 miles	6-10	-	2	2	-	-
10	18 miles	-	-	2	-	-	-
C	0 miles	3	-	7	4	4	0
W	22 miles	3	-	1	1	0	0

*(5) No. of surface water quality samples

(6) No. of integr. depth sed. samples

(7) No. of point sed. samples

(8) No. of soil samples

Figure A.6.1. Schematic map of the confluence area showing location of selected cross sections. The inset table summarizes information on the selected cross sections.

solutes and suspended sediment and these water discharges, the daily mass flux of dissolved constituents and of transported suspended sediment was calculated for sections 1, 2 and 8 (Figure A.6.1). Note that the mass flows of solutes and suspended sediment in section 2 were nearly identical to those of section 8. This is attributed primarily to the low flow in the Price River which contributed only 0.4% of the total discharge of section 8.

Table A.6.1. Water quality data for the confluence of the Price and Green Rivers, May 20-23, 1976.

Description of Stations	SC (mg/l)	Turb. (JTU)	SS (mg/l)
Green R., 500 ft above confluence center	283	260	749
Price R*, 600 ft above confluence, center	2,032	9,750	31,911
Green R., 100 ft below confluence			
30 ft from right bank	399	250	831
50 ft from left bank	282	260	781
Green R., 500 ft below confluence			
30 ft from right bank	405	370	2,170
30 ft from left	286	235	710
Green R., 4 mi below confluence 70 ft from right bank	289	250	744

*The Price River discharges into the right bank of the Green River.

Taking the measured data from sections 1 and 2 and assuming complete mixing, the calculated flow weighted average concentration of solutes and suspended sediment downstream of the confluence should be 290 mg/l (an increase of only 7 mg/l) and 866 mg/l, respectively. As far as SC is concerned, the calculated value of 290 mg/l is in excellent agreement with the measured value of 289 mg/l at section 8 (Table A.6.1). However, 866 mg/l suspended sediment is far in excess of the measured 744 mg/l at section 8. This discrepancy attests to deposition of suspended sediment downstream of the confluence. Integrated suspended sediment samples taken 30 feet from the right banks show that sediment concentration decreases from 31,900 to 2,170 mg/l, a 93% reduction, between the confluence proper and 500 feet downstream of it. This decrease substantiates the hypothesis that most of the Price River sediment is deposited immediately downstream of the confluence.

Examination of field EC measurements (Table A.6.2) indicates that a narrow plume, 10-50 ft wide, is formed along the right bank of the Green River under these base (low) flow conditions for quite some distance. The cross sectioned sample located 30 feet from the right bank and 100 feet downstream of the confluence (section 2, Table A.6.1 and A.6.2) is at the plume interface. Although the plume widens further

Table A.6.2. Summary of EC values at the studied cross-sections and at selected distances from the right bank, Price and Green Rivers, May 20-23, 1976.

Section No.	Section width (ft)	Distance from right bank (ft)	EC at water surface (μmho/cm)	EC for integrated Depth (μmho/cm)
1	60	15		2483
		25	3923	3778
		30	3547	3725
0	60	average	2318	2267
2	140	0	418	
		50	429	417
		70	432	425
		90	429	414
3	140	5	1159	
		30	600	1185
		50	495	652
		70	432	407
		90	429	421
4	200	30	607	564
		80	567	560
		170	436	418
5	400	30	573	555
		75	440	431
		155	432	407
6	400	30	537	492
		50	464	450
		350	432	401
7	300	10	515	497
		50	453	457
		265	411	404
8	300	30	447	427
		70	447	435
		260	443	435
		20	436	427
9	400	370	438	427
10	450	0	447	
		450	455	

downstream (section 3), it is still detectable there 30 feet from the right bank. In fact, the mixing length for the plume for these dates is substantially greater than 0.7 miles (3,600 feet) but only slightly less than 4 miles. It is interesting to note that complete mixing is achieved in such a long stretch during high turbulence (5 fps average and as much as 10 fps in riffles) in the Green River.

Some of the water samples were subjected to detailed chemical analyses (Table A.6.3), part of which are plotted in Figure A.6.2. The variations in chemical composition clearly demonstrate the inherent difference between the Price and the Green Rivers.

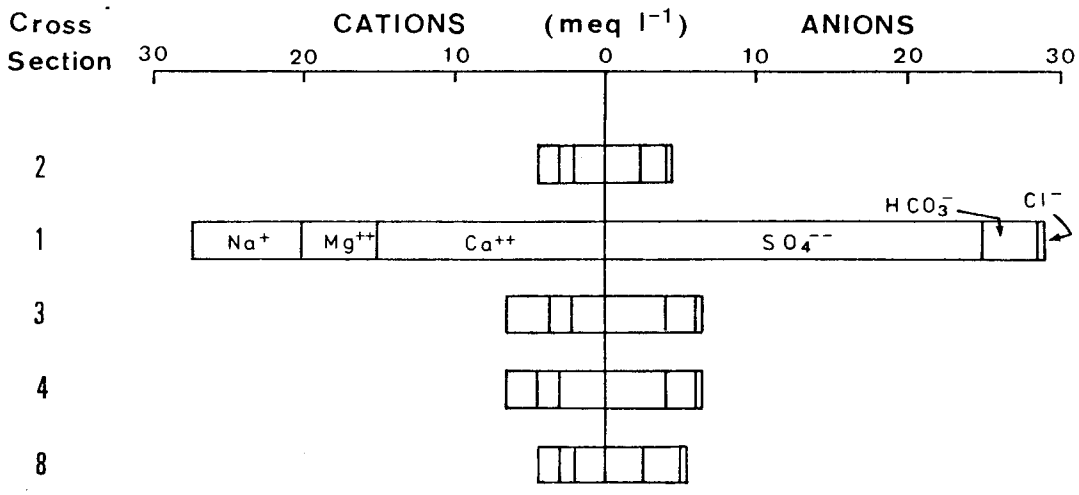

Figure A.6.2. Water quality at the confluence and vicinity.

Table A.6.3. Water chemistry data for the Price and Green River confluence study, May 20-23, 1976.

Description of Stations	pH	Na	Ca	Mg	K	Total Cations	HCO_3	Cl	SO_4	Total Anions
		meq. per liter								
Section 2, center	8.2	1.33	2.05	1.10	0.08	4.56	2.16	0.24	2.35	4.75
Section 1, center	8.0	7.08	15.0	5.0	0.33	27.41	3.48	0.44	25.0	28.92
Section 3, 30 ft from right bank	8.2	2.60	2.25	1.50	0.10	6.45	2.16	0.30	3.90	6.36
Section 3, 50 ft from left bank	8.0	1.31	2.10	1.10	0.05	4.56	2.12	0.22	2.30	4.64
Section 4, 30 ft from right bank	8.2	1.89	3.00	1.55	0.15	6.59	2.16	0.28	4.10	6.54
Section 4, 30 ft from left bank	8.1	1.36	1.95	1.10	0.08	4.49	2.08	0.22	2.30	4.60
Section 8, 70 ft from left bank	8.0	1.36	2.05	1.20	0.08	4.69	2.30	0.20	2.55	5.05

The latter is a low-salinity $CaHCO_3$-$CaSO_4$ type water shile the former is a high-salinity Ca (Na, Mg)- SO_4 (HCO_3) system. Figure A.6.2 shows that the detailed water chemistry of the Green River above the confluence is identical to its nature 4 miles downstream of the confluence. This supports the earlier observation regarding mixing length.

Note that the increase in SC within the Green River was only 7 mg/l. It is possible that additional solutes had been released from sediment transported by the Price River into the Green River. This release is not documented in the data presented herein because it would have amounted to 1-3 mg/l (i.e. less than 1% accuracy), a figure below detectability associated with the sampling and laboratory tecniques used in this study.

A.6.2 Occasional Sampling of Runoff

Results of grab water samples from the Price River at Woodside, Utah from where it leaves the Mancos Shale terrain, and from the Green River at Green River, Utah (below the confluence with the Price River) are given in Table A.6.4.

Table A.6.4. Water quality data for grab samples.

Description \ Location	Price River at Woodside, Utah		Green River at Green River, Utah	
Sampling date	7/30/76	3/24/77	7/30/76	3/25/77
EC, µmho/cm	2,160	5,100	761	844
SC, mg/liter	1,840	4,980	467	573
Turbidity, JTU	375	---	220	---
SS, mg/liter	975	42	429	118
pH	7.9	8.4	7.9	8.6
Solutes, meq/liter				
Na	13.00	33.50	2.35	2.95
Ca	8.00	12.50	3.00	3.25
Mg	9.75	20.50	2.10	2.30
K	0.31	0.39	0.10	0.08
HCO_3	4.54	4.07	3.13	3.24
Cl	1.28	2.72	0.66	0.69
SO_4	26.00	61.00	4.30	5.00

A.7 TRIBUTARY STUDY

The Price, San Rafael and Dirty Devil Rivers with drainage areas of 1,500, 1,670, and 4,200 square miles, respectively, were chosen because they contribute significant solute loads to the Green and Colorado Rivers (Iorns, Hembree and Oakland, 1965; USBR, 1974).

Runoff from these major tributaries was sampled in order a) to supplement the meager water quality data available for these rivers, and b) to determine whether appreciable quantities of solutes are released from sediment transported in sampled runoff. It should be noted that the timing of the sampling program was initially dependant on the presence of investigations near the tributaries. No long-term estimates of mass transport of solutes and of sediment may, therefore, be based uniquely on this set of data. Moreover, none except one of the runoff events were characterized by high solute and sediment concentrations typical of thunderstorm-induced flash floods.

A.7.1 Mass Flow of Dissolved and Suspended Matter

The location of runoff sampling collected during June 22-26, 1976 from the Price, San Rafael and Dirty Devil River is shown in Figures A.7.1a, A.7.1b and A.7.1c, respectively. Table A.7.1 summarizes the pertinent data for these sampling events. The salinity of the sampled runoff was consistently high (2,000 to 3,400 mg/l). These solute concentrations are substantially higher than those of the receiving waters in the Green and Colorado Rivers.

Suspended sediment concentrations were low during the June, 1976 sampling period with the exception of higher concentrations associated with a storm event in the Grassy Trail Creek Basin. The sample

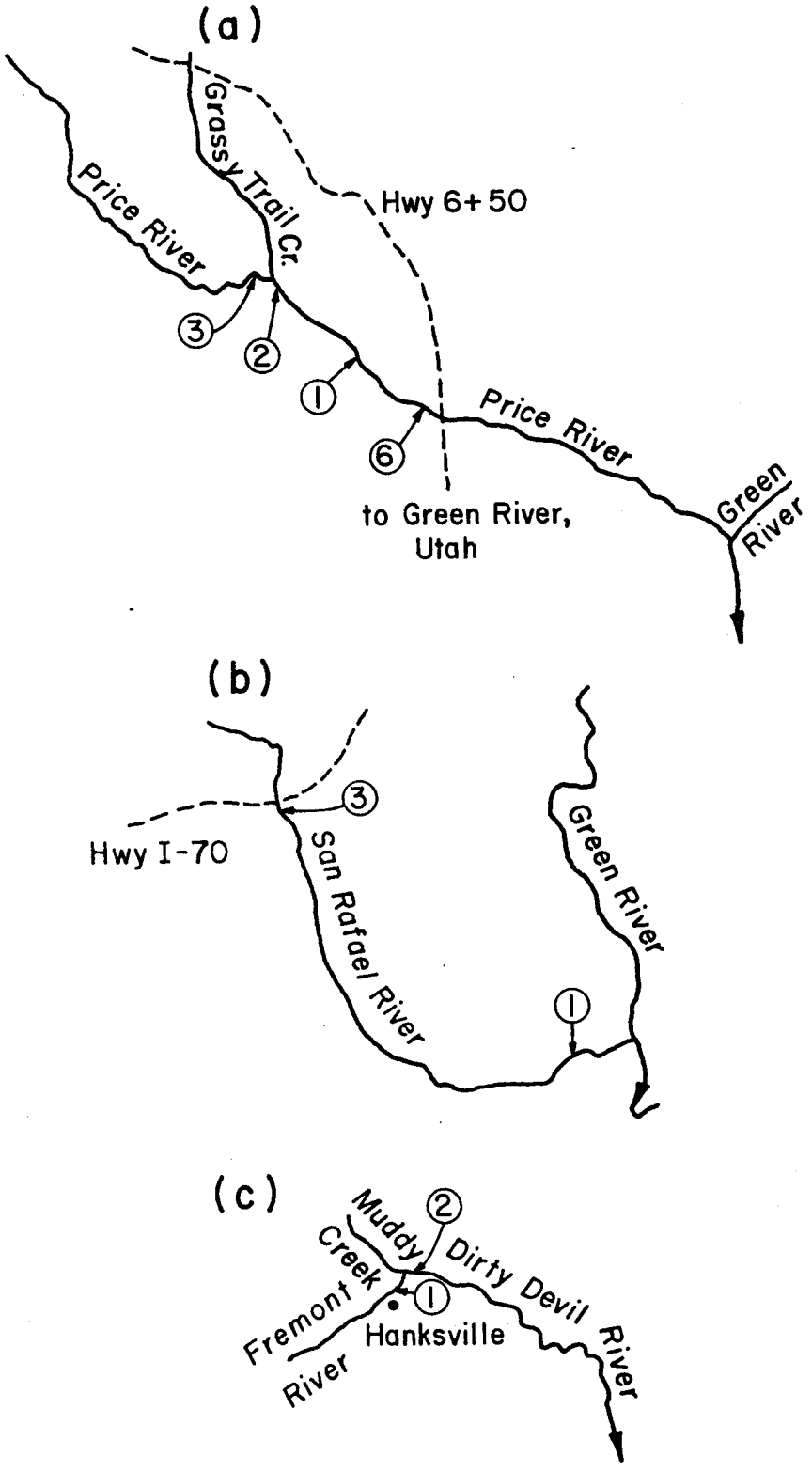

Figure A.7.1. Schematic maps showing sampling locations in the Price (a), San Rafael (b) and Dirty Devil (c) Rivers.

collected during the runoff event at section 2 (Figure A.7.1.a) contained 44673 mg/ℓ suspended matter but its solute content was only slightly higher than that of the Price River further upstream. Most of the drainage basin of Grassy Trail Creek is comprised of thick alluvial fills covering Mancos Shale pediments - hence, this area is not expected to yield large quantities of solutes. The sample collected at section 6 two days after the peak associated with the flow event from Grassy Trail Creek contained a substantially lower sediment concentration. Baseflow in the San Rafael and Dirty Devil Rivers was characterized by moderately high solute concentrations and low sediment concentrations.

Taking the estimated flow discharges and the gravimetric parameters, the calculated mass flows of solutes and sediments are presented in Table A.7.1. Note that except for section 2, the fluxes of solutes in various reaches of the Price River during baseflow in June, 1976 were of about the same order of magnitude as that determined for the outlet of the Price River into the Green River in the May, 1976 confluence study (see section A.6). However, the flux of sediment was considerably lower during June than during May, 1976, except for section 2.

The water sample collected at section 2 in the Price River, containing about 4.5% suspended sediments, was subjected to a tenfold dilution with distilled water. This dilution was undertaken in order to determine whether the suspended sediment would yield additional solutes. Table A.7.2 summarizes sediment and ion specie concentrations for the undiluted and diluted sample. The EC in the diluted sample was higher one-tenth of the one in the undiluted sample due to common

Table A.7.1. Flow, quality and mass transfer in the Price, San Rafael and Dirty Devil Rivers.

River	Section	Sampling date	EC µmho/cm	Turbidity JTU	Q cfs	TDS mg/ℓ	TDS tons/day	SS mg/ℓ	SS tons/day
Price	3	6/22/76	3,446	47	69	2,970	552	78	14
	2	6/22/76	3,571	3,571	145	3,400	1,330	44,673	17,480
	1	6/22/76	3,000	24	27	2,529	184	28	2
	6	6/24/76	3,500	850	42	2,956	335	6,182	701
San Rafael	3	6/24/76	3,091	69	73	2,671	526	118	23
	1	6/24/76	3,400	130	50	3,033	409	256	347
Dirty Devil	1	6/26/76	2,550	19	3	2,066	17	46	0.4
	2	6/26/76	2,318	22	4	2,004	22	38	0.4

Table A.7.2. Effects of tenfold dilution with distilled water of an unfiltered Price River water sample obtained from Section 2 on June 22, 1976.

Parameter	Water sampled on 6/22/76; analyzed on 7/7/76	Water sampled on 6/22/76; diluted on9/20/76; analyzed on 9/21/76;
SS, mg/ℓ	44,673	4,467
EC, μmho/cm	3,571	464
SC*, mg/ℓ	3,176	319
Cations, meq/ℓ		
Na	17.75	1.83
Ca	14.62	1.45
Mg	13.75	0.98
K	0.36	0.05
Total	46.48	4.31
Anions, meq/ℓ		
HCO_3	5.40	0.73
Cl	1.88	0.21
SO_4	39.50	3.80
Total	46.78	4.74

*Sum of mg/liter of cations and anions.

ion effects (Tanji, 1969). In this test the sediments did not yield additional solutes as evidenced by a one-tenth decrease in ion specie concentrations. Note, however, that the water sample was analyzed two weeks after being collected; this was sufficient time for the soluble mineral originally present in the sediment to dissolve. This dilution experiment must, therefore, be considered inconclusive.

A.7.2 Filtration of Sediment from Runoff Samples

Additional water samples collected from the tributaries were filtered at the time of sampling. A comparison of SC between filtered and unfiltered samples would indicate the quantity of solute released from suspended matter. Sediment was filtered by vacuum filtration using a No. 41 Whatman filter paper.

Table A.7.3 shows no significant difference in solute content between the filtered and unfiltered samples of runoff collected during March, 1977 from three locations in the Price River and from the Green River at Green River, Utah. The reason for this similarity is the low concentration of suspended sediment in the sampled runoff, i.e., sediment concentrations were so small that even if evaporite minerals had dissolved, they would yield undetectable quantities of additional solutes.

It may also be inferred that the collected water samples were undersaturated to only slightly saturated with respects to the more soluble evaporite minerals, and that such minerals were not present in significant quantities in the transported sediment. This is substantiated by the nearly identical ion specie concentrations in both filtered and unfiltered samples (Table A.7.3). The concentration of

A.7.3. Comparison of unfiltered and on-site filtered water samples from the tributary sampling program, March 23-27, 1977.

Sample Location	Sampling date	Nature of sample*	EC (μmho/cm)	SC (mg/ℓ)	SS (mg/ℓ)
Price River at Woodside	3/23/77	U	5,000	4,830	23
		F	5,050	4,750	1
	3/24/77	U	5,100	4,980	1
		F	5,210	4,900	1
	3/27/77	U	4,900	4,630	5
		F	4,990	4,700	2
Price River above Grassy Trail Creek	3/24/77	U	5,320	5,110	5
		F	5,320	5,070	4
Price River at Highway 10	3/24/77	U	1,630	1,300	303
		F	1,630	1,340	8
Miller Creek at Highway 10	3/24/77	U	3,160	2,950	3
		F	3,160	2,920	5
Green River at Green River	3/25/77	U	844	570	118
		F	844	570	3

*U = unfiltered, F = filtered through No. 41 Whatman filter paper.

Ca, HCO_3 and the pH, however, indicate that the runoff was saturated with respect to carbonate minerals such as Calcite.

On July 29, 1976 one more set of filtered and unfiltered water samples were obtained from the Price River at Woodside and from the Green River at Green River. The analyses are reported in Table A.7.4 giving similar results as those in Table A.7.3.

Table A.7.4. EC, SC, suspended sediment concentration (SS) and stoichiometric ion concentrations of unfiltered and on-site filtered water samples.

Sampling Location	Sampling date	Sample type	EC (µmho/cm)	SC (mg/ℓ)	SS (mg/ℓ)	pH	Na	Ca	Mg	K	Total Cations	HCO_3	Cl	SO_4	Total Anions
							meq. per liter								
Price River at	3/23/77	U	5000	4830	23	8.5	32.5	12.0	20.5	0.4	65.40	4.07	2.66	60.0	66.73
Woodside		F	5050	4750	1	8.5	33.5	11.5	20.5	0.38	65.88	4.07	2.66	60.0	66.73
	3/24/77	U	5100	4980	1	8.4	33.5	12.5	20.5	0.39	66.89	4.07	2.72	61.0	67.79
		F	5210	4900	1	8.5	32.5	13.0	21.5	0.39	67.39	4.18	2.72	61.0	67.90
	3/27/77	U	4900	4630	5	8.2	30.0	13.5	19.5	0.38	63.38	4.91	2.49	57.0	64.40
		F	4990	4700	2	8.6	30.5	14.0	19.5	0.38	64.38	5.01	2.55	57.0	64.56
Price River at	3/24/77	U	5320	5110	5	8.1	34.0	13.5	21.5	0.38	69.38	5.22	2.72	62.0	69.94
Grassy Trail Creek		F	5320	5070	4	8.5	34.5	13.0	21.5	0.38	69.38	4.91	2.66	62.0	69.57
Price River	3/24/77	U	1630	1300	303	8.4	4.5	6.8	8.3	0.16	19.76	5.53	1.20	14.0	20.73
Highway 10		F	1630	1340	8	8.4	4.5	6.9	8.3	0.16	19.86	5.53	1.25	13.5	20.28
Miller Creek at	3/24/77	U	3160	2950	3	8.2	12.5	10.0	19.0	0.28	41.78	4.59	2.89	33.0	40.48
Highway 10		F	3160	2920	5	8.5	12.3	10.5	18.2	0.28	41.28	5.12	2.77	30.0	37.89
Green River at	3/25/77	U	844	570	118	8.6	2.95	3.25	2.3	0.08	8.58	3.24	0.69	5.0	8.93
Green River		F	844	570	3	8.6	2.95	3.20	2.4	0.08	8.63	3.34	0.75	5.2	9.29

*U = unfiltered water subsample, F = on-site